

University of Southampton Research Repository ePrints Soton

Copyright © and Moral Rights for this thesis are retained by the author and/or other copyright owners. A copy can be downloaded for personal non-commercial research or study, without prior permission or charge. This thesis cannot be reproduced or quoted extensively from without first obtaining permission in writing from the copyright holder/s. The content must not be changed in any way or sold commercially in any format or medium without the formal permission of the copyright holders.

When referring to this work, full bibliographic details including the author, title, awarding institution and date of the thesis must be given e.g.

AUTHOR (year of submission) "Full thesis title", University of Southampton, name of the University School or Department, PhD Thesis, pagination

UNIVERSITY OF SOUTHAMPTON
FACULTY OF MEDICINE

**PHOSPHOLIPID KINETICS IN ACUTE
RESPIRATORY DISTRESS SYNDROME**

Ahilanandan Dushianthan

MBBS MRCP

Thesis for the degree of Doctor of Philosophy

February 2014

UNIVERSITY OF SOUTHAMPTON

ABSTRACT

FACULTY OF MEDICINE

Doctor of Philosophy

**PHOSPHOLIPID KINETICS IN ACUTE
RESPIRATORY DISTRESS SYNDROME**

by Ahilanandan Dushianthan

Acute respiratory distress syndrome (ARDS) is a life-threatening critical illness, characterised by qualitative and quantitative surfactant compositional changes associated with premature airway collapse, gas-exchange abnormalities and acute hypoxic respiratory failure. The underlying mechanisms for this dysregulation in surfactant metabolisms are not fully understood. Lack of therapeutic benefits from clinical trials highlight the importance of detailed *in-vivo* analysis and characterisation of ARDS patients according to patterns of surfactant synthesis and metabolism.

Phosphatidylcholine (PC) is not only a major constituent of pulmonary surfactant, it is also an essential part of the cell membrane cytoskeleton with diverse functions. The endogenous synthesis of PC depends on two main pathways. While all eukaryotic cells utilise cytidine diphosphate-choline (CDP-choline) pathway, hepatocytes generates 30% of their PC by three sequential methylations of phosphatidylethanolamine catalysed by the actions of a specific enzyme phosphatidylethanolamine methyltransferase (PEMT). This thesis explores the PC compositional alterations and synthetic patterns *in-vivo* in patients with ARDS. Stable isotope labelling and electrospray ionisation mass spectrometry (ESI-MS/MS) enabled highly specific PC molecular assessment through analysis of patterns of *methyl-D₉*-choline incorporation.

Patients with ARDS had significant abnormalities in surfactant phospholipid composition with diminished levels of PC16:0/16:0. This was associated with variations in surfactant PC synthesis. To refine surfactant isolation methods for future studies, phospholipid composition and kinetics from various endobronchial compartments of healthy volunteers were characterised. This suggested that secretions from tracheal wash were qualitatively similar to those from small volume bronchoalveolar lavage phospholipids, both in composition and dynamic *methyl-D₉*-choline incorporation. Analysis of patient's plasma revealed significant alterations in the fractional concentrations and compositions of lipoproteins and PC, with a specific fractional increase in PC16:0/18:1. This was accompanied by an increase in overall flux through CDP-choline pathway. PEMT pathway was investigated by two different analytical methods. ARDS patients had significantly lower levels of PC flux through this pathway. Cellular PC analysis from patients also revealed significant changes with increased PC16:0/18:1 in red blood cells, PC18:0/18:2 in neutrophils and decreased arachidonyl-PC species in lymphocytes.

This study demonstrates the feasibility of using stable isotope labelling in combination with ESI-MS/MS technology to characterise surfactant, cellular, plasma and hepatic PC metabolic pathways in patients with ARDS. Ongoing recruitment may possibly detect underlying phenotypic variations of patients according to de-novo synthesis of specific PC molecular species from various tissue types.

TABLE OF CONTENTS

ABSTRACT	III
LIST OF TABLES	IX
LIST OF FIGURES	XI
DECLARATION OF AUTHORSHIP	XXI
ACKNOWLEDGEMENTS	XXIII
LIST OF ABBREVIATIONS	XXV
CHAPTER 1 INTRODUCTION	1
1.1 ACUTE RESPIRATORY DISTRESS SYNDROME	1
1.1.1 DEFINITIONS	1
1.1.2 CLINICAL IMPACT OF ARDS	5
1.2.3 PATHOPHYSIOLOGY	7
1.2.4 AETIOLOGY AND ASSOCIATIONS	10
1.1.5 MANAGEMENT OF ARDS	11
1.2 PULMONARY SURFACTANT SYSTEM	11
1.2.1 SURFACTANT COMPOSITION	12
1.2.2 SURFACTANT SYNTHESIS, TURNOVER AND METABOLISM	12
1.2.3 ENDOGENOUS SURFACTANT ALTERATIONS IN ARDS	15
1.2.4 PATHOPHYSIOLOGY OF DYSFUNCTIONAL SURFACTANT	17
1.2.5 EXOGENOUS SURFACTANT REPLACEMENT	21
1.3 PHOSPHOLIPID METABOLISM IN HUMANS	22
1.3.1 GLYCEROPHOSPHOLIPIDS	22
1.3.2 SYNTHETIC PATHWAYS OF GLYCEROPHOSPHOLIPIDS	23
1.3.3 CHOLINE AND PHOSPHATIDYLCHOLINE METABOLISM	25
1.3.4 HEPATIC LIPID METABOLISM	26
1.4 DYNAMIC SURFACTANT PHOSPHOLIPID ASSESSMENT	28
1.4.1 ELECTROSPRAY IONISATION MASS SPECTROMETRY	29
1.4.2 STABLE ISOTOPE LABELLING WITH <i>METHYL-D₉</i> CHOLINE CHLORIDE	31
1.5 CELL ISOLATION BY MAGNETIC BEAD LABELLING	33
1.6 THESIS AIMS	34
CHAPTER 2 METHODOLOGY	37
2.1 MATERIALS	37
2.2 ETHICS AND RESEARCH DEVELOPMENT APPROVAL	38
2.3 PATIENT SELECTION	38
2.4 <i>METHYL-D₉</i>- CHOLINE INFUSION AND SAMPLE COLLECTION	39
2.5 SAMPLE PROCESSING	41
2.6 PHOSPHOLIPID EXTRACTION	41
2.7 EXTRACTION OF CHOLINE METABOLITES	43

2.8 ANALYSIS BY ESI-MS/MS	43
2.9 LC-MS/MS FOR CHOLINE AND ITS METABOLITES	44
2.10 ELISA FOR SP-D ASSESSMENT	46
2.11 NEUTROPHIL AND LYMPHOCYTE ISOLATION	47
2.12 FLOW CYTOMETRY OF NEUTROPHILS	47
2.13 EX-VIVO INCUBATION OF NEUTROPHILS WITH FATTY ACID SUPPLEMENTATION	48
2.14 PLASMA CHOLESTEROL AND LIPOPROTEIN ANALYSIS	48
2.15 DATA EXTRACTION	48
2.16 STATISTICAL ANALYSIS	48

CHAPTER 3 SURFACTANT PHOSPHOLIPID KINETICS IN ARDS **51**

3.1 INTRODUCTION	51
3.2 OBJECTIVES	52
3.3 SUMMARY OF METHODS	52
3.4 RESULTS	53
3.4.1 PATIENT'S CHARACTERISTICS	53
3.4.2 MASS SPECTROMETRY ANALYSIS OF BALF PC	55
3.4.3 TOTAL SURFACTANT PC AND FRACTIONAL PC16:0/16:0 CONCENTRATIONS	56
3.4.4 SURFACTANT PC MOLECULAR COMPOSITION AT ENROLMENT	58
3.4.5 SURFACTANT PC MOLECULAR COMPOSITION OVER TIME	58
3.4.6 VARIATION IN SURFACTANT PC COMPOSITION BETWEEN PATIENTS	60
3.4.7 MOLECULAR COMPOSITION OF <i>METHYL-D₉</i> - LABELLED PC SPECIES	62
3.4.8 TOTAL SURFACTANT PC <i>METHYL-D₉</i> - INCORPORATION	66
3.4.9 FRACTIONAL PC16:0/16:0- <i>METHYL-D₉</i> INCORPORATION	67
3.5 DISCUSSION	69
3.6 CONCLUSIONS	72

CHAPTER 4 IN-VIVO CHARACTERISATION OF PC SYNTHETIC PATHWAYS IN ARDS **73**

4.1 INTRODUCTION	73
4.2 OBJECTIVES	75
4.3 SUMMARY OF METHODS	75
4.4 RESULTS	76
4.4.1 PLASMA CHOLINE AND BETAINE CONCENTRATIONS AND ENRICHMENT	76
4.4.2 PLASMA LIPID CONCENTRATIONS AND COMPOSITION	78
4.4.3 CHARACTERISATION OF CDP-CHOLINE PATHWAY	83
4.4.4 CHARACTERISATION OF PEMT PATHWAY	90
4.5 DISCUSSION	99
4.6 CONCLUSIONS	103

CHAPTER 5 CELLULAR PHOSPHOLIPID PROFILE AND TURNOVER IN ARDS **105**

5.1 INTRODUCTION	105
5.2 OBJECTIVES	106
5.3 SUMMARY OF METHODS	106
5.4 RESULTS	107
5.4.1 PC COMPOSITIONAL VARIATION AMONG CELLS	108
5.4.2 RED BLOOD CELL PHOSPHOLIPID PROFILE	109
5.4.3 PC COMPOSITION AND KINETICS OF CD15+ NEUTROPHILS	118

5.4.4 CD3+ LYMPHOCYTE PC MOLECULAR COMPOSITION	122
5.4.5 EX-VIVO INCUBATION OF CD15+ NEUTROPHILS WITH FATTY ACIDS	123
5.4.6 FUNCTIONAL VARIATION OF NEUTROPHILS AFTER FATTY ACID SUPPLEMENTATION	128
5.5 DISCUSSION	129
5.6 CONCLUSIONS	133
<u>CHAPTER 6 EXAMINATION OF PHOSPHOLIPID COMPOSITION AND KINETICS FROM VARIOUS ENDOBRONCHIAL COMPARTMENTS IN HUMAN HEALTHY ADULTS</u>	135
<hr/>	
6.1 INTRODUCTION	135
6.2 OBJECTIVES	137
6.3 SUMMARY OF METHODS	137
6.4 RESULTS	137
6.4.1 DEMOGRAPHICS	137
6.4.2 TOTAL PHOSPHOLIPID, PC AND SP-D CONCENTRATIONS	138
6.4.3 SURFACTANT PHOSPHOLIPID COMPOSITION	142
6.4.4 TOTAL AND FRACTIONAL PC <i>METHYL-D₉</i> INCORPORATION	146
6.4.5 MOLECULAR SPECIFICITY OF <i>METHYL-D₉</i> LABELLED PC SPECIES	150
6.4.6 BALF LPC ASSESSMENT AND FRACTIONAL LABELLING	151
6.5 DISCUSSION	153
6.6 CONCLUSIONS	156
<u>CHAPTER 7 GENERAL DISCUSSION AND FUTURE DIRECTIONS</u>	159
<hr/>	
<u>APPENDIX 1. PUBLICATIONS</u>	167
<hr/>	
<u>REFERENCES</u>	168
<hr/>	

LIST OF TABLES

<u>TABLE 1;</u> Expanded definition of acute respiratory distress syndrome/ Murray’s lung injury score (LIS).	3
<u>TABLE 2;</u> American European Consensus Criteria for the diagnosis of acute respiratory distress syndrome and acute lung injury.....	4
<u>TABLE 3;</u> Berlin definition of acute respiratory distress syndrome.	4
<u>TABLE 4;</u> Incidence and mortality of acute lung injury and acute respiratory distress syndrome across the world	5
<u>TABLE 5;</u> Mortality data from Acute Respiratory Distress Syndrome Network randomised controlled trials published between 2000- 2011.	6
<u>TABLE 6;</u> Clinical conditions associated with aetiology of acute respiratory distress syndrome.	10
<u>TABLE 7;</u> Summary table of bronchoalveolar lavage surfactant fractional compositional abnormalities in patients with ARDS.	17
<u>TABLE 8;</u> Quantity of biological samples used for phospholipid extraction.	42
<u>TABLE 9;</u> Internal standards and quantities used for biological samples.....	42
<u>TABLE 10;</u> Mass charge ratio (m/z) assignments for most prominent components of PC determined by precursor scans of m/z184+, m/z187+ and m/z193+ for positive ionization fragmentation.....	44

TABLE 11; Ultra performance liquid chromatography (UPLC) gradient (A) and multiple reaction monitoring (MRM) transitions for plasma choline, betaine and their *methyl-D₉* labelled counterparts (B).....45

TABLE 12; Baseline characteristics and outcomes of recruited ARDS patients.....54

TABLE 13; Plasma cholesterol, low density lipoproteins (LDL) - cholesterol, high density lipoproteins (HDL) - cholesterol and triacylglycerol concentrations at enrolment (T=0) between patients (N=10) and controls (N=10).....79

TABLE 14; Characteristics of healthy subjects recruited138

TABLE 15; Total phospholipid, phosphatidylcholine and surfactant protein D concentrations for all sampling methods139

TABLE 16; Phosphatidylcholine molecular composition of phospholipid fraction from all sampling methods143

TABLE 17; Fractional *methyl-D₉* labelled phosphatidylcholine composition at 24 and 48 hours.....150

LIST OF FIGURES

FIGURE 1; Pictorial view of injured alveolus with pulmonary oedema in ARDS.....	9
FIGURE 2; Basic schematic representation of pulmonary surfactant synthesis, secretion and recycling by alveolar type-II cells.	14
FIGURE 3; Structure of glycerophospholipids, the head group of sub-classes and sphingomyelin.	23
FIGURE 4; Synthetic pathways for major glycerophospholipids found in pulmonary surfactant.	24
FIGURE 5; Illustration of phosphatidylethanolamine-N-methyl transferase (PEMT) and cytidine diphosphate (CDP) choline pathways for the endogenous synthesis of phosphatidylcholines (PC) from <i>methyl-D₉</i> choline.	32
FIGURE 6; Multiple reaction monitoring chromatograms of 12 channels ES+ (A), choline 103.8→59.8 (B), <i>methyl-D₉</i> choline 112.9→68.9 (C), betaine 117.9→ 58.9 (D) and <i>methyl-D₉</i> betaine 126.9→67.9 (E) transitions	46
FIGURE 7; Example of a typical mass spectrum for pulmonary surfactant phosphatidylcholine composition from a healthy control.	55
FIGURE 8; Total surfactant phosphatidylcholine concentration (nmol/ml) isolated from bronchoalveolar lavage over time in patients (N=10) compared to healthy adult controls (N=9) at first time point (T=24Hrs).....	56
FIGURE 9; Clinical correlations of total phosphatidylcholine and fractional PC16:0/16:0 concentrations with oxygenation at enrolment and death	57

FIGURE 10; Bronchoalveolar lavage phosphatidylcholine molecular composition at enrolment (T=0Hrs) in patients compared to healthy adult controls.	58
FIGURE 11; Bronchoalveolar lavage surfactant phosphatidylcholine fractional molecular composition over time in patients	59
FIGURE 12; Time course variation of sum of all selected saturated and unsaturated phosphatidylcholine composition in patients.	59
FIGURE 13; Relationships of relative composition of PC16:0/16:0 with other major (A) and minor (B) phosphatidylcholine species over time for the corresponding time points.....	60
FIGURE 14; Fractional compositional variation of bronchoalveolar surfactant phosphatidylcholine species from individual patients at enrolment (T=0Hrs) (A) and healthy controls at T=24Hrs (B)	61
FIGURE 15; Individual variation of fractional PC16:0/16:0 composition among patients (N=10) at enrolment compared with controls (N=9).	61
FIGURE 16; Molecular composition of <i>methyl-D₉</i> labelled phosphatidylcholine fraction in patients over time.....	62
FIGURE 17; Comparison of <i>methyl-D₉</i> labelled and unlabelled fractional phosphatidylcholine composition at time points 6 (A), 12 (B), 24 (C), 48 (D), 72 (E) and 96 (F) hours after <i>methyl-D₉</i> choline infusion in patients.....	63
FIGURE 18; Comparison of <i>methyl-D₉</i> labelled and unlabelled fractional phosphatidylcholine composition at time points 24Hrs (A) and 48Hrs (B) after <i>methyl-D₉</i> choline infusion in healthy controls.....	64

FIGURE 19; Individual variation in *methyl-D₉* labelled surfactant phosphatidylcholine composition at peak incorporation (T=48Hrs after *methyl-D₉* choline infusion) from patients (A) and healthy controls (B) 65

FIGURE 20; Relationship between unlabelled PC16:0/16:0 composition (% of total unlabelled phosphatidylcholine) and the *methyl-D₉* labelled PC16:0/16:0 (% of total labelled phosphatidylcholine) among patients and controls at (T=48Hrs) at maximal incorporation (T=48Hrs). 66

FIGURE 21; Mean total bronchoalveolar lavage phosphatidylcholine *methyl-D₉* choline incorporation (A) and the rate of total bronchoalveolar lavage phosphatidylcholine *methyl-D₉* choline incorporation (B) in patients (N=10) compared to controls (N=9)..... 67

FIGURE 22; Individual variation in mean total bronchoalveolar lavage phosphatidylcholine *methyl-D₉* choline incorporation in patients (N=10) among patients over time..... 67

FIGURE 23; Bronchoalveolar lavage fractional *Methyl-D₉* PC16:0/16:0 incorporation (A) and rate of fractional *methyl-D₉* PC16:0/16:0 incorporation (B) in patients (N=10) compared to controls (N=9). 68

FIGURE 24; Individual variation in bronchoalveolar lavage fractional *methyl-D₉* PC16:0/16:0 incorporation in patients (N=10) over time..... 68

FIGURE 25; Plasma choline concentrations ($\mu\text{M/l}$) (A) and fractional plasma *methyl-D₉*-choline enrichment (%) (B) for both patients (N=10) and healthy controls (N=10) over time..... 77

FIGURE 26; Fractional plasma *methyl-D₉*-betaine enrichment (%) for patients (N=10) and healthy controls (N=10)..... 77

FIGURE 27; Comparison of plasma phosphatidylcholine concentrations (mmol/l) between patients (N=10) and controls (N=10) at enrolment (T=0Hrs).....78

FIGURE 28; Changes in plasma fractional PC molecular concentrations (mmol/l) in patients (N=10) corrected for control values (N=10) at enrolment (T=0Hrs).79

FIGURE 29; Plasma phosphatidylcholine concentrations (mmol/l) over time between patients (N=10) and controls (N=10).79

FIGURE 30; Concentrations of polyunsaturated based phosphatidylcholine species (mmol/l) between patients (N=10) and controls (N=10) at enrolment (T=0Hrs).80

FIGURE 31; Plasma cholesterol, low density lipoproteins (LDL) - cholesterol, high density lipoproteins (HDL) - cholesterol and triacylglycerol concentrations over time in ARDS patients (N=10).....81

FIGURE 32; Plasma phosphatidylcholine molecular composition at T=0Hrs in patients (N=10) compared with healthy controls (N=10).....82

FIGURE 33; Plasma 1-alkyl 2-acyl phosphatidylcholine composition molecular composition at T=0Hrs in patients (N=10) compared with healthy controls (N=10).83

FIGURE 34; Typical mass spectra of precursor scans of m/z184 (A) and m/z193 (B) from plasma of controls at peak incorporation (T=24Hrs).....84

FIGURE 35; Plasma phosphatidylcholine *methyl-D₉* incorporation for patients (N=10) and healthy controls (N=10) over time.85

FIGURE 36; Rate of total plasma phosphatidylcholine *methyl-D₉* incorporation for patients (N=10) and healthy controls (N=10).85

FIGURE 37; Fractional *methyl-D₉*-incorporation of plasma PC species from healthy controls (N=10) (**A**) and patients (N=10) (**B**)..... 86

FIGURE 38; Individual variation in plasma total *methyl-D₉* PC incorporation among healthy controls (N=10) (**A**) and patients (N=10) (**B**) over time..... 87

FIGURE 39; Correlation between plasma phosphatidylcholine concentrations and peak total *methyl-D₉* PC incorporations (T=24Hrs)..... 87

FIGURE 40; Plasma fractional *methyl-D₉*-phosphatidylcholine concentration changes (mean) from control values (mean) for appropriate times..... 88

FIGURE 41; Comparison of plasma 1-alkyl 2-acyl *methyl-D₉*-phosphatidylcholine incorporation for patients (N=10) and controls (N=10). 89

FIGURE 42; Fractional *methyl-D₉* incorporation of plasma 1-alkyl 2-acyl phosphatidylcholine species in healthy controls (N=10) (**A**) and patients (N=10) (**B**).... 90

FIGURE 43; Fractional composition of *methyl-D₉* labelled phosphatidylcholine in plasma from healthy controls (N=10) (**A**) and patients (N=10) (**B**)..... 90

FIGURE 44; Parent scans for plasma phosphatidylcholine composition. Mass spectra for unlabelled (**A**), *methyl-D₃* (**B**) and *methyl-D₆* (**C**) compositions from plasma phosphatidylcholine of healthy controls..... 91

FIGURE 45; Plasma *methyl-D₃* phosphatidylcholine incorporation, comparison between patients (N=10) and healthy controls (N=10) over time. 92

FIGURE 46; Plasma *methyl-D₆* phosphatidylcholine incorporation, comparison between patients (N=10) and controls (N=10) over time. 92

FIGURE 47; Plasma phosphatidylcholine fractional <i>methyl-D₃</i> incorporation in controls (N=10) (A) and patients (N=10) (B).....	93
FIGURE 48; Plasma phosphatidylcholine fractional <i>methyl-D₆</i> incorporation in controls (N=10) (A) and patients (N=10) (B).....	94
FIGURE 49; Neutral loss scan for PC18:0/22:6.....	95
FIGURE 50; Correlation between precursor and neutral loss scans for plasma phosphatidylcholine <i>methyl-D₃</i> and <i>methyl-D₆</i> enrichment for controls and patients.	95
FIGURE 51; <i>Methyl-D₃</i> S-adenosyl methionine enrichment for all time points in controls (A) and patients (B).	96
FIGURE 52; <i>Methyl-D₃</i> S-adenosyl methionine enrichment in controls (A) and patients (B) as estimated by both precursor and neutral loss scans.....	97
FIGURE 53; Fractional synthesis (A) and rate of synthesis (B) of phosphatidylcholine via phosphatidylethanolamine N- methyltransferase pathway.	98
FIGURE 54; Individual variation in total phosphatidylcholine synthesis (% of total PC) by phosphatidylethanolamine N- methyltransferase pathway among controls (N=10) (A) and patients (N=10) (B).	98
FIGURE 55; Molecular specificity of labelled phosphatidylcholine by phosphatidylethanolamine N- methyltransferase pathway in controls (N=10) (A) and patients (N=10) (B).....	99
FIGURE 56; Purity assessment of the CD3+ cells by flow cytometry.	107

FIGURE 57; Purity assessment of the CD15+ cells by flow cytometry.....	108
FIGURE 58; Example of typical mass spectra for the PC composition of red blood cells (A), CD15+ neutrophils (B), and CD3+ T- lymphocytes (C) in healthy human volunteers.	108
FIGURE 59; Phosphatidylcholine molecular composition of red blood cells (N=30), CD15+ neutrophils (N=42) and CD3+ T lymphocytes (N=36) in healthy humans.	109
FIGURE 60; Comparison of red blood cell total phosphatidylcholine concentrations ($\mu\text{mol/ml}$) for all time points measured between patients (N=8, 56 time points) and controls (N=5, 30 time points).	110
FIGURE 61; Red blood cell phosphatidylcholine molecular composition in patients (N=8) over time. Control data (N=5) for T=0 at enrolment.....	111
FIGURE 62; Correlation between plasma PC16:0/18:1 and red blood cell PC6:0/18:1 concentration ($\mu\text{mol/ml}$), in patients (N= 8 with 55 total time points) (A), controls (N=5 with total 30 time points) (B)	112
FIGURE 63; Red blood cell phosphatidylethanolamine molecular composition in patients (N=8) over time and control data (N=5) for T=0 at enrolment	113
FIGURE 64; Red blood cell phosphatidylinositol molecular composition in patients (N=8) over time and control data (N=5) for T=0 at enrolment.	113
FIGURE 65; Red blood cell phosphatidylserine molecular composition in patients (N=8) over time and control data (N=5) for T=0 at enrolment.	114
FIGURE 66; Red blood cell sphingomyelin molecular composition in patients (N=8) over time and control data (N=5) for T=0 at enrolment	114

FIGURE 67; Time course variation of red blood cell unlabelled and *methyl-D₉* labelled phosphatidylcholine molecular composition in controls (N=5) and patients (N=8).....115

FIGURE 68; Red blood cell phosphatidylcholine *methyl-D₉* incorporation for both patients (N=8) and controls (N=5).....116

FIGURE 69; Red blood cell fractional phosphatidylcholine *methyl-D₉* incorporation (% of total PC) in controls (N=5) (**A**) and patients (N=8) (**B**)117

FIGURE 70; Changes in unlabelled (A) and *methyl-D₉* labelled (B) red blood cell fractional PC molecular concentrations (mmol/l) in patients (N=8) corrected for control values (N=5) at peak incorporation (T=96Hrs).....118

FIGURE 71; CD15+ neutrophil phosphatidylcholine concentrations (nmol/ml) for all time points measured in patients (N=9 with 58 time points) and healthy controls (N=6 with 33 time points)118

FIGURE 72; CD15+ neutrophil phosphatidylcholine composition in patients (N=9) over time compared to controls (N=6) at T=0119

FIGURE 73; Unlabelled and *methyl-D₉*-labelled choline PC composition of CD15+ neutrophils from controls (N=6) and patients (N=9)120

FIGURE 74; *Methyl-D₉* choline phosphatidylcholine incorporation of CD15+ neutrophils (% of total PC) from patients (N=9) and healthy controls (N=6)121

FIGURE 75; Fractional *methyl-D₉* incorporation of diacyl and 1-alkyl 2-acyl phosphatidylcholine species of CD15+ neutrophils from controls (N=6) and patients (N=9).....121

FIGURE 76; Phosphatidylcholine molecular composition of CD3+ T- lymphocytes in patients (N=4) over time, compared to healthy controls (N=4) at enrolment	122
FIGURE 77; Composition of arachidonyl (20:4) containing PC species of CD3+ T- lymphocytes for all time points measured between patients (n=4, 26 time points) and controls (n=4, 18 time points)	123
FIGURE 78; Unlabelled phosphatidylcholine composition of CD15+ neutrophils after fatty acid supplementation.....	125
FIGURE 79; Fractional composition of <i>methyl-D₉</i> labelled PC fraction in CD15+ neutrophils after fatty acid supplementation	126
FIGURE 80; Fractional <i>methyl-D₉</i> incorporation in CD15+ neutrophils after fatty acids supplementation.....	127
FIGURE 81; Human whole blood was incubated with fatty acids and neutrophils were assessed for their cell surface expression of activation markers (CD11a, CD11b, CD62L) on flow cytometry	128
FIGURE 82; Mean channel fluorescence shift for CD62L(A), CD11b (B) and CD11a (C) after fatty acid supplementation.	129
FIGURE 83; Correlations of bronchoalveolar lavage and tracheal wash phospholipid concentrations (nmol/l) for both time points studied (24 and 48 hours).	140
FIGURE 84; Correlation between bronchoalveolar lavage fluid (BALF), tracheal wash (TW), and induced sputum (IS) phospholipid (PL) and phosphatidylcholine (PC) concentrations.....	141

FIGURE 85; Variation in the total phosphatidylcholine concentrations (nmol/ml) from all sampling methods between subjects.	141
FIGURE 86; Fractional phospholipid composition from all sampling methods.	142
FIGURE 87; Comparison of surfactant phospholipid subclass molecular composition from all sampling methods.....	146
FIGURE 88; Total phosphatidylcholine (A) and fractional PC16:0/16:0 <i>methyl-D₉</i> -incorporation (B) for all sampling methods.	147
FIGURE 89; Correlation graphs for the total phosphatidylcholine and fractional PC16:0/16:0 <i>methyl-D₉</i> -incorporations for all isolation methods.	148
FIGURE 90; Fractional <i>methyl-D₉</i> -incorporation of major surfactant phosphatidylcholine species (PC16:0/14:0, PC16:1/16:0, PC16:0/16:0 and PC16:0/18:1) for all sampling methods.....	149
FIGURE 91; Individual variation in total phosphatidylcholine (A) and fractional <i>methyl-D₉</i> -PC16:0/16:0 incorporation (B).....	149
FIGURE 92; Molecular specificity of <i>methyl-D₉</i> -choline incorporation into PC16:0/16:0 synthesis (black bars), expressed as a percentage of <i>methyl-D₉</i> labelled PC, was compared with that of unlabelled PC16:0/16:0 (grey bars) at both 24 and 48 hours for bronchoalveolar lavage fluid (BALF), tracheal wash (TW) and induced sputum (IS)...	151
FIGURE 93; Comparison of bronchoalveolar lavage unlabelled and <i>methyl-D₉</i> labelled lysophosphatidylcholine composition at 24 and 48 hours.	152
FIGURE 94; Correlation between LPC16:0 and PC16:0/16:0 <i>methyl-D₉</i> incorporation of bronchoalveolar lavage surfactant from healthy volunteers.	152

DECLARATION OF AUTHORSHIP

I, Dr Ahilanandan Dushianthan, declare that the thesis entitled

PHOSPHOLIPID KINETICS IN ACUTE RESPIRATORY DISTRESS SYNDROME

and the work presented in the thesis are both my own, and have been generated by me as the result of my own original research. I confirm that:

this work was done wholly or mainly while in candidature for a research degree at this University;

where any part of this thesis has previously been submitted for a degree or any other qualification at this University or any other institution, this has been clearly stated;

where I have consulted the published work of others, this is always clearly attributed;

where I have quoted from the work of others, the source is always given. With the exception of such quotations, this thesis is entirely my own work;

I have acknowledged all main sources of help;

where the thesis is based on work done by myself jointly with others, I have made clear exactly what was done by others and what I have contributed myself;

parts of this work have been published as:

- Phospholipid composition and kinetics in different endobronchial fractions from healthy volunteers. **Dushianthan A**, Goss V, Cusack R, Grocott MPW, Postle AD (2014). *BMC Pulmonary Medicine*; 14: 10.
- Surfactant phospholipid kinetics in patients with acute respiratory distress syndrome (ARDS). **Dushianthan A**, Cusack R, Pappachan J, Goss V, Postle AD, Grocott MPW (2013). *Journal of Intensive Care Society*; 14(1); S08-S09.

- Altered phosphatidylcholine synthetic pathways in acute respiratory distress syndrome (ARDS). **Dushianthan A**, Cusack R, Goss V, Postle AD, Grocott MPW (2013). *British Journal of Anaesthesia*; 110 (5); 860-885.
- Neutrophil phospholipid profiling in patients with Acute Respiratory Distress syndrome (ARDS). **Dushianthan A**, Cusack R, Goss V, Grocott M, Postle AD (2012). *Intensive Care Med*; 38(Suppl 1):S258.
- Phenotypic characterisation of patients with Acute Respiratory Distress syndrome (ARDS) according to surfactant synthetic function. **Dushianthan A**, Cusack R, Goss V, Pappachan J, Postle A, Grocott MPW (2012). *Intensive Care Med*; 38(Suppl 1): S258.
- Surfactant phospholipid kinetics in patients with Acute Respiratory Distress syndrome (ARDS). **Dushianthan A**, Cusack R, Goss V, Postle AD, Grocott MPW (2012). *Thorax*;67(Suppl 2); A11.
- Bronchoalveolar lavage, tracheal wash and induced sputum surfactant phospholipid kinetics from healthy volunteers. **Dushianthan A**, Cusack R, Goss V, Grocott MPW, Postle AD (2012). *Thorax*;67 (Suppl 2); A30.
- Exogenous surfactant therapy for acute lung injury/acute respiratory distress syndrome – where do we go from here? **Dushianthan A**, Cusack R, Goss V, Postle AD, Grocott MPW (2012). *Critical Care*;16(6):238.
- Exogenous surfactant therapy in acute lung injury/acute respiratory distress syndrome: the need for a revised paradigm approach. **Dushianthan A**, Cusack R, Grocott M, Postle AD (2012). *J Cardiothorac Vasc Anesth*;26(5):e50.
- Acute Respiratory distress Syndrome and Acute Lung Injury. **Dushianthan A**, Grocott MP, Postle AD, Cusack R (2011). *Postgrad Med J*;87(1031):612-22.

Signed.....

Date.....

ACKNOWLEDGEMENTS

I would like to express my sincere gratitude to Professor Mike Grocott and Professor Tony Postle for giving me the opportunity to undertake these research studies and for their continued support, supervision, guidance, patience and encouragement throughout this period. I would also like to thank Dr Victoria Goss and Dr Rebecca Cusack, for their advice and practical support in establishing clinical and laboratory methodologies, which were instrumental for the preparation of this thesis.

I would also like to thank Dr Grietof Koster, Paul Townsend and Dr Rosie Mackay for their invaluable help, staff of University Hospital Southampton General Intensive Care Unit particularly consultants, nurses and technicians, staff at NIHR Southampton Respiratory and Critical Care Biomedical Research Unit and NIHR Wellcome Trust Clinical Research Facility. My heartfelt thanks to all my volunteers, patients and their families, without them this could not have been possible. I also like to thank my closest friend Dr Khan, for his helpful comments and suggestions. The studies presented in this thesis are funded by NIHR Southampton Respiratory and Critical Care Biomedical Research Unit, and by a grant from National Institute of Academic Anaesthesia UK.

Most importantly: to my wife, daughter, mum, siblings, in-laws and friends. For your patience, unconditional love, support and understanding for the past three or more years. And finally, my dad, despite leaving an empty space, you are the inspiration for my life. Thank you.

LIST OF ABBREVIATIONS

ABCA	ATP-binding cassette sub-family A
ACE	Angiotension converting enzyme
AECC	American European Consensus Conference
ALI	Acute lung injury
ALIVE	Acute lung injury ventilator evaluation trial
ALTA	Albuterol for the treatment of ALI trial
ALVEOLI	Assessment of low tidal volume and elevated end-expiratory volume to obviate lung injury trial
APACHE	Acute physiology and chronic health evaluation
apoA	Apolipoprotein A
ARDS	Acute respiratory distress syndrome
ARMA	Tidal volume positive pressure ventilation for treatment of ALI and ARDS
AT-I	Alveolar type-I cells
AT-II	Alveolar type-II cells
ATP	Adenosine tri-phosphate
BADH	Betaine aldehyde dehydrogenase
BAL	Bronchoalveolar lavage
BALF	Bronchoalveolar lavage fluid
BALTI-2	β -2 agonist treatment on clinical outcomes in ARDS trial
BHMT	Betaine- homocysteine S- methyltransferase
BHT	Butylated hydroxytoulene
BSA	Bovine serum albumin
cAMP	Cyclic adenosine mono-phosphate
CDH	Choline dehydrogenase
CDP	Cytidine diphosphate
CETP	Cholesterylester transfer protein
CK	Choline kinase
CPT	Cholinephosphotransferase
CT	Choline phosphate cytidyltransferase
DAG	Diacylglycerol
DHA	Docosahexaenoic acid
DPPC	Dipalmitoyl phosphatidylcholine

EDEN-OMEGA	Early versus delayed enteral feeding and Omega-3 Fatty acid/antioxidant supplementation for treating people with ALI and ARDS trial
EDTA	Ethylenediaminetetra acetic acid
ELISA	Enzyme- linked immunosorbent assay
EPA	Eicosapentaenoic acid
ER	Endoplasmic reticulum
ERS	European Respiratory Society
ESI-MS/MS	Electrospray ionisation mass spectrometry
FACS	Fluorescence activated cell sorter
FACTT	Fluid and catheter treatment trial
FEV ₁	Forced expiratory volume at one second
FiO ₂	Fraction of inspired oxygen
FSR	Fractional synthetic rate
GA	Golgi apparatus
GC-IRMS	Gas chromatography combustion isotope ratio mass spectrometry
GM-CSF	Granulocyte colony stimulating factor
HDL	High density lipoproteins
HMD	Hyaline membrane disease
HMG-CoA	3-hydroxy-3-methylglutaryl-CoA
HPLC	High performance liquid chromatography
IBW	Ideal body weight
ICU	Intensive care unit
IL	Interleukin
IS	Induced sputum
KARMA	Ketoconazole and respiratory management in ALI and ARDS trial
LARMA	Lisophylline and respiratory management in ALI and ARDS trial
LaSRS	Late steroids rescue study
LCAT	Lecithin—cholesterol acyltransferase
LDL	Low density lipoproteins
LIS	Lung injury score
LLL	Left lower lobe
LML	Left middle lobe
LPC	Lysophosphatidylcholine

LPL	Lipoprotein lipase
LPS	Lipopolysaccharide
m/z	Mass-charge ratio
MD	Mean difference
MIDA	Multiple isotopomer distribution analysis
MRM	Multiple reaction monitoring
NADPH	Nicotinamide adenine dinucleotide phosphate-oxidase
NNNMG	N-nitroso-N-methylurethane
OSCAR	High Frequency oscillation in ARDS
PA	Phosphatidic acid
PaO ₂	Partial pressure of arterial oxygen
PBS	Phosphate buffered saline
PC	Phosphatidylcholine
PC-TP	Phospholipid transfer proteins
PE	Phosphatidylethanolamine
PEEP	Positive end expiratory pressure
PEFR	Peak expiratory flow rate
PEMT	Phosphatidylethanolamine- N- methyltransferase
PG	Phosphatidylglycerol
PL	Phospholipids
PS	Phosphatidylserine
PTSD	Post-traumatic stress disorder
PUFA	Polyunsaturated fatty acid
RBC	Red blood cells
RCT	Randomised controlled trial
RDS	Respiratory distress syndrome
RLL	Right lower lobe
RML	Right middle lobe
ROS	Reactive oxygen species
RPMI- 1640	Roswell Park Memorial Institute medium
SAM	S-adenosyl methionine
SatPC	Saturated phosphatidylcholine
SD	Standard deviation
SEM	Standard error of mean
SOD	Supraoxide dismutase
SP-A	Surfactant protein-A
SP-B	Surfactant protein-B

SP-C	Surfactant protein-C
SP-D	Surfactant protein-D
SPH	Sphingomyelin
sPLA ₂	Secretory phospholipase A ₂
TLC	Thin layer chromatography
TMB	3,3',5,5' Tetramethylbenzidine
TNF	Tumour necrosis factor
TW	Tracheal wash
VLDL	Very low density lipoprotein

CHAPTER 1

INTRODUCTION

1.1 Acute Respiratory Distress Syndrome

1.1.1 Definitions

Acute respiratory distress syndrome (ARDS) is a severe form of hypoxic respiratory failure in the critical care setting. Early documentation of lung injury was noted in World War II battlefields, where soldiers developed lung complications following trauma and this was termed “wet lung of trauma”. It was observed that these patients had the highest mortality, were difficult to resuscitate, and tolerated surgical procedures badly. The application of intermittent positive pressure oxygenation through a rudimentary device was seen to improve respiratory signs (Burford TH and Burbank B 1945) (Brewer LA and Burbank B 1946). Only in 1967, was the term “acute respiratory distress syndrome” coined by Ashbaugh and colleagues, describing 12 patients with refractory hypoxemia and bilateral pulmonary infiltrates with decreased static lung compliance. The pathological features from post mortem studies of these patients showed similarities to neonatal respiratory distress syndrome, with collapsed congested alveoli, and hyaline membrane formation (Ashbaugh DG et al. 1967).

The diagnostic definitions encapsulating these characteristic clinical features have evolved over the years, and in 1988, an expanded definition of ARDS was proposed with a quantitative physiological scoring classification. This criterion incorporated four essential components; chest radiographic abnormalities, the degree of hypoxemia, respiratory system compliance, and the amount of positive end expiratory pressure (PEEP) applied (Murray JF et al. 1988) (Table 1). Subsequent attempts at improving the classification led to the formation of the American European Consensus Conference (AECC) criteria which

refined the previous definitions and helped to unify a simple diagnostic pathway. According to these criteria, ARDS was defined as acute hypoxic illness with $\text{PaO}_2/\text{FiO}_2 < 200$ mmHg (26.7kPa), with bilateral chest radiographic infiltrates in the absence of raised pulmonary artery wedge pressure of more than 18mmHg or the absence of clinically raised left atrial pressure. When the $\text{PaO}_2/\text{FiO}_2$ was >200 mmHg and < 300 mmHg (40kPa), it was termed acute lung injury (ALI) (Table 2) (Bernard GR et al. 1994). This simple definition was adopted readily and subsequently used to identify patients in several ARDS randomised controlled clinical trials.

Further changes to this definition in 1998 were inclusions of additional information regarding aetiology, co-existing diseases and the number of non-pulmonary organ system failures, (GOCA; G-Gas exchange, O-organ failure, C- cause and A- associated diseases) that led to a more complex but informative scoring system (Artigas A et al. 1998). However, the earlier AECC classification proposed in 1994, remains the most widely accepted definition to date.

The AECC diagnostic definition is not without pitfalls. All four components of these criteria have been scrutinised since its proposal in 1994. First, although most use an arbitrary time frame of 72 hours as an “acute event”, this was not clearly defined as part of this definition. Secondly, there is a significant inter-observer variability in interpreting the chest radiographic features of ARDS, leading to poor reproducibility (Rubenfeld GD et al. 1999). Thirdly, in mechanically ventilated patients, the degree of hypoxemia in general is dependent on the amount of positive end expiratory pressure (PEEP) applied. The lack of inclusion of PEEP in this definition, exposes its vulnerability to subjective bias. Finally, ongoing controversy also exists in the use of pulmonary artery occlusion pressure as part of the diagnostic criteria. The use of pulmonary artery catheters is in decline due to the lack of clinical benefit with associated cardiovascular complications (Connors AF et al. 1996), (Wheeler AP et al. 2006).

Defining components		Lung injury Score
Chest Radiography (Alveolar consolidation)	No consolidation	Score 0
	1 quadrant	Score 1
	2 quadrant	Score 2
	3 quadrant	Score 3
	4 quadrant	Score 4
Hypoxemia	PaO ₂ /FiO ₂ ≥ 300	Score 0
	PaO ₂ /FiO ₂ 225-299	Score 1
	PaO ₂ /FiO ₂ 175-224	Score 2
	PaO ₂ /FiO ₂ 100-174	Score 3
	PaO ₂ /FiO ₂ < 100	Score 4
Compliance	≥80mL/cm H ₂ O	Score 0
	≥60-79mL/cm H ₂ O	Score 1
	≥40-59mL/cm H ₂ O	Score 2
	≥20-39mL/cm H ₂ O	Score 3
	≤19mL/cm H ₂ O	Score 4
Positive end expiratory pressure (PEEP)	≤ 5	Score 0
	6-8	Score 1
	9-11	Score 2
	12-14	Score 3
	≥ 15	Score 4

For total lung injury score divide the aggregate sum by the number of components that were used;

No Lung Injury	Score 0
Mild to moderate	Score 0.1-2.5
Severe lung injury	Score > 2.5

Table 1; Expanded definition of acute respiratory distress syndrome/ Murray's lung injury score (LIS). A scoring system based on four clinically defined components; chest radiographic changes, degree of hypoxemia and compliance and the amount of positive end expiratory pressure applied. A total score divided by the aggregate sum by the number of components defines the degree of severity (Murray JF et al. 1988).

Diagnosis	Timing	Oxygenation	Chest radiograph	Exclusion of Cardiogenic pulmonary oedema
ALI	Acute onset	$\text{PaO}_2/\text{FiO}_2 \leq 300\text{mmHg}$ (40kPa)	Bilateral infiltrates	$\leq 18\text{mmHg}$ when measured or no clinical evidence of left atrial hypertension
ARDS	Acute onset	$\text{PaO}_2/\text{FiO}_2 \leq 200\text{mmHg}$ (26.7kPa)	Bilateral infiltrates	$\leq 18\text{mmHg}$ when measured or no clinical evidence of left atrial hypertension

Table 2; American European Consensus Criteria for the diagnosis of acute respiratory distress syndrome and acute lung injury. There were three clinically defining components; degree of hypoxemia as defined by $\text{PaO}_2/\text{FiO}_2$ ratio, the presence of chest radiographic infiltrates in the absence of raised left atrial pressure. Acute lung injury is diagnosed, when there is a lesser degree of hypoxemia, as defined as $\text{PaO}_2/\text{FiO}_2$ ratio of between 300-200mmHg or 40kPa. $\text{PaO}_2/\text{FiO}_2$ ratio is the fraction of arterial oxygen over inspired oxygen (Bernhard GR et al. 1994).

Lack of therapeutic benefits from ARDS randomised clinical trials has been attributed to patient's heterogeneity, coupled with the limitations of the existing diagnostic definitions mentioned above. This stimulated further discussions and led to the proposal of "Berlin definition of ARDS". In this definition, ARDS was sub-categorised further according to the degree of hypoxemia as mild ($\text{PaO}_2/\text{FiO}_2$ of 200-300mmHg), moderate ($\text{PaO}_2/\text{FiO}_2$ of 100-200mmHg) and severe ($\text{PaO}_2/\text{FiO}_2 < 100\text{mmHg}$) (Table 3) (Ranieri VM et al. 2012). However, despite these attempts, ARDS remains a heterogeneous disease with variations in aetiology, response to treatment and natural progression.

Onset	Oxygenation $\text{PaO}_2/\text{FiO}_2$	Chest radiograph	Exclusion of Cardiac pulmonary oedema
< 7 days	<ul style="list-style-type: none"> • Mild (200-300mmHg) • Moderate (100-200mmHg) • Severe (<100mmHg) And PEEP $\geq 5\text{cmH}_2\text{O}$	Bilateral opacities	Respiratory failure not fully explained by cardiac failure or fluid overload

Table 3; Berlin definition of acute respiratory distress syndrome. There are four clinically defining components. In this definition ARDS is defined according to the severity of hypoxemia in the presence of bilateral opacities on chest radiograph in the absence of cardiac failure (Ranieri VM et al. 2012).

1.1.2 Clinical impact of ARDS

In the UK, there have been no prospective epidemiological studies of ARDS to date. The main reasons for this are; the dependency of the diagnosis on a multi-component syndromic definition, where the diagnostic criteria itself is limited by reliability and validity in identifying a homogeneous population. ARDS is also characterised by a longer duration of hospital stay and high mortality, which proves difficult to assess its exact prevalence. Attributable mortality is also difficult to measure as many patients die with ARDS rather than primarily of ARDS.

Despite these limitations, a number of epidemiological studies around the world suggest that the incidence of ARDS ranges between 13.5- 58 per 100,000 person-years (Table 4). In the UK estimates were lower, with an incidence of 4.5 per 100,000 person years (Webster NR et al. 1988). However, this was extrapolated from a survey conducted in 1988, and robust prospective epidemiological studies are lacking.

	<u>USA</u> (Rubenfeld GD et al 2005)	<u>Scandinavia</u> (Luhr OR et al 1999)	<u>Australia</u> (Bersten AD et al 2002)	<u>Europe</u> (Brun-Buisson C et al 2004)
<u>ALI</u>				
Incidence†	78.9	17.9	34.0	
Mortality (%)	38.5	41.4	32.0	49.4
<u>ARDS</u>				
Incidence†	58.7	13.5	22.0	
Mortality (%)	41.1	41.2	34.0	57.9

Table 4; Incidence and mortality of acute lung injury and acute respiratory distress syndrome across the world (†- cases per 100,000). ALI, acute lung injury; ARDS, acute respiratory distress syndrome.

Reported mortality rates also vary widely. A systematic review suggested that the mortality of ARDS among the published observational and randomised controlled trials was between 36-44%, without any significant decline in the last two decades (Phua J et al. 2009). A

recent multi-centre observational study conducted in Spain also suggested the mortality of ARDS may be as high as 50% (Villar J et al. 2011). Contrary to these findings, there has been a gradual decline in mortality among the ARDS Network clinical trials study population over the past two decades (Table 5).

Clinical Trial	Intervention	Study period	Mortality (%)	
			Controls	Intervention
KARMA (ARDS network 2000b)	Ketoconazole	1996-1998	34.1	35.2
ARMA (ARDS network 2000a)	Low tidal volume	1996-1999	39.8	31.0
LARMA (ARDS network 2002)	Lisofylline	1998-1999	24.1	31.9
La SRS (Steinberg KP et al. 2004)	Late corticosteroids	1997-2003	28.6	29.2
ALVEOLI (Brower RG et al. 2004)	Low PEEP	1999-2002	27.5	24.9
FACTT (Wiedemann HP et al 2006)	Fluid management	2000-2005	28.4	25.5
ALTA (Matthay MA et al. 2011)	Albuterol	2007-2008	17.7	23.1
OMEGA (Rice TW et al 2011)	Immunonutrition	2008-2009	16.3	26.6
EDEN (Rice TW et al 2011)	Trophic feeding	2006-2011	22.2	23.2

Table 5; Mortality data from Acute Respiratory Distress Syndrome Network randomised controlled trials published between 2000-2011. The mortality is expressed as percentage of total patients for author defined durations (30 days /60 days / hospital discharge). There is a trend towards declining mortality over this period.

Mortality data for the UK is limited. A single centre observational study conducted in the UK between years 1990-1997, suggested that the mortality of ARDS has declined over this period from 66% to 44% (Able SJ et al. 1998). However, a Scottish ARDS audit performed in 1999 reported mortality rates exceeding 50% (Hughes M et al. 2003). The acute lung injury verification of epidemiology (ALIVE) study, that recruited patients across Europe including the UK, showed hospital death rates of ALI and ARDS were 33% and 58% respectively (Brun-Brussion C et al. 2004). However, in the recent interventional

RCTs of intravenous salbutamol (BALTI-2) and high frequency oscillatory ventilation (OSCAR) for patients with ARDS, the overall mortality was 29% and 41% respectively (Gao SF et al. 2012) (Young D et al. 2013). These studies confirm the existence of significant variations in reported mortality with a promising overall downward trend, despite the lack of any established pharmacotherapies. The reasons for this mortality decline is not clear, this may be due to a combination of protective lung ventilation, with improved aggressive supportive measures such as institution of early antibiotics, ulcer and thrombosis prophylaxis with improved fluid, nutritional, and multi-organ support.

Survivors from ARDS are debilitated by significant physical and psychological morbidity. Limitations in physical ability and poor quality of life with depression, anxiety and post-traumatic stress disorder (PTSD) are frequently seen in these patients. Cognitive impairment with reduced memory, attention and task execution are also common (Herridge MS et al. 2003) (Hopkins RO et al. 2005). Despite having a normal or near normal lung function, patients had persistently reduced exercise capacity even after five years (Herridge MS et al. 2011). Such morbidity remains a significant economic and health burden among critically ill patients.

1.1.3 Pathophysiology

Infective or non-infective processes may lead to ARDS/ALI, where there is a significant acute inflammatory process causing alveolar epithelial and vascular endothelial injury. Early stages of ARDS are characterised by alveolar flooding with protein rich fluid due to increased vascular permeability. Injury to AT-I (alveolar type 1) epithelial cells contributes to the pulmonary oedema and the breakdown of this epithelial barrier exposes the underlying basement membrane, predisposing to pulmonary bacteraemia and sepsis.

It is postulated that Injury to AT-II (alveolar type 2) cells may impair surfactant synthesis and metabolism resulting in increased alveolar surface tension and alveolar collapse (Ware

LB et al. 2000). However, the exact underlying mechanisms for these alterations in surfactant synthesis and metabolism in in-vivo human models of acute lung injury are not fully explored. Histopathologically there is diffuse alveolar damage with infiltrations of neutrophils, macrophages and erythrocytes and alveolar haemorrhage with hyaline membrane formation (Bachofen M et al. 1977).

The acute phase is followed by a fibro-proliferative phase in some patients with various degrees of fibrosis, neovascularisation, and later resolution (Gattinoni L et al. 1994). However, these stages can often overlap. Figure 1, illustrates the complex pathophysiological processes leading to the development of ARDS. Surfactant abnormalities are a characteristic feature of ARDS and are detailed later.

Neutrophils are an essential part of human innate immune system, and their interaction and activation defines the host's immune response against microbial pathogens. There is a significant body of evidence suggesting their involvement in pathogenesis of ARDS/ALI (Grommes J et al. 2011). First, there is histological and radiological evidence of neutrophil accumulation into lungs during early stages of ARDS (Bachofen M et al. 1977). Second, there are also increased amount of neutrophils and their secretory materials in the bronchoalveolar lavage of patients with ARDS (McGuire WW et al. 1982). Although patients with neutropenia can develop ARDS, animal models with neutrophil depletion have shown a marked reduction in the degree of acute lung injury, implicating their contribution in ARDS (Abraham E et al. 2000).

Activated neutrophils release a vast array of harmful mediators, including cytokines, proteases, reactive oxygen species and matrix metalloproteinases, leading to endothelial and epithelial injury. Certain cytokines secreted by neutrophils such as interleukin-1 (IL-1), IL-6, IL-8, tumour necrosis factor (TNF) are pro-inflammatory, and also involved in the inflammatory cascade leading to lung injury (Lee WL et al. 2001).

Arachidonic acid from membrane phospholipids can become enzymatically oxidised to form active metabolites such as prostaglandins and leukotrienes, which are powerful inflammatory mediators potentiating lung injury (Bonnans C et al 2007). The contribution of specific neutrophil membrane phospholipid species during this phospholipase mediated generation of oxidised metabolites have not yet been characterised in patients with ALI/ARDS.

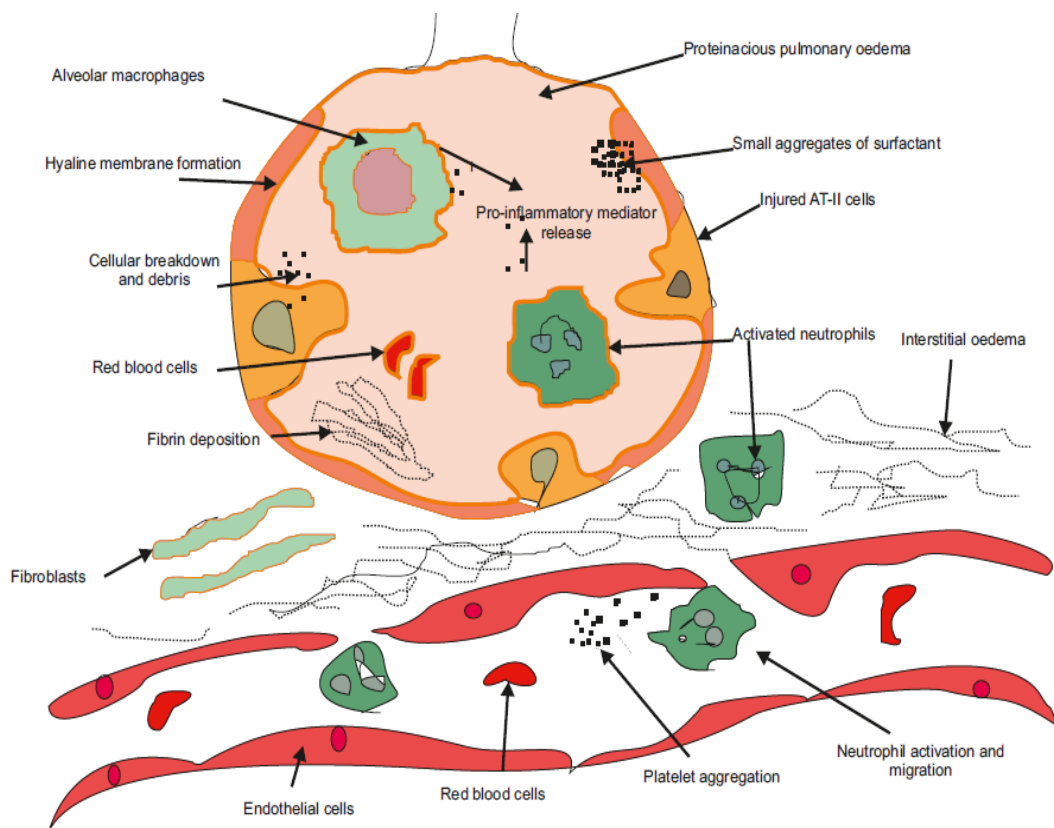


Figure 1; Pictorial view of injured alveolus with pulmonary oedema in ARDS. There is breakdown of alveolar endothelial and epithelial membranes with invasion of neutrophils and plasma constituents into alveolus. Injured alveolar type-II cells unable to secrete surfactant and there is increased surfactant breakdown leading to accumulation of small aggregates. Activated neutrophils and macrophages secrete potent pro-inflammatory cytokines. The influx of protein-rich oedema fluid into the alveolus, leads to the inactivation of surfactant. There is denuded alveolar membrane with hyaline membrane formation with interstitial oedema further hastening the impairment of gas-exchange. Following the acute phase, there is infiltration of fibroblasts and collagen deposition, which may lead to fibrosis. Platelet aggregation may lead to activation of pro-thrombotic factors and enhanced coagulation.

1.1.4 Aetiology and associations

The aetiological factors for the development of ARDS/ALI can be either direct, such as in the case of pneumonia or indirect. Sepsis is the commonest indirect insult (Rubenfeld GD et al. 2005) (Table 6). Chronic alcohol abuse (Moss M et al. 2003) and older age (Rubenfeld GD et al.2005) are reported to be independent risk factors for the developing ARDS and, surprisingly, diabetes mellitus is protective (Moss M et al. 2000). Additionally, there is emerging evidence supporting the hypothesis, that various genetic factors may influence the host's susceptibility and response to an insult such as sepsis. A number of genetic polymorphisms, at various levels (E.g. human angiotensin converting enzyme [ACE] gene, extracellular superoxide dismutase [SOD3], IL-10, mannose binding lectin [MBL], surfactant protein- B) are currently being studied as potential pathogenesis for the susceptibility and the effect on the evolution of disease process (Reddy AJ and Kleeberger SR 2009).

Direct lung injury	Indirect lung injury
<u>Common causes</u>	<u>Common causes</u>
Pneumonia	Sepsis
Aspiration of gastric contents	Severe trauma with multiple transfusions
<u>Less common causes</u>	<u>Less common causes</u>
Pulmonary contusion	Cardiopulmonary bypass
Fat emboli	Drug overdose
Near- drowning	Acute pancreatitis
Inhalational injury	Transfusion of blood products
Reperfusion pulmonary oedema	

Table 6; Clinical conditions associated with aetiology of acute respiratory distress syndrome. Several direct and indirect causes are implicated in the development of acute respiratory distress syndrome (Adopted from Ware LB et al. 2000 with permission).

1.1.5 Management of ARDS

The treatment of ARDS involves general supportive measures with lung protective ventilator strategies, and appropriate therapy for the underlying clinical condition such as infection. In the year 2000, ARDS network published a landmark study, which showed an absolute 9% reduction in mortality following a low tidal volume ventilation strategy (6ml/kg of ideal body weight (IBW)) than conventional ventilation (10ml/kg of IBW) (ARDS Network 2000a). Although several pharmacotherapies including exogenous surfactants, corticosteroids, ketoconazole and N-acetyl cysteine were investigated in patients with ARDS, so far they have shown no proven benefit in improving mortality (Adhikari NK et al. 2004) (Table 5). This highlights the importance of ongoing research in this area to improve clinical outcome.

In summary, ARDS imposes significant morbidity and mortality and remains a therapeutic challenge. Current diagnostic definitions fail to identify a homogenous population, and are limited by lack of specificity and information regarding possible underlying genophenotypes.

1.2 *Pulmonary surfactant system*

Recognition of the importance of alveolar surface tension forces in respiratory mechanics originated from the pioneering work by von Neergaard in 1929 (von Neergaard K 1929). Later in the 1950's, Pattle's and Clements's description of surface active material (Pattle RE 1955) (Clements JA 1957), followed by the appreciation of its role in respiratory distress syndrome {Hyaline membrane disease (HMD)} in neonates by Avery and Mead (Avery ME and Mead J 1959), provided the foundation for the explosion of subsequent research in this area. Over the last six decades, the understanding of the role of pulmonary surfactant in alveolar physiology and pathophysiology has developed substantially. Pulmonary surfactant in humans is now well described, and comprises of a complex mixture of lipids and proteins, which lines the alveolar airspaces. As the water molecules

have a tendency to attract each other, there are strong forces at the alveolar air-liquid interface, generating a surface tension for the spherical alveolar surface to collapse. Surfactant, with its amphipathic (contains both hydrophobic and hydrophilic) properties reduces this surface tension, keeping the alveolus patent for adequate gas exchange. The importance of pulmonary surfactant is classically illustrated in immature lungs from premature neonates, where there is an inadequate surfactant material, leading to significant respiratory compromise.

1.2.1 Surfactant composition

Pulmonary surfactant system is a unique mixture of lipids and proteins. The lipid component consists mainly of phospholipids which make up approximately 80-85% of the total composition, whereas neutral lipids such as cholesterol and surfactant proteins account for the rest. Among the phospholipid classes 80% are phosphatidylcholines (PC), and the remainder is made up by phosphatidylglycerol (PG), phosphatidylinositol (PI), phosphatidylserine (PS) and phosphatidylethanolamine (PE). Dipalmitoyl-PC (DPPC or PC 16:0/16:0) is the most abundant surface active PC molecule, accounting for 50-60% of total PC (Postle AD et al. 2001). The role of other PC species, which are enriched in pulmonary surfactant (PC16:0/14:0 and PC16:1/16:0) is not well established. The relative composition of phospholipid subclass and PC molecular composition varies between animal species, suggesting the possibility of functional variation. Four surfactant proteins have been identified called SP-A, SP-B, SP-C and SP-D. While SP-B and SP-C are hydrophobic, involved in enhancing the absorption of lipid to the surface of the alveoli, SP-A and SP-D are hydrophilic and they are involved in host's innate immune system (Haagsman HP et al. 2001).

1.2.2 Surfactant synthesis, turnover and metabolism

Surfactant lipids are synthesised in the endoplasmic reticulum (ER) of the AT-II cells, subsequently transported to cytoplasm and stored in lamellar body organelles prior to

secretion into alveolar hypophase (Figure 2). The Golgi apparatus within the cytoplasm is thought to be involved in surfactant processing and intracellular trafficking prior to subsequent storage. This has been demonstrated in animal models with radiolabelled $^3\text{[H]}$ choline and electron microscopy studies (Chevalier G et al. 1972). However, these findings were disputed recently in cultured AT-II cells, where the disruption of Golgi apparatus by brefeldin A resulted in no interference of PC incorporation but cessation of protein secretion (Osanai K et al. 2001) (Osanai K et al. 2006). This suggests pathways of phospholipid transfer, can be both dependant and independent of Golgi apparatus (Andreeva AV et al. 2007).

Several phospholipid transfer proteins (PC-TP) have been identified and are thought to be involved in the transfer of phospholipids from ER to lamellar body (Andreeva AV et al. 2007). Since studies of PC-TP $-/-$ knockout gene mice had preserved surfactant synthesis (van Helvoort A et al 1999), the exact functions of these proteins in alveolar phospholipid transfer still remains to be explored.

ABCA3 is a transport protein and part of ATP-binding cassette transporter family expressed in membranes of lamellar bodies. Mutations of ABCA3 gene are associated with varying degree of neonatal RDS and surfactant and lamellar body deficiency (Garmany TH et al. 2006). It is possible that ABCA3 plays a vital role in phospholipid import into LB and lamellar body maturation. Lamellar body maturation and subsequent transport lead to surfactant secretion into alveolar space by exocytosis. Surfactant secretion is a highly regulated process, where there is annexin-II mediated reorganisation of AT-II cell cytoskeleton (Singh TK et al. 2004), and fusion of membranes induced by calcium (Burgoyne RD et al. 2002), F-actin and annexin VII (Chander A et al. 2007).

Surfactant secretion can be stimulated by several factors. Mechanical stretch (Wirtz HR et al 1990) and labour are physiological mechanisms leading to increased surfactant secretion. Signalling messengers (protein kinases, Ca^{2+} , calmodulin dependant protein kinase, cAMP, ATP, diacylglycerol) and drugs such as β_2 agonists (terbutaline), platelet

activating factor, LPS, TNF- α , LDL and HDL can all stimulate surfactant secretion (Andreeva AV et al. 2007).

Surfactant is continuously renewed by a recycle process. AT-II cells are actively involved in the degradation of surfactant phospholipids. Active internalisation into AT-II cells is facilitated by surfactant protein A (Jain D et al. 2005). Once internalised surfactant phospholipids are destined for either recycling or degradation. Alveolar macrophages are also involved in the catabolism of surfactant lipids (Miles PR et al. 1988), but their exact role in the maintenance of alveolar phospholipid balance is not well established.

Granulocyte colony stimulating factor (GM-CSF) is important in the regulation of surfactant clearance. In transgenic mice, conditional deletion of GM-CSF gene results in pulmonary alveolar proteinosis, and highlights the importance of GM-CSF in the regulation of surfactant homeostasis (Trapnell BC et al. 2002).

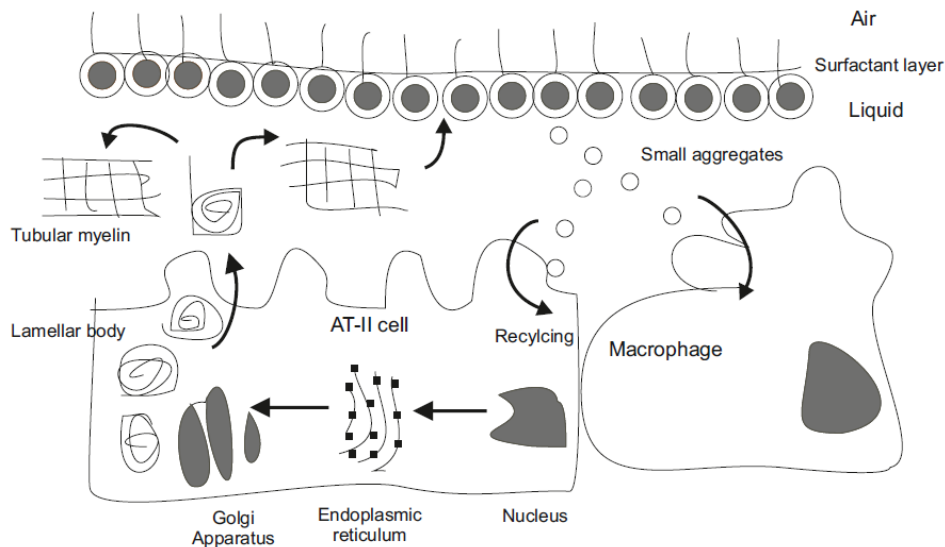


Figure 2: Basic schematic representation of pulmonary surfactant synthesis, secretion and recycling by alveolar type-II cells. Surfactant lipids are synthesised in the endoplasmic reticulum and subsequently processed by Golgi apparatus prior to storage in the lamellar body. Following secretion into alveolar hypophase lamellar bodies unravel to form tubular myelin and the surfactant monolayer. Subsequent breakdown involves formation of small aggregates, either destined for recycling in alveolar type-II cells or degradation and removal by the macrophages.

1.2.3 Endogenous surfactant alterations in ARDS

When Ashbaugh et al described the initial syndrome of ARDS in patients with respiratory failure they postulated defective surfactant may be a contributory factor (Ashbaugh DG et al. 1967). Subsequent post mortem studies by Petty and co-workers showed reduced compliance of lungs with increased alveolar fluid surface film compressibility in patients who died from ARDS (Petty TL et al. 1979). Since then a number of studies that have assessed functional and compositional changes in surfactant in patients with ARDS. Despite these studies having both variable patient characteristics and study methodology, surfactant compositional changes are consistently evident in patients with ARDS (Table 7).

1.2.3.1 Surface activity and surfactant aggregates

The surfactant extracted from patients with and at risk of developing ARDS, has abnormal physiological characteristics with reduced biophysical surface activity, resulting in increased minimum surface tension (Hallman M et al. 1982) (Gregory TJ et al. 1991). These changes were not specific to ARDS and also seen in patients with pneumonia but not those with cardiogenic pulmonary oedema (Gunther A et al. 1996).

Large surfactant aggregates (composed of lamellar bodies, tubular myelin and large multilamellar vesicles) are highly surface active (Veldhuizen RA et al. 1993). In in-vitro experimental models, during surfactant turnover prior to endocytosis, these large aggregates are converted to inactive small aggregates composed of unilamellar vesicles. The exact mechanism leading to this conversion is not fully understood. Reduction in large surfactant aggregates with a relative increase in small aggregates is characteristic of bronchoalveolar lavage fluid (BALF) surfactant from patients with ARDS (Schmidt R et al. 2007) (Gunther A et al. 1996). Reduced levels of large surfactant aggregates are also associated with low survival rates in ARDS (Schmidt R et al. 2007), but not in cystic fibrosis (Mander A et al. 2002).

1.2.3.2 Total Phospholipid concentrations

Determining absolute total phospholipid (PL) concentrations in the alveolar surfactant pool is difficult, and depends on several factors including lavage technique, amount of fluid used for lavage, surface areas lavaged and recovery (Haslam PL et al.1999). This reflects on the variability of the results published in clinical studies. While the initial study by Hallman and colleagues showed similar PL levels in ARDS and controls (Hallman M et al. 1982), subsequent investigators have shown reductions in PL concentrations, particularly in patients whom the precipitating cause was pneumonia (Gregory TJ et al. 1988) (Nakos G et al. 1998) (Gunther A et al. 1996).

1.2.3.3 Phospholipid and phosphatidylcholine composition

BALF phospholipid composition in ARDS is characterised by a relative decrease in the fractional concentrations of PC and PG with increases in PI, PE and PS. The assessment of phospholipid fractions has been limited by the analytical methods available to quantify PC composition, which have lacked precision in identifying molecular species. Two methodological limitations are particularly important. First, quantifying total disaturated PC as a surrogate for PC16:0/16:0 using osmium tetroxide (OsO₄) (Hallman M et al. 1982) (Mason RJ et al. 1976) has an inherent limitation because this technique also measures other disaturated PC molecular species. Second, assessment of relative content of individual fatty acids by chromatographic techniques does not reveal the specific molecular structure of individual phospholipid species (Schmidt R et al. 2001). However, when high performance liquid chromatography (HPLC) was used to analyse specific molecular PC species in a study of BALF from patients with ARDS, lower concentrations of PC16:0/16:0 and increases in unsaturated PC species were demonstrated (Schmidt R et al. 2007).

1.2.3.4 Surfactant proteins

There is an increased total protein concentration in BALF of patients with ARDS (Nakos G et al. 1998). This is coupled by reductions in surfactant associated proteins SP-A and

SP-B during early stages in patients at risk of ARDS and early lung injury, even before clinically apparent ARDS. SP-A and SP-B may remain low for up to 2 weeks (Gregory TJ et al. 1991) (Greene KE et al. 1999). However, SP-D concentrations were relatively unchanged during the disease process. Although all the surfactant related proteins are secreted by AT- II cells, this disparity in levels and variation in changes during the disease course may suggest specific impairment in regulatory mechanisms of surfactant proteins in ARDS (Greene KE et al. 1999). SP- C levels were also reduced in early stages of ARDS and may continue to remain low as long as up to 14 days after the onset (Schmidt R et al. 2007).

Surfactant characteristics	Abnormalities in ALI/ARDS
Surface activity	Increased surface tension
Phospholipid profile	Reduced levels of PC & PG with increase in PI, PE, PS and SPH
PC composition	Reduced levels of PC16:0/16:0 with increased levels of unsaturated species.
Surfactant aggregates	Reduced proportion of large aggregates to small aggregates
Surfactant Apo proteins	Decreased alveolar surfactant proteins and increased plasma surfactant proteins

Table 7; Summary table of bronchoalveolar lavage surfactant fractional compositional abnormalities in patients with acute respiratory distress syndrome. PC, phosphatidylcholine; PG, phosphatidylglycerol; PI, phosphatidylinositol; PE, phosphatidylethanolamine; PS, phosphatidylserine; SPH, sphingomyelin; DPPC, dipalmitoyl phosphatidylcholine.

1.2.4 Pathophysiology of dysfunctional surfactant

The pathogenesis of surfactant changes in ARDS is poorly understood. Although several animal lung injury models have been utilised, the relevance and applicability of these in human ARDS remains uncertain. Translation from animal and in-vitro models of surfactant dysfunction, suggests the possibility of several pathological mechanisms

causing surfactant compositional, and functional alterations during lung injury. These include; reduced synthesis by AT-II cells, surfactant functional inhibition by invading plasma constituents and increased breakdown from activated oxidative and hydrolytic pathways. It is likely that each of these mechanisms contributes to surfactant dysfunction to varying degrees, in individual patients.

1.2.4.1 Synthetic dysfunction

In ARDS, surfactant synthetic or secretory dysfunction may result from direct or indirect injury to AT-II cells. However, human studies investigating in-vivo models of surfactant metabolism during disease states are lacking. In an experimental animal model, hyperoxia induced direct lung injury resulted in decreased PC synthesis from isolated AT-II cells (Holm BA et al. 1988). In contrast, subcutaneous injection of nitrogenated urethane compound, which has an indirect toxic effects on AT- II cells, leads to an increased surfactant saturated PC synthesis and secretion (Lewis JF et al. 1990). These paradoxical findings indicate that surfactant PC synthesis may be influenced by the type of AT-II cell injury endured. However, animal experimental lung injury models so far proved to be of limited value in studying surfactant metabolism for translational approach in human ARDS.

Stable isotope labelling of surfactant precursors is a novel approach to study surfactant kinetics in humans (Postle AD et al. 2009). One in-vivo study using such method suggests there is an increased fractional surfactant PC synthesis in ARDS patients, compared to ventilated controls (Simonato M et al. 2011). In contrast, sequential quantitative BALF studies in ARDS patients, have shown consistently lower concentrations of PC and PC16:0/16:0 (Schmidt R et al. 2007). Surfactant SP-D is primarily secreted by AT-II cells and can be used as a surrogate biomarker for alveolar epithelial injury (Ware LB et al. 2010). Although BALF SP-D levels remain relatively unchanged during ARDS disease course, lower SP-D levels are evident in a subgroup of patients, and are associated with a

significant increase in mortality (Greene KE et al. 1999). These studies imply existence of patients with variable surfactant synthetic and secretory capacity with similar clinical pictures: in other words, phenotypic variation that can only be identified through in-vivo characterisation of surfactant metabolism.

1.2.4.2 Surfactant functional inhibition

During the early stages of ARDS, there is flooding of plasma material including plasma proteins into the alveolar space. These plasma constituents have surfactant functional inhibitory properties and in experimental models, plasma proteins in particular albumin (Fuchimukai T et al. 1987), haemoglobin (Holm BA et al. 1987), fibrinogen and fibrin monomers (Seeger W et al. 1993) were shown to impair surfactant function. The exact mechanisms of surfactant functional inhibition by plasma constituents are not known. However, competitive adsorption of plasma proteins and dysfunctional surfactant film formation are some of the postulated reasons (Holm BA et al. 1999) (Gunasekara L et al. 2008). In ARDS, there are also increased levels of neutral lipids such as cholesterol present in pulmonary surfactant (Markart P et al. 2007). Increased levels of these in endogenous surfactant also appear to impair surfactant function (Vockeroth D et al. 2010). It seems that surfactant preparations with hydrophobic apoproteins are less vulnerable to functional inhibition by plasma constituents (Seeger W et al. 1993).

1.2.4.3 Oxidation of surfactant phospholipids

Increased release of inflammatory mediators with generation of oxygen radical species, lipid mediators and enzymes such as phospholipases, and proteases are characteristic in ARDS. Reactive oxygen species (ROS) are generated as a part of metabolism of oxygen, and they are physiologically involved in cell signalling. These are highly reactive molecules and abnormal levels of ROS are associated with cellular damage, and can modify properties of molecules such as phospholipids. ROS such as H₂O₂, superoxide and nitric oxide are released by inflammatory cells and are generated by enzyme reactions (xanthine oxidase/glucose oxidase/ NADPH oxidase). Their involvement in disruption of

lipid and protein components leads to surfactant dysfunction, and it has long been postulated to contribute to lung injury (Lamb NJ et al. 1999). When exogenous natural surfactant is oxidised, its surface reduction capacity is greatly reduced (Rodriguez-Capote K et al. 2006). ROS can also contribute to cellular injury leading to reduced synthesis of surfactant by AT- II cells (Rice KL et al. 1992). SP-A and SP-D have potent antioxidant properties (Bridges JP et al. 2000) and the presence of un-oxidised SP-B and SP-C in exogenous surfactant environment seem to reduce surfactant dysfunction by oxidation (Rodriguez-Capote et al. 2006).

1.2.4.4 Hydrolysis of surfactant phospholipids

Hydrolysis of surfactant phospholipids by lipases also contribute to surfactant dysfunction. There are several types (~10) of secretory phospholipase-A₂ (sPLA₂) identified so far of which, sPLA₂-IIA, sPLA₂-V and sPLA₂-X are involved in hydrolysis of pulmonary surfactant (Chabot S et al. 2003). In BALF of ARDS patients, there is increased activity of (sPLA₂) which correlate with disease severity (Kim DK et al. 1995). Furthermore, tracheal instillation of PLA₂ in animal models leads to severe lung injury (Edelson JD et al. 1991). Secretory PLA₂ mediated hydrolysis of surfactant phospholipids generates lysophospholipids and free fatty acids, which are also inhibitors of surfactant function (Cockshutt AM et al. 1991) (Hite RD et al. 2005). Furthermore, free unesterified polyunsaturated fatty acids are precursors for several potential pro-inflammatory and pro-resolution mediators generated by enzymes cyclooxygenase (COX), lipoxygenase (LOX), and cytochrome P450 (CYP) (Haworth O and Levy BD 2007). In-vitro studies demonstrate that surfactant protein A is an inhibitor of sPLA₂-IIA and sPLA₂-X activity, and may abolish surfactant breakdown by hydrolysis (Arbibe L et al. 1998). Specific sPLA₂ inhibitors may provide additional therapeutic value in surfactant protection during exogenous surfactant replacement (Furue S et al. 2001).

In summary, the cause of surfactant dysfunction and compositional abnormalities in ARDS are complex, and multi-factorial. Studies are needed to better understand the underlying mechanism leading to these abnormalities in order to maximise the potential benefit from exogenous surfactant replacement.

1.2.5 Exogenous surfactant replacement in ARDS

Fujiwara et al reported the first positive, uncontrolled, clinical study of surfactant replacement in humans (Fujiwara T et al. 1980). In this study, 10 premature neonates with severe respiratory distress syndrome (RDS) were successfully treated with natural bovine surfactant supplemented with synthetic DPPC and PG. Subsequent randomised clinical trials (RCTs) with both natural and synthetic surfactant preparations have shown consistent improvements in lung mechanics, oxygenation and mortality in neonatal RDS (Halliday HL 2008).

Several RCTs of surfactant replacement in adults with ARDS have been conducted since 1994. These in general have shown improvements in oxygenation indices, but failed to produce any demonstrable survival benefits. This is confirmed by a recent systematic review and meta-analysis that included 9 RCTs with a total of 2575 patients. However, the validity of these results were limited by the substantial clinical heterogeneity of the studies included in this analysis (Meng H et al. 2012). Possible reasons for this failure of a theoretically promising therapy include the differences in the exogenous surfactant composition, drug delivery methods and the presence of variation in surfactant biology among the target population.

ARDS encompasses a variety of aetiologies, leading to an apparently common diffuse alveolar damage. Consequently, surfactant alterations are attributed to several pathological mechanisms, which have not been fully explored in humans. Specifically, patterns of surfactant synthesis and metabolism have not been characterised in ARDS. As mentioned earlier, current ARDS diagnostic definitions are uninformative with regards to the degree

of alveolar injury, the dynamic surfactant pool and surfactant metabolism. Phenotypic characterisation according to surfactant metabolism may help to selectively target those patients most likely to benefit from exogenous surfactant replacement.

1.3 *Phospholipid metabolism in humans*

Phospholipids are amphiphilic lipids with two fatty acyl hydrophobic chains esterified to either a glycerol backbone (glycerophospholipids) or sphingolipids and are linked to a hydrophilic phosphate based head group. If they are attached to a glycerol backbone, they are called glycerophospholipids and if sphingosine instead of glycerol, then they are termed sphingomyelin. Phospholipids have several essential functions and their constituents play crucial roles in structural formation of cell membranes, pulmonary surfactant, and intracellular signal transduction.

1.3.1 Glycerophospholipids

Phospholipids are commonly found as glycerophospholipids. They are the major components of all eukaryotic cell membrane and pulmonary surfactant. The class of a glycerophospholipid (i.e. phosphatidylcholine (PC), phosphatidylethanolamine (PE), phosphatidylinositol (PI), phosphatidylglycerol (PG) or phosphatidylserine (PS)) is defined by the type of head group esterified to the glycerol backbone. If the head group contains choline group, then they will be termed as PC. Other head groups are glycerol, ethanolamine, inositol and serine corresponding to the rest of the classes of glycerophospholipids (Figure 3).

The molecular species of glycerophospholipids can be classified according to the nature of esterified bond at the sn-1 (carbon-1) and sn-2 (carbon-2) positions of glycerol backbone, the of number carbon atoms in the fatty acid chains and the number of double bonds. The number of carbon atoms in the fatty acid chain determines the length of the chain and the number of double bonds in the side chain denotes their degree of saturation/unsaturation. For instance, dipalmitoyl PC is denoted as PC16:0/16:0, where

there are two saturated fatty acids chains with sixteen carbons length. The nature of the linkage at the sn-1 position between fatty acids and the glycerol backbone defines whether the molecular species are acyl, alkyl or alkenyl species. If there is an ester bond, they are acyl species and if there are either alkyl ether or vinyl ether bonds, they are termed alkyl and alkenyl (plasmalogen) species respectively.

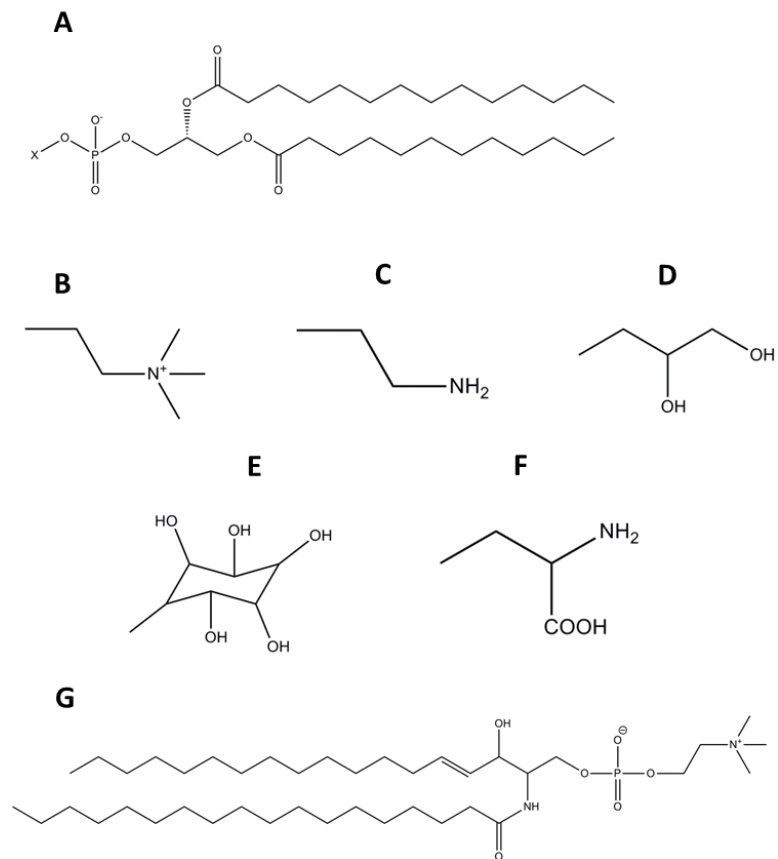


Figure 3; Structure of glycerophospholipids, the head group of sub-classes and sphingomyelin. X, head group specific for phospholipid subclass. **A**, phospholipid structure; **B**, phosphatidylcholine head group; **C**, phosphatidylethanolamine head group; **D**, phosphatidylglycerol head group; **E**, phosphatidylinositol head group; **F**, phosphatidylserine head group; **G**, sphingomyelin.

1.3.2 Synthetic pathways of glycerophospholipids

Glucose, glycogen and glycerol are essential precursors for the generation of phosphatidic acid (PA), a major intermediate in glycerophospholipid biosynthesis. Phosphorylation of

these leads to the formation of glycerol-3-phosphate. Subsequent additions of a series of fatty acyl-CoA result in the generation of phosphatidic acid via lyso-phosphatidic acid (1-acyl-*sn*-glycerol-3-phosphate) by the sequential actions of glycerol-3-phosphate acyltransferase and acylglycerol-3-acyltransferase. The formation of PA and the generation diacylglycerol (DAG) by hydrolysis from the actions of phosphatidic acid phosphatase is the precursor for the subsequent surfactant PC and PE biosynthesis. PA can also be converted to CDP-diacylglycerol by CDP-diacylglycerol synthase which utilizes the CTP (cytidine triphosphate). CDP-diacylglycerol is also used to synthesise PG and PI by phosphatidyl-glycerophosphatase and CDP-diacylglycerolinositol phosphatidyltransferase respectively (Figure 4). Further addition of acyl-CoA to DAG by diacylglycerol acyltransferase results in the formation of triacylglycerol which is a major source of energy in eukaryotic cells.

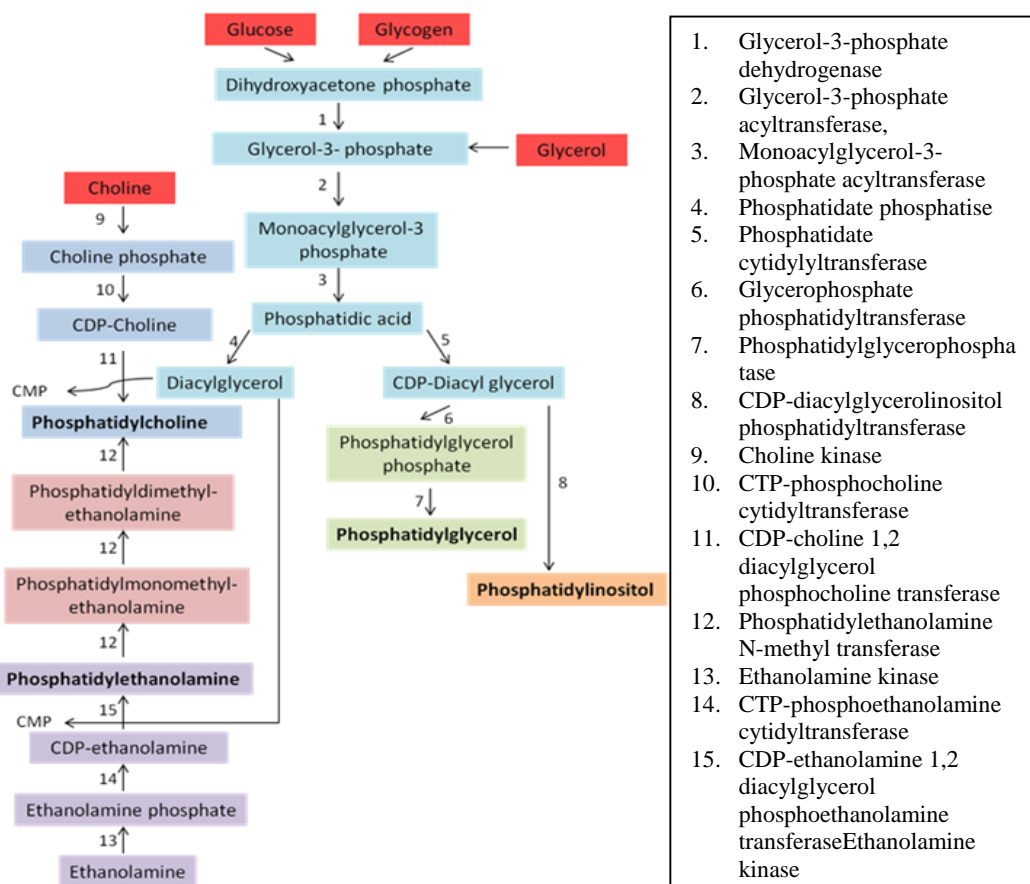


Figure 4; Synthetic pathways for major glycerophospholipids found in pulmonary surfactant. The numbers 1-15 represent catalytic enzymes.

1.3.3 Choline and phosphatidylcholine metabolism

Choline is an amino alcohol classified as an essential nutrient. Choline can be acquired from diet and via de-novo biosynthesis by methylation of PE to PC, catalysed by phosphatidylethanolamine N-methyltransferase (PEMT) by the action of phospholipases. This PEMT/phospholipase mediated de novo biosynthesis is the only known endogenous biosynthetic source for choline (Li Z and Vance DE 2008). Despite this capability of de novo biosynthesis of choline in animals, choline is classified as an essential nutrient as this pathway alone is inadequate to meet the daily requirements. Choline as part of PC is an essential component of pulmonary surfactant and mammalian cell membrane. Choline metabolites are also critically important for intracellular cell signalling and neuromodulation. The majority of endogenous choline is in the form of PC (95%) and about 5% is in the forms of free choline, choline phosphate and acetylcholine (Zeisel SH 2000).

Beef, pork, eggs and soybean are some of the common items enriched with choline (Zeisel SH et al. 2003). Recommended daily intake of choline is 425mg/day for women and 550mg/day for men. Choline deficiency is implicated in many disease processes such as fatty liver, atherosclerosis, memory impairment and metabolic syndrome. Genetic polymorphisms of genes encoding for enzymes (such as PEMT) involved in choline metabolism have been identified (Figure 4). If present, these polymorphisms may alter the daily requirement threshold for an individual (Ueland PM 2011).

Dietary choline is absorbed by the small intestine and transported into cells by choline transporters. In all eukaryotic cells, PC is primarily synthesised by CDP-choline pathway. Upon entry into the cell, choline is immediately phosphorylated by choline kinase (CK) to choline phosphate or oxidised to betaine by certain cells such as hepatocytes. In the second reaction, CDP-choline is produced from phosphocholine by the catalytic action of CTP: phosphocholine cytidyltransferase (CT) is the rate-limiting event of PC biosynthesis. The eventual synthesis of PC is catalysed by the action of CDP-

choline: 1,2-diacylglycerol cholinephosphotransferase (CPT), where the phosphocholine from CDP-choline is transferred to 1,2-diacylglycerol. Phosphocholine is converted to CDP-choline by the action of CTP: phosphocholine cytidylyltransferase and PC is an eventual result of the condensation of diacylglycerol and CDP-choline by cholinephosphotransferase (Li Z and Vance DE 2008) (Figure 4).

The enzymes responsible for CDP-choline pathway are not specific for the generation of large amount of PC16:0/16:0 in the lungs. However, the AT-II cells are enriched in palmitoyl-CoA, an enzyme responsible for acyl remodelling of PC16:0/16:0 (Post M et al. 1983). In isolated AT-II cells about 45% of surfactant PC16:0/16:0 is synthesised de-novo via CDP-choline pathway (den Breejen JN et al. 1989). The rest of the PC16:0/16:0 is synthesised by acyl remodelling mechanisms, where the PC molecule can be cleaved at sn-2 position by phospholipase-A₂, followed by re-esterification catalysed by lysoPC acyltransferase (Okuyama H et al. 1983).

1.3.4 Hepatic lipid metabolism

The liver is the major source of phospholipids in the body. PC can be also generated by sequential methylation of PE by PEMT which accounts for about 30% of PC synthesis in the liver. S-Adenosylmethionine (SAM) is an important methyl donor for this reaction (Li Z and Vance DE 2008). However, this is not the major PC pathway for the synthesis of pulmonary surfactant. Hepatic phospholipid metabolism is essential for the export of lipids to peripheral tissues including lung. The utilisation of PEMT mediated PC biosynthetic pathway by hepatocytes, produces an arrangement of specific molecular PC species that are enriched in polyunsaturated fatty-acids. Where PC synthesised from CDP-choline pathway by other cells including AT-II cells is dominated by saturated or mono-unsaturated PC species (Pynn CJ et al. 2011). The pathophysiological mechanisms for this molecular variation in synthetic patterns have not been investigated before.

Phospholipids synthesised by the liver are packaged and transported as lipoproteins into the systemic circulation. Hepatic PC synthesis is essential for adequate very low density lipoprotein (VLDL) secretion from the liver (Yao ZM and Vance DE 1988). Mice models with conditional deletions of PEMT and CT α (Cytidyltransferase) genes suggest both PC synthetic pathways are essential for the hepatic VLDL secretion (Jacobs RL et al. 2004) (Noga AA and Vance DE 2003). This has been extensively studied in animal models of hepatic steatosis (Cole LK et al. 2012). Alterations in PC synthesis also lead to a reduction in high density lipoproteins (HDL) levels and are thought to be due to down regulation of ABCA1 expression (in the case of CT α deficiency), and increased HDL uptake in the liver during PEMT deficiency (Jacobs RL et al. 2008).

Surfactant phospholipids are synthesised de-novo by AT-II cells. However, phospholipid synthesis requires substrates such as fatty acids which can also be produced de-novo or obtained from circulating plasma lipids (Batenburg JJ 1992). In neonatal animal models, surfactant synthesis can be stimulated by increased maternal supply of VLDL (Ryan AJ et al. 2002). Additionally, there is also evidence that AT-II cells are capable of VLDL uptake and catabolism mediated by lipoprotein lipase (LPL) for the generation of fatty acid substrates (Mallampalli RK et al. 1997). In neonatal rats, the fractional surfactant molecular composition can be also influenced by exogenous supply of myristate (Pynn CJ et al. 2010). Furthermore, incubated AT-II cells demonstrate variable surfactant PC molecular composition depending on their culture medium (Caesar PA et al. 1988). These studies imply, that surfactant metabolism may be manipulated by the availability of precursor substrates and deficiency of these substrates during disease states may have pathological consequence which has not been studied before. ARDS is a systemic disease with multi-organ involvement and hepatic dysfunction is a recognised feature. As liver is the primary source for circulating plasma lipids, alterations in hepatic phospholipid metabolism during disease states may have implications in the export and supply of lipids essential for the synthesis of pulmonary surfactant.

1.4 Dynamic surfactant phospholipid assessment

Surfactant phospholipid metabolism in humans particularly in disease states such as ARDS is not well characterised. Several investigators have used sequential BALF to study surfactant abnormalities in ARDS (Greene KE et al 1999, Schmidt R et al 2001). This method of surfactant isolation provides a snap-shot assessment of surfactant phospholipids and is limited by variability in recovery and lack of information regarding dynamic synthesis and metabolism. Radio isotope labelling of choline, free fatty acids and phosphate provided early surfactant profiling and dynamics in animal models and ex-vivo cell cultures, but are not applicable to study humans (Jacobs H et al. 1982). Such animal studies have demonstrated slower surfactant turnover in pre-term and term lungs compared to adult lungs (Jobe A 1980) (Jobe A 1988).

Stable isotope labelling of surfactant phospholipid precursors is a desirable method to study surfactant metabolism in humans. The use of ^{13}C -glucose and free fatty acids such as ^{13}C -palmitate (16:0) has been used successfully to investigate surfactant metabolism in neonates (Carnielli VP et al. 2009). These studies provided novel insights into in-vivo human models of surfactant metabolism. Inevitably, they had employed a complex sample processing and analytical methodology. Surfactant phospholipid was isolated from tracheal aspirates and disaturated PC (SatPC) was separated by thin layer chromatography (TLC) following oxidation with osmium tetroxide. SatPC was further derivatised to methyl esters and subsequent measurements were made by gas chromatography. From the measurements of enrichment, the fractional synthetic rate (FSR) of SatPC was expressed as percentage of total surfactant PC synthesised per day. A consistent pattern of much slower alveolar fractional PC turnover was demonstrated by these studies in neonates with RDS compared with term infants (Carnielli VP et al. 2009). A study conducted on adult population with ARDS using deuteriated water as a stable isotope and same methodology mentioned above, showed an increased surfactant fractional PC turnover in patients with ARDS. This finding suggests the possibility of a compensatory increase of surfactant

synthesis in ARDS (Simonato M et al. 2011). In this study tracheal epithelial lining fluid was used as a surrogate for alveolar surfactant pool. However, so far no studies have evaluated the surfactant phospholipid composition and kinetics of tracheal epithelial lining fluid in relation to alveolar surfactant pool in adults, particularly in disease states such as ARDS.

1.4.1 Electrospray ionisation tandem mass spectrometry (ESI-MS/MS)

Recent developments in the study of lipids (lipidomics) are closely mirrored by the advances in the utility of mass spectrometry (MS). Coupling soft ionisation methods such as electrospray ionisation (ESI) allows precise molecular analysis of intact phospholipid species in mammalian tissues. During electrospray interface, the biological samples dissolved in volatile organic solvents are infused through a charged capillary to form an aerosol of charged droplets. Dry nitrogen gas is then used to evaporate the solvent, leaving the ionised analyte to be transferred into the mass analyser.

The common platforms used by ESI-MS are direct infusion or coupled with liquid chromatography (LC). Adaptations with nanospray technique, (with a narrow-bore capillary) allows lower flow rate with high resolution, particularly useful for small volumes of samples. The interface of the ESI can be set at positive (following protonation $[M+H]^+$), negative (following deprotonation $[M-H]^-$) or a combination of both positive and negative ion modes.

High performance liquid chromatography (HPLC) is an analytical technique commonly used to separate different classes of lipids. This can be done in either normal phase or reversed phase. Class separation can be achieved with normal phase chromatography according to their polar head group, while reversed phase enables identification of individual molecular species in a particular class. Coupling HPLC-MS/MS methods has improved sensitivity of phospholipids analysis and quantification.

Once the ionisation phase is achieved, the gas phase ions are separated and analysed according to the mass charge ratio (m/z) in the mass analyser. There are several types of mass analysers available such as ion trap (IT), triple quadrupole (TQ), time of flight (TOF) and Fourier transform ion cyclotron resonance (FT-ICR). In this thesis, only triple quadrupole mass analyser was used to analyse all biological samples. In quadrupole analysers, there are 4 parallel metal rods with an oscillating electrical field, allowing selective filtration of lipid ions according to their m/z ratio. The first (Q1) and third (Q3) quadrupoles are mass analysers used for scanning or ion selection. The central quadrupole is a collision cell, where selected ions undergo fragmentation in the presence of a collision gas. This process is called collision induced dissociation (CID). The combination of two independent mass analysers with a dissociation process leading to multiple steps of ion selection and fragmentation forms the basis of tandem mass spectrometry (MS/MS).

ESI-MS/MS uses various analytical methods such as product ion scans, precursor ion scans, neutral loss scans and multiple reactions monitoring (MRM). Precursor ion scanning involves selection of a product ion and subsequent determination of precursor ions. This mode of analysis is often used to assess glycerophospholipids and the fragmentation identifies different head groups unique to that particular phospholipid class, according to their mass to charge ratio. For example, a precursor scan of m/z 184 identifies PC species that have common PC head group. Other diagnostic scans with m/z 153 (PG) and m/z 241 (PI) allows assessment of relative abundance of these molecular species.

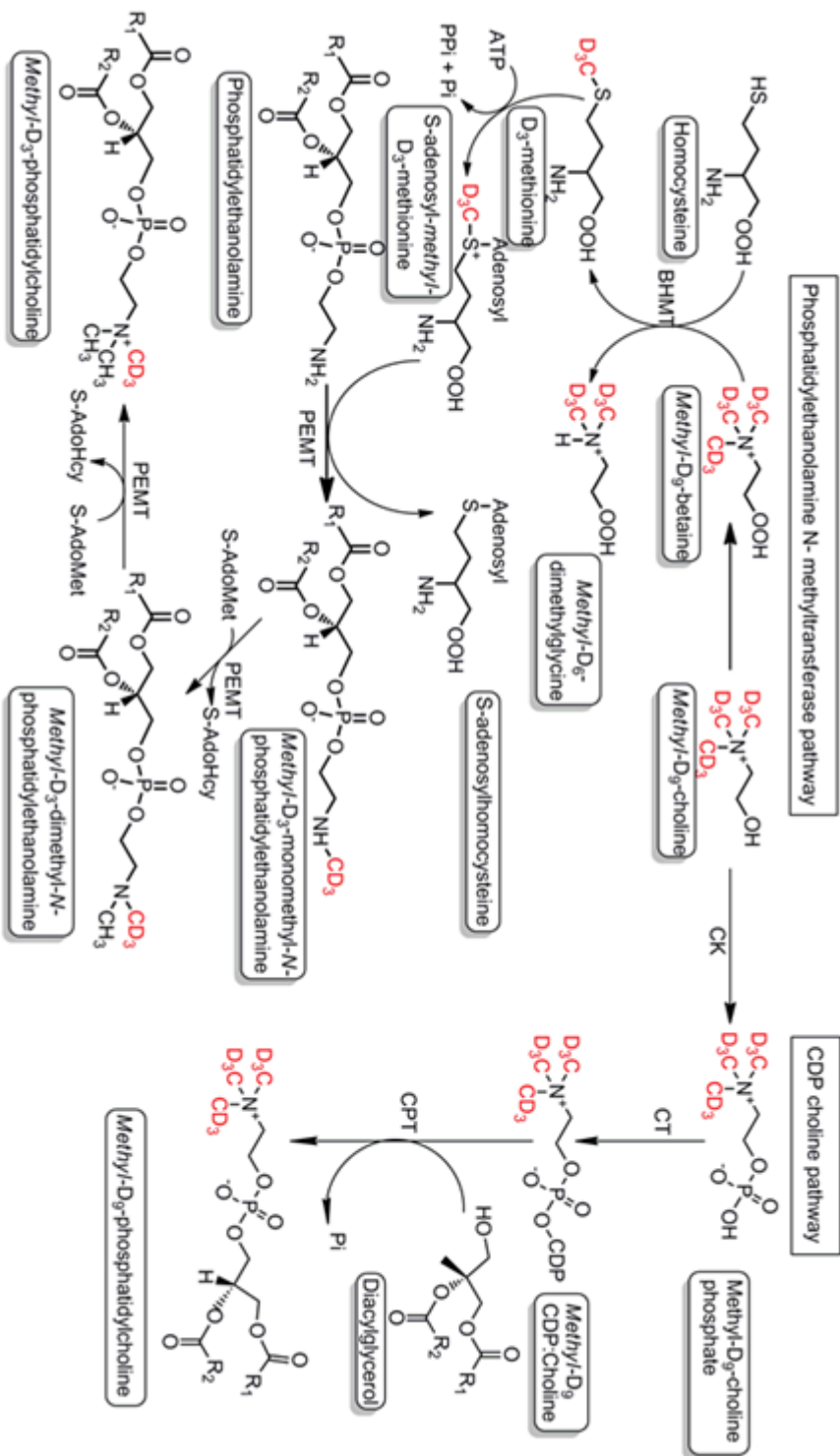
Another alternative approach is neutral loss scanning where there is selection of a neutral fragment offset by a defined mass. This mode of scanning was used to identify molecular composition of phosphatidylserine (NL87) and phosphatidylethanolamine (NL141). In multiple reaction monitoring (MRM) a precursor ion is preselected at Q1 and fragmented in the collision cell but instead of a full scan, only a specified fragmented ion is chosen in Q3. MRM acquisitions allows maximum sensitivity for the detection of targeted product

ions of interest and particularly useful when the lipid content is low. This can be used when analysing samples of known mass transition.

1.4.2 Stable isotope labelling with *methyl-D₉*-choline chloride

Using stable isotope labelling with deuteriated choline (*methyl-D₉*-choline chloride) in combination with analytical methods of electrospray-ionisation mass spectrometry (ESI-MS/MS), is a novel way to evaluate phospholipid metabolism (Postle AD and Hunt A 2009). The *methyl-D₉*-labelled PC with incorporation of nine additional deuterium atoms produces a fragment which is 9 mass units higher at m/z 193 than the unlabelled fraction. From sequential precursor scans of the m/z 184 and 193, it is possible to assess the composition of labelled and unlabelled PC species in biological samples. This highly specialised analytical method enables characterisation of essential PC metabolic pathways (CDP-choline and PEMT) with precise molecular assessment of *methyl-D₉* enrichment (Postle AD et al. 2011) (Bernhard W et al. 2004) (Pynn CJ et al. 2011). The incorporation pattern of *methyl-D₉* choline into both metabolic pathways for the synthesis of endogenous phosphatidylcholines is illustrated in Figure 5. This novel technique provided the foundation which formed the basis of this thesis and has enabled the application of such novel methodology in a selective human patient cohort for the first time.

Figure 5: Illustration of phosphatidylethanolamine-N-methyl transferase (PEMT) and cytidine diphosphate (CDP) choline pathways for the endogenous synthesis of phosphatidylcholine (PC) from methyl-D₉ choline.



1.5 Cell isolation by magnetic bead labelling

The neutrophil extraction techniques necessitate a sensitive method to obtain a selective cell population with high purity and functional viability. Traditional methods involved separation techniques utilising the variability of density between cell populations, where sedimentation of cells occurs into separate zones according to their density (Boyum A et al. 1991). The separation zones are produced with various materials such as percoll or polysaccharide (Boyum A 1968). The mechanical strain during separation may potentially lead to activation of cells and may even result in less viable cell population and impaired function (Glasser L and Fiederlein RL 1990). Subsequent immunological labelling of cells depending on their cell specific epitopes and isolation through fluorescence- activated cell sorter (FACS) yielded higher purity of cell populations. However, the latter method is laborious and time consuming.

Magnetic cell sorting also rely on the similar principle of immunological labelling, but with the use of magnetically labelled antibodies and separation through a magnetic cell separator. Magnetic cell separation is an evolving technique with more rapid process time and high purity cell yield. In addition there is less mechanical stress during separation compared to traditional centrifugation methods leading to better viability of extracted cells (Thiel A et al. 1998).

CD 15 (LeuM1, Lewis X, 3-fucosyl-N-acetyl-lactosamine) is a carbohydrate based epitope expressed on the surfaces of leukocytes and some cancer cell lines such as lymphoma cells. It is generated by fucosyltransferases (an enzyme catalyses the transfer of a fucose to acceptor molecules), which lead to covalent binding of these carbohydrate antigens to the surface of cells. CD15 is involved in leukocyte adhesion and the specificity towards this cell line makes it an ideal surface marker. CD15 is highly specific to neutrophils although expressed in eosinophils and malignant cell lines such as lymphoma (Kerr MA and Stocks SC 1992).

Plasma T-lymphocytes are involved in adoptive immune responses and can be identified according to their cell surface epitope CD3. This is a protein complex associated with T-cell receptor (TCR) and TCR: CD3 complex is essential for intracellular signaling. CD3+ subsets of lymphocytes form a readily available source of peripheral blood cells that can be extracted by magnetic labelling technique. In this thesis CD15+ neutrophils and CD3+ subsets of T- lymphocytes were isolated by specific epitope labelling and isolation by magnetic cell separation technique.

1.6 Thesis aim and objectives

ARDS is a heterogeneous disease with variations in pathogenesis, severity, response to clinical treatment and outcome. Lack of specificity coupled with failure to identify a homogenous population according to a defined pathological phenotype are some of the limitations of existing ARDS definitions. Although alterations in surfactant phospholipids and proteins are a recognised feature of ARDS, underlying mechanisms leading up to these changes are not known. The overall aim of this thesis is to conduct a detailed, *in-vivo*, dynamic molecular analysis of phospholipid metabolism in patients with ARDS. Such information may improve our understanding of ARDS pathogenesis. The specific objectives of this thesis are the following;

1. To assess the surfactant phospholipid composition and kinetics among patients with ARDS. To characterise surfactant PC molecular composition, dynamic *methyl-D₉*-PC incorporation, fractional synthesis of PC and PC16:0/16:0 of individual patients with ARDS. Exploring these mechanisms of surfactant disturbance and subsequent phenotypic characterisation of ARDS patients according to surfactant phospholipid metabolism may provide valuable insight into the pathogenesis of ARDS and could facilitate surfactant related clinical trials in the future.

2. ARDS is a systemic disease frequently leading to by multi-organ failure and death. Consequently, this thesis is also aimed to assess the global changes in phospholipid metabolism by characterising circulating plasma lipid profile, relative compositional alterations of plasma PC in ARDS and molecular specificity of PC biosynthesis from both CDP-choline and PEMT pathways.

3. Cellular phospholipid alterations in particular inflammatory cells can influence down-stream metabolic pathways of inflammation and resolution. Phospholipid profile and dynamic PC turnover of red blood cells, CD15+ neutrophils and CD3+ lymphocytes were assessed in ARDS patients. Furthermore isolated CD15+ neutrophils were incubated ex-vivo following supplementation of fatty acids to assess the molecular specificity of PC biosynthesis and expression of cell surface activation markers.

4. Dynamic surfactant phospholipid assessment requires isolation of surfactant material from alveolar compartment and typically involves bronchoalveolar lavage, which is an invasive procedure. Analysis of surfactant kinetics using less invasive isolation techniques may have potential clinical benefits. Consequently, this study was further aimed to assess molecular specificity of surfactant phospholipid synthesis extracted from small volume bronchoalveolar lavage fluid, tracheal wash and induced sputum, representing secretions from various endobronchial compartments in healthy adults.

CHAPTER 2

Methodology

2.1 *Materials*

Deuterated *methyl-D₉* choline chloride (99% enrichment) from CK GAS Products Ltd

EDTA blood tubes from BD Diagnostics

0.9% and 4.5% saline from B. Braun Medical Inc.

Butylated Hydroxy Toluene (BHT) from Sigma-Aldrich

Hanks Buffered Salt Solution (HBSS) from Invitrogen

All phospholipids internal standards from Avanti Polar Lipids

All solvents are HPLC gradient from Fisher Scientific

Fatty acids (oleic acid, linoleic acid, palmitic acid and arachidonic acid) from Sigma-Aldrich

Acquity UPLC BEH- HILIC column from Waters

CD15+, CD3+ magnetic beads and AutoMACS solvents from Miltenyi Biotech

Native Human SP-D in- house preparation from Southampton NIHR BRU

Nunc MaxiSorp ELISA plate for SP-D from Fisher Scientific

Streptavidin horse radish peroxidase 1:10,000 from Sigma-Aldrich

3,3',5,5' Tetramethylbenzidine (TMB) and H₂SO₄ from Sigma-Aldrich

Cholesterol, HDL, LDL analysis by Konelab 20 (ThermoFisher)

Triglycerides Reagent Kits from Microgenics ThermoFisher

Lipotrol from Microgenics Thermofisher

Antibodies (CD11b, CD11a, CD-62L, CD45 PerCP-Cy5) and reagents for flow cytometry from BD sciences

RPMI-1640 medium from Sigma-Aldrich

2.2 Ethics and Research and development approval

Two clinical studies formed the basis for this thesis. “**Pulmonary surfactant in adult patients with acute respiratory distress syndrome**” (Study 1) was conducted in the General Intensive Care Unit at University Hospital Southampton. The second study “**Comparison of bronchoalveolar lavage and induced sputum surfactant phospholipid kinetics in healthy adult volunteers**” (Study 2) was conducted in the Wellcome Trust Clinical Research facility at University Hospital Southampton. Both studies were approved by national ethics committees {(10/WNo01/52), (11/SC/0185)} and was sponsored by University Hospital Southampton NHS Foundation Trust {(RHMCR10244) and (RHMCR10254)} respectively.

2.3 Patient selection

Patients with ARDS were identified from the General Intensive Care Unit at University Hospital Southampton NHS Foundation Trust, according to the American European Consensus Conference diagnostic criteria (Bernard GR et al. 1994). This involved patients fulfilling all three components of the following definition.

1. Acute onset with a ratio of PaO_2 to the fraction inspired oxygen (FiO_2) ≤ 26.7 kPa
2. Bilateral pulmonary infiltrates
3. Pulmonary artery wedge pressure of ≤ 18 mmHg (if performed) or the absence of clinical evidence of raised left atrial pressure.

All eligible patients were enrolled after informed assent was obtained from patient’s next of kin. As all patients were sedated and on mechanical ventilation, the consent was only sought once their cognitive function returned to normal. Patients with the following were excluded;

- Failure to obtain informed consent from patient’s next of kin/ legal representative or patient’s negation to participate when they recover

- Extreme cardiovascular instability
- Intractable intra cranial hypertension
- Pulmonary haemorrhage or persistent pulmonary air leak
- Advanced malignancy
- Imminent death
- Pregnant women
- Immediate families of investigators or site personnel directly affiliated with the study Immediate family is defined as child or sibling, whether biological or legally adopted
- Participation in an investigational clinical trial

Volunteers who were non-smokers without any previous medical history or respiratory problems were recruited for the second study.

2.4 *Methyl-D₉-choline infusion and sample collection*

After informed assent ventilated, sedated patients with pre-existing arterial and venous cannula were given an intravenous infusion of sterile, pyrogen free *methyl-D₉-choline chloride* (3.6mg/kg) over a three-hour period (Bernhard W et al. 2004). Blood samples (2ml- EDTA tubes) were then collected from an indwelling arterial line at baseline and then at 6, 12, 24, 48, 72 and 96 hours after the start of *methyl-D₉-choline chloride* infusion. Urine samples were collected from catheter bags at 0,6,12,24,48,72 and 96 hours.

Bronchoalveolar lavage (BAL) in patients was performed via a fibre-optic bronchoscope (Olympus BF P60). All patients were intubated with an endotracheal tube (size 7-9) and mechanically ventilated. Prior to the bronchoscopy, patients were pre-oxygenated with 100% oxygen and this was continued throughout the procedure. Most patients needed additional sedation but none had paralysing agents. Bronchoscopy was not performed on patients with inspired oxygen (FiO₂) of >80% and was abandoned if there was a significant desaturation defined as pulse oximetry oxygen saturation of <85%.

Small volumes of bronchoalveolar lavage fluid (BALF) were collected by suctioning after instillation of 10-20 ml of warm sterile saline from a single lobar bronchus (either from middle or lower lobes). This was then rotated (in the order of right middle lobe, left middle lobe, right lower lobe and left lower lobe) for the subsequent lavages to minimise theoretical concerns that repeated lavage of the same lobe could be detrimental to surfactant concentration or function in that lobe. The BALF was performed at baseline before the administration of *methyl-D₉*-choline chloride infusion and at 6, 12, 24, 48, 72, 96 hours after the infusion. The reason for the frequent sampling recovery in the early stages was to ensure adequate analysis is performed at this stage, which could be utilised to target therapeutic interventions.

For the second study, once healthy volunteers were consented, they had an infusion of 3.6mg/kg *methyl-D₉*-choline chloride followed by sample collection of blood, induced sputum and urine at 0,8,24,48,72 and 96 hours. Small volume BALF and tracheal wash was performed at 24 and 48 hours. Sputum was induced by nebulised 4.5% hypertonic saline in accordance to ERS guidelines (Paggiaro PL et al. 2002). The induction was performed up to 20 minutes and stopped after sufficient material was obtained (~2mls). There was no individual events of bronchospams or significant drop (>10%) in peak expiratory flow (PEFR) during or after the process.

Tracheal wash (TW) and small volume BALF samples were obtained by a fibre-optic bronchoscope. This was done under local anaesthesia, without any pre-medication. Bronchoscope was passed through mouth with the application of topical lidocaine maximum of 4 ml of 2% above vocal cords and 8 ml of 1% below vocal cords. Ten ml of warmed saline (37°C) was applied at the distal end of right lower lobe lobar bronchus and was suctioned. A greater than 50% recovery was deemed to be adequate, but if there was <50% recovery, then a further 10mls of warmed saline was applied. The trachea was flushed with 10mls of warmed saline and recovered by suction. The subsequent BALF

sampling was performed from left lower lobe lobar bronchus next day. There was no significant decline in the FEV₁ noted after the bronchoscopy.

The mean total lignocaine used was 180(±40) mgs and 190(±30) mgs for the first and second bronchoscopy respectively. The lowest oxygen saturation documented was 87% with a mean pre and post oxygen saturation of 99% and 94% respectively. The mean recovery of TW (30%) was lower than that of BALF (42%). There were no significant changes in FEV₁ following bronchoscopy for both days.

2.5 Sample processing

Blood samples obtained from patients and volunteers were transferred in an ice box at 4°C. 10µl of Butylated Hydroxy Toluene (BHT) (20g/L) solution was added to all samples as an anti-oxidant. Then the samples are centrifuged at 400g for 15 minutes at 4°C. The plasma supernatant and the red blood cell isolates were stored in aliquots of 250µl in a freezer at -80°C.

Induced sputum, BALF and TW samples were transferred at 4°C to the processing lab. Then the samples were filtered through a 100µm nylon cell strainer and centrifuged at 100g for 20 seconds at 4°C. The resultant liquid material was further centrifuged at 400g for 10 minutes at 4°C. The supernatant was aliquoted in volumes of 500µl in eppendorfs and stored in a -80°C freezer.

If a cell pellet forms, this was re-suspended in Hanks buffered salt solution (HBSS) and centrifuged again at 400g for 10 minutes. The supernatant was discarded and the cells were re-suspended in 50µl of HBSS and stored in a -80°C freezer.

2.6 Phospholipid extraction

Total lipid extraction was performed from biological samples using Bligh and Dyer method (Bligh EG and Dyer WJ 1959). Volume of samples used for phospholipid extraction was dependent on the type of biological sample (Table 8). Isolated samples were

made up to a volume of 800µl and specified internal standards (IS) were added. The internal standard was a non- native, commercially available phospholipid, chosen appropriate for the mass range and phospholipid class analysed (Table 9). One ml of chloroform and 2ml of methanol was added to the samples, followed by further 1ml of chloroform and 1ml of distilled water. Separation was achieved by centrifuging at 400g at 20°C for 20 minutes. The lower lipid rich layer was then removed and dried under a nitrogen concentrator at 40°C. Once dried, a further 1ml of chloroform was added and dried again and stored in -20°C freezer.

Type of sample	Quantity
Bronchoalveolar lavage fluid	800µl
Tracheal wash	800µl
Induced sputum	800µl
Plasma	100µl
Red blood cells	100µl

Table 8; Quantity of biological samples used for phospholipid extraction.

Biological samples	Internal standards
Broncholaveolar lavage, tracheal wash and induced sputum	<ul style="list-style-type: none"> • DMPC- 1.0nmol • DMPG- 0.2nmol • LHPC- 0.1nmol
Plasma and Red blood cells	<ul style="list-style-type: none"> • DMPC- 10nmol • DMPG- 2.0nmol • LHPC- 1.0nmol • D₄-choline 100µmol
Neutrophils and lymphocytes	<ul style="list-style-type: none"> • DMPC- 1.0nmol

Table 9; Internal standards and quantities used for biological samples. DMPC; dimyristoylglycerophosphocholine, DMPG; dimyristoylglycerophosphoglycerol, LHPC; 1-heptadecanoylglycerophosphocholine

2.7 Extraction of choline metabolites

Choline and its metabolites were isolated from 100µl of plasma samples from the aqueous layer (top) during the lipid extraction process (detailed in 2.6). 100pmol of D₄-choline added as internal standard. Then the samples were freeze dried overnight and stored at -80°C for further analysis.

2.8 Analysis by ESI-MS/MS

The dried phospholipid fraction from biological samples was suspended in a mixture of 250µl of methanol-butanol-water-concentratedNH₄OH (6:2:1.6:0.4 v/v), and was injected at a rate of 5µl/min to be analysed by ESI-MS/MS (Waters, UK). Samples were injected by direct infusion, except for neutrophils, where nanoflow spray was used to enhance intensity and specificity.

The mass spectra was acquired in both positive (ES⁺) and negative (ES⁻) ionisation modes with m/z range of 2-3000. Typical MS/MS conditions were; capillary-2.80KV, cone- 30V, source temperature- 150°C, collision energy of 30eV and a scan time of 12 seconds for each ionisation modes. Collision induced dissociation (CID) produced diagnostic fragmentation, which enabled identification of PC (m/z184⁺), LPC (m/z184⁺), SPH (m/z184⁺), PG (m/z153⁻) and PI (m/z241⁻). Neutral loss scans were used to identify PE (m/z141⁺) and PS (m/z87⁻).

For specific diagnostic scans m/z ratio range was 400-900. *Methyl*-D₉ labelled PC and LPC was identified by precursor scan of m/z193⁺. The precursor scans of m/z187⁺ and m/z190⁺ enabled the characterisation of labelled *methyl*-D₃-PC and *methyl*-D₆-PC respectively. Table 10, illustrates the m/z assignments according to fragmentation of m/z184⁺ (unlabeled), m/z187⁺ (labelled via N-methylation) and m/z193⁺ (labelled via CDP-choline pathway).

PC molecular species	Unlabelled fragmentation transition (m/z)	Labelled fragmentation N-methylation (m/z)	Labelled fragmentation CDP-choline transition (m/z)
PC14:0/ 16:0 or PC30:0	706.6 → 184	709.6 → 187	715.6 → 193
PC16:0a/ 16:0 or PC32a:0	720.6 → 184	723.6 → 187	729.6 → 193
PC16:0/16:0 or PC32:0	734.6 → 184	737.6 → 187	743.6 → 193
PC16:0a/18:2 or PC34a:2	744.6 → 184	747.6 → 187	753.6 → 193
PC16:0a/18:1 or PC34a:1	746.6 → 184	749.6 → 187	755.6 → 193
PC16:0/ 18:2 or PC34:2	758.6 → 184	761.6 → 187	767.6 → 193
PC16:0/ 18:1 or PC34:1	760.6 → 184	763.6 → 187	769.6 → 193
PC16:0a/ 20:4 or PC36a:4	768.6 → 184	771.6 → 187	777.6 → 193
PC18:1a/ 18:2 or PC36a:3	770.6 → 184	773.6 → 187	779.6 → 193
PC18:0a/ 18:2 or PC36a:2	772.6 → 184	775.6 → 187	781.6 → 193
PC18:0a/ 18:1 or PC36a:1	774.6 → 184	777.6 → 187	783.6 → 193
PC14:0/ 22:6 or PC36:6	778.6 → 184	781.6 → 187	787.6 → 193
PC16:0/ 20:4 or PC36:4	782.6 → 184	785.6 → 187	791.6 → 193
PC18:1/ 18:2 or PC36:3	784.6 → 184	787.6 → 187	793.6 → 193
PC18:0/ 18:2 or PC36:2	786.6 → 184	789.6 → 187	795.6 → 193
PC18:0/ 18:1 or PC36:1	788.6 → 184	791.6 → 187	797.6 → 193
PC18:1a/22:4 or PC40a:5	794.6 → 184	797.6 → 187	803.6 → 193
PC18:0a/20:4 or PC38a:4	796.6 → 184	799.6 → 187	805.6 → 193
PC16:0/ 22:6 or PC38:6	806.6 → 184	809.6 → 187	815.6 → 193
PC18:1/ 20:4 or PC38:5	808.6 → 184	811.6 → 187	817.6 → 193
PC18:0/20:4 or PC38:4	810.6 → 184	813.6 → 187	819.6 → 193
PC20:4/20:4 or PC40:8	830.6 → 184	833.6 → 187	839.6 → 193
PC18:0/22:6 or PC40:6	834.6 → 184	837.6 → 187	843.6 → 193

Table 10; Mass charge ratio (m/z) assignments for most prominent components of PC determined by precursor scans of m/z184⁺, m/z187⁺ and m/z193⁺ for positive ionisation fragmentation.

2.9 LC-MS/MS for plasma choline and betaine

To assess choline, betaine and their corresponding deuterium labelled counterparts in plasma, a reverse phase LC method was utilised. The frozen samples were thawed at room temperature. Samples (100µl) were deproteinised with 100µl of acetonitrile and centrifuged at 300 rpm for 15 minutes at room temperature. The supernatant was aspirated and placed in an insert within a 2ml mass spectrometry vial in a sample tray. The samples were separated by an Acquity UPLC system (Waters, UK) with a BEH-Hilic column

(2.1mm×100mm×1.7µm) at 30°C. The mobile phase was produced by solvent A (ammonium formate 0.5M/L, pH 4.1 in water) and solution B (0.5% formic acid in acetonitrile). The column was eluted at a flow rate of 0.2ml/min with a gradient condition tabulated below (Table 11). Typical MRM chromatograms for choline, betaine and their deuterated counterparts are shown in Figure 6. Absolute concentrations of choline and betaine was not quantified due to the lack of reference standards. However, plasma choline concentrations were estimated based on the recovery of the internal standard (D₄-choline), whereas, plasma betaine enrichment was presented as relative abundance.

A				B	
Time (Min)	Solvent A (%)	Solvent B (%)	Flow rate (ml/min)	Metabolites	Precursor → Product ion (m/z)
Initial	1	99	0.2		
1	20	80	0.2	Choline	103.8 → 59.8
3.5	40	60	0.2		
4.0	70	30	0.2	D ₉ -choline	112.9 → 68.9
4.1	98	2	0.2		
6.6	10	90	0.2	Betaine	117.9 → 58.9
7.6	10	90	0.2		
8.6	1	99	0.2		
8.7	1	99	0.2	D ₉ -betaine	126.9 → 67.9
9.0	1	99	0.2		

Table 11; Ultra performance liquid chromatography (ULPC) gradient (**A**) and multiple reaction monitoring (MRM) transitions for plasma choline, betaine and their *methyl-D₉* labelled counterparts (**B**).

MS/MS was used for mass determination in positive ionisation MRM mode with following conditions: source temperature 150°C, capillary voltage of 3.8KV and cone voltage of 50V, the collision energy was 28eV, desolvation gas flow of 800L/h at 200°C, collision gas flow 0.15L/min, inter-scan delay 0.02s and dwell time 0.03s. MRM transitions for choline, *methyl-D₉*-choline, betaine and *methyl-D₉*-betaine are tabulated (Table 11). The molecular abundance was quantified using MassLynx software according to area under the peak for

that specific molecule. *Methyl-D*₄ choline enabled absolute quantification of choline and *methyl-D*₉ choline.

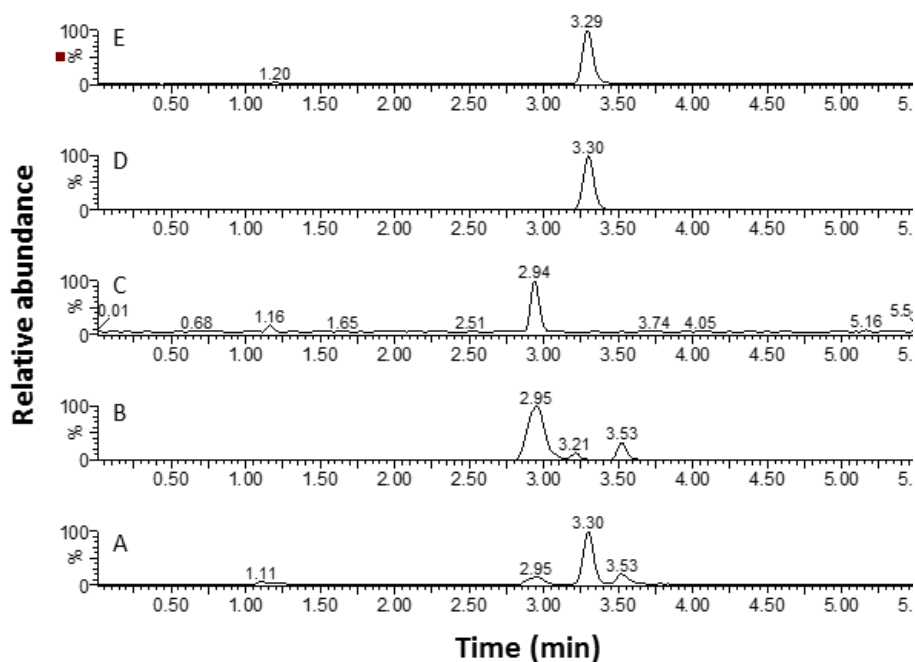


Figure 6: Multiple reaction monitoring chromatograms of 12 channels ES+ (A), choline 103.8→59.8 (B), *methyl-D*₉ choline 112.9→68.9 (C), betaine 117.9→ 58.9 (D) and *methyl-D*₉ betaine 126.9→67.9 (E) transitions.

2.10 ELISA for SP-D Assessment

The SP-D content was determined by enzyme- linked immunosorbent assay (ELISA). Native human SP-D (NhSP-D) used as a standard for ELISA was purified from BALF from patients with alveolar proteinosis by maltose affinity chromatography then further by gel filtration. The purity of all proteins was verified through SDS-PAGE and N-terminal sequencing (Strong P et al. 1998) (Suwabe A et al. 1996) conducted by surfactant protein analyst Dr MaKay from the Respiratory Biomedical Unit at University Hospital Southampton NHS foundation Trust. The plates (96-well Nunc MaxiSorb) were coated with capture antibody rfhSP-D 1ug/100ul per well in carbonate binding buffer and incubated at 4^oC overnight. Plates were washed three times (PBS/T 0.05% (v/v) Tween 20) and blocked for one hour (PBS/T with 2% BSA) at room temperature. After further wash, samples and standards were incubated for one hour at room temperature. After

washing again the plates were incubated with streptavidin horseradish peroxidase 1:10,000 for one hour at room temperature. The plates were developed with TMB, reaction was stopped with 0.5M H₂SO₄ and plates were read at 450nm.

2.11 Neutrophil and lymphocyte isolation

CD15⁺ neutrophils and CD3⁺ lymphocytes were extracted from whole blood with CD15⁺ and CD3⁺ microbeads using the autoMACS system. 1ml of venous blood sample was mixed with 50ul of either CD15⁺ or CD3⁺ microbeads and was incubated for 15 minutes at 4°C. The cells were then washed with 4ml of autoMACS running buffer (phosphate buffered saline pH 7.2 + 2mM EDTA+0.5% BSA+ 0.05% of v/v sodium azide) and centrifuged at 400g for 10 minutes at room temperature. The supernatant was discarded and the resulting cell pellet was re-suspended in 2mls of autoMACS running buffer. The samples were then passed through a high density magnetic cell separator and specific cells were eluted as positive fraction. The eluted positive fraction was centrifuged at 400g and 4°C for 10 minutes. Visible neutrophil or lymphocyte pellet was obtained by discarding the supernatant.

2.12 Flow cytometry of neutrophils

Isolated CD15⁺ and CD3⁺ cells were analysed further by flow cytometry for their purity. Following isolation and determination of cell number, cells were fluorescently stained with CD45-PE. Analysis was based on scatter signals and propidium iodide fluorescence. For functional analysis, whole blood neutrophils were used. Neutrophils were identified by light and size scattering using anti-CD45 PerCP-Cy5 labelled monoclonal antibodies. Cells were added with 5ul of anti-CD11b, anti-CD11a and anti-CD62L fluorescent antibodies and incubated for 15min in dark at room temperature. The expression of CD11b, CD11a and CD62L was assessed by flow cytometry (FACSCanto II from BD Biosciences).

2.13 Ex-vivo incubation of neutrophil with fatty acid supplementation

Extracted neutrophils from healthy volunteers were suspended in 0.5mg *methyl-D₉*-choline chloride in 1mL of RPMI 1640, supplemented with L-glutamine and 25mM Hepes. 30µM of oleic acid, linoleic acid, palmitic acid and arachidonic acid were added separately to each neutrophil suspension. This was incubated at 37°C for 3 hours. Once the incubation is complete, the suspension was centrifuged at 3000rpm at 4°C for 10 minutes. The resultant cellular pellet was stored at -80°C for further analysis.

2.14 Plasma Cholesterol and lipoprotein analysis

Plasma lipid profile (cholesterol, HDL-cholesterol, LDL-cholesterol and triacylglycerol) was quantified by automated Konelab 20 Autoanalyser at NIHR Southampton Biomedical Research Centre (Nutrition). Lipotrol (ThermoFisher) was used as quality control sample.

2.15 Data extraction

The MS/MS data was visually screened with Masslynx software (Version 4). The extraction and analysis of data was performed by two dedicated excel spread sheets (extractor/analyser) programmed by Dr Grielof Koster from Southampton Biomedical Research Unit. The ion peaks was quantified after correction for adducts formation (such as Sodiation) and for ¹³C isotopic effects. The phospholipid relative abundance was quantified from dedicated precursor and neutral loss fragmentations. The *methyl-D₉* labelled and unlabelled PC compositions were calculated from MS/MS fragmentations of precursor ion m/z184⁺ and m/z193⁺ respectively. The fractional incorporation of PC species was calculated from labelled fraction (m/z193⁺) corrected for relative total abundance [$\Sigma(m/z184^+ + m/z193^+)$].

2.16 Statistical analysis

The data was normally distributed as assessed by D'Agostino & Pearson omnibus normality test. It was summarised by means and standard deviations (SD) or standard errors of means (SEM). The difference in composition in each group was examined by

calculating the difference in means. Single comparisons were analysed by two-tailed student's t-test, unpaired or paired where applicable, and multiple comparisons by ANOVA of variance with Bonferroni's corrections. Correlation between continuous variables were assessed using the Pearson correlation coefficient. A probability value of $P < 0.05$ was considered to be statistical significance. All statistical analysis was performed by GraphPad Prism version 6.0 (Prism Software INC. California, USA).

CHAPTER 3

Surfactant phospholipid kinetics in Acute Respiratory Distress Syndrome

3.1 Introduction

Acute respiratory distress syndrome is characterised by significant alterations in surfactant biology. Quantitative and qualitative changes in fractional phospholipids with decreased contents of PC and PG are common findings (Dushianthan A et al. 2012). Concomitant reductions in the concentrations of PC16:0/16:0 is associated with increased minimum surface tension, leading to poor lung compliance and premature alveolar collapse during the early stages of ARDS (Gunther A et al. 1996). Despite significant advances in pulmonary surfactant research, there remains a lack of understanding in mechanistic reasons for the marked surfactant compositional changes that manifest in ARDS. However, observations from in-vitro experimental studies suggest, several potential underlying mechanisms such as impaired surfactant synthesis, increased breakdown by hydrolysis or oxidation of surfactant phospholipids and surfactant functional inhibition by invading plasma and cellular constituents may all contribute to these dysfunctional changes (Holm BA et al. 1999).

The disappointing results from surfactant replacement clinical trials in adults, reiterate the necessity for in-vivo human studies, to explore the exact underlying mechanisms leading to the disordered surfactant metabolism evident in ARDS. Such studies may enable biochemical phenotyping of patients according to their intrinsic surfactant synthetic function and turnover. Identification of such patients primarily with AT-II cell synthetic dysfunction may facilitate an individualised exogenous surfactant replacement strategy. The heterogeneous nature of the existing ARDS diagnostic definitions, coupled with the

lack of specific information regarding surfactant biology prior to replacement strategy, may have contributed to the negative clinical outcomes in previous surfactant replacement randomised controlled trials.

Traditional assessments of pulmonary surfactant consisted of isolation with sequential BALF and subsequent separation of surfactant phospholipids by liquid chromatography (Hallman M et al. 1982) (Gunther A et al. 1996). Such studies provided significant insights into surfactant compositional abnormalities in patients with ARDS. However, quantitative phospholipid assessments were unpredictable due to the variability of surfactant recovery by BALF. Furthermore, such approaches lack specific information regarding the dynamics of surfactant synthesis and turnover. Stable isotope labelling, coupled with ESI-MS/MS provides a novel approach to the dynamic assessment of surfactant metabolism in addition to highly specific molecular analysis of surfactant phospholipids. Consequently this methodology was utilised to characterise surfactant phospholipid kinetics in patients with ARDS.

3.2 Objectives

1. To assess surfactant PC molecular composition in patients with ARDS
2. To explore the variations in dynamic *methyl-D₉* choline incorporation into surfactant PC
3. To correlate any clinical variables with surfactant PC metabolism

3.3 Summary of methods

Once patients were identified, they were infused with *methyl-D₉* choline chloride and small volume BALF samples were taken at 0,6,12,24,48,96 hours. Healthy adult volunteers were infused with *methyl-D₉*-choline and BALF were performed at 24 and 48 hours. Samples were filtered by 100µm cell strainer to remove mucus and centrifuged at 400×g×10 minutes to remove cellular material. Phospholipid extraction was performed according to Bligh and Dyer method and PC 14:0/14:0 (dimyristoyl PC) was added as internal standard.

The samples were directly infused for the analysis by ESI-MS/MS. The labelled and unlabelled PC species were identified according to phosphocholine head group fragments of m/z184 and m/z193 scans respectively. The resultant peaks for each molecular species were quantified in dedicated excel spread sheets according to the relative intensity corrected for the recovery of the internal standard. The results were expressed in means and standard error of the mean (SEM), unless stated otherwise. (For detailed methods see Chapter 2).

3.4 Results

3.4.1 Patient characteristics

Ten patients with severe ARDS were recruited. This included 5 males and 5 females with a mean age of 61 and a range of 38-90. The mean PaO₂/FiO₂ ratio was 15.1 (\pm 1.4) suggesting severe hypoxic respiratory failure. The mean lung injury score was 3.2 (\pm 0.1). The APACHE II score, which defines the overall severity of their illness was 23.2 (\pm 1.3), predicting the mortality as high as 40-50%. All patients were intubated for respiratory failure and were managed with invasive ventilation. The duration of mechanical ventilation was 8.9 (SD \pm 4.9) days. The mean length of ICU and hospital stay was 12.4 (SD \pm 9.3) and 18.6 (SD \pm 13.8) respectively. Five patients died in ICU (50%), and one patient died in hospital after ICU discharge (Table 12).

The majority of patients (90%) presented with pneumonia, and most (80%) needed at least one other organ support in addition to invasive mechanical ventilation. One patient did not survive beyond 24 hours of enrolment, and hence only had biological samples up to 12 hours after *methyl-D₉*-choline infusion. While all patients had BALF at least until 48 hours, some did not have their BALF performed at later time points (72 and 96 hours) due to either planned extubation or death. All patients were enrolled within 72 hours of diagnosis of ARDS, and the actual mean enrolment time was <48 hours. The summary of patient's characteristics is listed in Table 12.

Patient's Characteristics	
Age	61 (38-90)
M:F	5:5
PaO ₂ /FiO ₂ ratio (mmHg)	113.4 (63.5-169.3)
Lung Injury Score	3.2 (2.5-3.5)
APACHE II Score	23.2 (17-30)
Tidal volumes (ml/kg IBW)	6.7 ± 1.3 [†]
PEEP (cm of H ₂ O)	10.8 ± 3.1 [†]
Ventilation days	8.9 (3-19)
Length of ICU stay	12.4 (3-35)
Length of hospital stay	18.6 (9-53)
ICU survival	50%

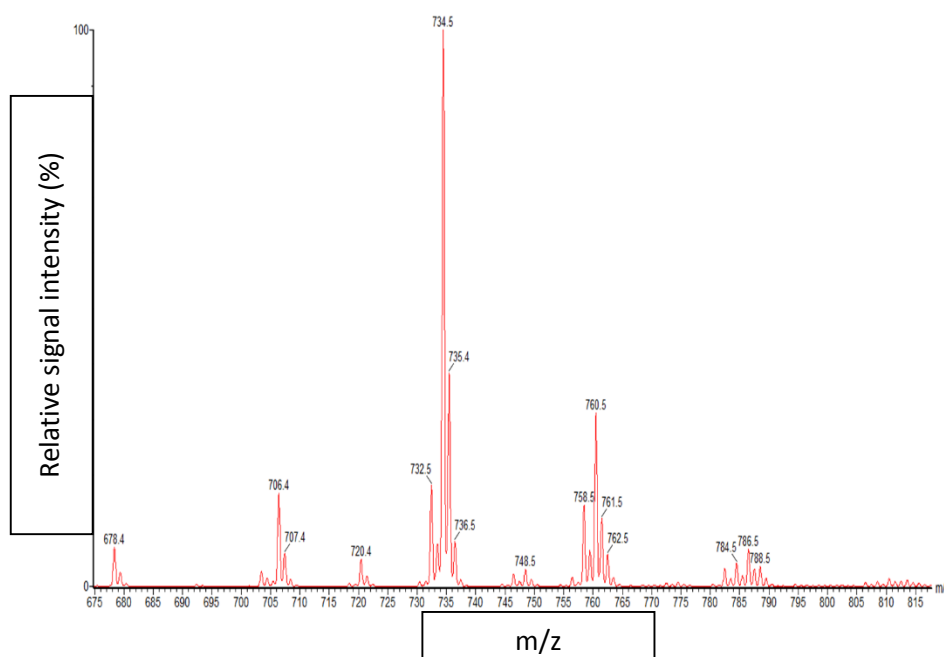
Table 12; Baseline characteristics and outcomes of recruited ARDS patients. M, male; F, female; PaO₂/FiO₂ ratio, ratio of partial pressure of arterial oxygen and fraction of inspired oxygen; APACHE, acute physiology and chronic health evaluation; IBW, ideal body weight; PEEP, positive end expiratory pressure; ICU, intensive care unit. Data expressed as mean ± standard deviation[†] or mean (range).

BALF was tolerated by all without any significant immediate complications. There were no pneumothoraces. On average patients needed additional sedation with boluses of propofol (40±3mgs) or midazolam (2±0.3mgs) for the procedure. There were no significant step-up in oxygen requirement (FiO₂) post procedure (pre 54±10%, post 55±9%). The average oxygen saturation pre- procedure was 94±2% and post procedure was 91±3%. There were no cardiac arrhythmias noted during the procedure.

Nine healthy volunteers were recruited as controls (5 males and 4 females) with a mean age of 25.7 (range 18-36) and small volume BALF was obtained at 24 and 48 hours after *methyl-D₉*-choline infusion.

3.4.2 Mass spectrometry analysis of BALF PC

The PC molecular composition was identified by precursor scans of m/z 184 on ESI-MS/MS. The typical mass spectra for BALF PC composition is shown below with PC species for that particular mass charge ratio (Figure 7). In general, the most abundant PC species were PC16:0/16:0, PC16:0/18:1, PC16:0/14:0 and PC16:0/16:1. This distinctive PC composition mainly consisted of saturated PC species. In contrast, plasma and cellular PC compositions consisted mainly of unsaturated PC species and this is detailed later in chapter four and five.



(m/z)	PC Species	(m/z)	PC species
678	Internal STD	760	PC16:0/18:1
706	PC16:0/14:0	782	PC16:0/20:4
720	PC16:0a/16:0	784	PC18:1/18:2
732	PC16:0/16:1	786	PC18:0/18:2
734	PC16:0/16:0	788	PC18:0/18:1
758	PC16:0/18:2	810	PC18:0/20:4

Figure 7; Example of a typical mass spectrum for pulmonary surfactant phosphatidylcholine composition from a healthy control. The range for m/z was 675-815. The peak at m/z 678 was PC14:0/14:0 (internal standard). The molecular m/z for each corresponding phosphatidylcholine is listed on subsequent table. m/z , mass to charge ratio.

3.4.3 Total Surfactant PC and fractional PC16:0/16:0 concentration

Total surfactant PC concentration was estimated by the sum of total major PC species and corrected for the internal standard (PC14:0/14:0). There was a significant reduction ($P<0.0001$) in the total BALF PC isolated in patients, compared to healthy controls (Figure 8). At enrolment ($T=0$) the mean total PC concentration in patient group was $13(\pm 4)$ nmol/ml and accounted for only 30% of the controls. A further reduction in PC concentration was noted at 12 hours after enrolment. Additionally, in patients, there was no significant recovery in total PC concentration over the investigative period up to 96 hours (Figure 8). Moreover, at enrolment ($T=0$), there were no significant positive correlation between BALF total PC concentrations and PaO_2/FiO_2 ratio of patients (Figure 9A).

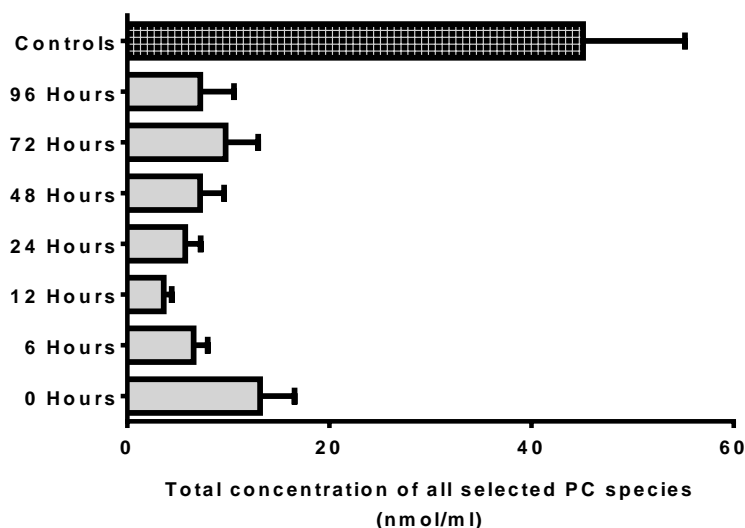


Figure 8; Total surfactant phosphatidylcholine concentration (nmol/ml) isolated from bronchoalveolar lavage over time in patients ($N=10$) compared to healthy adult controls ($N=9$) at first time point ($T=24$ Hrs). This is estimated from sum of all selected phosphatidylcholine species. Data expressed as mean \pm SEM. PC, phosphatidylcholine.

PC16:0/16:0 concentrations were also much lower in patients at enrolment (2.6 ± 0.3 nmol/ml), and only accounted for about 10% of the healthy control values. There were significant variations in the PC16:0/16:0 concentrations among both patients and controls [(patients range; 0.76-7.52nmol/ml), controls range; 8.8-74.1nmol/ml)]. This is

likely to be due to the variability in BALF surfactant recovery. The PC16:0/16:0 concentrations at enrolment and overall mean fractional concentrations of PC16:0/16:0 did not show any positive correlation with neither PaO₂/FiO₂ ratio nor the overall survival (Figure 9B and 9D). Although patients who died had lower overall mean concentrations of PC16:0/16:0 (1.4±0.4nmol/ml) than survivors (2.7±0.9nmol/ml), over the investigative period, the significant variation among survivors resulted in no overall statistical difference between the groups analysed. There was also no significant difference in PC16:0/16:0 concentrations at T=0 between survivors and non-survivors (Figure 9C).

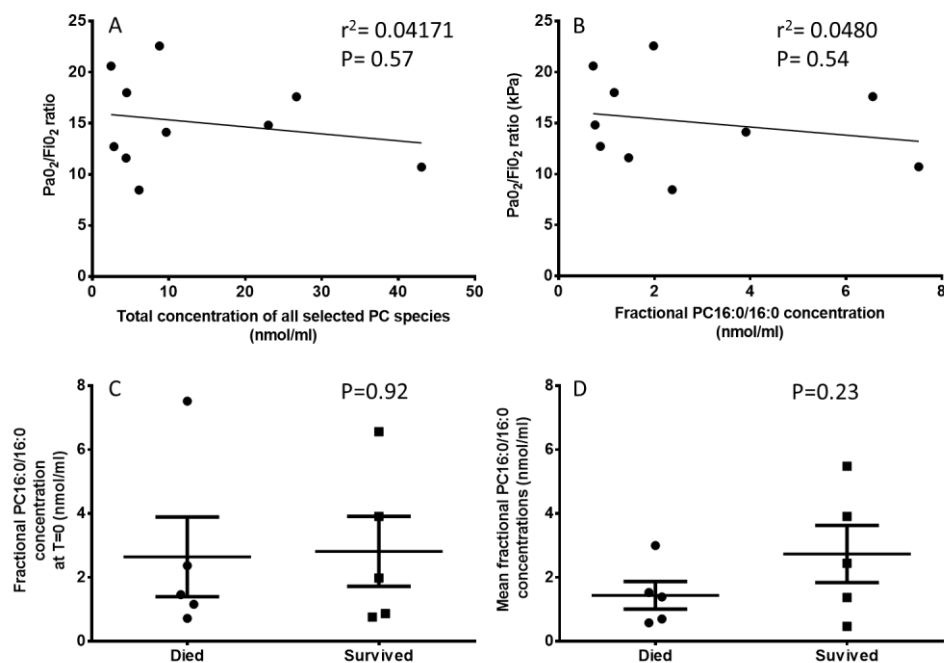


Figure 9; Clinical correlations of total phosphatidylcholine and fractional PC16:0/16:0 concentrations with oxygenation at enrolment and death. PC, phosphatidylcholine; PaO₂/FiO₂, the ratio of arterial oxygen to fraction of inspired oxygen. **A;** total surfactant PC concentrations and PaO₂/FiO₂ ratio at enrolment, **B;** PC16:0/16:0 concentration and PaO₂/FiO₂ ratio at enrolment, **C;** Overall mean PC16:0/16:0 fractional concentrations throughout study period with survival, **D;** PC16:0/16:0 fractional concentrations at enrolment with survival. Comparison A and B by Pearson correlation coefficient and were not statistically significant. Comparison C and D by student t- test and were not statistically significant.

3.4.4 Surfactant PC molecular composition at enrolment (T=0)

At enrolment (T=0), the surfactant PC composition of patients consisted of PC16:0/16:0 (27.4±2.8%), PC16:0/18:1 (23.2±1.2%), PC16:0/18:2 (10.6±1.6%) and PC18:0/18:2 (9.7±1.0%), with other PC species were in much lower abundance. Compared to the controls, surfactant recovered from ARDS patients had significantly lower proportions of surfactant specific PC species, PC16:0/16:0 (MD of 29% reduction, P<0.0001) and PC16:0/14:0 (MD of 4% reduction, P=0.02). There was no significant difference in relative composition of PC16:0/16:1 between groups. Additionally there were higher compositions of PC16:0/18:1 (MD 11% higher, P<0.0001), PC16:0/18:2 (MD 5.2% higher, P=0.0013) and PC18:0/18:2 (MD of 7.4% higher, P<0.0001) in patients (Figure 10).

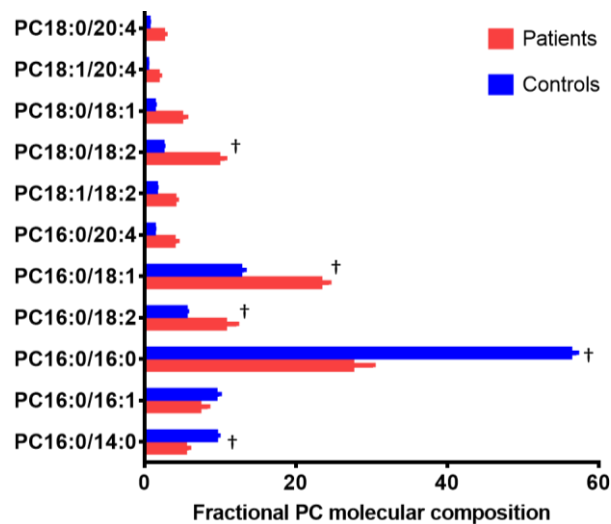


Figure 10; Bronchoalveolar lavage phosphatidylcholine molecular composition at enrolment (T=0Hrs) in patients compared to healthy adult controls. PC, phosphatidylcholine. Comparison by two way ANOVA with Bonferroni's corrections for multiple tests and data are expressed as mean ± SEM percentage of total PC, †; P<0.05.

3.4.5 Surfactant PC molecular composition over time

Among patients there was an improvement in the surfactant PC composition over time, with gradual increment in fractional compositions of saturated PC species such as PC16:0/16:0 and PC16:0/14:0 with decreases in unsaturated PC species including PC16:0/18:1 and PC18:0/18:2. Despite these improvements, even at 96 hours, the relative

total composition of unsaturated PC species remained significantly elevated in patients. The fractional improvement in PC16:0/16:0 composition was coupled with alterations in other PC species for the corresponding time points (Figures 11, 12, and 13). The relative proportional increase in PC16:0/16:0 was associated with reductions in unsaturated PC species (Figure 13).

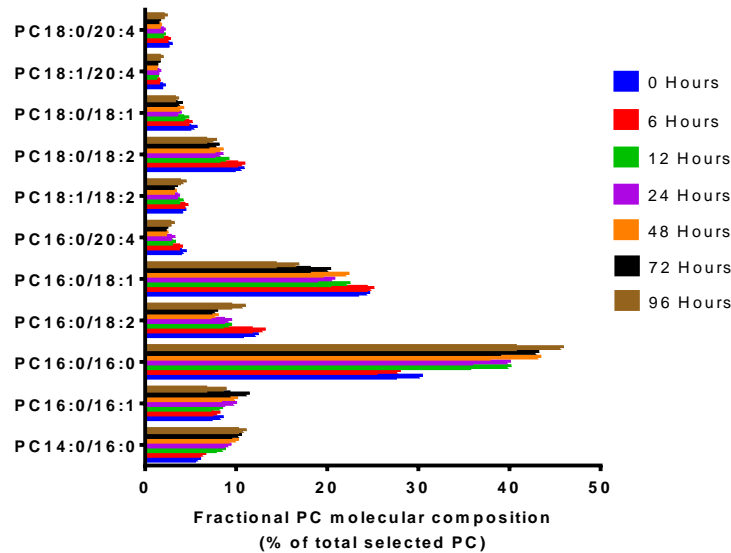


Figure 11; Bronchoalveolar lavage surfactant phosphatidylcholine fractional molecular composition over time in patients. Expressed as mean± SEM.

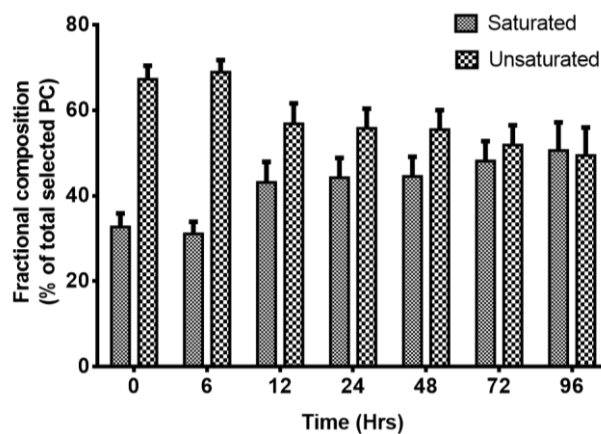


Figure 12; Time course variation of sum of all selected saturated and unsaturated phosphatidylcholine composition in patients. The saturated species were PC16:0/16:0 and PC16:0/14:0. The unsaturated species consisted of PC16:1/16:0, PC16:0/18:2, PC16:0/18:1, PC16:0/20:4, PC18:1/18:2, PC18:0/18:2, PC18:0/18:1, PC18:1/20:4 and PC18:0/20:4. There was a gradual increment in total saturated PC species with subsequent decline in unsaturated PC species over time.

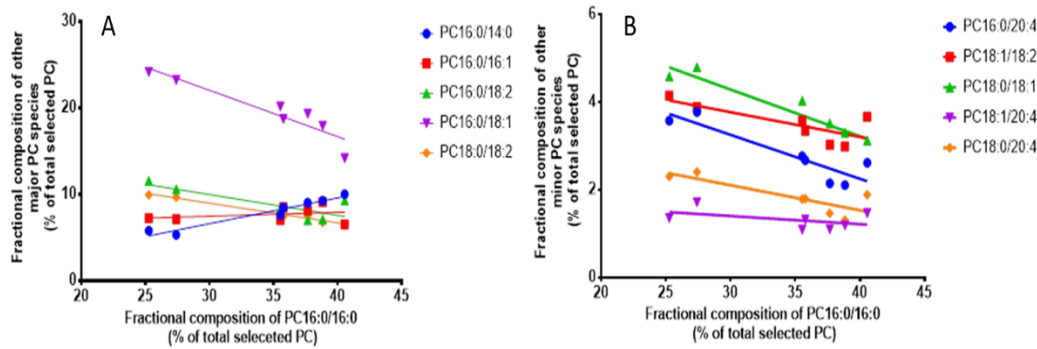


Figure 13; Relationships of relative composition of PC16:0/16:0 with other major (A) and minor (B) phosphatidylcholine molecular species over time for the corresponding time points. PC, phosphatidylcholine. There were increases in PC16:0/14:0 and decreases in PC16:0/18:1, PC16:0/18:2, PC18:0/18:2 and all other minor unsaturated PC species in relation to PC16:0/16:0.

3.4.6 Variations in surfactant PC composition between patients

There were significant differences in surfactant PC composition among patients. In controls the sum of all surfactant specific PC species PC16:0/16:0, PC16:0/14:0 and PC16:0/16:1 accounted for 75% of total PC. In patients at enrolment this varied from 14-59% (mean 40%) (Figure 14). The fractional composition of PC16:0/16:0 was significantly lower in patients compared to healthy controls (Figure 15).

There were also increases in unsaturated PC species as demonstrated by the ratio of saturated to unsaturated PC ratio. This ratio was 1.9 for controls but significantly varied between patients with an overall decreased mean ratio of 0.5 (range 0.2-0.8). The three arachidonoyl PC species (PC16:0/20:4, PC18:1/20:4 and PC18:1/20:4) accounted for <2% of PC composition in controls compared to patients, where there was a fractional increase in their composition up to 8%.

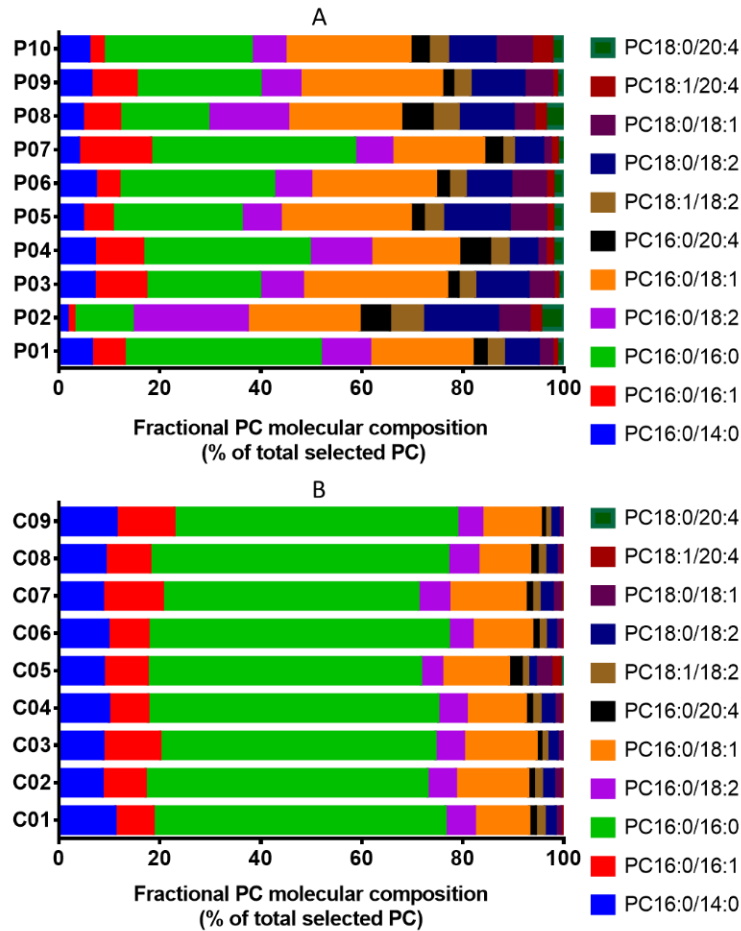


Figure 14; Fractional compositional variation of bronchoalveolar surfactant phosphatidylcholine species from individual patients at enrolment (T=0Hrs) (A) and healthy controls at T=24Hrs (B).

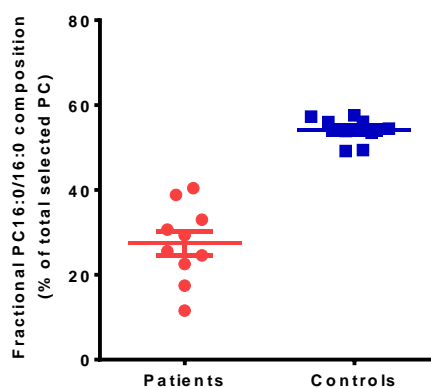


Figure 15; Individual variation of fractional PC16:0/16:0 composition among patients (N=10) at enrolment compared with controls (N=9). PC, phosphatidylcholine. Data presented as mean \pm SEM. There was a significant difference between patients and controls compared by student t-test with a mean difference of 29%, $P < 0.0001$.

3.4.7 Molecular composition of *methyl-D₉*-labelled PC species

In patients, the molecular composition of labelled PC varied at different time points. For instance, at 6 hours (the earliest time point after *methyl-D₉* choline infusion), the PC composition was dominated by unsaturated PC species such as PC16:0/18:1 (22%) and PC16:0/18:2 (13%) (Figure 16). There was a gradual increment in *methyl-D₉* labelled PC16:0/16:0 from 11% at 6 hours to 32% and 35% of total labelled PC at 48 and 72 hours. In addition, there was a gradual decline in *methyl-D₉* labelled PC16:0/18:1, which was 22% at 6 hours and 14% at 96 hours after choline infusion (Figure 16). The other PC species showed no significant time course variation over the investigative period.

In healthy controls, the *methyl-D₉* labelled PC16:0/16:0 was 47% and 51% of total labelled PC at 24 and 48 hours respectively (both time points studied). In patients, at the earliest time point (T=6hrs), the *methyl-D₉*-labelled fraction of PC16:0/16:0 was proportionally lower compared to the unlabelled fraction and only became near equilibrium at 48 hours (Figure 17). This was similar to the controls (Figure 18).

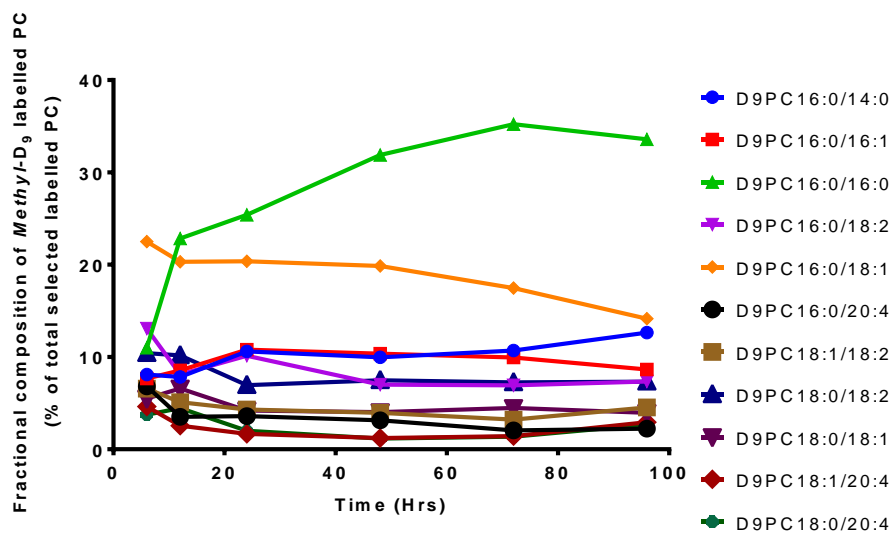


Figure 16; Molecular composition of *methyl-D₉* labelled phosphatidylcholine fraction in patients over time. PC, phosphatidylcholine. This is expressed as percentage of total labelled phosphatidylcholine.

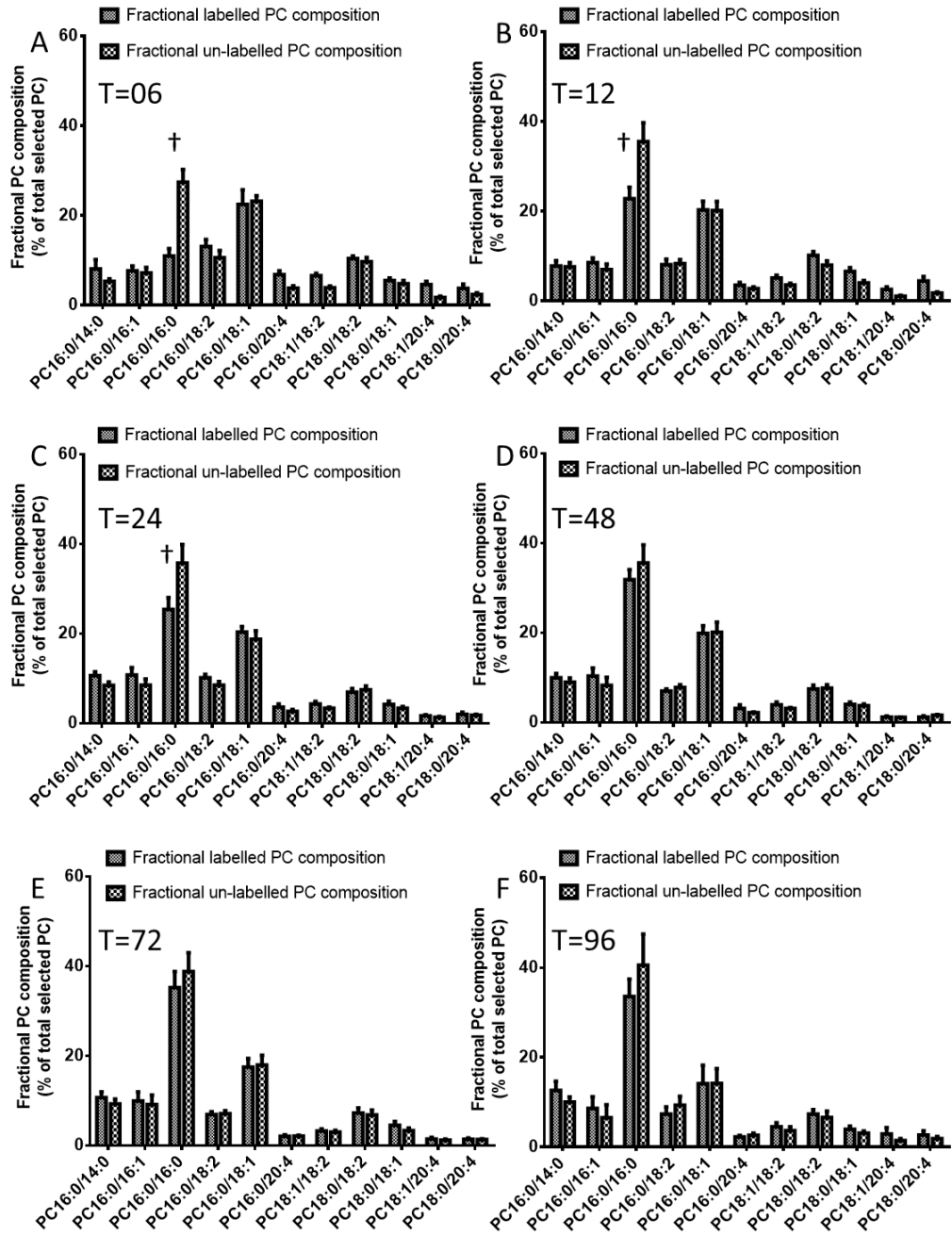


Figure 17; Comparison of *methyl-D₉* labelled and unlabelled fractional phosphatidylcholine composition at time points 6 (A), 12 (B), 24 (C), 48 (D), 72 (E) and 96 (F) hours after *methyl-D₉* choline infusion in patients. PC16:0/16:0 labelled fraction was much lower at earlier time points and only equilibrated with unlabelled fraction at 48 hours. Data presented as mean \pm SEM. Comparisons were made by two way ANOVA with Bonferroni's corrections for multiple tests and †P<0.05.

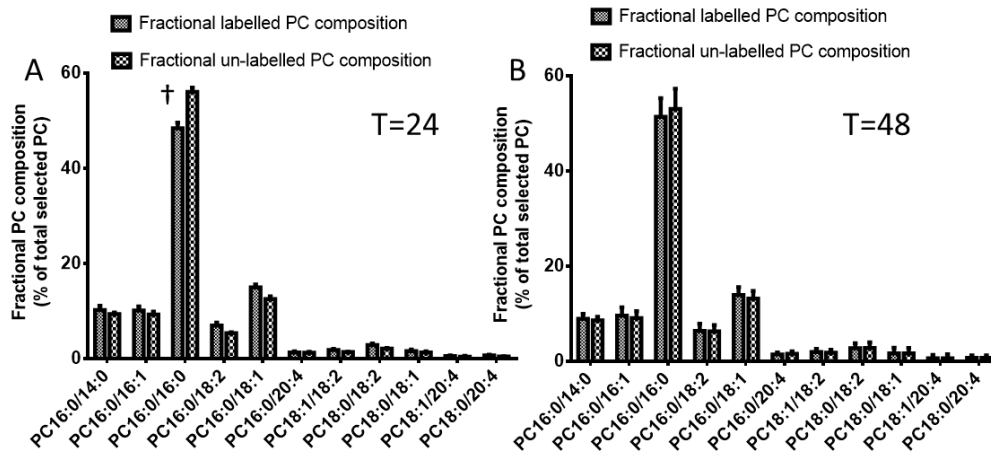


Figure 18; Comparison of *methyl-D₉* labelled and unlabelled fractional phosphatidylcholine composition at time points 24Hrs (**A**) and 48Hrs (**B**) after *methyl-D₉* choline infusion in healthy controls. PC16:0/16:0 labelled fraction was much lower at 24 hours and only equilibrated with unlabelled fraction at 48 hours. Data presented as mean \pm SEM. Comparisons were made by two way ANOVA with Bonferroni's corrections for multiple tests and †P<0.05.

There were considerable variations in the relative proportions of labelled PC16:0/16:0 among patients at the time of equilibrium (T=48Hrs), which ranged from 12-44% of total *methyl-D₉*-labelled PC (Figure 19). This variation was much less in healthy controls. Even though there was no significant correlation between the fractional synthesis of PC16:0/16:0 and mortality, patients who have had the lowest *methyl-D₉* labelled PC16:0/16:0 at 72 hours (P04 and P05) did not survive ICU.

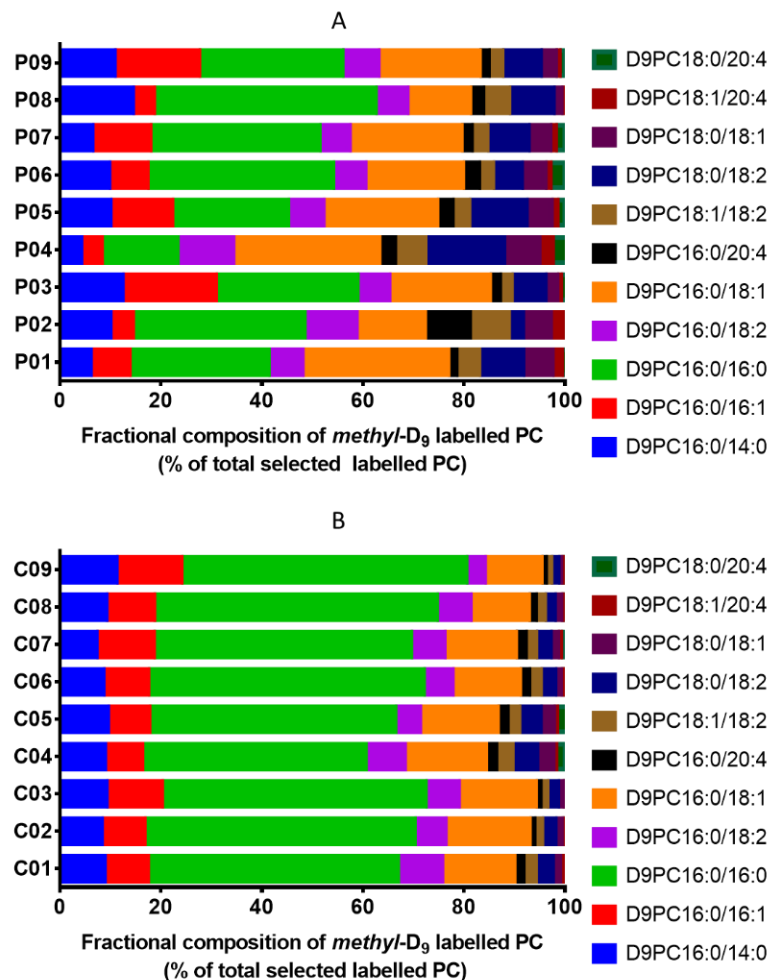


Figure 19; Individual variation in *methyl-D₉* labelled surfactant phosphatidylcholine composition at peak incorporation (T=48Hrs after *methyl-D₉* choline infusion) from patients (A) and healthy controls (B).

There was a significant correlation between unlabelled and labelled PC16:0/16:0 at maximal incorporation, suggesting the possibility of a linear relationship ($r^2=0.9051$, $P<0.0001$). This implies that at 48 hours the *methyl-D₉* labelled PC16:0/16:0 composition is in equilibrium with unlabelled PC16:0/16:0 fraction (Figure 20). But, some patients had much lower PC16:0/16:0 composition with similar corresponding *methyl-D₉* labelled PC16:0/16:0. One patient (P04) had <20% of endogenous PC16:0/16:0 and at maximal incorporation, the fractional *methyl-D₉* labelled PC16:0/16:0 was also consisted of <20%. Interestingly this patient did not survive his acute illness.

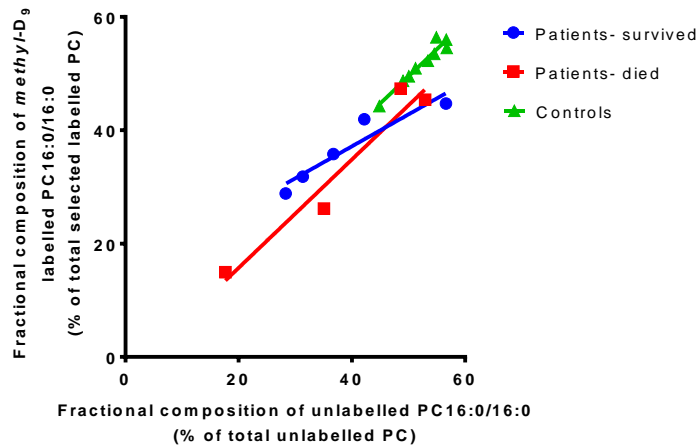


Figure 20; Relationship between unlabelled PC16:0/16:0 composition (% of total unlabelled phosphatidylcholine) and the *methyl-D₉* labelled PC16:0/16:0 (% of total labelled phosphatidylcholine) among patients and controls at (T=48Hrs) at maximal incorporation (T=48Hrs). (Blue dots- patients survived (N=5, red squares- patients died (N=4) and green triangles are healthy controls (N=9).

3.4.8 Total surfactant PC *methyl-D₉*-choline incorporation

In ARDS patients, the *methyl-D₉*- total PC incorporation was noticeable at 6 hours at 0.19% of total PC. There was a non-linear increase in enrichment which peaked at 48 hours at 0.90%, followed by a relative steady state until 96 hours. In comparison to controls, this was a 49% and 73% increase in total enrichments at 24 and 48 hours respectively (Figure 21A).

In patients, the rate of *methyl-D₉* incorporation peaked at 6 hours ($0.03 \pm 0.007\%/h$) with a linear decline ($r^2=0.9902$, $P=0.0004$) until 96 hours, but with a higher regression rate compared to controls (Figure 21B). This suggests that at 24 hours, the rate of incorporation was much faster in patients compared to controls. But this difference in the rates become smaller at later time points (e.g. at 48 hours).

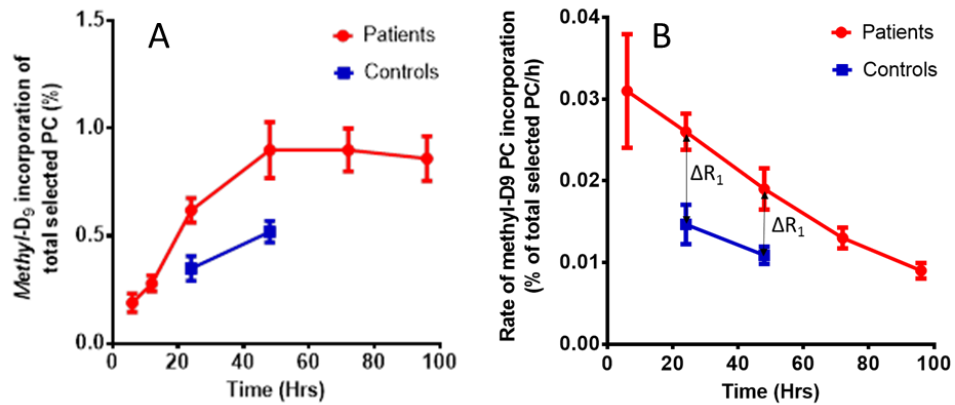


Figure 21; Mean total bronchoalveolar lavage phosphatidylcholine *methyl-D₉* choline incorporation (**A**) and the rate of total bronchoalveolar lavage phosphatidylcholine *methyl-D₉* choline incorporation (**B**) in patients (N=10) compared to controls (N=9). Expressed as mean \pm SEM. Patients had 6 time points (6, 12, 24, 48, 72, and 96 hours) and controls had 2 time points (24 and 48 hours). $\Delta R_1 = 0.011\%/h$, $\Delta R_2 = 0.008\%/h$.

There were significant variations in the *methyl-D₉*- PC fractional incorporation among patients and 48 hours, and it ranged between 0.49-1.19% (Figure 22). Despite these variations, there was no significant differences in the mean total *methyl-D₉*- PC incorporation between survivors and non-survivors.

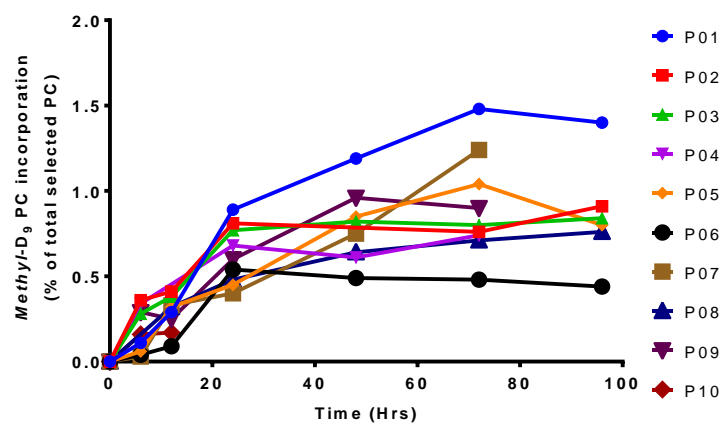


Figure 22; Individual variation in mean total bronchoalveolar lavage phosphatidylcholine *methyl-D₉* choline incorporation in patients (N=10) among patients over time.

3.4.9 Fractional PC16:0/16:0 *methyl-D₉* choline incorporation

In patients, the fractional PC16:0/16:0 *methyl-D₉* incorporation at 6 hours was $0.09 \pm 0.03\%$, and was much lower than total PC incorporation for this time point. Maximal

methyl-D₉-choline PC16:0/16:0 incorporation was noted at 72 hours with $0.79 \pm 0.08\%$. Compared to healthy controls, there was a 39% and 47% increase in PC16:0/16:0 *methyl-D₉* incorporation at 24 and 48 hours respectively (Figure 23A).

The rate of incorporation at 6 hours was $0.014 \pm 0.004/h$ and peaked at 24 hours to $0.018 \pm 0.003/h$ (Figure 23B). This was a much slower incorporation rate than the rate of overall total PC enrichment. In addition, the pattern of rate of incorporation was non-linear. There were also significant variations in the *methyl-D₉* PC16:0/16:0 incorporation among patients, ranging between 0.48-1.27% at maximal incorporation (Figure 24).

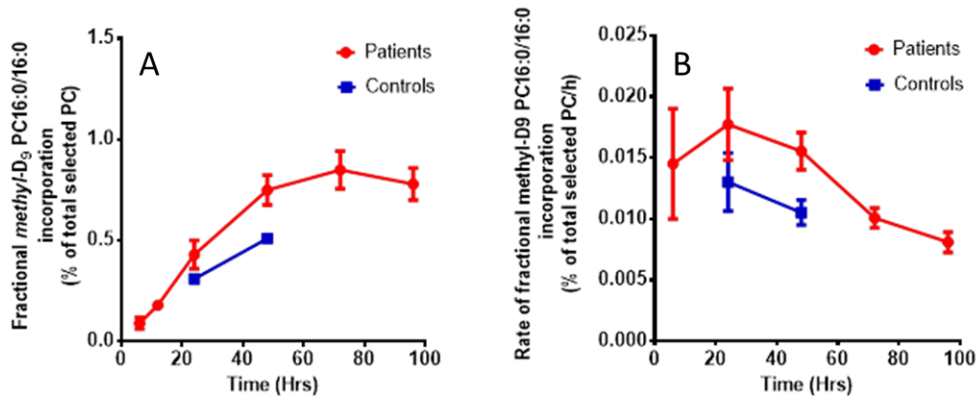


Figure 23; Bronchoalveolar lavage fractional *Methyl-D₉* PC16:0/16:0 incorporation (**A**) and rate of fractional *methyl-D₉* PC16:0/16:0 incorporation (**B**) in patients (N=10) compared to controls (N=9). Expressed as mean \pm SEM. Patients had 6 time points (6, 12, 24, 48, 72, and 96 hours) and controls had 2 time points (24 and 48 hours).

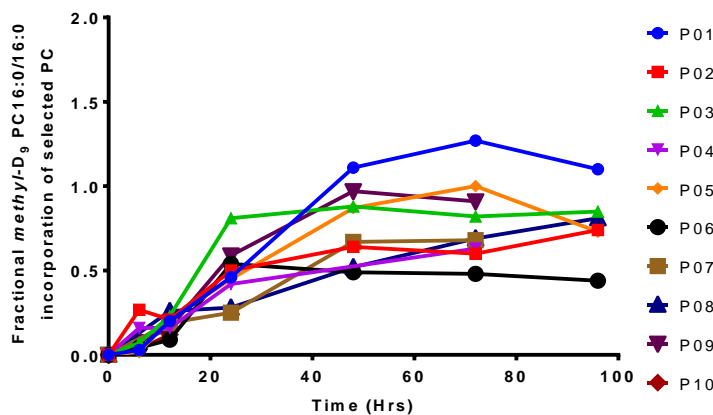


Figure 24; Individual variation in bronchoalveolar lavage fractional *methyl-D₉* PC16:0/16:0 incorporation in patients (N=10) over time.

3.5 Discussion

This study conducted on a small number of patients, illustrates the feasibility of performing stable isotope labelling in combination with ESI-MS/MS analytical methods, to investigate surfactant phospholipid metabolism in a defined human patient cohort. This is the first study to characterise the molecular specificity of surfactant synthesis in adult ARDS population. The study group composed of patients with severe ARDS, as defined by the degree of hypoxemia with poor lung compliance and multi-organ involvement. Most patients (90%) had pneumonia as the single precipitating factor.

Despite the significant variability, ARDS patients had persistently lower BALF PC concentration compared to healthy controls (Figure 8). This findings is consistent with previous studies (Hallman M et al. 1982). This deficit in PC concentration may be due to reduced synthesis, increased breakdown, or dilution by pulmonary oedema. The BALF fractional PC16:0/16:0 concentration was also much lower in patients and only accounted for about 10% of the healthy controls. This degree in the loss of surfactant PC16:0/16:0 could explain the severity of hypoxemia, evident in this study population. However, there were no direct correlations between the total PC and PC16:0/16:0 concentrations at enrolment with clinical variables studied ($\text{PaO}_2/\text{FiO}_2$ ratio/ compliance or mortality) (Figure 9).

Characterisation of surfactant phospholipids in the past involved chromatographic separation methods to quantify derivatised fatty acids such as palmitic acid (16:0), which was used as a surrogate for PC16:0/16:0 (Hallman M et al. 1982) (Schmidt R et al. 2001). This methodology always produced higher fractional compositional values (70-80%) for palmitic acid (16:0), which may have come from PC species other than PC16:0/16:0 and have no clinical relevance. The assessment of surfactant PC molecular composition in healthy controls reveals principal enrichment of PC16:0/16:0 (50-60%), in accordance with previous studies (Wright SM et al. 2000) (Schmidt R et al. 2007) (Figure 10). In comparison, patients had significantly lower proportions of both disaturated PC species

(PC16:0/16:0 and PC16:0/14:0) and higher compositions of unsaturated PC species. Moreover, there were considerable improvements in the relative proportions of total disaturated PC species over time (Figure 11).

The incorporation of *methyl-D₉*-choline into surfactant PC enabled for the first time, the assessment of surfactant PC molecular synthesis via CDP-choline pathway, in adult ARDS population. This study demonstrate that at earlier time points (before 24 hours), the molecular composition of *methyl-D₉* labelled surfactant PC fraction is completely different to that of unlabelled endogenous composition (Figure 16). This finding is consistent with a previous study of healthy adult volunteers, and indicates that not all alveolar surfactant is acyl remodelled prior to secretion (Bernard W et al. 2004). In patients and healthy controls, the fractional *methyl-D₉*-labelled PC16:0/16:0 composition was at equilibrium with the unlabelled PC16:0/16:0 fraction at 48 hours, suggesting that acyl remodelling mechanisms are complete only by this time point (Figures 17 and 18). There was a considerable variation in the proportion of labelled PC16:0/16:0 at peak incorporation among patients. One patient had significantly lower compositions of both unlabelled (<20% of total PC) and *methyl-D₉*-labelled PC16:0/16:0 (<20% of *methyl-D₉* labelled PC), and did not survive his acute illness.

Total PC and fractional *methyl-D₉*-PC16:0/16:0 enrichment was nearly doubled in patients compared to controls (Figure 21A). Other investigators have also shown increased synthesis of surfactant disaturated PC (SatPC) in ARDS patients (Simonato M et al. 2011). This increased enrichment noted in our study could be due to several reasons. It is entirely plausible, there could be a compensatory increase in surfactant synthesis by AT- II cells during acute lung injury. Other possibility is related to the approach how enrichment values were estimated. As the calculation of fractional enrichment is dependent on the unlabelled endogenous concentrations, and lower fractional concentrations may have influenced the estimated incorporation values. Moreover, damaged alveolar epithelial and endothelial lining could have resulted in a contaminated pool of phospholipids and the extracted

material may have come from non-surfactant origin. However, PC16:0/16:0 is a relatively unique di-saturated PC enriched in pulmonary surfactant and the incorporation pattern of PC16:0/16:0 is likely to represent alveolar surfactant origin. Nevertheless, there was a consistent increase in both total surfactant PC and fractional PC16:0/16:0 enrichment in all patients, albeit with substantial individual variability, indicating the presence of underlying phenotypes corresponding to AT-II cell surfactant synthetic capacity.

This is the first study to use small volume bronchoalveolar lavage fluid (BALF) to investigate surfactant metabolism in patients with ARDS. In the past, investigators have used large volume (quantitative) BALF to quantify surfactant phospholipid composition and alterations in ARDS. Although in general this is a safe procedure, repetitive large volume BALF may theoretically deplete alveolar surfactant and may produce a negative clinical impact. Moreover, desaturations are much more common during quantitative BALF than small volume BALF. The surfactant PC composition in our control group is similar to that of previous publications, which has utilised large volume BALF (Wright SM et al. 2000) (Schmidt R et al. 2007). This suggests, at least in physiological conditions small volume BALF is comparable to quantitative BALF for the study of surfactant phospholipid composition. Induced sputum and tracheal aspirates also have been used as alternates for BALF for surfactant isolation (Bernhard W et al. 2004) (Simonato M et al. 2011). However, so far no studies have made any direct comparisons of phospholipid metabolism from all these three bronchoalveolar compartments in an adult human model. Small volume BALF were tolerated by all, without any significant immediate complications. Although few oxygen desaturations were noted during the procedure, these were not sustained post procedure. Despite no cardiovascular or respiratory compromise, all patients in general needed additional sedation, on average of 30mgs of propofol to perform this procedure.

The lack of clinical correlations (death or PaO₂/FiO₂ ratio) with surfactant composition and synthesis is more likely to be due to the small number of patients enrolled into the study

so far. Continued recruitment may help to identify potential phenotypes of patients with variations in surfactant metabolism.

3.6 Conclusions

This preliminary data suggest the feasibility of using stable isotope labelling technique to study surfactant kinetics in patients with ARDS. The assessment of composition and isotope labelling indicate significant variability in the surfactant PC composition, fractional synthesis and fractional enrichment of *methyl-D₉*-choline into surfactant PC among patients. This individual variability may pave the way for phenotypic characterisation of patients, according to surfactant metabolism and subsequent therapeutic targets. Continued enrolment of patients is essential to establish clinical correlations.

CHAPTER 4

In-vivo characterisation of plasma PC synthetic pathways in Acute Respiratory Distress Syndrome

4.1 Introduction

Human *de-novo* biosynthesis of PC is dependent on two distinct molecular pathways. While all nucleated mammalian cells utilise CDP-choline pathway for the biosynthesis of PC, hepatocytes are capable of converting phosphatidylethanolamine (PE) into PC by three sequential methylation of PE from the action of PE N-methyltransferase (PEMT) (Li Z and Vance DE 2008). The preference of PEMT to selectively synthesise polyunsaturated fatty acid (PUFA) containing PC species, highlights the possibility of functional variation between these two pathways (DeLong CJ et al. 1999) (Pynn CJ et al. 2011).

ARDS is characterised by severe systematic inflammatory response with multi-organ involvement, and hepatic dysfunction is a recognised feature (Schwartz DB et al. 1989). As lipid metabolism is highly orchestrated by the liver, alterations in hepatic PC synthesis may have clinical implications in ARDS, and have not been investigated before. Furthermore, phospholipids in particular phosphatidylcholines are precursors for several biosynthetic pathways of inflammation and resolution (Serhan CN 2010). Fatty acids esterified to phosphatidylcholines can be hydrolysed by the action of phospholipase-A₂, and subsequent generations of oxidative metabolites are regulators of inflammation and have been implicated at least in part in the pathogenesis of ARDS (Caironi P et al. 2005) (Gust R et al. 1999). Besides, docosahexaenoic acid (DHA; sn-2 22:6) can generate mediators which are involved in resolution of inflammation (Uddin M and Levy BD 2011).

Patients with ARDS characteristically have reduced plasma concentrations of PUFA (Kumar KV 2000), and mechanisms underlying these are not been elucidated. Further, there may be clinical consequences of these alterations in PC metabolism, influencing the degree of inflammation, initiation of resolution and progression into chronic inflammation.

Studies have demonstrated that in PEMT knockout mice models, there is a selective reduction in docosahexaenoic acid [22:6] from both plasma and hepatic PC (Watkins SM et al. 2003). It is possible that the reductions in plasma PUFAs in ARDS may be as a result of alterations in PC metabolic pathways, which has not been investigated before. Consequently, this chapter was aimed to assess the molecular specificity of PC synthesis, via both synthetic pathways in patients with ARDS.

Chapter 3 demonstrated that there were significant alterations in surfactant phospholipid metabolism in patients with ARDS. However, it is not clear whether these changes were specific to lung compartment, or that there were global disturbances in overall phospholipid metabolism. Human plasma provides a readily available source of PC. To investigate the effect of ARDS on phospholipid metabolism, plasma PC concentrations with relative molecular compositions and additional information regarding in-vivo *methyl-D₉* choline enrichment via PC synthetic pathways were characterised in patients with ARDS and healthy humans. Using stable isotope labelling with *methyl-D₉*-choline chloride and analytical methods of ESI-MS/MS, it is possible to quantify molecular PC flux through both CDP-choline and PEMT synthetic pathways. Furthermore, two types of scan modes (neutral loss and precursor scans) on ESI-MS/MS was used to assess the fractional enrichment of single (*methyl-D₃*) and two deuterium (*methyl-D₆*) labelled PC species, which has enabled the estimation of *methyl-D₃*-S-adenosyl methionine enrichment in the liver (Pynn CJ et al. 2011).

4.2 Objectives

The objectives of this chapter are to assess the following in patients with ARDS with subsequent correlation with healthy controls.

1. Circulating plasma lipid concentrations
2. Relative plasma PC molecular compositional alterations in ARDS
3. Molecular specificity of PC synthesis via both CDP-choline and PEMT pathways

4.3 Summary of methods

After ethical approval, human healthy volunteers and ARDS patients were infused with 3.6mg/kg *methyl-D₉*-choline chloride. Blood samples were collected in EDTA specimen bottles at 0, 6, 12, 24, 48, 72 and 96 hours after choline infusion for patients and at 0, 8, 24, 48, 72 and 96 hours for healthy controls. The collected samples were centrifuged at 1000g at 4°C for 15 minutes. The plasma supernatant was aspirated and stored at -80°C. Lipid extraction was performed by a modified Bligh and Dyer method (Bligh EG and Dyer WJ 1959). The lower lipid fraction was analysed by ESI-MS/MS after dissolving with methanol: butanol: H₂O: 25% NH₄OH (6:2:1.6:0.4 v/v) by direct infusion. The upper aqueous layer obtained during the lipid extraction process was used to measure plasma choline and betaine concentrations. PC_{14:0/14:0} for PC and *methyl-D₄*-choline for choline were used as internal standards. Plasma choline, *methyl-D₉*-choline and betaine was measured on HPLC-MS/MS. Plasma lipoprotein concentrations (cholesterol, HDL-cholesterol, LDL-cholesterol and triglycerides) were measured by Konelab 20 Autoanalyser.

Collision induced decomposition resulted in protonated phosphocholine head group with m/z of 184⁺ for PC, m/z187⁺ for the incorporation of one deuterated-*methyl* PC group and m/z190⁺ for the incorporation of two deuterated-*methyl* PC groups. By applying specific precursor scans, it is possible to quantify unlabelled and one and two deuterium labelled

PC molecular composition. Four PUFA-PC species were chosen for diagnostic neutral loss scans of $m/z +599$ (PC16:0/20:4), $m/z +623$ (PC16:0/22:6), $m/z +627$ (PC18:0/20:4) and $m/z +651$ (PC18:0/22:6). This enabled quantification of one (M+3) and two (M+6) deuterated-*methyl* groups from the dedicated molecular mass of that particular PC. For instance, PC 16:0/20:4 has a molecular m/z of 782, the incorporation of one and two deuterium labelled *methyl* groups will result in m/z of 785 and 788 respectively. The ion peaks were quantified using Masslynx software and dedicated excel spread sheets. For detailed methodology see chapter 2.

4.4 Results

4.4.1 Plasma choline and betaine concentrations and enrichment

Due to the lack of reference standards, plasma choline concentrations were only estimated based on the recovery of internal standard (D_4 -choline). This showed no significant difference between patients and controls. Prior to enrolment, ARDS patients and healthy controls had choline levels of $3.6 \pm 1.3 \mu\text{M/l}$ and $4.2 \pm 0.9 \mu\text{M/l}$ respectively. Subsequent infusion of *methyl*- D_9 -choline, did not increase the endogenous choline concentrations in the plasma and there were no significant changes over time (Figure 25A).

In addition, the *methyl*- D_9 -choline enrichment was similar for earlier time points, and contributed to about 9% of total choline in patients at 6 hours and 8% in healthy controls at 8 hours after the infusion. By 96 hours, the labelled choline accounted for only <2% of total choline present in the plasma for both patients and controls. However, this decay was much faster in patients suggesting increased usage of choline for endogenous metabolism (Figure 25B).

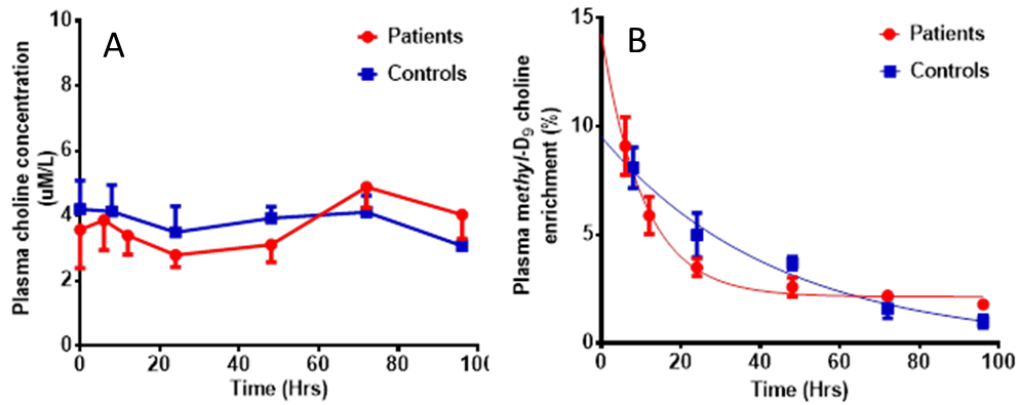


Figure 25; Plasma choline concentrations ($\mu\text{M/L}$) (**A**) and fractional plasma *methyl-D₉*-choline enrichment (%) (**B**) for both patients (N=10) and healthy controls (N=10) over time. Data are presented as mean \pm SEM. There was no significant difference between both groups even after the infusion of *methyl-D₉* choline.

Choline is metabolised to betaine in the liver. Absolute betaine concentrations were not calculated in the absence of an internal standard. The plasma *methyl-D₉*-betaine enrichment presented as fractional abundance was similar at earlier time points for both patients and controls. However, the decay was much faster in patients suggesting increased flux (Figure 26).

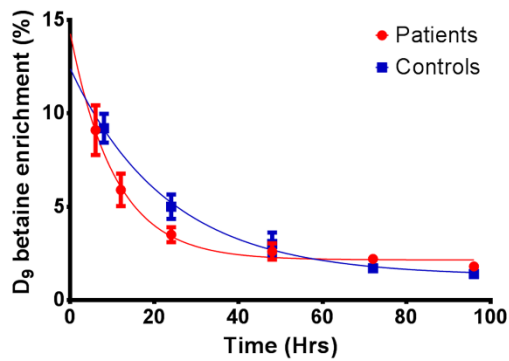


Figure 26; Fractional plasma *methyl-D₉*-betaine enrichment (%) for patients (N=10) and healthy controls (N=10). There was no significant difference between both groups and as analysed by two way ANOVA of variance. Data presented as mean \pm SEM.

4.4.2 Plasma lipid concentrations and compositions

4.4.2.1 Plasma PC concentrations

Plasma PC concentration was assessed as the sum of selected major PC species (>1% abundance) in both patients and controls and the mean total PC was 1.5 ± 0.5 mmol/l and 2.0 ± 0.1 mmol/l respectively ($P<0.0001$). This was a 25% reduction in the plasma PC concentration in patients compared to healthy controls (Figure 27). However, this reduction was not uniform among all PC species. In fact, the fractional concentrations of PC16:0/18:1 and PC18:0/18:1 were elevated in patients by 16% and 13% respectively compared to controls (Figure 28). Greatest reductions were seen in diunsaturated and polyunsaturated PC species such as PC16:0/18:2 (39%), PC16:0/20:4 (37%), PC16:0/22:6 (43%) and PC18:1/20:4 (33%) (Figure 28). In addition, there was no real improvement in the total PC concentration over time in patients (Figure 29). 1-alkyl 2-acyl PC species were in lesser abundance (<8% of total PC) and the concentrations in patients and controls were 0.09 ± 0.0017 mmol/l and 0.16 ± 0.05 mmol/l respectively. This was a 44% reduction in total 1-alkyl 2-acyl PC concentration in patients.

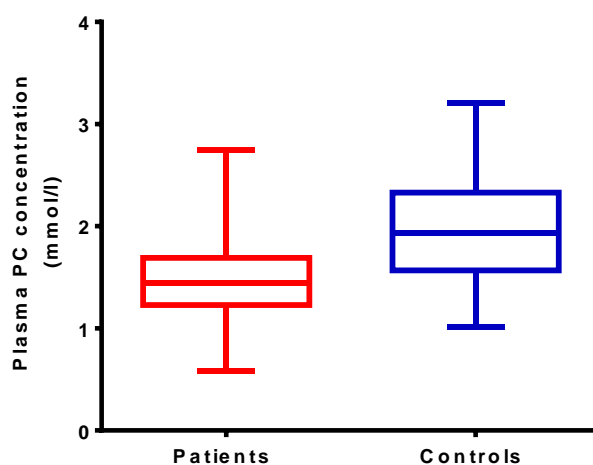


Figure 27; Comparison of plasma phosphatidylcholine concentrations (mmol/l) between patients (N=10) and controls (N=10) at enrolment (T=0Hrs). Data presented as Box and Whiskers plot, with means and minimum to maximum values. There was a significant difference between groups with a mean difference of 0.48 ± 0.08 mmol/l, $P<0.0001$, as assessed by student's t- test. PC, phosphatidylcholine.

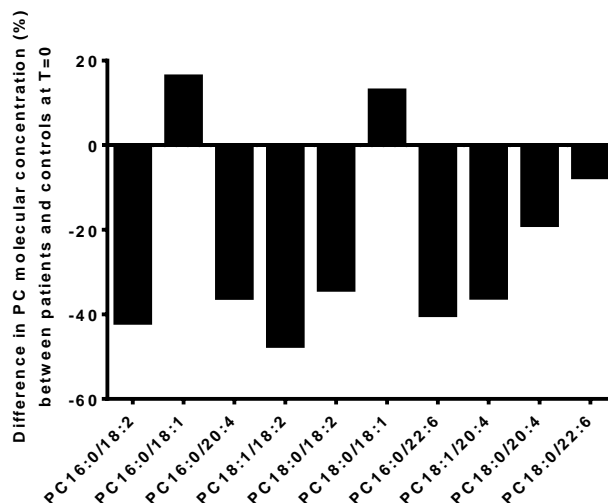


Figure 28; Changes in plasma fractional PC molecular concentrations (mmol/l) in patients (N=10) corrected for control values (N=10) at enrolment (T=0). Positive bar indicates an increase (%) and negative bar indicates a decrease (%) in plasma PC concentration from patients. Data expressed as percentage (%) change from controls at enrolment. PC, phosphatidylcholine.

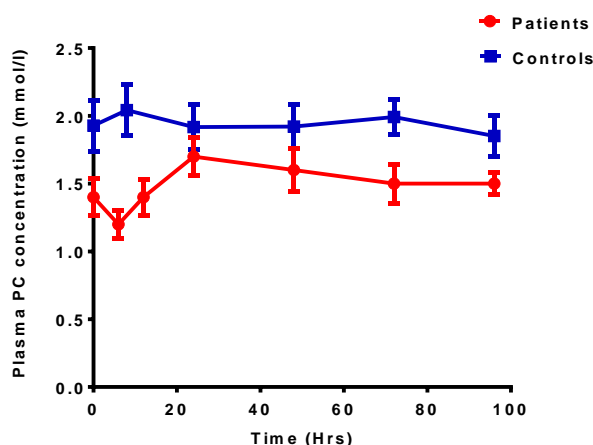


Figure 29; Plasma phosphatidylcholine concentrations (mmol/l) over time between patients (N=10) and controls (N=10). Data presented as mean \pm SEM. PC, phosphatidylcholine.

In a previous study of ARDS patients, the plasma fatty acid analysis by gas chromatographic measurements, suggest a 25% reduction in docosahexaenoic acid (DHA 22:6) concentrations (Kumar KV et al. 2000). However, studies dealing with plasma PC molecular assessment in ARDS are lacking. Consequently, selective molecular quantification of major plasma PUFA containing PC species was performed. This showed

a 34% reduction in all PUFA PC species (Figure 30) and 36% reduction in sn-2 22:6 PC species (PC16:0/22:6 and PC18:0/22:6) concentration compared to controls.

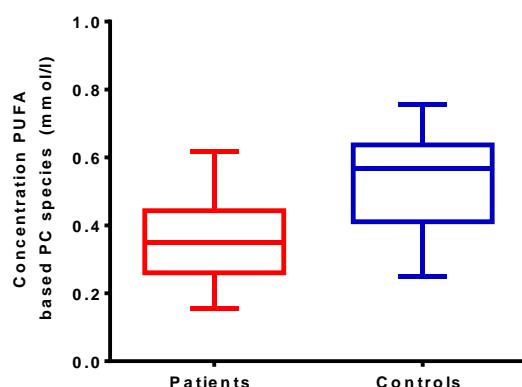


Figure 30; Concentrations of polyunsaturated based phosphatidylcholine species (mmol/l) between patients (N=10) and controls (N=10) at enrolment (T=0Hrs). Data presented as Box and Whiskers plot, with means and minimum to maximum values. There was a significant difference between groups with a mean difference of 0.18 ± 0.02 mmol/l, $P < 0.0001$, as assessed by student's t- test.

4.4.2.2 Plasma cholesterol, LDL, HDL and Triacylglycerol concentrations

Phosphatidylcholines are closely inter-related with lipid metabolism in humans and make up 20-40% of lipoprotein complex. Any alterations in the PC concentrations may lead to changes in the lipid metabolism. Consequently, plasma cholesterol-lipoproteins were quantified for patients at all-time points and controls at enrolment. In patients, there were significant reductions in total phosphatidylcholine (25%), total cholesterol (52%), LDL-cholesterol (70%), and HDL-cholesterol (75%) at enrolment. The triacylglycerol concentrations were similar for both patients and controls (Table 13). In patients, there was a gradual increment in concentrations of plasma total cholesterol, low density lipoproteins (LDL) - cholesterol, high density lipoproteins (HDL) - cholesterol and triacylglycerol concentrations over time (Figure 31).

Lipid concentrations	Patients	Controls
Total PC (mmol/l)	1.46 ± 0.09*	1.94 ± 0.15
Cholesterol (mmol/l)	2.12 ± 0.20*	4.37 ± 0.27
HDL (mmol/l)	0.31 ± 0.07*	1.24 ± 0.16
LDL (mmol/l)	0.79 ± 0.16*	2.66 ± 0.22
Triacylglycerol (mmol/l)	1.33 ± 0.16	1.24 ± 0.22

Table 13; Plasma cholesterol, low density lipoproteins (LDL) - cholesterol, high density lipoproteins (HDL) - cholesterol and triacylglycerol concentrations at enrolment (T=0Hrs) between patients (N=10) and controls (N=10). Data presented as mean ± SEM, *P<0.05 as analysed by student's T- test. PC, phosphatidylcholine; LDL, low density lipoproteins; HDL, high density lipoproteins.

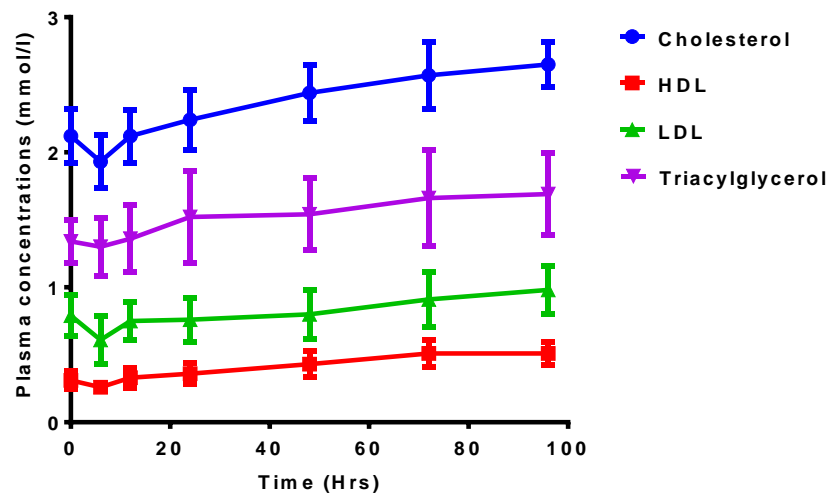


Figure 31; Plasma cholesterol, low density lipoproteins (LDL) - cholesterol, high density lipoproteins (HDL) - cholesterol and triacylglycerol concentrations over time in ARDS patients (N=10). Data presented as mean ± SEM.

4.4.2.3 Plasma PC molecular composition

The relative PC molecular composition was assessed by the fraction of individual PCs, in relation to sum of all selected PC composition. In controls, plasma diacyl-PC molecular composition consisted mainly of unsaturated PC species such as PC16:0/18:2 (30%),

PC18:0/18:2 (16%), PC16:0/18:1 (14%) and PC16:0/20:4 (12%). There was no significant time course variation in PC composition in either patients or controls. At enrolment (T=0), patients had significantly lower proportions of PC16:0/18:2 and higher content of PC16:0/18:1 compared to controls (Figure 32). There was an overall reduction in 1-acyl sn-2 18:2 PC species, and increase in sn-2 PC 18:1 species in patients compared to healthy controls. However, statistically significant differences were only noted for two PC species (PC16:0/18:1 and PC16:0/18:2) (Figure 32).

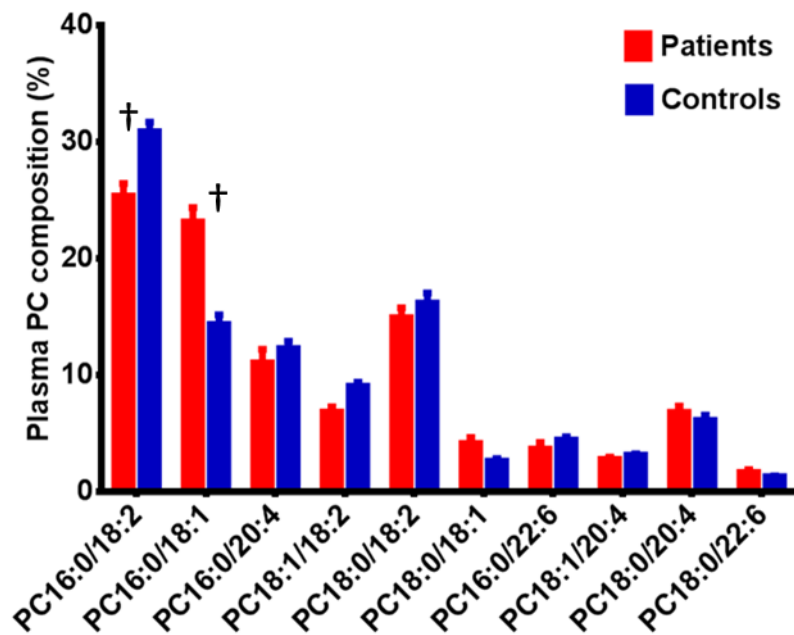


Figure 32; Plasma phosphatidylcholine molecular composition at T=0Hrs in patients (N=10) compared with healthy controls (N=10). Data presented as Mean \pm SEM, †P<0.05 as analysed by two way ANOVA of variance and corrected by Bonferroni's correction for multiple comparisons. PC, phosphatidylcholine.

1-alkyl 2-acyl species accounted for 5.8% and 7.6% of total PC in patients and controls respectively. In controls, molecular 1-alkyl 2-acyl PC composition was primarily composed of PC16:0a/20:4 (16%), PC18:1a/20:4 (16%), PC18:0a/18:2 (11%), PC18:0a/20:4 (11%) and PC16:0a/18:2 (10%). At enrolment (T=0), there were significant differences noted in patients with increases in PC16:0a/18:1, PC18:0a/18:1 and PC18:1a/20:4 and decreases in PC16:0a/18:2, PC16:1a/20:4 and PC16:0a/20:4 compared to healthy controls (Figure 33). Variable changes in arachidonyl species (20:4) were noted

in patients, where sn1-palmitoyl and sn1-palmitoleic alkyl-20:4-PC species were reduced, while sn1-oleoyl species were increased. Overall there was a reduction in alkyl sn-2 18:2 species and increases in sn-2 18:1 alkyl PC species. These changes were similar to the changes of diacyl- PC species.

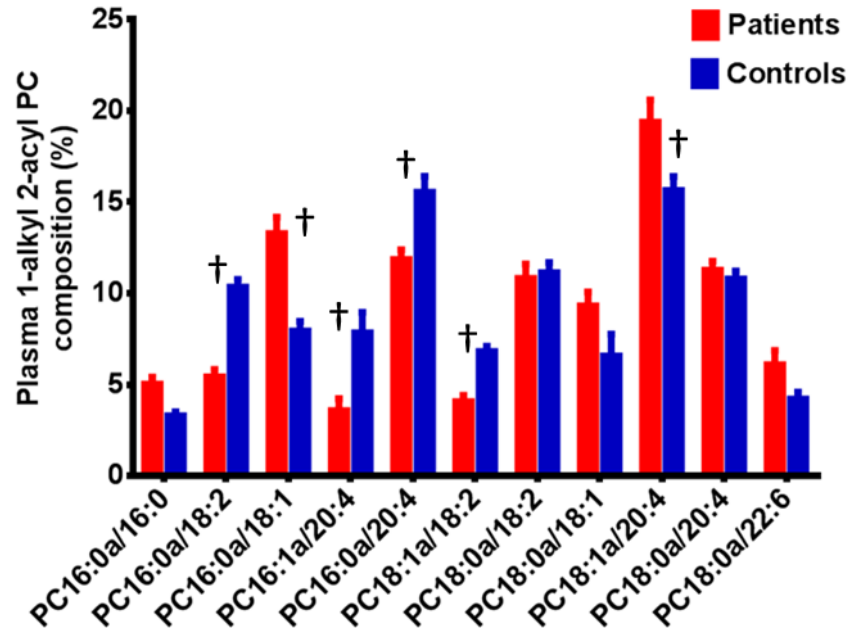


Figure 33; Plasma 1-alkyl 2-acyl phosphatidylcholine composition molecular composition at T=0Hrs in patients (N=10) compared with healthy controls (N=10). Data presented as Mean \pm SEM, †P<0.05 as analysed by two way ANOVA of variance and corrected by Bonferroni's correction for multiple comparisons.

4.4.3 Characterisation of CDP-choline pathway

4.4.3.1 Total PC methyl-D₉ incorporation by CDP-choline pathway

Precursor scans of m/z184⁺ and m/z193⁺ enabled quantification of unlabelled and methyl-D₉ labelled PC fraction in the plasma (Figure 34). The fractional incorporation was calculated from the equation (Pyn CJ et al. 2011);

$$\text{Fractional incorporation (\%)} = \frac{P_{193}}{\Sigma(P_{193}+P_{184})} \times 100$$

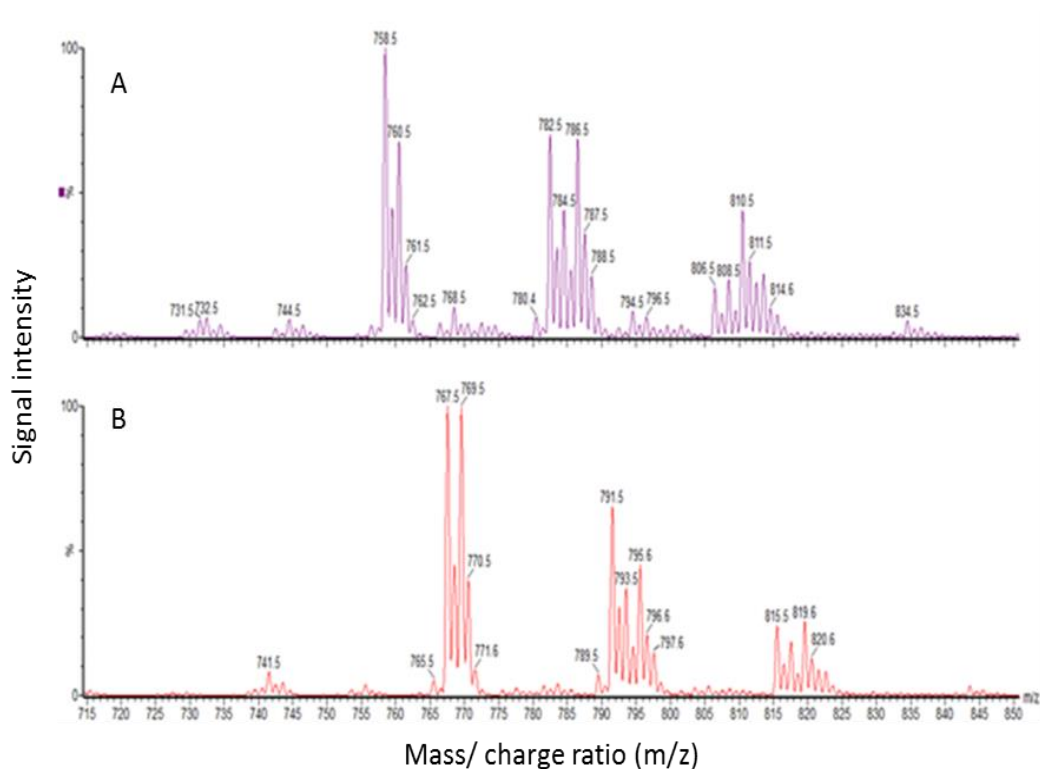


Figure 34; Typical mass spectra of precursor scans of $m/z184^+$ (**A**) and $m/z193^+$ (**B**) from plasma of controls at peak incorporation ($T=24\text{Hrs}$). The signal intensity of spectra B is about 100^{th} less than that of spectra A.

In healthy controls, the *methyl-D₉* incorporation at the earliest time point ($T=8\text{Hrs}$) was $0.20\pm 0.02\%$ of total PC and showed a linear increase ($r^2=0.9950$, $P=0.04$) up to 24 hours, where it peaked at $0.51\pm 0.03\%$ of total PC. This was followed by a linear decline ($r^2=0.9882$, $P=0.006$) until 96 hours (Figure 35).

In patients, the total *methyl-D₉* incorporation was noticeable at 6 hours at 0.20% (± 0.08) and was maximal ($0.75\% \pm 0.06$) at 24 hours. The pattern of incorporation was similar, with a linear increase up to 24 hours ($r^2=0.9846$, $P=0.008$) followed by a linear decay until 96 hours ($r^2=0.9903$, $P=0.005$). However, patients had much higher *methyl-D₉* incorporation, compared to controls at all-time points (Figure 35). In fact, at peak incorporation (at 24 hours), the total *methyl-D₉* incorporation was 47% higher than that of controls.

The rate of incorporation was a linear increase for both patients ($r^2=0.9846$, $P<0.05$ at $0.031\pm 0.003\%/h$) and controls ($r^2=0.9950$, $P<0.05$ at $0.021\pm 0.001\%/h$) until 24 hours. The rate decay was $0.003\pm 0.0002\%/h$ and $0.0025\pm 0.0002\%/h$ for patients and controls respectively (Figure 36). This implies that the total flux of PC synthesis via CDP-choline pathway is much higher and faster in patients, but the utilisation of the incorporated material was at a similar rate for both groups.

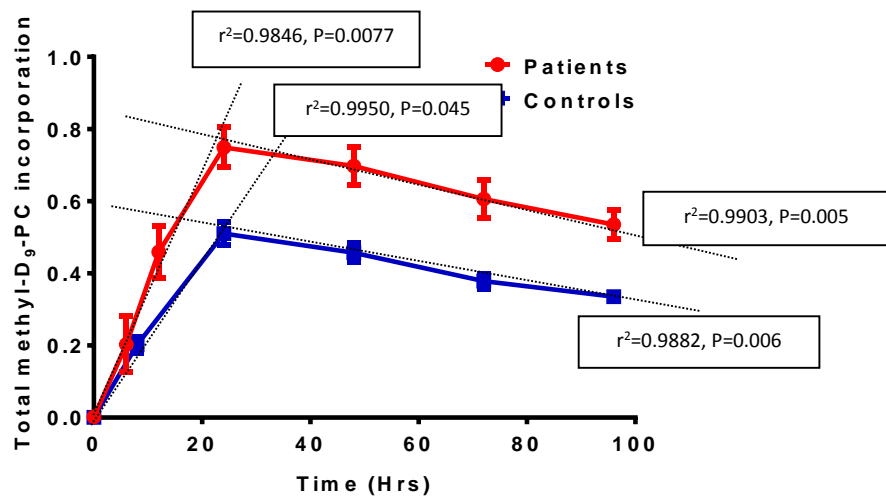


Figure 35; Plasma phosphatidylcholine *methyl-D₉* incorporation for patients (N=10) and healthy controls (N=10) over time. Data presented as mean \pm SEM. Control group showed as linear increase ($r^2=0.9950$, $P=0.04$) until 24 hours followed by a linear decline ($r^2=0.9882$, $P=0.006$). Patients also showed similar pattern with linear increase ($r^2=0.9846$, $P=0.008$) and linear decrease ($r^2=0.9903$, $P=0.005$).

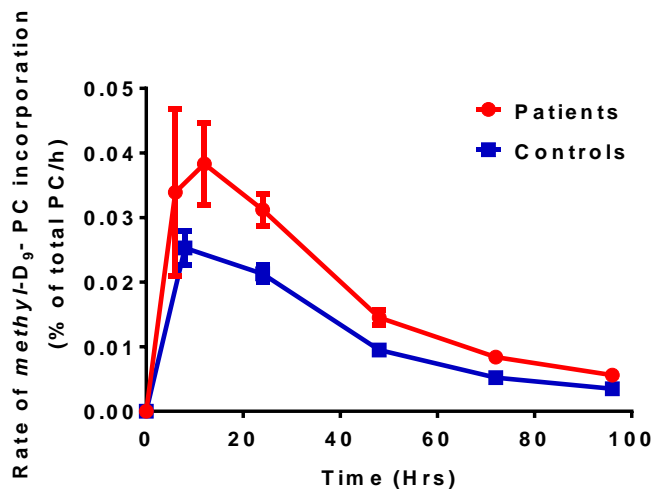


Figure 36; Rate of total plasma phosphatidylcholine *methyl-D₉* incorporation for patients (N=10) and healthy controls (N=10). Data presented as mean \pm SEM.

In healthy controls, the fractional *methyl-D₉* incorporation of individual PC species revealed a selective preferential incorporation pattern, where short chain unsaturated PC species (PC16:0/18:1 and PC16:0/18:2) had higher incorporation than long chain polyunsaturated PC species (PC18:0/22:6 and PC18:0/20:4). Most PC species had maximal incorporation at 24 hours (except for PC18:1/18:2, PC18:0/18:2 and PC18:0/18:1). For this time point, the highest fractional incorporation was noted in PC16:0/18:1 (0.77±0.04%), followed by PC16:0/18:2 (0.57±0.03%). The sn-2 arachidonyl PC species were in the order of PC16:0/20:4 (0.49±0.03%), PC18:1/20:4 (0.43±0.03%) and PC18:0/20:4 (0.37±0.02%). The peak fractional *methyl-D₉* incorporation for sn-2 22:6 PC species were 0.54±0.06% for PC16:0/22:6 and 0.23±0.02% for PC18:0/22:6 (Figure 37).

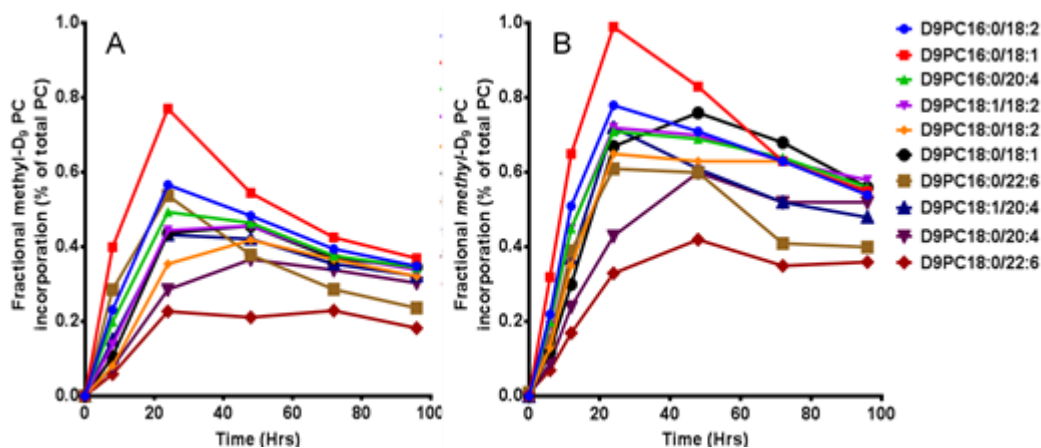


Figure 37; Fractional *methyl-D₉*-incorporation of plasma PC species from healthy controls (N=10) (A) and patients (N=10) (B).

In patients, the fractional *methyl-D₉* incorporation was increased in all PC species, but this relative increase was variable between PC species (Figure 37). At peak incorporation (T=24hrs), compared to controls, the most increases were noted in PC18:0/18:2 (85%), PC18:1/20:4 (66%) followed by PC18:1/18:2 (62%). There were significant variations in the total *methyl-D₉* incorporation among patients (Figure 38). For instance, *methyl-D₉* incorporation was comparatively much higher (0.96%) for patient P09 than patient P03 (0.49%) at 24 hours.

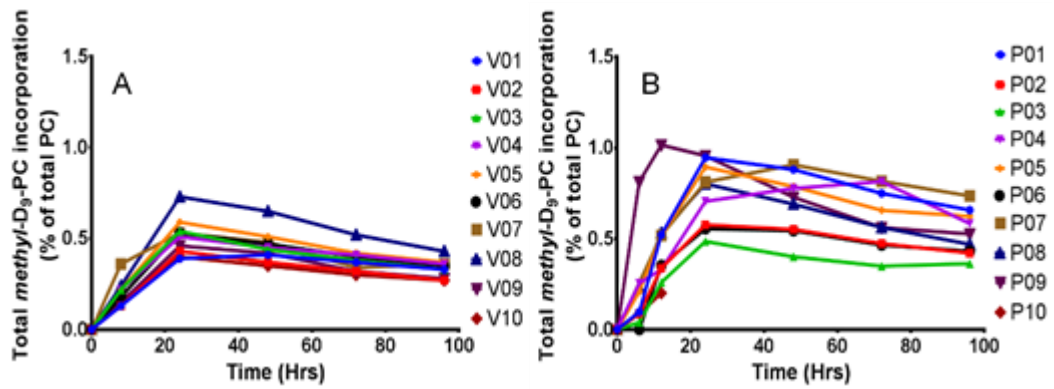


Figure 38; Individual variation in plasma total *methyl-D₉* PC incorporation among healthy controls (N=10) (A) and patients (N=10) (B) over time.

Although there was a trend suggestive of increasing plasma PC concentrations were associated with decreased *methyl-D₉* incorporations. However, this was not statistically significant. Patients tended to have higher *methyl-D₉* PC incorporation with lower plasma PC concentrations. However, in both patients and controls increases in plasma PC concentrations were not correlated with total PC *methyl-D₉* incorporation (Figure 39). This implies that plasma PC concentrations may not solely dependent on the endogenous PC synthesis by CDP-choline pathway, as assessed by total *methyl-D₉* PC incorporation.

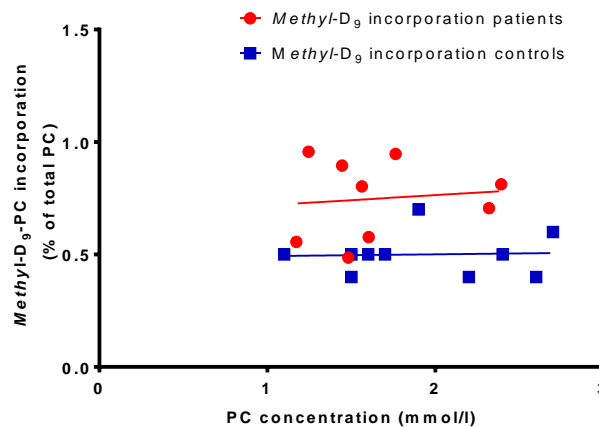


Figure 39; Correlation between plasma phosphatidylcholine concentrations and peak total *methyl-D₉* PC incorporations (T=24). There was no significant correlation between plasma PC concentration and *methyl-D₉* incorporation at peak (T=24) for both patients (N=9) and controls (N=10) as assessed by Pearson’s correlation coefficient. Blue dots - controls and red dots- patients.

The fractional *methyl-D₉* incorporation was calculated from the *methyl-D₉* labelled PC fraction corrected for the unlabelled PC. As these calculations were dependent on the unlabelled endogenous composition, any changes in the latter will likely to influence the calculations above. There was evidence that some PC species had much lower endogenous unlabelled fractional concentrations than others. For instance, the concentrations of PC16:0/18:2 and PC18:0/18:2 were significantly reduced in patients and would have influenced the calculations for fractional incorporations. For this reason, absolute *methyl-D₉* PC concentration, which directly reflects the labelled PC material was also measured. When absolute *methyl-D₉* PC concentrations were corrected for the control values, a different pattern emerged. This showed a selective increase in the labelling of several PC species by CDP-choline pathway. Particularly, fractional *methyl-D₉*-concentrations of PC16:0/18:1 and PC18:0/18:1 was significantly increased, when compared to controls and demonstrated a hierarchy of selectivity in PC labelling via CDP-choline pathway. This was in the order of: monounsaturated PC species PC18:0/18:1>PC16:0/18:1, di-unsaturated species PC18:0/18:2> PC18:1/18:2> PC16:0/18:2 and among PUFA based PC species, PC18:0/22:6> PC18:0/20:4> PC18:1/20:4> PC16:0/20:4. There was no increase in fractional concentrations of *methyl-D₉* PC16:0/22:6 in patients (Figure 40).

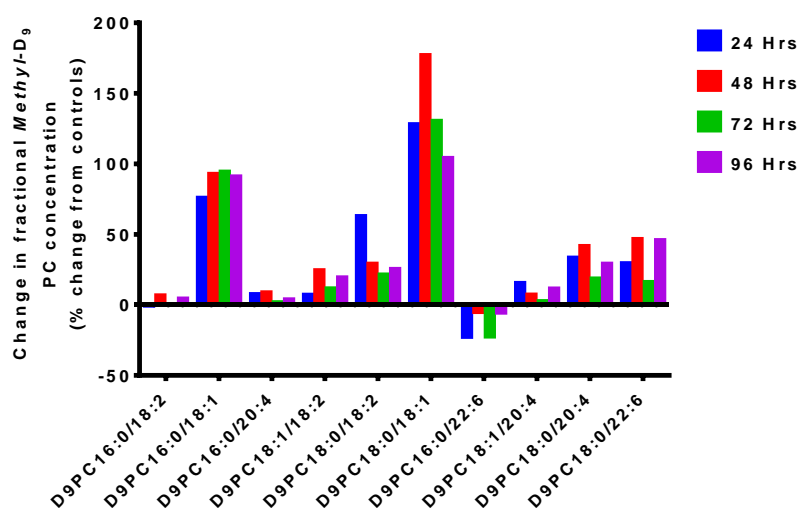


Figure 40; Plasma fractional *methyl-D₉*-phosphatidylcholine concentration changes (mean) from control values (mean) for appropriate times. Expressed as % change from control values for each time points. Patients N=10, Controls N=10.

In controls, 1-alkyl 2-acyl PC species *methyl-D₉*-incorporation was linear until 24 hours ($r^2=0.9990$, $p<0.02$), peaked at 48 hours at $0.31\pm 0.05\%$ and achieved a steady state of incorporation after 48 hours until 96 hours (Figure 41). These PC species had much slower and overall lower rate of incorporation compared to diacyl PC species. The steady state of incorporation suggests a continued *methyl-D₉* incorporation of recycled material.

Patients had similar incorporation pattern, but with much higher incorporation at all-time points. At peak incorporation (48 hours) it was 84% higher in patients at 0.57 ± 0.05 compared to controls (Figure 41). The assessment of fractional incorporation of individual species showed a pattern similar to that of diacyl-PC species. The sn-2 monounsaturated species had the highest incorporation followed by di-unsaturated, and finally the polyunsaturated species had much slower and lower rate of incorporation. Overall patients had higher incorporation in all 1-alkyl 2-acyl PC species compared to healthy controls (Figure 42).

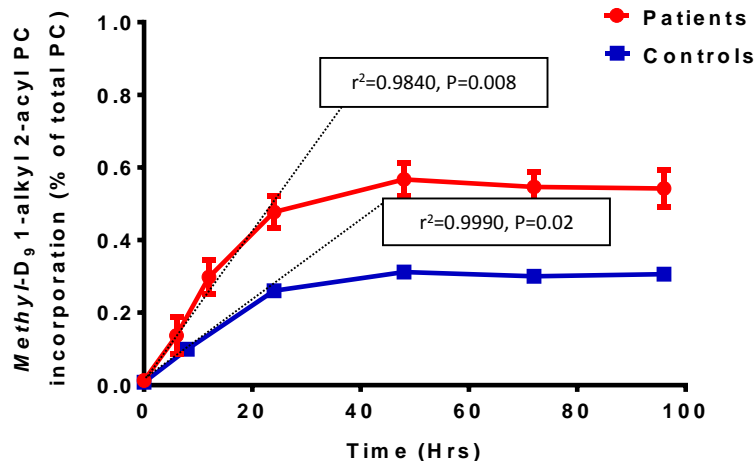


Figure 41; Comparison of plasma 1-alkyl 2-acyl *methyl-D₉*-phosphatidylcholine incorporation for patients (N=10) and controls (N=10). Data presented as mean \pm SEM. Both patients and control group showed as linear increase ($r^2=0.9840$, $P=0.008$ and $r^2=0.9990$, $P=0.02$ respectively) until 24 hours followed by a steady state incorporation.

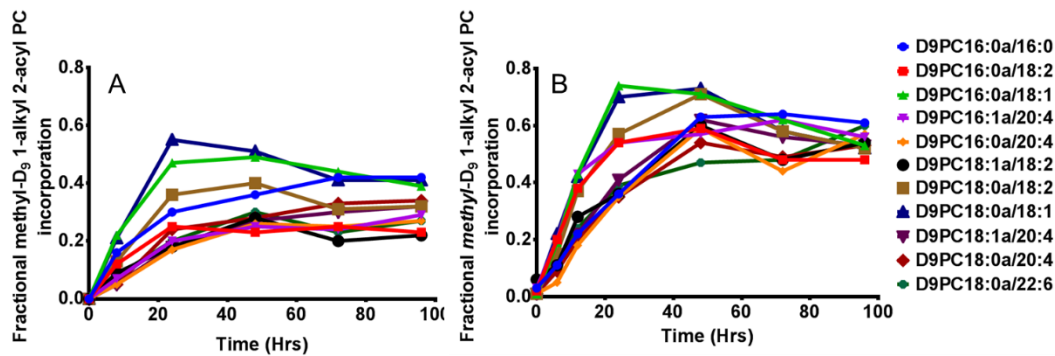


Figure 42; Fractional *methyl-D₉* incorporation of plasma 1-alkyl 2-acyl phosphatidylcholine in healthy controls (N=10) (A) and patients (N=10) (B).

4.4.3.2 Molecular specificity of PC synthesis via CDP-choline pathway

The fraction of *methyl-D₉* labelled PC primarily consisted of PC16:0/18:2, PC16:0/18:1, PC18:0/18:2 and PC16:0/20:4. In controls, PC16:0/18:2 is the principle PC. However, in patients, there was an increase in relative composition of PC16:0/18:1 at earlier time points, exceeding the PC16:0/18:2 until 24 hours. Although PC16:0/18:2 fractional synthesis remained relatively stable throughout the time course in both groups, overall composition was much lower in patients than controls (Figure 43).

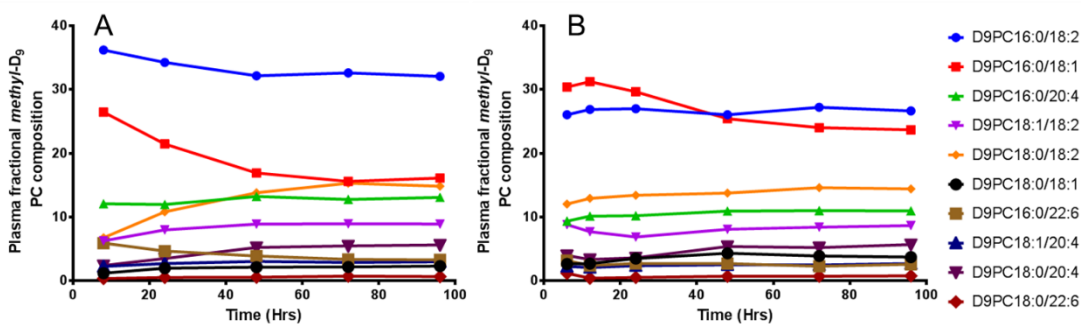


Figure 43; Fractional composition of *methyl-D₉* labelled phosphatidylcholine in plasma from healthy controls (N=10) (A) and patients (N=10) (B).

4.4.4 Characterisation of PEMT pathway

The infused *methyl-D₉*-choline is oxidised to betaine in the liver. Further metabolism of betaine via dimethylglycine by the action of betaine homocysteine S-methyltransferase (3HMT) yields a single *methyl-D₃* (M+3) labelled methionine. The subsequent generation

of S-adenosylmethionine is an important methyl donor for the synthesis of PC via PEMT pathway (Figure 5). PC synthesised this way can be quantified by precursor scans for one ($m/z187^+$) labelled *methyl-D₃* of the PC head group and two ($m/z190^+$) labelled *methyl-D₆* of the PC head group. From these relative quantifications, it is possible to characterise *methyl-D₃* and *methyl-D₆* incorporation patterns and the molecular specificity of PC synthesis from this pathway (Figure 44).

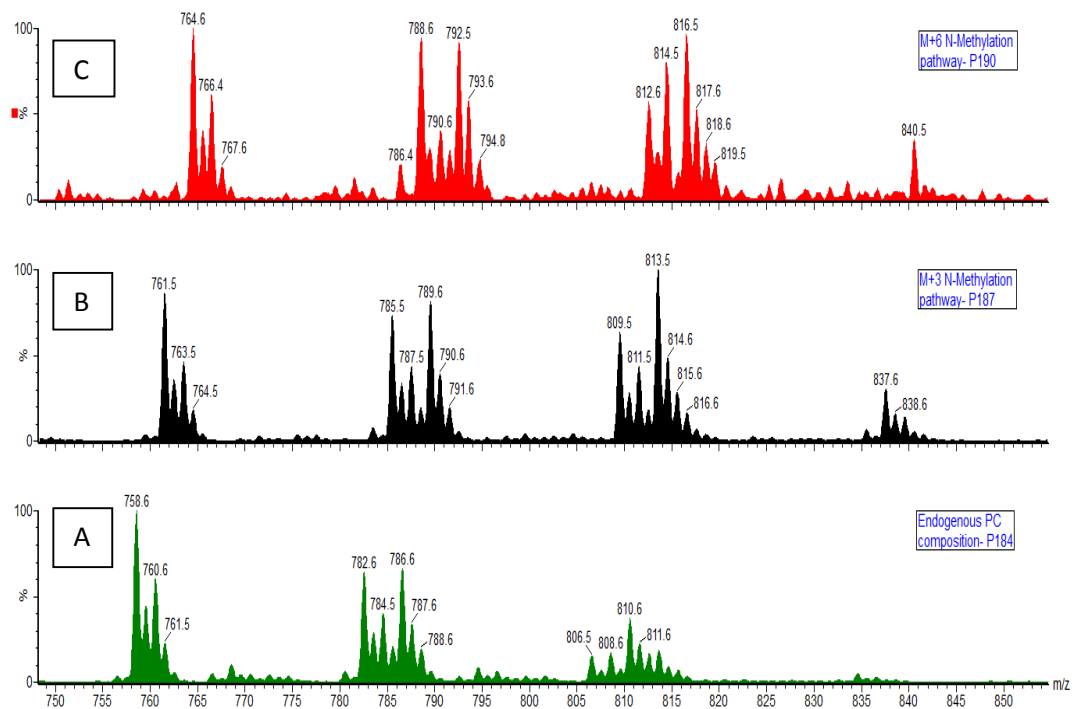


Figure 44; Spectra of precursor scans for the plasma PC composition (A) with subsequent *methyl-D₃* (B) and *methyl-D₆* (C) incorporations from healthy controls.

4.4.4.1 *Methyl-D₃* PC and *methyl-D₆* PC incorporation

The fractional *methyl-D₃* and *methyl-D₆* enrichments were much lower in patients compared to healthy controls. In controls, *methyl-D₃* PC incorporation was linear ($r^2=0.9923$, $P=0.04$), at a rate of $0.012 \pm 0.001\%/h$ until 24 hours and was maximal at 48 hours at $0.32 \pm 0.05\%$. This was followed by a linear decline in the incorporation at a rate of $0.001 \pm 0.0001\%/h$. In patients, the incorporation was a linear increase ($r^2=0.9835$, $P=0.008$) until 24 hours but with much slower rate of $0.004 \pm 0.00038\%/h$ compared to controls (Figure 45). The peak incorporation of $0.13 \pm 0.03\%$ was achieved at 48 hours,

which was only 40% of the incorporation achieved by healthy controls. After 48 hours there was a steady state of incorporation until 96 hours (Figure 45).

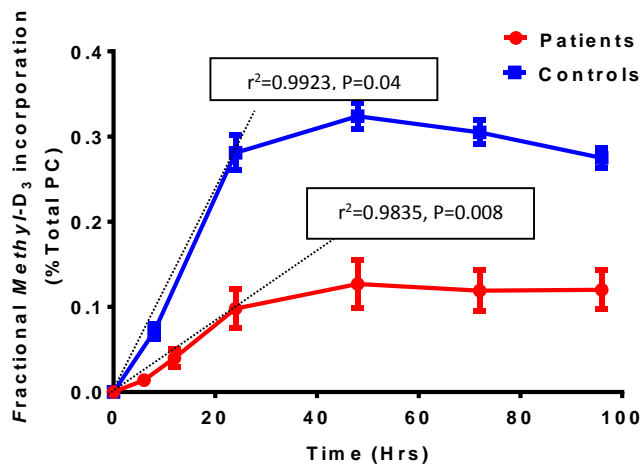


Figure 45; Plasma *methyl-D₃* phosphatidylcholine incorporation, comparison between patients (N=10) and healthy controls (N=10) over time. Data presented as mean \pm SEM. Both patients and control group, showed as linear increase ($r^2=0.9835$, $P=0.008$ and $r^2=0.9923$, $P=0.04$ respectively) until 24 hours followed by a steady state incorporation in controls and non-linear decline in patients.

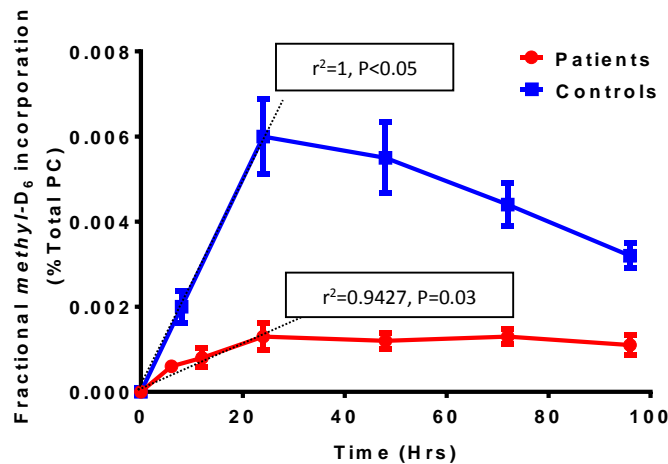


Figure 46; Plasma *methyl-D₆* phosphatidylcholine incorporation, comparison between patients (N=10) and controls (N=10) over time. Data presented as mean \pm SEM. Both patients and control group, showed as linear increase ($r^2=0.9427$, $P=0.03$ and $r^2=1$, $P<0.05$ respectively) until 24 hours followed by a steady state incorporation in patients and non-linear decline in controls. PC, phosphatidylcholine.

In controls, *methyl-D*₆ total PC incorporation was linear ($r^2=1.0$), at a rate of $25.00e^{-5}\%/h$ until 24 hours and maximal incorporation was achieved at $0.006\pm 0.0009\%$ at this time point. This was followed by a linear decline ($r^2=0.9710$) at a rate of $4.0e^{-5}\%/h$. Patient's incorporations was much lower and showed linear incorporation ($r^2=0.9427$, $P=0.03$) until 24 hours at a rate of $5.1e^{-5}\%/h$. The maximal incorporation was noted at 24 hours ($0.0013\pm 0.0003\%$) and this was only 20% of the incorporation achieved by healthy controls. This was followed by a steady state if incorporation until 96 hours (Figure 46).

4.4.4.2 Molecular specificity of *methyl-D*₃ PC and *methyl-D*₆ PC labelling

The molecular specificity of *methyl-D*₃ labelling was similar to that of *methyl-D*₆ labelling, where the PUFA containing PC species in particular the PC22:6 species, had the highest incorporation followed by PC20:4 species. The mono and di-unsaturated PC species showed much less labelling. PC16:0/20:4 incorporation showed close resemblance with mono and di-unsaturated PC species rather than other PUFA based PC species (Figures 47 and 48). For patients, the pattern of incorporation was similar to that of the controls but with a lesser relative proportion of incorporation (Figures 47 and 48).

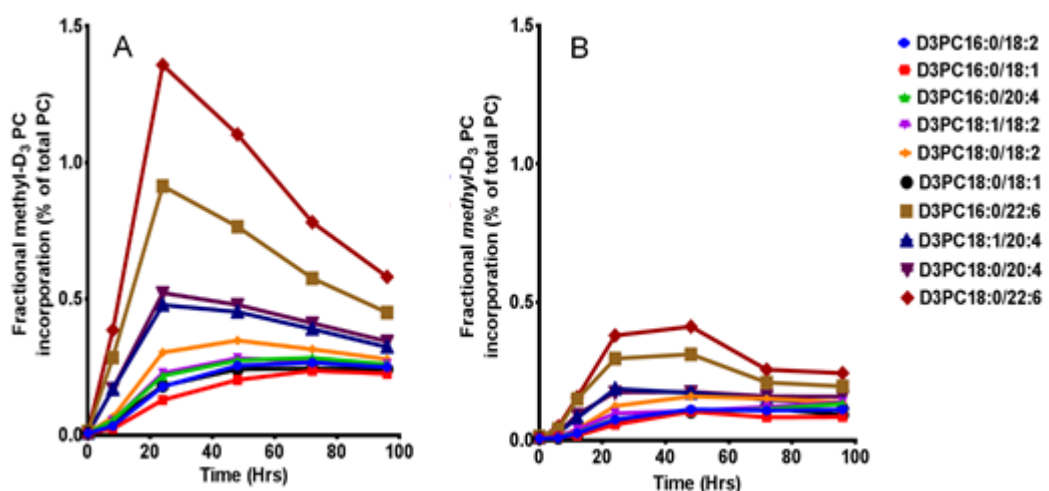


Figure 47; Plasma phosphatidylcholine fractional *methyl-D*₃ incorporation in controls (N=10) (A) and patients (N=10) (B). Compared to *methyl-D*₉ incorporation PC22:6 followed by PC20:4 based PC species have the highest incorporation in both patients and controls. But patients have a much lower *methyl-D*₃ incorporation compared to controls.

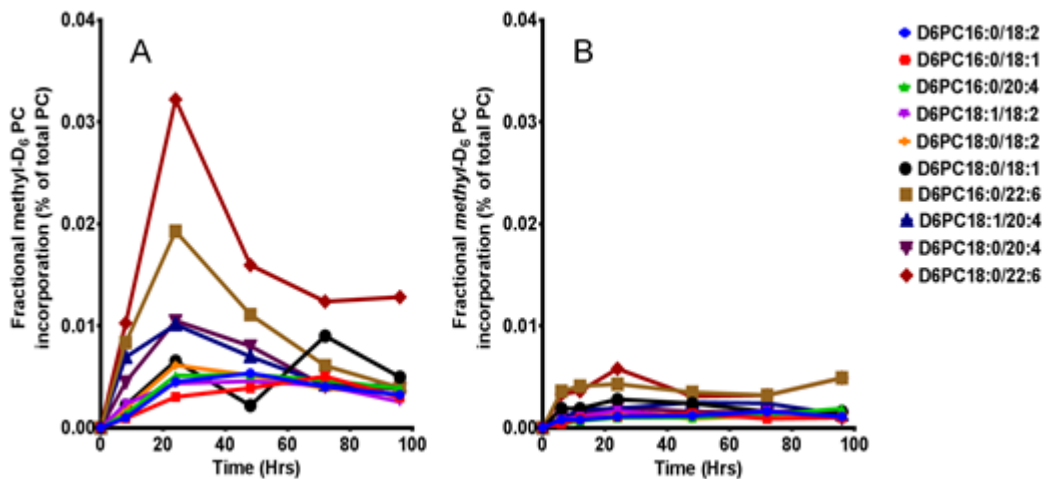


Figure 48; Plasma phosphatidylcholine fractional *methyl-D₆* incorporation in controls (N=10) (A) and patients (N=10) (B). Compared to *methyl-D₉* incorporation PC22:6 followed by PC20:4 based PC species have the highest incorporation in both patients and controls. But patients have a much lower *methyl-D₆* incorporation compared to controls.

4.4.4.3 Analytical methods

When precursor scans were used to assess fractional enrichment, the overall incorporation was much lower for the analysis of *methyl-D₆* enrichment ($m/z190^+$) in some patients. Due to this additional neutral loss scans (NL) were used to complement the assessment of *methyl-D₃* and *methyl-D₆* fractional and total incorporations. Since polyunsaturated fatty acid (PUFA) containing PC species are preferentially synthesised by this pathway, four PUFA-PC species (PC16:0/20:4, PC16:0/22:6, PC18:0/20:4 and PC18:0/22:6) were chosen to be analysed by neutral loss scans. From the NL scans, the fractional incorporation for *methyl-D₃* (M+3) and *methyl-D₆* (M+6) into these selected PC species was assessed by the quantification of peaks for the corresponding M+3 and M+6 from the unlabelled peak, after isotopic reduction. Figure 49, shows an example of a NL scan spectra for the unlabelled- PC18:0/22:6 and subsequent peaks for *methyl-D₃*-PC18:0/22:6 and *methyl-D₆*-PC18:0/22:6 plasma incorporation. Correlations graphs of NL and precursor scans suggest significant correlation between these analyses for both *methyl-D₃* and *methyl-D₆* PC enrichment for all-time points assessed, among healthy controls (*methyl-D₃*;

$r^2=0.9906$, $P<0.0001$ and *methyl-D₆*; $r^2=0.8157$, $P<0.001$) and patients (*methyl-D₃*; $r^2=0.9848$, $P<0.0001$ and *methyl-D₆*; $r^2=0.6303$, $P<0.001$) (Figure 50).

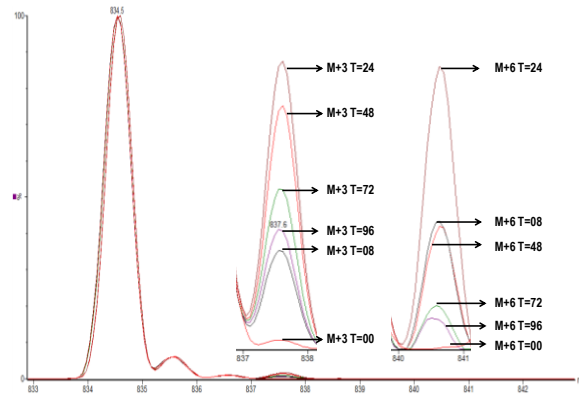


Figure 49; Neutral loss scan for PC18:0/22:6. The largest peak at m/z of 834 is the unlabelled PC18:0/22:6, subsequent peaks represent *methyl-D₃* (M+3) and *methyl-D₆* (M+6) labelled PC18:0/22:6 at various time points. The spectrum two is about 1% and peak three is 0.05% of the unlabelled peak.

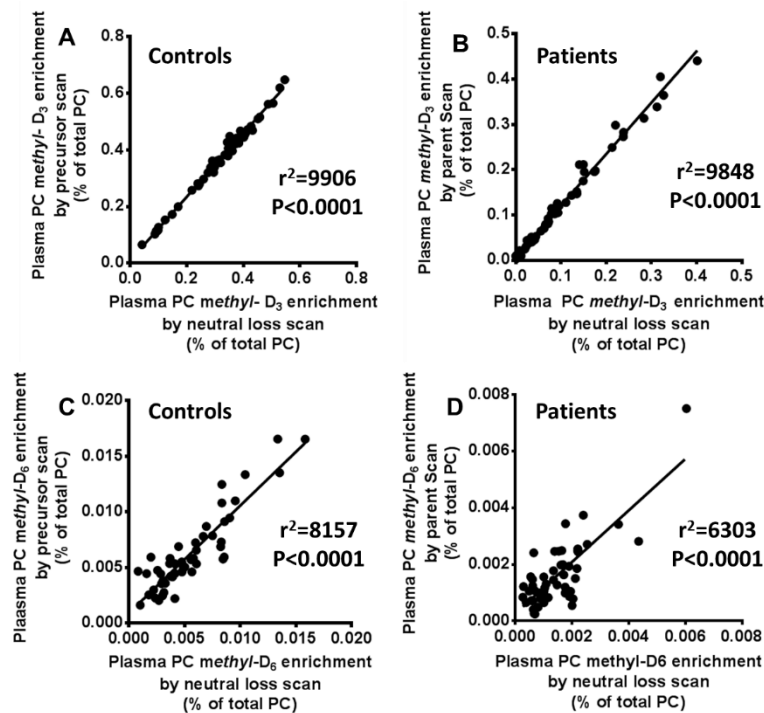


Figure 50; Correlation between precursor and neutral loss scans for plasma phosphatidylcholine *methyl-D₃* and *methyl-D₆* enrichment for controls and patients. **A**, *methyl-D₃* enrichment for controls; **B**, *methyl-D₃* enrichment for patients; **C**, *methyl-D₆* enrichment for controls; **D**, *methyl-D₆* enrichment for patients. For patients N=10 with 52 time points and controls N=10 with 50 time points. Correlation was assessed by Pearson correlation coefficient. $P<0.05$ is statistical significance.

4.4.4.4 Estimation of methyl-D₃ S-adenosyl methionine (SAM) enrichment

Both precursor and NL scans were used to estimate *methyl-D₃-SAM* enrichment in healthy controls and patients. The *methyl-D₃-SAM* enrichment was estimated by parent scans of P187 for *methyl-D₃* and P190 for *methyl-D₆* with the equation $P190/\Sigma(187+P190)$ and for neutral loss scans $M+6/\Sigma(M+6+M+3)$. The derivation of this equation for the quantification of *methyl-D₃-SAM* enrichment has been discussed elsewhere (Pynn CJ et al. 2011). There was a significant correlation between the *methyl-D₃-SAM* enrichment estimates from precursor and NL scans in both controls ($r^2=0.7838$, $P<0.0001$) and patients ($r^2=0.8432$, $P<0.0001$) (Figure 51). For the controls, when measured by neutral loss scans, the *methyl-D₃-SAM* enrichment was maximal at 6 hours and subsequently showed exponential decay, with a half-life of 30.5 hours and a rate constant (k) of $0.023(\pm 0.01)\%/h$. The *methyl-D₃-SAM* enrichment for patients was maximal at the earliest time point similar to controls. However, there was a rapid decline with much shorter half-life of 3.9 hours and a higher rate constant (k) of $0.18(\pm 0.04)\%/h$ compared to healthy controls (Figure 52). Both mass spectrometry analytical methods were consistent for the assessment of *methyl-D₃* and *methyl-D₆* PC enrichment, which has enabled the estimation of *methyl-D₃* SAM enrichment.

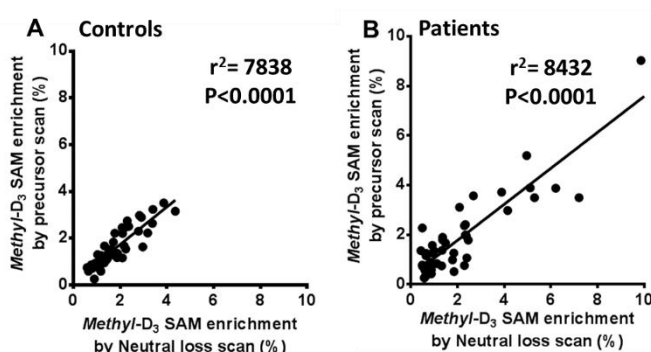


Figure 51; *Methyl-D₃* S-adenosyl methionine enrichment for all time points in controls (A) and patients (B). For patients N=10 with 47 time points and controls N=10 with 50 time points. Correlation was assessed by Pearson correlation coefficient. $P<0.05$ is statistical significance. PC, phosphatidylcholine; PEMT, phosphatidylethanolamine N-methyltransferase; SAM, S-adenosyl methionine

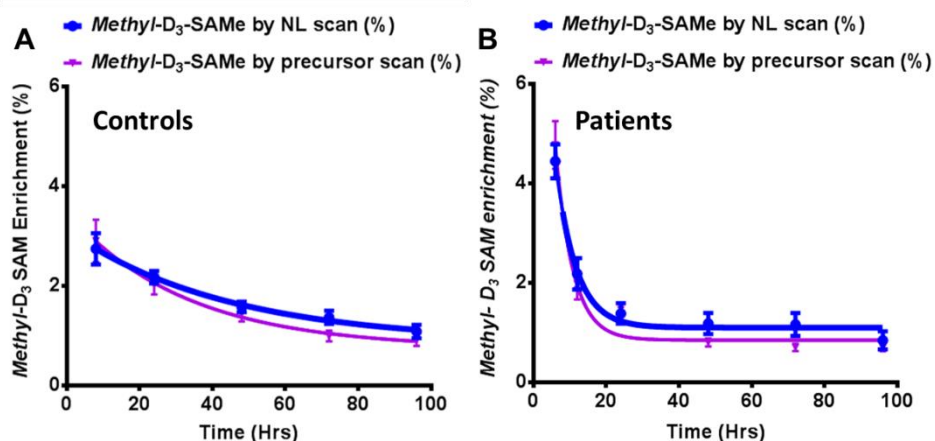


Figure 52; *Methyl-D₃* S-adenosyl methionine enrichment in controls (A) and patients (B) as estimated by both precursor and neutral loss scans. There was no significant difference between these two mass spectrometry analytical modes for the estimation of S-adenosyl methionine enrichment. Data presented as mean \pm SEM. Patients N=10, Controls N=10.

4.4.4.5 Total PC flux through PEMT pathway

As there was no significant difference between the both analytical modes for the estimation of *methyl-D₃* SAM enrichment, subsequent calculations of total PC flux through PEMT pathway was estimated only using precursor scans. Total flux of PC through the PEMT pathway was estimated by using *methyl-D₃*-SAM enrichment values corrected for the corresponding *methyl-D₃* enrichment. The maximal total PC synthesis in controls was $25 \pm 1\%$ of total PC at 96 hours (Figure 53A). The total rate of synthesis was $0.3 \pm 0.04\%/h$ up to 8 hours and was maximal at 24 hours $0.52 \pm 0.04\%/h$. There was a linear decline from 24-96 hours ($0.003 \pm 0.0005\%/h$, $r^2 = 0.9699$, $P < 0.0001$) (Figure 53B).

In patients, the flux through PEMT pathway was globally reduced for all PC species. The maximal total PC synthesis via PEMT pathway was $14 \pm 9\%$ at 96 hours (Figure 53A). This is an absolute decline of 44% when compared with controls. The rate of synthesis was non-linear and maximal at 24 hours at $0.34 \pm 0.27\%/h$. This was followed by a linear decline between 24-96 hours at $0.002 \pm 0.0003\%/h$ (Figure 53B). There was variation among patients in total PC synthesis, where some patients had significantly lower proportion of PC synthesised by this pathway (Figure 54).

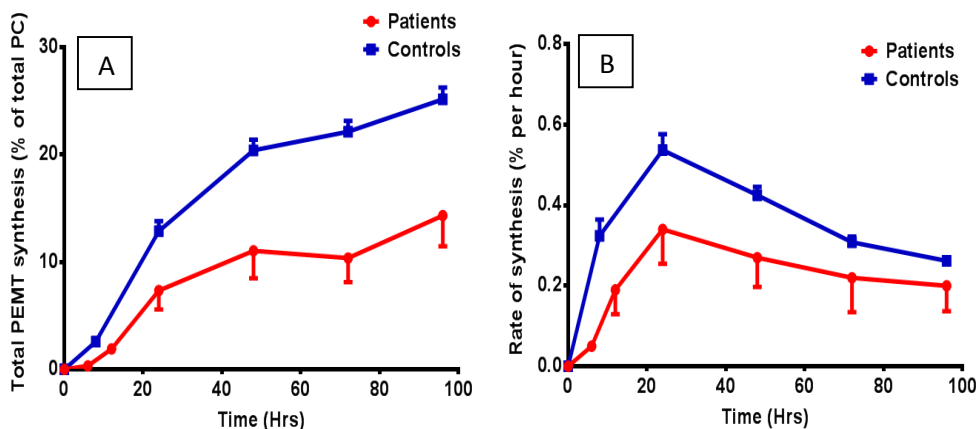


Figure 53; Fractional synthesis (A) and rate of synthesis (B) of phosphatidylcholine via phosphatidylethanolamine N- methyltransferase pathway. Expressed as mean \pm SEM percentage of total PC and rate of PC synthesis mean \pm SEM of total PC /h. Patients N=10, controls N=10. PC, phosphatidylcholine; PEMT, phosphatidylethanolamine N-methyltransferase

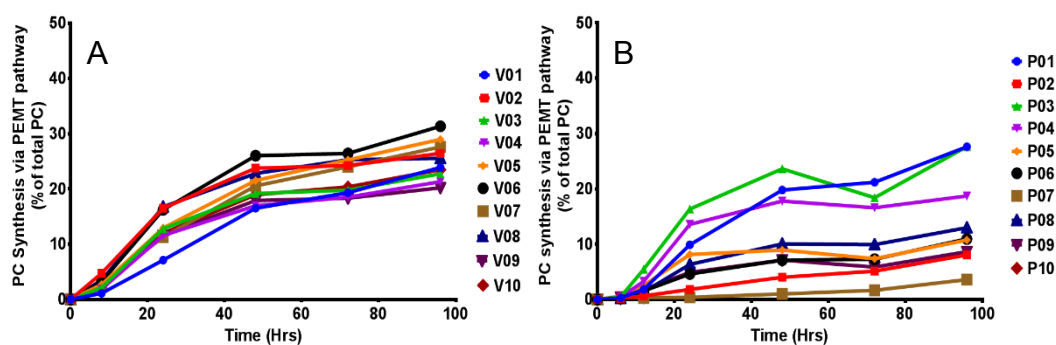


Figure 54; Individual variation in total phosphatidylcholine synthesis (% of total PC) by phosphatidylethanolamine N- methyltransferase pathway among controls (N=10) (A) and patients (N=10) (B). PC, phosphatidylcholine; PEMT, phosphatidylethanolamine N-methyltransferase

4.4.4.6 PC Molecular specificity of PEMT flux in patients

There were significant variations in PC synthesis via PEMT pathway between individuals, and each molecular species even in healthy controls. The molecular biosynthesis showed a particular pattern, where PC22:6 followed by PC20:4 species were much higher than mono or di-unsaturated species. Maximal synthesis was noted at 96 hours for most PC species and for this time point the fractional synthesis was PC18:0/22:6 (53%), PC16:0/22:6 (41%), PC18:0/20:4 (31%), PC18:1/20:4 (30%), PC16:0/18:2 (22%) and

PC16:0/18:1 (21%) (Figure 55). Same methodology was used to assess PEMT synthesis in patients with ARDS.

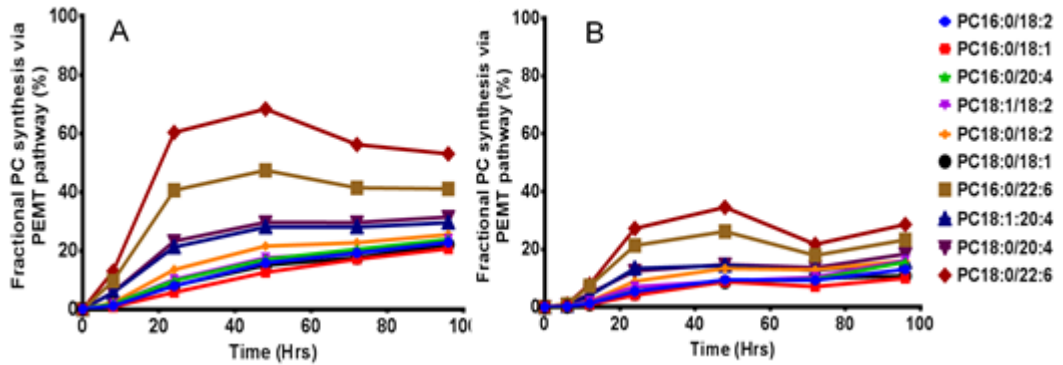


Figure 55; Molecular specificity of labelled phosphatidylcholine by phosphatidylethanolamine N- methyltransferase pathway in controls (N=10) (A) and patients (N=10) (B). PC, phosphatidylcholine.

4.5 Discussion

Patients with ARDS had significantly lower plasma PC, total cholesterol, LDL-cholesterol and HDL-cholesterol concentrations (Table 13 and Figure 29). PC metabolism was also significantly altered with increased flux through CDP-choline pathway, and subsequent changes in overall plasma PC composition. In addition, there was a global reduction in PC synthesis by PEMT pathway. This is the first study to demonstrate these findings in patients with ARDS.

Several studies have suggested systemic inflammatory response is associated with reduction in the circulating levels of cholesterol, LDL and HDL concentrations which correlates with disease severity (Gordon BR et al. 1996). In addition to these findings, studies have also shown that there were reductions in cholesterol synthesis, apoA-1, apoA-2, LCAT, CETP, LPL activity and changes in reverse cholesterol transport in LPS and endotoxemia induced sepsis models (Wendel M et al. 2007). Contrary to these, triacylglycerol concentrations may be increased during sepsis and critical illness and possibly due to increased synthesis by the liver as an acute phase response (Khovidhunkit W et al. 2004). Although the results presented here does agree with previous studies, this

is the first study to show these findings in ARDS patients (Figure 31). From the results above, it is possible to conclude that in patients with ARDS, there are significant alterations in lipid metabolism, which may have potential therapeutic value in the future. For instance, dietary or therapeutic modifications to augment HDL and reverse cholesterol transport may potentially alter clinical outcome. HMG-CoA reductase inhibitors and polyunsaturated fatty acids such as EPA and DHA may modify circulating plasma lipids and have been shown to modulate systemic inflammatory response (Mermis JD and Simpson HQ 2012) (Calder PC 2012).

The reductions in the plasma PC concentrations were not uniform. There were selective increases in the concentrations of monounsaturated PC species (PC16:0/18:1 and PC18:0/18:1), coupled with significant reductions in polyunsaturated PC species in patients (Figure 28). These changes were also seen in alkyl PC species, where sn-2 arachidonyl species (PC16:1a/20:4, PC16:0a/20:4, PC18:1a/20:4) were reduced with increases in PC16:0a/18:1 and PC18:0a/18:1 were noted in patients. These findings indicate that there are specific changes in plasma PC molecular concentrations in patients with ARDS and the clinical consequence of these changes are not clear.

PC synthesis from CDP-choline pathway is characterised by the incorporation of *methyl-D₉* choline chloride into plasma PC. There was a 50% increase in *methyl-D₉* incorporation into plasma PC in patients, suggesting increased flux through this pathway (Figure 35). However, despite this increase, the total plasma PC concentrations remained low. One possible reason for this could be increased utilisation of PC by cells to produce inflammatory mediators. But this was not evident in the rate of hydrolysis of labelled PC which was similar to that of controls. The fractional synthesis of two PC species (PC16:0/18:1 and PC18:0/18:1) were significantly increased compared to controls (Figure 40). This is also a reflection of the unlabelled PC composition, and suggesting a selective increase in their synthesis via CDP-choline pathway.

PEMT is an intracellular organelle membrane bound enzyme that catalyses sequential methylations leading to the conversion of PE to PC in the liver (Li Z and Vance DE 2008). PEMT knockout mice models provided novel insights into the importance of this previously thought aberrant PC synthetic pathway (Walkey CJ et al. 1997). These studies highlight not only the significance of PEMT activity in states of choline deprivation, but also provide supporting evidence for the requirement of this pathway for VLDL secretion from the liver (Vance DE 2013). Although there are functional similarities between both CDP-choline and PEMT pathways, the molecular specificity of PC secreted into plasma from these pathways show a substantial compositional variation (Pynn CJ et al. 2011).

Studies investigating PC biosynthesis and molecular variations between these synthetic pathways are lacking, and are not fully explored in humans. This is due to the lack of accessibility of human hepatic tissue and methodological limitations in determining *in-vivo* PEMT activity. Since hepatic PC synthesised from PEMT is predominantly polyunsaturated, plasma PC-DHA concentrations have been shown to reflect hepatic PEMT activity (da Costa KA et al. 2011). Others have utilised stable isotope labelling with combination of isotope ratio mass spectrometry (MS) and multiple isotopomer distribution analysis (MIDA) to determine *in-vivo* triacylglycerol synthesis and VLDL secretion from the liver (Parks EJ and Hellerstein MK 2006). However, both of these methods are limited by the lack of information regarding dynamic hepatic PC synthesis and turnover. Stable isotope labelling of choline with deuterium and analytical methods using ESI-MS/MS has enabled assessment of hepatic PC molecular synthetic patterns in isolated rat primary hepatocytes and more recently in healthy human volunteers (Pynn CJ et al 2011). However, this is the first study to utilise this methodology and demonstrate the feasibility of performing such investigations to assess PC molecular synthetic patterns in a specific disease cohort, characterised by systemic inflammatory response with severe hypoxic respiratory failure.

The assessment of *methyl-D₃* and *methyl-D₆* deuterium labelling enabled the estimation *methyl-D₃-SAM* enrichment in the liver. The assessments of *methyl-D₃-PC*, *methyl-D₆-PC* and the estimation of *methyl-D₃-SAM* enrichment were highly correlated between both methods (neutral loss and precursor scans) in healthy controls and patients (Figures 50, 51 and 52). However, in patients, it was not possible to assess *methyl-D₆* PC enrichment reliably by precursor scans of $m/z190^+$ due to low signal intensity. Consequently, specific NL scans were used for a selective group of PUFA containing PC to estimate the *methyl-D₃-SAM* enrichment in the liver. Despite significant correlation between these two ESI-MS/MS analytical modes for the estimation of *methyl-D₃-SAM* enrichment, the variation was much smaller, particularly at earlier time points with NL scan. Nevertheless, the results were reassuring as both ESI-MS/MS analytical methods yielded similar low values for *methyl-D₆* enrichment with significant correlation ($P<0.0001$) in both patients and controls (Figure 50).

In addition to a decreased total PC concentration, there were lower concentrations of PUFA based PC species, with global reduction in the total PC flux through PEMT pathway in most patients (Figures 29, 30 and 53). This could be due to several reasons. Firstly, ARDS patients tend to have multi-organ involvement including hepatic dysfunction and this reduction in synthesis may be an indication of the degree of hepatic synthetic dysfunction endured. Only one patient in our study had clinically overt liver failure and this patient had dramatically reduced PEMT PC synthesis. Other patients with reduced PEMT PC synthesis had no significant evidence of liver enzyme abnormalities in their plasma. It is possible, that this reduction in PEMT activity may be a reflection of early hepatic synthetic dysfunction prior to biochemical evidence of liver damage. Other possibility is the lack of available SAM for optimal hepatic PC synthesis. The *methyl-D₃-SAM* enrichment in patients was higher at earliest time point and showed a rapid decline until 24 hours, followed by a steady state decay which is lower than that of controls, indicating that SAM may be prioritised for other methyl dependent pathways (Figure 52).

Recent randomised controlled studies suggest a lack of clinical response from external supplementation of dietary PUFA in patients with ARDS (Rice TW et al. 2011). Despite this, one can postulate, that there may be underlying phenotypes with reduced alterations in hepatic PC synthesis coupled with lower endogenous concentrations of PUFA based PC in ARDS. Inadequate secretion of endogenous PUFA may have clinical implications (i.e. may prolong the natural progression/ or delay resolution), which has not been investigated before.

4.6 Conclusions

This chapter demonstrates significant alterations in the plasma lipoproteins and PC molecular composition in patients with ARDS. Enrichment studies illustrate changes in PC metabolic pathways with increased flux through CDP-choline coupled with reductions in hepatic PC synthesis by PEMT pathway. These novel analytical methods presented here enabled a non-invasive approach, to the assessment of hepatic PC synthesis and quantification of S-adenosyl methionine enrichment. This study highlights the feasibility of using stable isotope labelling with combination of ESI-MS/MS technology, to characterise hepatic PC metabolic pathways in a specified disease cohort.

CHAPTER 5

Cellular phospholipid profile and turnover in patients with Acute Respiratory Distress Syndrome

5.1 *Introduction*

Mammalian cell membranes composed of a mixture of glycerophospholipids and proteins. PC followed by PE are the most abundant glycerophospholipids (Hermansson M et al. 2011). The relative molecular composition of membrane phospholipids can vary between cells, and depends on the function of that particular cell. In addition to the structural role, membrane phospholipids are involved in cellular regulatory mechanisms. For instance, phosphatidic acid generated by the action of phospholipase-D on membrane PC results in the activation of neutrophil NADPH oxidase, a membrane bound enzyme complex involved in activation of neutrophils and the respiratory burst oxidase response (McPhail LC et al. 1993). Additionally, phospholipase-A₂ induced hydrolysis of membrane phospholipids generates arachidonic acid mediated pro-inflammatory active metabolites such as prostaglandins, thromboxanes and leukotrienes and resolution mediators such as E and D- series resolvins (Uddin M and Levy BD 2011).

The composition of membrane phospholipids can be manipulated with external supplementation of fatty acids and has been demonstrated in several in-vitro cell lines (Spector AA and Yorek MA 1985). This suggest that cells are readily capable of either de-novo PC biosynthesis, or remodelling of endogenous phospholipids according to their functional need. Importantly, the plasma PC changes evident in ARDS patients may lead to alterations in circulating inflammatory cell phospholipid profile and synthesis. These

changes may have clinical implications for both underlying pathophysiology of ARDS disease processes and the possibility for potential therapeutic targets in the future.

There were significant alterations in plasma PC molecular composition, with altered hepatic PC synthetic pathways in patients with ARDS, as demonstrated in Chapter Four. Consequently, this chapter aims to assess the impact of these plasma PC alterations on composition and turnover of cellular phospholipids from circulating peripheral red blood cells (RBC), CD15+ neutrophils and CD3+ T-lymphocytes. Furthermore, specific PC molecular changes and cell surface expression of activation markers following external free fatty acid supplementation in ex-vivo human neutrophils were also assessed.

5.2 Objectives

The objectives of this chapter are to assess the following;

1. Phospholipid profile of peripheral red blood cell, CD15+ neutrophil and CD3+ lymphocyte populations in ARDS
2. Dynamic cellular PC turnover in ARDS
3. Molecular specificity of PC biosynthesis following supplementation of free-fatty acids in isolated CD15+ neutrophils from healthy volunteers
4. Alterations of whole blood neutrophil's surface expressions of CD62L, CD11a and CD11b following incubation with free fatty acids

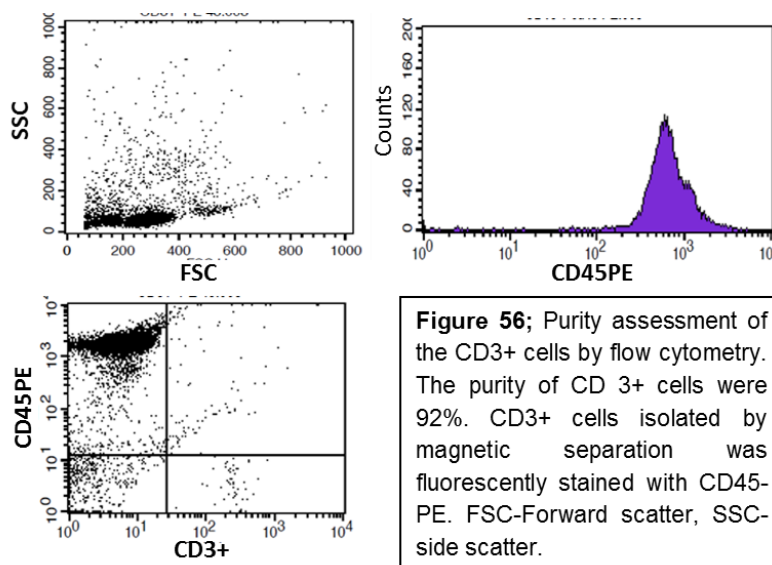
5.3 Summary of methods

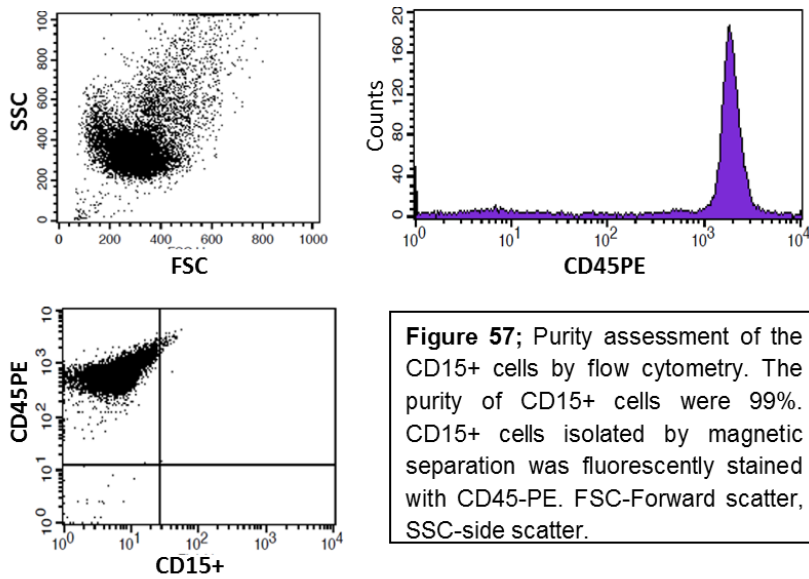
Two ml of blood samples were collected in EDTA specimen bottles at base line and 6, 12, 24, 48, 72 and 96 hours after *methyl-D₉* choline infusion for ARDS patients and at 8, 24, 48, 72 and 96 hours for healthy controls. Red blood cells were extracted from the 100µl of packed cell pellet formed when whole blood was centrifuged at 400g at room temperature for 15 minutes. They were then washed with 0.9% saline (w/v) followed by repeated centrifugation twice prior to lipid extraction. 1ml of whole blood was used to purify CD15+ neutrophils and CD3+ T-lymphocytes by magnetic bead antibodies using

AutoMACS automated cell separator (Miltenyibiotec). Peripheral blood CD15+ neutrophils were also isolated from healthy volunteers who did not have choline infusion and were incubated with 0.5mg of *methyl-D₉* choline chloride at 37°C for 3 hours, separately supplemented with 30µM of palmitate, oleate, linoleate and arachidonate. Total lipid was extracted from all cell populations by modified Bligh and Dyer method after addition of PC14:0/14:0 as internal standard. RBC phospholipids were analysed by direct infusion with diagnostic ESI-MS/MS scans. However, due to the small quantity of cells compared to RBC, only PC composition was assessed for both CD15+ neutrophils and CD3+ lymphocytes by ESI-MS/MS with nanoflow infusion. The purity of neutrophils and lymphocytes subpopulations was assessed by flow cytometry. Neutrophil functional assessment by leukocyte surface L-selectin (CD62L) and beta-2 integrin (CD11a and CD11b) expression was also performed after incubation of whole blood neutrophils in fatty acids. For more detailed methodology see chapter 2.

5.4 Results

Purity of magnetically eluted CD3+ T-lymphocytes and CD15+ neutrophils were assessed by flow cytometry. CD15+ and CD3+ cells were fluorescently stained with CD45-PE and excellent purity was achieved reaching 99% and 92% respectively (Figures 56 and 57).





5.4.1 PC molecular compositional variation among cells

The PC molecular variation was investigated among peripheral RBC, CD15+ neutrophils and CD3+ T- lymphocytes in healthy controls (Figure 58). Seventeen major PC species were chosen for this comparison.

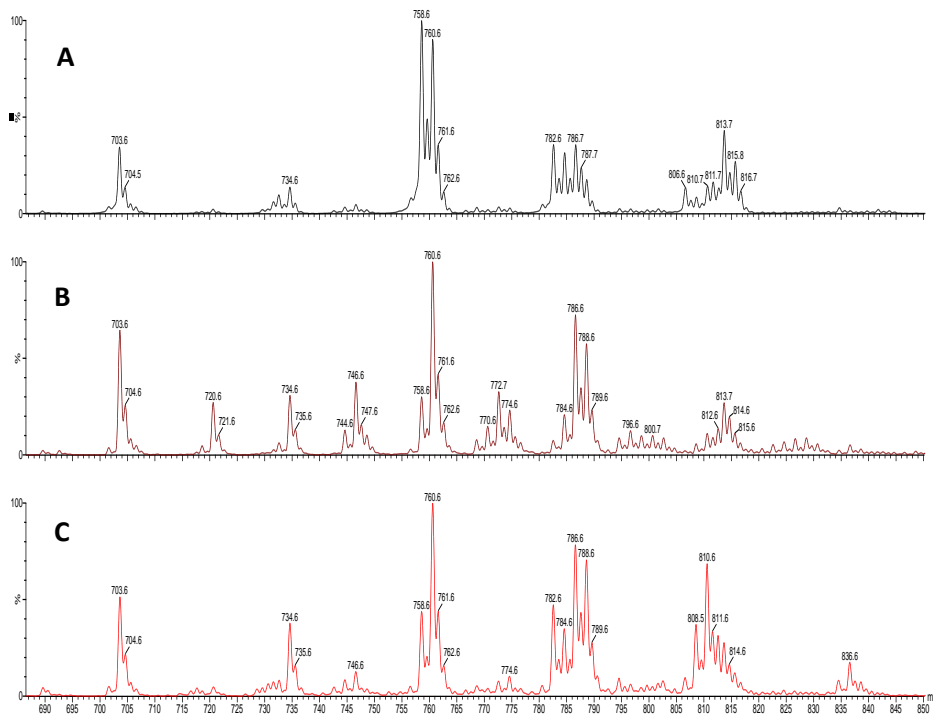


Figure 58; Example of typical mass spectra for the PC composition of red blood cells (A), CD15+ neutrophils (B), and CD3+ T- lymphocytes (C) in healthy human volunteers. Y-axis indicates signal intensity and X-axis represents mass/charge ratio (m/z).

The principle PC in both CD15+ neutrophils and CD3+ lymphocytes was PC16:0/18:1. In red blood cells PC16:0/18:2 was the major PC. The CD15+neutrophils were enriched with much higher fractional composition of 1-alkyl 2-acyl PC species (27%) compared to RBCs (4%) or CD3+ lymphocytes (7%). The CD3+ lymphocytes had much higher fractional composition of arachidonyl PC species (25%), such as PC16:0/20:4, PC18:1/20:4 and PC18:0/20:4 compared to CD15+neutrophils (6%) (Figure 59).

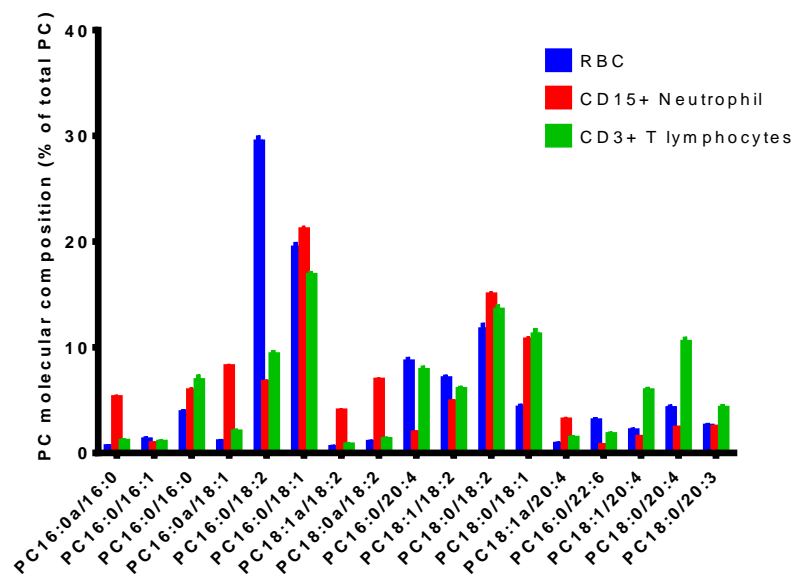


Figure 59; Phosphatidylcholine molecular composition of red blood cells (N=30), CD15+ neutrophils (N=42) and CD3+ T lymphocytes (N=36) in healthy humans, Data presented in mean ± SEM. PC, phosphatidylcholine.

5.4.2 Red blood cell phospholipid profile

Red blood cell molecular phospholipid compositions of PC, PE, PS, PI and SPH were measured with specific precursor and neutral loss scans on ESI-MS/MS and comparisons were made between patients with ARDS and healthy controls.

5.4.2.1 RBC PC fractional molecular concentration and composition

The mean total RBC PC concentration was measured using the internal standard and was $1.61 \pm 0.07 \mu\text{mol}$ for patients and $1.47 \pm 0.05 \mu\text{mol}$ for controls in 1ml of packed cell pellet.

There were no significant differences in total cumulative RBC PC concentrations between patients and controls (Figure 60).

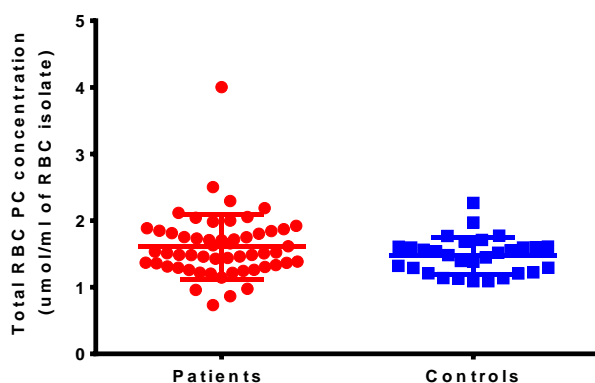


Figure 60; Comparison of red blood cell total phosphatidylcholine concentrations ($\mu\text{mol/ml}$ of packed cell pellet) for all time points measured between patients ($N=8$, 56 time points) and controls ($N=5$, 30 time points). There was no significant difference between groups as analysed by student's T-test. RBC, red blood cell; PC, phosphatidylcholine.

In healthy controls, the RBC PC molecular composition predominantly consisted of PC16:0/18:2 (31%) followed by PC16:0/18:1 (20%) and PC18:0/18:1 (12%), whereas, ARDS patient's had significantly ($P<0.0001$) elevated fractional composition of PC16:0/18:1 (25%), and decreased PC16:0/18:2 (24%). These changes were similar to that of plasma PC composition. In patients, variation in relative PC composition over time was noted for several PC species. However, this was only statistically significant ($P<0.05$) for two species (PC16:0/18:2 and PC16:0/20:4). At day 4, there were decreases in PC16:0/18:2 (12% decrease) and PC16:0/20:4 (35% decrease) compared to day one. This was only evident in patients and not in controls (Figure 61).

In red blood cells, 1-alkyl 2-acyl PC species were in much less abundance ($\sim 7\%$ of total PC) compared to diacyl PC species. The composition of these species mainly consisted of PC16:0a/18:1, PC16:0a/18:2, PC18:0a/18:2 and PC16:0a/20:4. Each of these species were $<2\%$ of total PC composition. In patients there were significant increases in PC16:0a/18:1, PC18:0a/18:2 and PC18:0a/18:1 and decreases in PC16:0a/18:2 and PC16:0a/20:4 noted compared to controls.

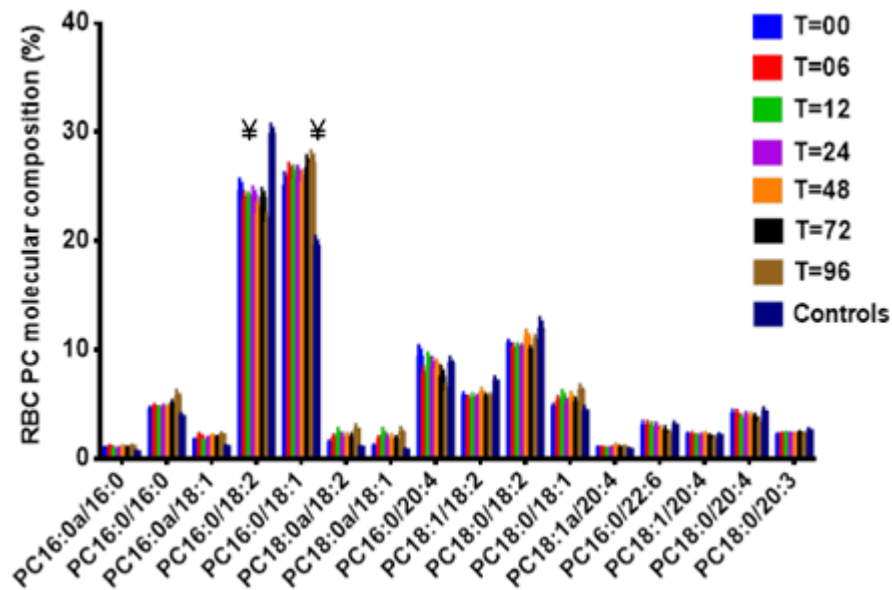


Figure 61; Red blood cell phosphatidylcholine molecular composition in patients (N=8) over time. Control data (N=5) for T=0 at enrolment. Results expressed in mean \pm SEM, * P<0.05 comparison between T=0 and T=96 in patients, ¥P<0.05 for comparison between patients and controls at T=0 as analysed by two way ANOVA of variance and corrected by Bonferroni's correction for multiple comparisons. RBC, red blood cell; PC, phosphatidylcholine.

There was a positive linear correlation between plasma PC16:0/18:1 and RBC PC16:0/18:1 concentrations in both patients and controls (patients $r^2= 0.1378$, $P=0.0053$; controls: $r^2=0.4618$, $P<0.0001$). However, patients had lesser increase in RBC PC16:0/18:1 concentration with plasma increases in PC16:0/18:1 compared to controls (Figure 62). This suggests, that RBC PC16:0/18:1 fractional concentrations may be dependent on plasma concentrations of PC16:0/18:1 and in patients RBC takes longer to equilibrate with plasma PC. There were no correlations in plasma and RBC concentrations for other PC species.

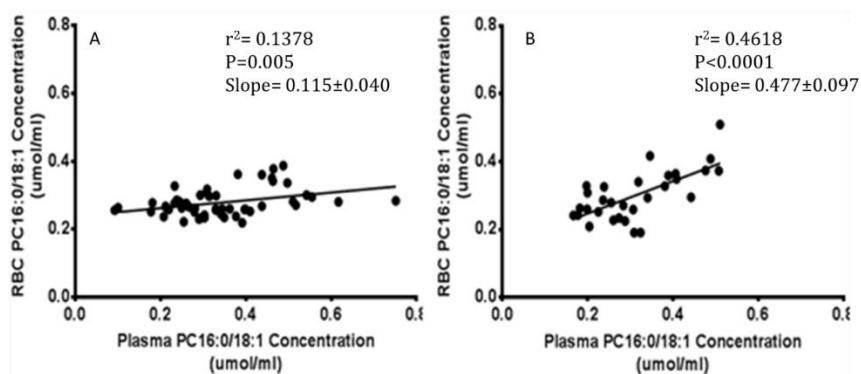


Figure 62; Correlation between plasma PC16:0/18:1 and red blood cell PC16:0/18:1 concentration ($\mu\text{mol/ml}$), in patients ($N= 8$ with 55 total time points) (**A**), controls ($N=5$ with total 30 time points) (**B**). Correlation was assessed by Pearson correlation coefficient. RBC, red blood cell; PC, phosphatidylcholine.

5.4.2.2 RBC PE, PI, PS and SPH molecular composition

The PE molecular composition was assessed by neutral loss (NL141+) scans on ESI-MS/MS and consisted of PE16:0/20:4 (13%), PE18:1/22:6 (13%), PE16:0/18:1 (11%), PE18:1/20:4 (10%) and PE18:0/20:4 (10%) (Figure 63). The molecular composition of PI was analysed by precursor scans of P241 and consisted of primarily PI18:0/20:4 (56%), PI18:0/18:2 (11%) and PI16:0/20:4 (7%) (Figure 64). There were no significant differences in PE or PI molecular composition between patients and controls. The PS molecular composition was analysed by neutral loss scans of NL87 and primarily consisted of polyunsaturated PS species, in particular PS18:0/20:4 (41%), PS18:0/22:6 (16%) and PS18:0/22:5 (11%). However, these polyunsaturated species did not differ in composition between patients and controls. Among the selected PS species, PS18:0/18:1 demonstrated higher relative composition in patients compared controls. In addition there was a time course increase in relative composition of PS18:0/18:1 among patients (Figure 65). The SPH molecular composition was characterised by precursor scans of P184 and consisted primarily of SPH24:1 (32%), SPH16:0 (29%), and SPH24:0 (19%). SPH16:0 was significantly elevated in patients compared to controls (Figure 66).

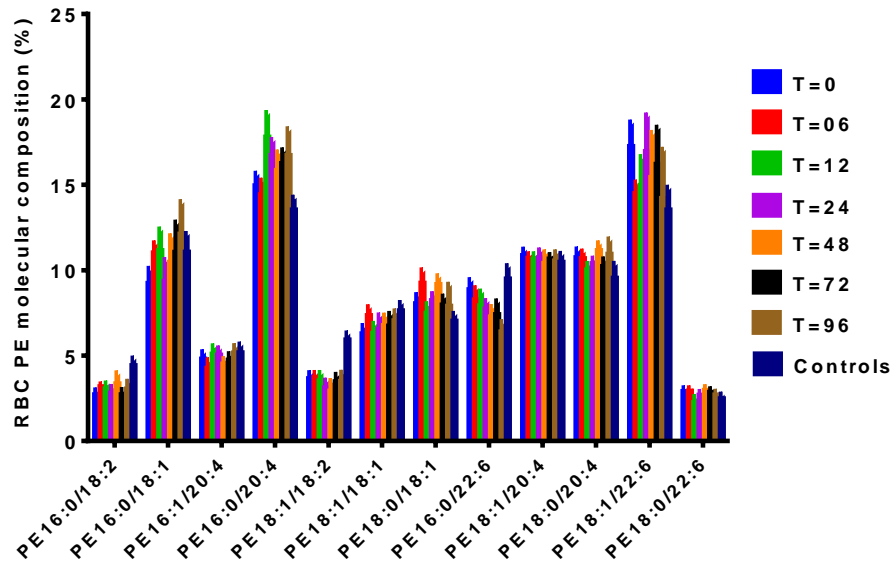


Figure 63; Red blood cell phosphatidylethanolamine molecular composition in patients (N=8) over time and control data (N=5) for T=0 at enrolment. Results expressed in mean \pm SEM, there was no significant difference for both comparisons between patients and controls at T=0 and between individual time points as analysed by two way ANOVA of variance and corrected by Bonferroni's correction for multiple comparisons. RBC, red blood cell; PE, phosphatidylethanolamine.

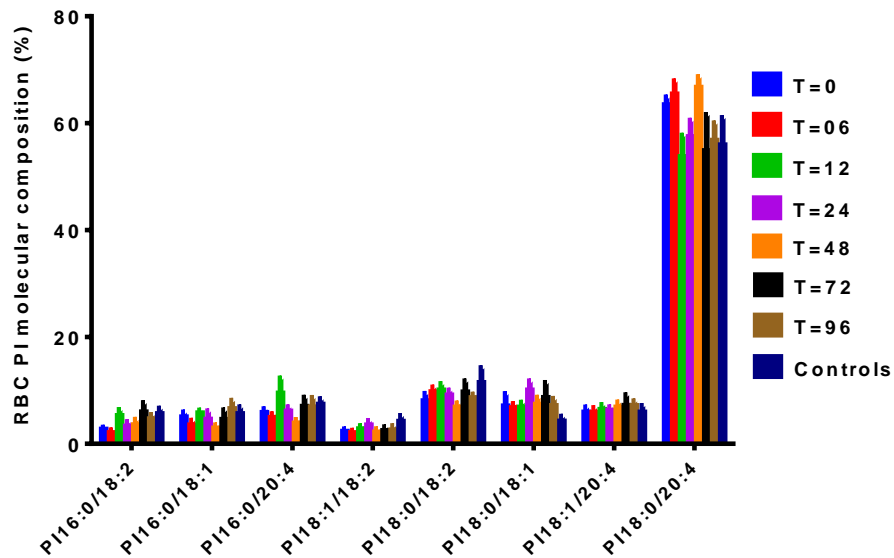


Figure 64; Red blood cell phosphatidylinositol molecular composition in patients (N=8) over time and control data (N=5) for T=0 at enrolment. Results expressed in mean \pm SEM, there was no significant difference for both comparisons between patients and controls at T=0 and between individual time points as analysed by two way ANOVA of variance and corrected by Bonferroni's correction for multiple comparisons. RBC, red blood cell; PI, phosphatidylinositol.

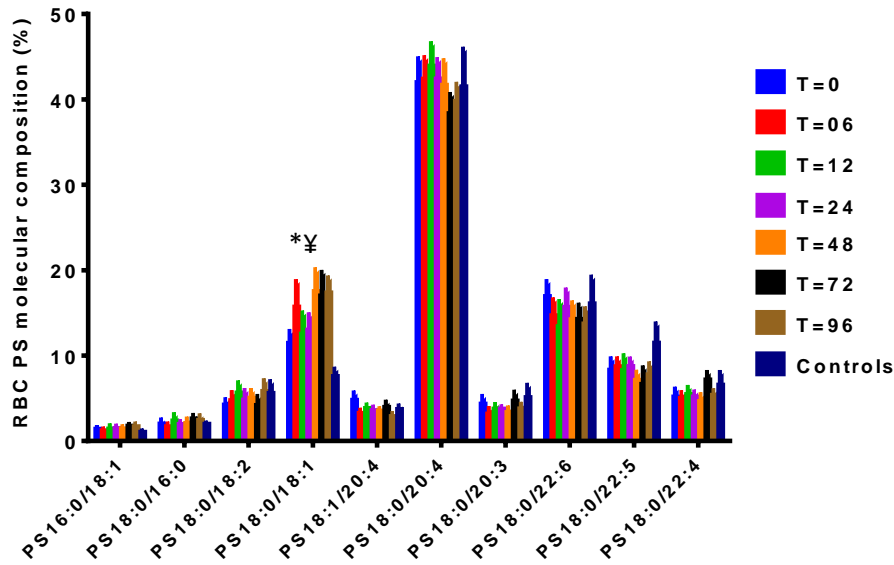


Figure 65; Red blood cell phosphatidylserine molecular composition in patients (N=8) over time and control data (N=5) for T=0 at enrolment. Results expressed in mean \pm SEM, *P<0.05 comparison between T=0 and T=96 in patients, ‡P<0.05 for comparison between patients and controls at T=0 as analysed by two way ANOVA of variance and corrected by Bonferroni’s correction for multiple comparisons. RBC, red blood cell; PS, phosphatidylserine.

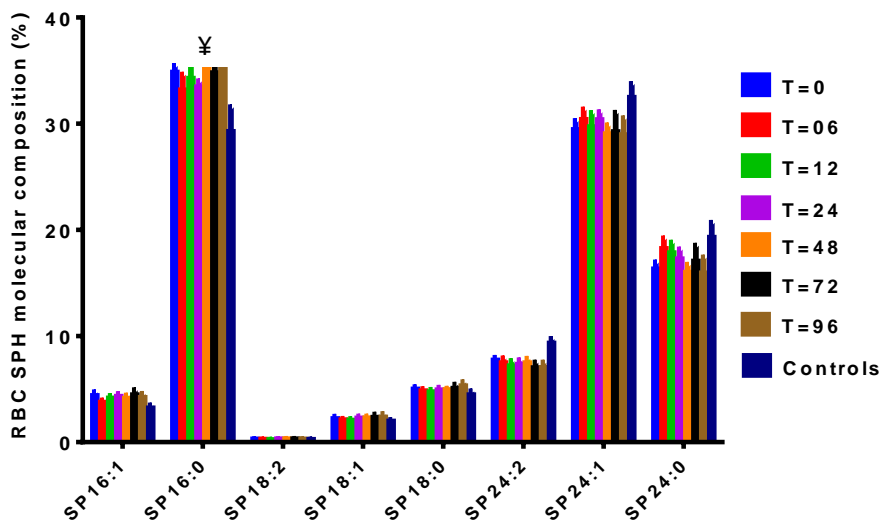


Figure 66; Red blood cell sphingomyelin molecular composition in patients (N=8) over time and control data (N=5) for T=0 at enrolment. Results expressed in mean \pm SEM, ‡P<0.05 for comparison between patients and controls at T=0 as analysed by two way ANOVA of variance and corrected by Bonferroni’s correction for multiple comparisons. RBC, red blood cell; SPH, sphingomyelin.

5.4.2.3 RBC *methyl-D₉* PC molecular composition and incorporation

In controls, PC16:0/18:2 followed by PC16:0/18:1 and PC16:0/20:4 were the major PC species among the *methyl-D₉* choline labelled fraction. In patients, there were significant increases in PC16:0/18:1 and decreases in PC16:0/18:2 compared to controls and this was a reflection of the RBC PC composition (Figure 67).

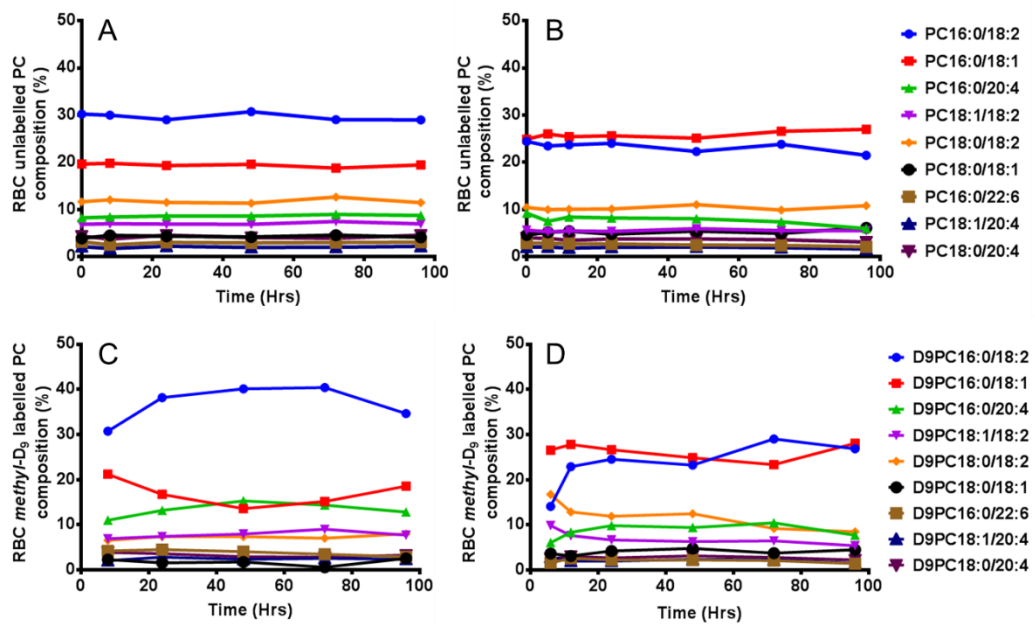


Figure 67; Time course variation of red blood cell unlabelled and *methyl-D₉* labelled phosphatidylcholine molecular composition in controls (N=5) and patients (N=8). **A;** Unlabelled PC composition for controls, **B;** Unlabelled PC composition for patients, **C;** *methyl-D₉* choline labelled PC composition in controls. **D;** *methyl-D₉* choline labelled PC composition in patients. RBC, red blood cell; PC, phosphatidylcholine.

Red blood cells lack nucleus and have no capacity to synthesise PC via CDP-choline pathway. However, they are capable of incorporating surrounding labelled PC as evidenced from studies of cultured cell lines. In controls, the *methyl-D₉* choline incorporation was noticeable at 8 hours of $0.07 \pm 0.006\%$ of total RBC's PC and continued to increase with a linear steady state, from 24 hours until 96 hours. In patients the incorporation was much higher compared to controls at all-time points. But this increase over time was not uniform. At 12 and 72 hours there was a drop in the percentage of

incorporation. The exact reason for this drop in the fractional incorporation was not clear. But this finding may be related to the plasma life span of RBC, reflecting the incorporation patterns of both old and newly generated RBCs. At 96 hours the *methyl-D₉* incorporation is almost doubled in patients compared to controls (Figure 68).

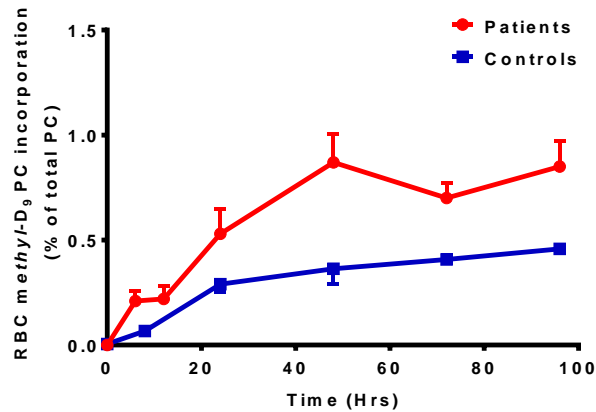


Figure 68; Red blood cell phosphatidylcholine *methyl-D₉* incorporation for both patients (N=8) and controls (N=5). Data presented as mean \pm SEM. RBC, red blood cell; PC, phosphatidylcholine.

In controls, the peak fractional molecular PC *methyl-D₉* choline incorporation (T=96) was in the order of PC16:0/20:4 (0.68%), PC16:0/18:2 (0.54%), PC18:1/18:2 (0.51%) and PC18:1/20:4 (0.49%). This pattern of fractional incorporation was different to that of plasma PC, where PC16:0/18:1 had the highest fractional *methyl-D₉* choline incorporation. In RBC, sn-2 arachidonyl PC species such as PC16:0/20:4 and PC18:1/20:4 had relatively higher fractional incorporation compared to other PC species (Figure 69A).

In patients, although PC16:0/20:4 was still demonstrated the highest incorporation, relative increase in its incorporation was not as high as some of the other PC species (PC16:0/18:1, PC18:0/18:1 and PC18:0/18:2) (Figure 69B). This selective increase in the incorporation was a reflection of plasma PC *methyl-D₉* choline incorporation pattern and highly suggestive that RBC PC *methyl-D₉* choline incorporation is dependent on the availability of plasma PC.

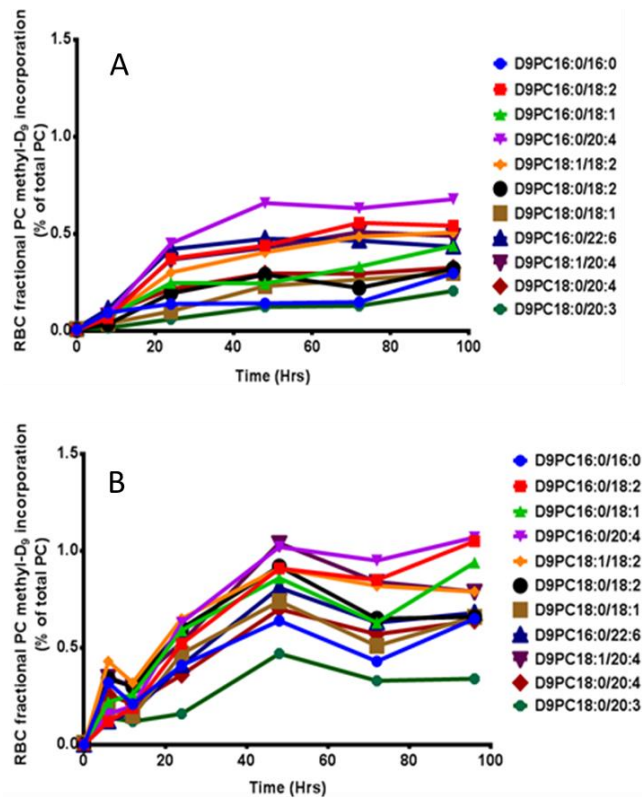


Figure 69; Red blood cell fractional phosphatidylcholine *methyl-D₉* incorporation (% of total PC) in controls (N=5) (A) and patients (N=8) (B). RBC, red blood cell; PC, phosphatidylcholine.

In red blood cells, although there were no significant differences in total PC concentration (Figure 60), variations in fractional PC concentrations were noted at all time points. At 96 hours (at peak *methyl-D₉* choline incorporation), there was a reduction in fractional concentrations of several RBC PC species with increases in PC16:0/16:0, PC16:0/18:1 and PC18:0/18:1 in patients compared to controls (Figure 70). This was coupled with an increase in the absolute concentrations of *methyl-D₉* choline labelled PC species in patients compared to controls and the most increment was noted particularly for the three PC species mentioned above. This suggests a selective pattern of PC incorporation in RBCs of patients enough to boost the endogenous pool of only certain PC species. The PUFA based PC species had relatively lesser *methyl-D₉* choline fractional concentrations compared to monounsaturated PC species, but the fractional incorporation was much higher due to the relative reduction in concentrations of unlabelled PC (Figure 70).

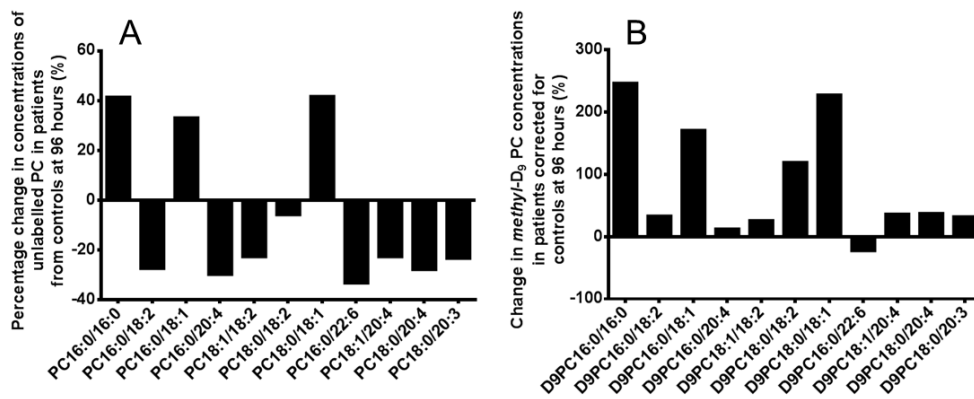


Figure 70; Changes in unlabelled (A) and *methyl-D₉* labelled (B) red blood cell fractional PC molecular concentrations (mmol/l) in patients (N=8) corrected for control values (N=5) at peak incorporation (T=96Hrs after *methyl-D₉* choline infusion). A positive value indicates greater abundance in the patients group for both panels. Data expressed as percentage (%) change from control values at peak incorporation which was at T=96Hrs after *methyl-D₉*-choline infusion.

5.4.3 PC composition and kinetics of CD15+ neutrophils

The CD15+ neutrophil mean total PC concentration was much higher in patients ($0.39 \pm 0.03 \text{ nmol/ml}$) than controls ($0.13 \pm 0.01 \text{ nmol/ml}$) (Figure 71). This is probably due to the quantitative increase in neutrophils in patients during the disease process.

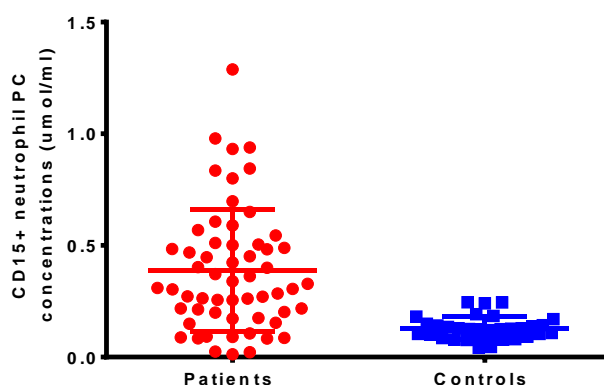


Figure 71; CD15+ neutrophil phosphatidylcholine concentrations (nmol/ml) for all time points measured in patients (N=9 with 58 time points) and healthy controls (N=6 with 33 time points). There is significant difference ($P < 0.001$) between mean phosphatidylcholine concentration between patients ($0.39 \pm 0.03 \text{ nmol/ml}$) and controls ($0.13 \pm 0.01 \text{ nmol/ml}$).

For CD15+ neutrophils, due to the nature of sampling and smaller quantity, only PC molecular composition was analysed. In controls, the CD15+ neutrophils primarily

composed of PC16:0/18:1 (22%), PC18:0/18:2 (16%) and PC18:0/18:1 (11%) (Figure 72). Occasionally the dedicated mass charge ratio (m/z) during mass spectrometry analysis, may be due to more than one PC species. For instance m/z of 786 could be due to either PC18:1/18:1 or PC18:0/18:2. In the case of neutrophils, this peak at m/z786 is likely to be due to PC18:1/18:1. However, this would need further clarification from specific analysis in the future. In CD15+ neutrophils, 1-alkyl 2-acyl species contributed to a greater proportion (27%), compared to red blood cells or lymphocytes.

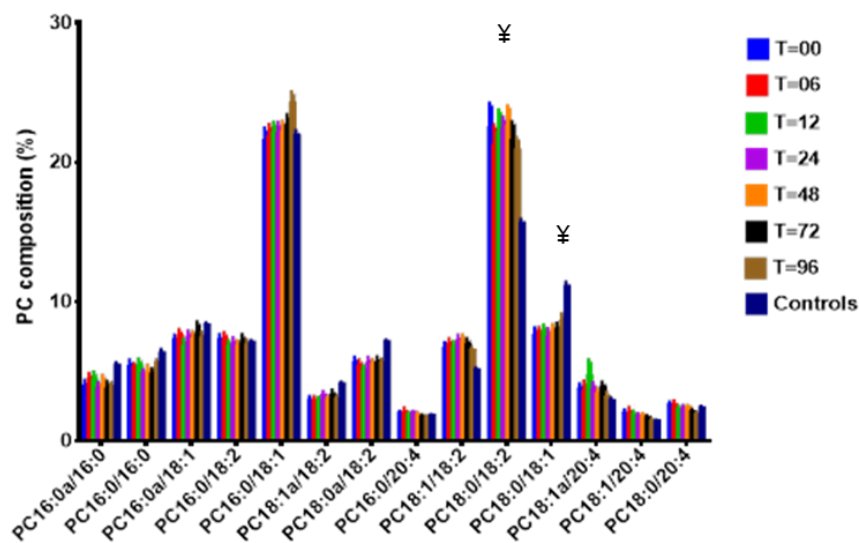


Figure 72; CD15+ neutrophil phosphatidylcholine composition in patients (N=9) over time compared to controls (N=6) at T=0. Data presented as mean \pm SEM, ¥P<0.05 for comparison between patients and controls at enrolment as analysed by two way ANOVA of variance with Bonferroni's corrections. PC, phosphatidylcholine.

In patients, there were statistically significant increases (P<0.0001) in PC18:0/18:2 (44% increase) and decreases in PC18:0/18:1 (32% decrease). Further, there was a gradual increase in relative composition of PC16:0/18:1 over time and at T=96, there was a statistical difference (P=0.004) between patients and controls. Significant increases (P=0.01) of PC18:1/18:2 was also noted at two time points (T=24 and 48) in patients compared to controls. In addition, there was a small but significant decrease (MD 4.9%, P<0.0001) in the sum of all 1-alkyl 2-acyl PC species composition. There were no

compositional variation in sn-2 arachidonyl PC species (20:4) between patients and controls (Figure 72).

In controls, the fractional composition of *methyl-D₉* choline labelled PC species reflected unlabelled endogenous composition for all time points, where PC16:0/18:1 was the major PC followed by PC18:0/18:2 and PC18:0/18:1. However, in patients the fractional synthesis of PC18:0/18:2 was significantly elevated and showed similar fraction to that of unlabelled endogenous PC composition (Figure 73). The total *methyl-D₉*-PC incorporation showed similar pattern for both patients and controls, but patients had an overall increased incorporation (Figure 74).

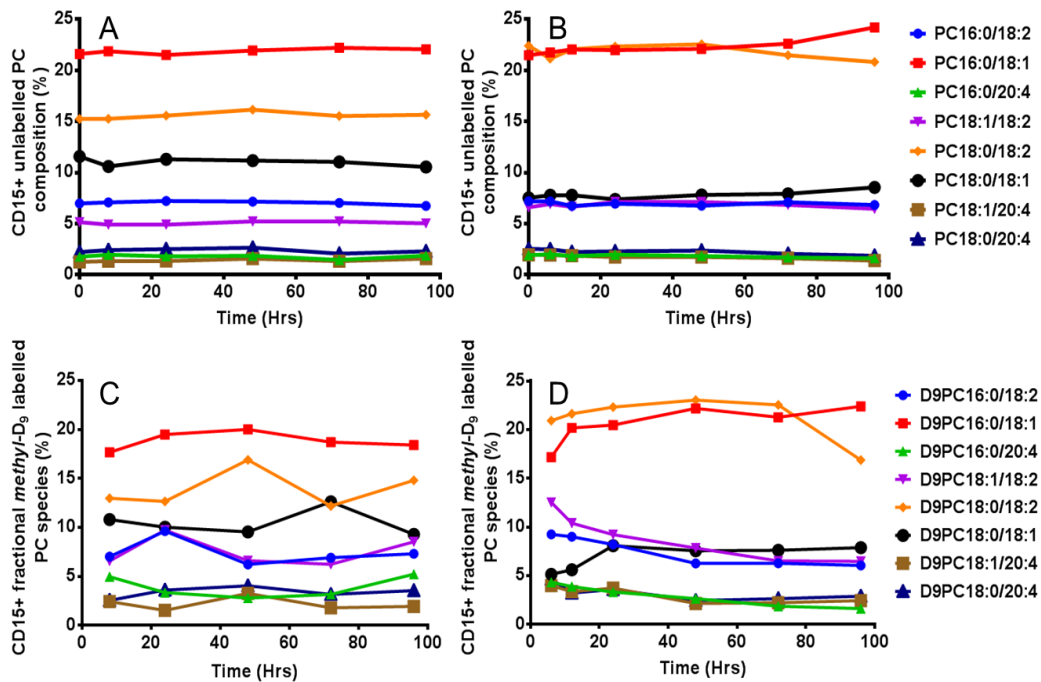


Figure 73; Unlabelled and *methyl-D₉*-labelled choline PC composition of CD15+ neutrophils from controls (N=6) and patients (N=9). **A;** Unlabelled PC composition for controls, **B;** Unlabelled PC composition for patients, **C;** *methyl-D₉* choline labelled PC composition in controls. **D;** *methyl-D₉* choline labelled PC composition in patients. PC, phosphatidylcholine.

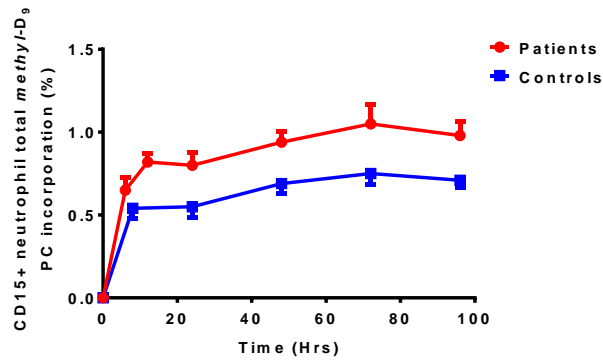


Figure 74; *Methyl-D₉* choline phosphatidylcholine incorporation of CD15+ neutrophils (% of total PC) from patients (N=9) and healthy controls (N=6). Data presented as mean \pm SEM. PC, phosphatidylcholine.

There were significant variations in the fractional *methyl-D₉*-choline incorporation patterns between PC molecular species. In controls, the fractional *methyl-D₉* choline incorporation was peaked at earliest time point (T=08Hrs) for all sn-2 arachidonyl PC species, whereas PC16:0/18:1, PC18:0/18:2, and PC18:0/18:1 showed gradual increases. 1-alkyl 2-acyl species also showed gradual increases in the incorporation. The magnitude of *methyl-D₉* incorporation was in the order of PC16:0/20:4, PC18:1/20:4, PC18:1/18:2 and PC18:0/20:4 and this pattern was similar for both patients and controls (Figure 75).

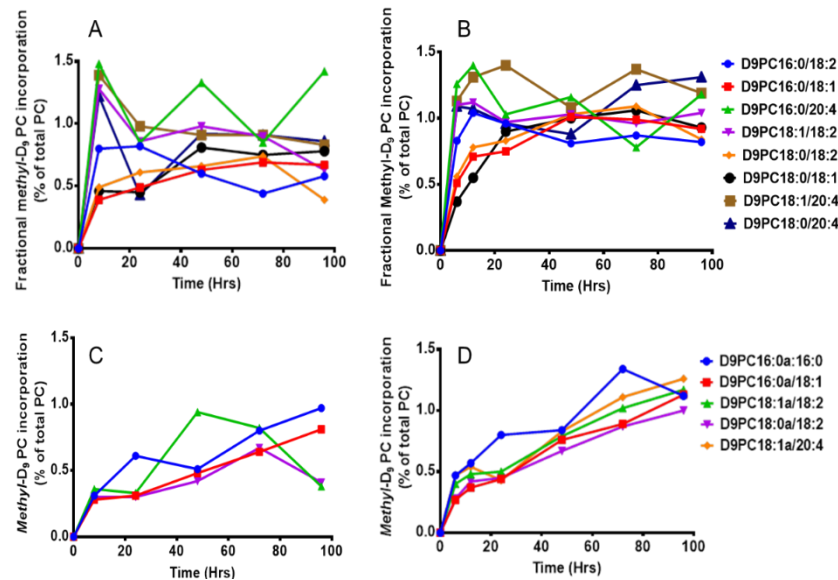


Figure 75; Fractional *methyl-D₉* incorporation of diacyl and 1-alkyl 2-acyl PC species of CD15+ neutrophils from controls (N=6) and patients (N=9). **A;** diacyl PC incorporation from controls, **B;** diacyl PC incorporation from patients, **C;** 1-alkyl 2-acyl incorporation from controls, **D;** 1-alkyl 2-acyl incorporation from patients. PC, phosphatidylcholine.

5.4.4 CD3+ T-lymphocyte PC molecular composition

Only PC molecular composition was analysed for CD3+ lymphocytes. Despite performing additional scans to assess incorporation patterns, these were not accurate due to small quantity and are not presented here. The PC molecular composition for CD3+ T-lymphocytes primarily consisted of PC16:0/18:1 (16%), PC18:0/18:2 (13%), PC18:0/18:1 (10%), and PC18:0/20:4 (11%). The prevalence of sn-2 arachidonyl PC species accounting for 25% of total PC. Additionally, they also contained higher proportions of PC16:0/16:0 (7%), PC18:0/20:3 (4%) and PC18:0/22:5 (3%) compared to other cell types. 1-alkyl 2-acyl PC species only accounted for 7% of total PC and this was much lower than neutrophils. In patients, there were significant ($P < 0.0001$) compositional differences noted with increases in PC16:0/18:2, PC16:0/18:1, PC18:0/18:2, and 18:0/18:1 with decreases in PC16:0/16:0 and all sn-2 arachidonyl PC species (Figure 76). The fractional composition of all arachidonyl (20:4) PC species were significantly reduced in patients (MD 12% reduction, $P < 0.0001$) (Figure 77).

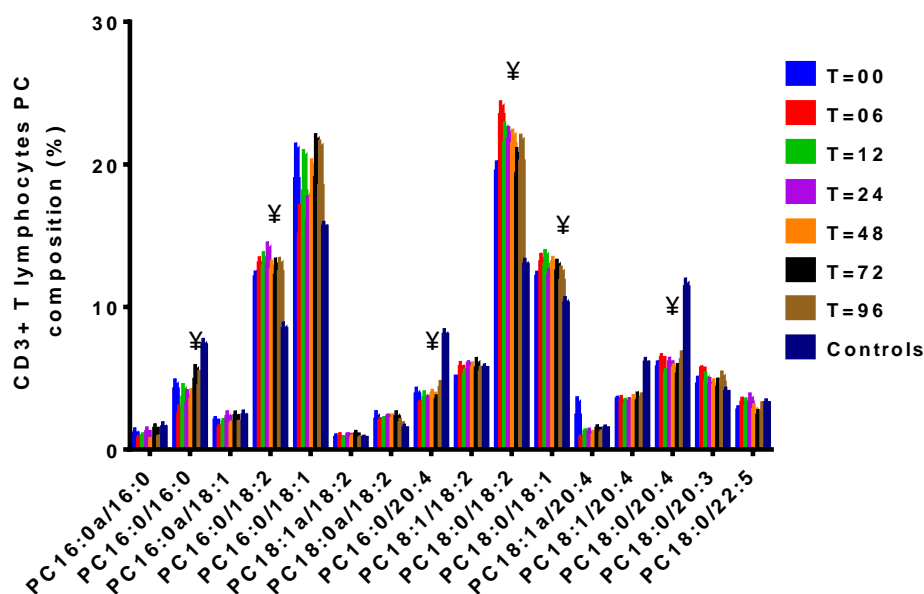


Figure 76; Phosphatidylcholine molecular composition of CD3+ T lymphocytes in patients (N=4) over time, compared to healthy controls (N=4) at enrolment. Data presented as mean \pm SEM. \neq $P < 0.05$ for comparison between patients and controls at enrolment T=0. PC, phosphatidylcholine.

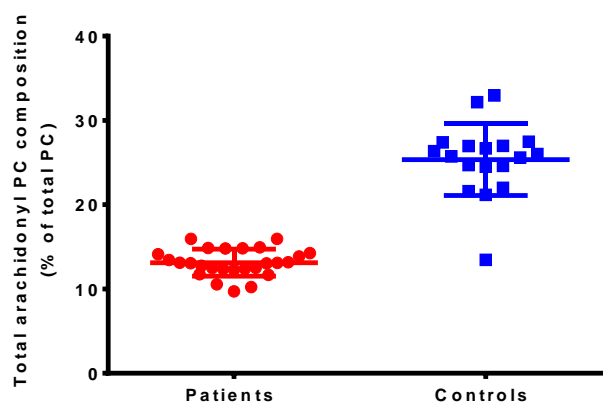


Figure 77; Composition of arachidonyl (20:4) containing phosphatidylcholine species (% of total PC) of CD3+ T lymphocytes for all time points measured between patients (N=4, 26 time points) and controls (N=4, 18 time points). Mean composition for patients ($13.1 \pm 0.3\%$) was much lower than controls ($25.4 \pm 1.0\%$), $P < 0.0001$ as assessed by Student's T- test. PC, phosphatidylcholine.

5.4.5 Ex-vivo incubation of CD15+ neutrophils with free fatty acids

From the results presented in this chapter so far, it seems that peripheral blood cells are capable of modifying their final PC composition, depending on the availability and supply of substrates from plasma. Cellular PC can also be modified by external supplementation of free fatty acids. However, the exact molecular arrangement of the newly synthesised PC following exogenous fatty acid supplementation is not well established. These modifications may have implications on cellular functions such as alterations in the capacity to synthesise oxylipins, intracellular signal transduction and apoptosis. CD15+ neutrophils from healthy volunteers were incubated with $30 \mu\text{mol}$ s of oleate, linoleate, arachidonate, and palmitate, separately and 0.5mg of *methyl-D₉*-choline chloride for a period of 3 hours. Although the degree of toxicity to the cells from this quantity was not measured, similar quantities of fatty acids were used in a previous study to assess PC synthesis in IMR-32 cells (Hunt AN et al. 2002). The incubation duration is a reflection of the life span of neutrophils *ex-vivo*. This Samples without any fatty acid supplements were used as controls. The labelled and unlabeled PC composition was assessed after individual fatty acid supplementation from all samples. All CD15+ neutrophils were unstimulated.

Although the unlabelled fractional PC composition remained unchanged (Figure 78), the fractional synthesis of labelled PC species was significantly altered after the additions of fatty acids (Figure 79). Following the addition of oleic acid, there was an increase in the fractional synthesis of PC18:1/18:1 (150%) and decrease in PC16:0/18:2. Linoleic acid supplementation resulted in increased fractional synthesis of PC18:2/18:2 (1320%). Arachidonic acid supplementation resulted in increases to all sn-2 arachidonoyl PC species in particular PC20:4/20:4 (2690%). Palmitic acid supplementation enriched dipalmitoyl-PC by 312%. These suggest there is a tendency to increase the fractional synthesis of PC species of both sn-1 and sn-2 of that particular FA supplemented (Figure 79).

The total *methyl-D₉*- choline enrichment was in the order of oleic acid ($0.52\pm 0.22\%$), no fatty acid ($0.87\pm 0.21\%$), arachidonic acid ($0.91\pm 0.25\%$), palmitic acid ($1.20\pm 0.28\%$) and linoleic acid ($1.36\pm 0.40\%$). This suggests that the presence of oleic acid may have a negative effect on neutrophil PC synthesis compared to other fatty acids. Fractional *methyl-D₉* enrichment of PC species in neutrophil was generally higher for sn-2 arachidonic acid PC species. There was no increase in *methyl-D₉* choline fractional enrichment for any other PC species following oleic acid supplementation. However, when other fatty acids were added, similar changes to the fractional synthesis were noted (Figure 80).

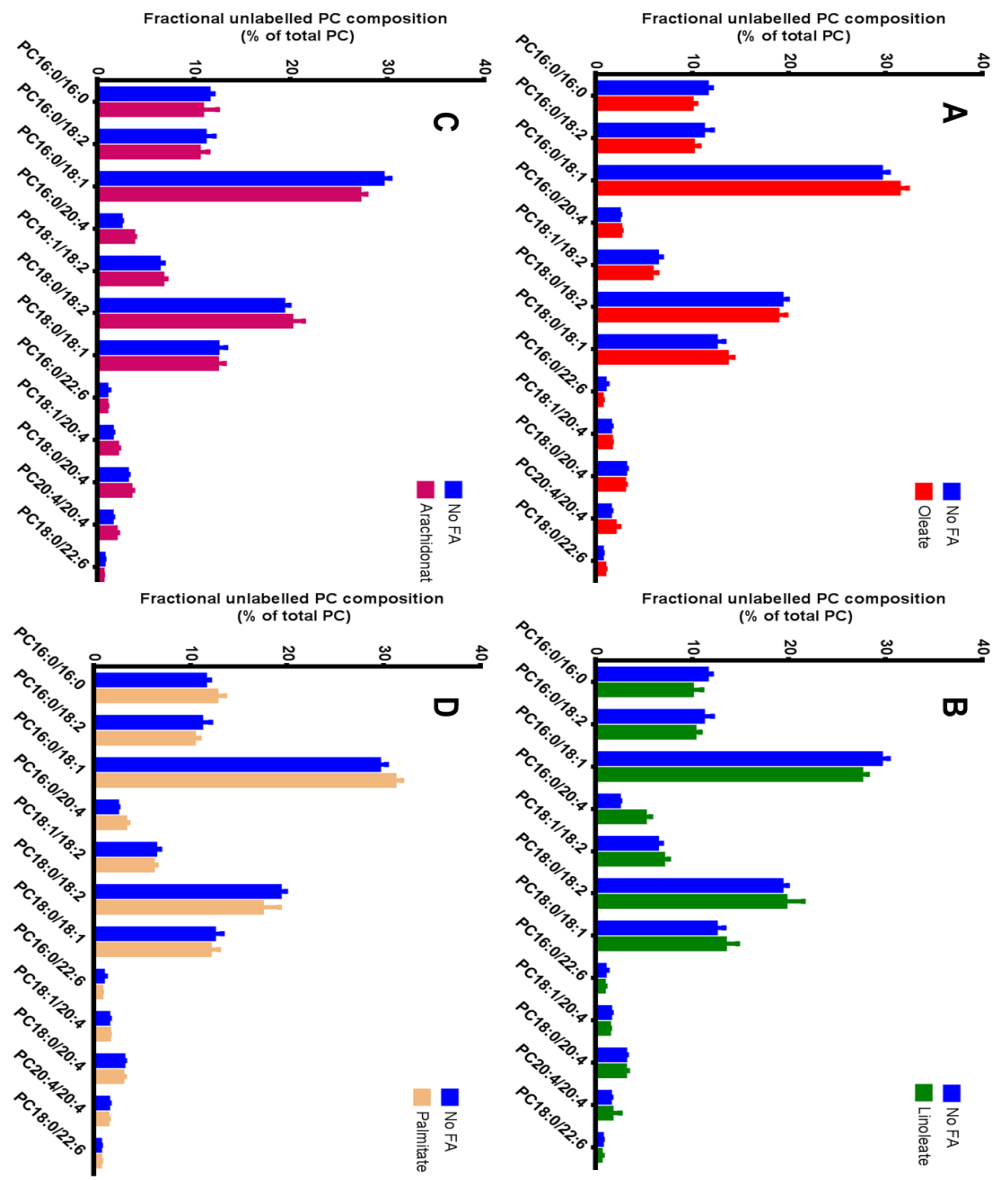


Figure 78: Unlabelled phosphatidylcholine composition of CD15+ neutrophils after fatty acid supplementation. **A;** Oleic acid (N=5), **B;** Linoleic acid (N=5), **C;** Arachidonic acid (N=5), **D;** Palmitic acid (N=5). Data presented as mean ± SEM. There was no significant difference in unlabelled PC fractional composition following fatty acid supplementation.

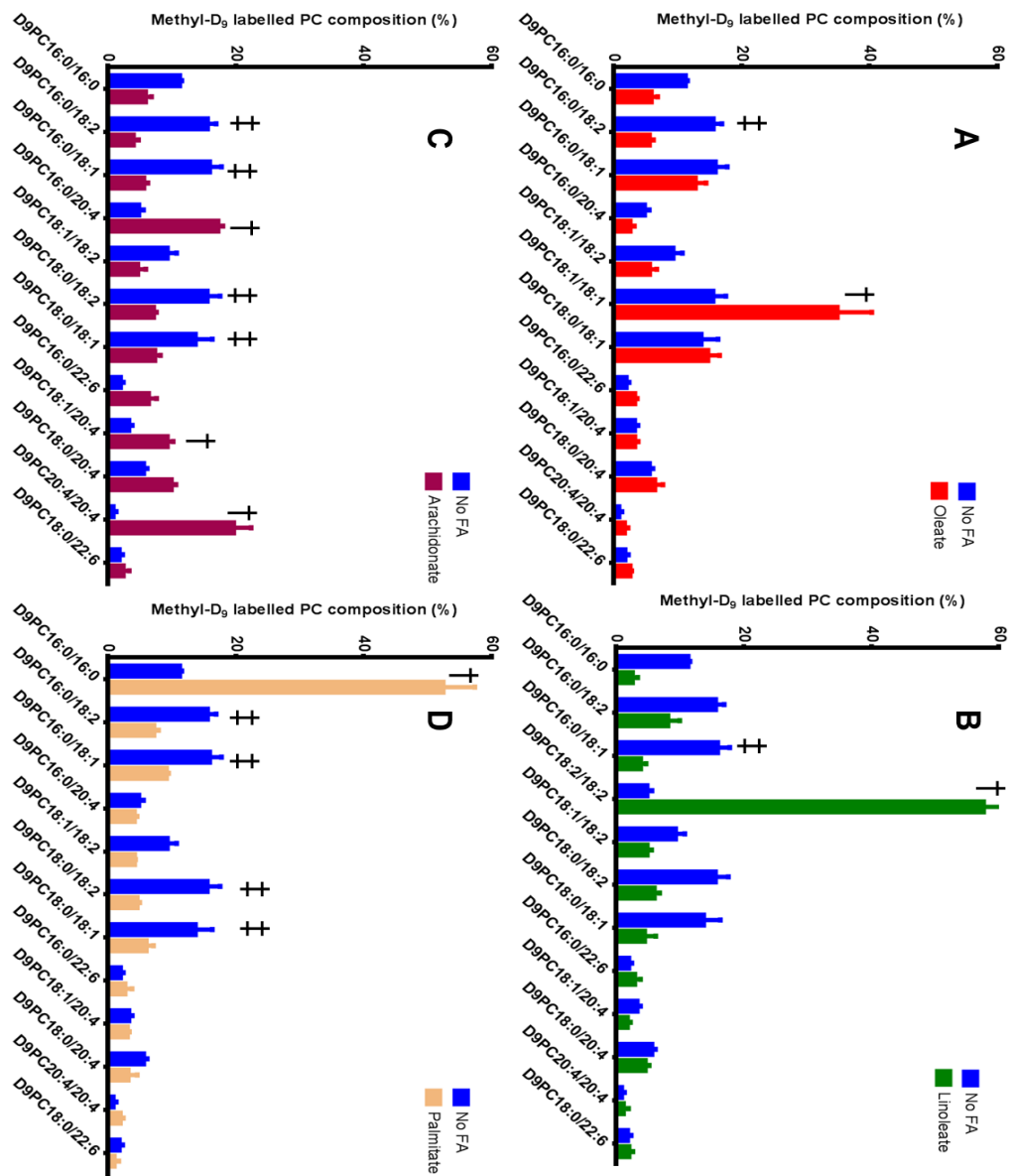


Figure 79: Fractional composition of methyl-D₉ labelled PC fraction in CD15+ neutrophils after fatty acid supplementation. **A;** Oleic acid (N=5), **B;** Linoleic acid (N=5), **C;** Arachidonic acid (N=5), **D;** Palmitic acid (N=5). Data presented as mean ± SEM, ‡; P<0.05 increase of fractional labelling, †; P<0.05 decrease in fractional labelling as assessed by two way ANOVA of variance with Bonferroni's corrections for multiple comparisons.

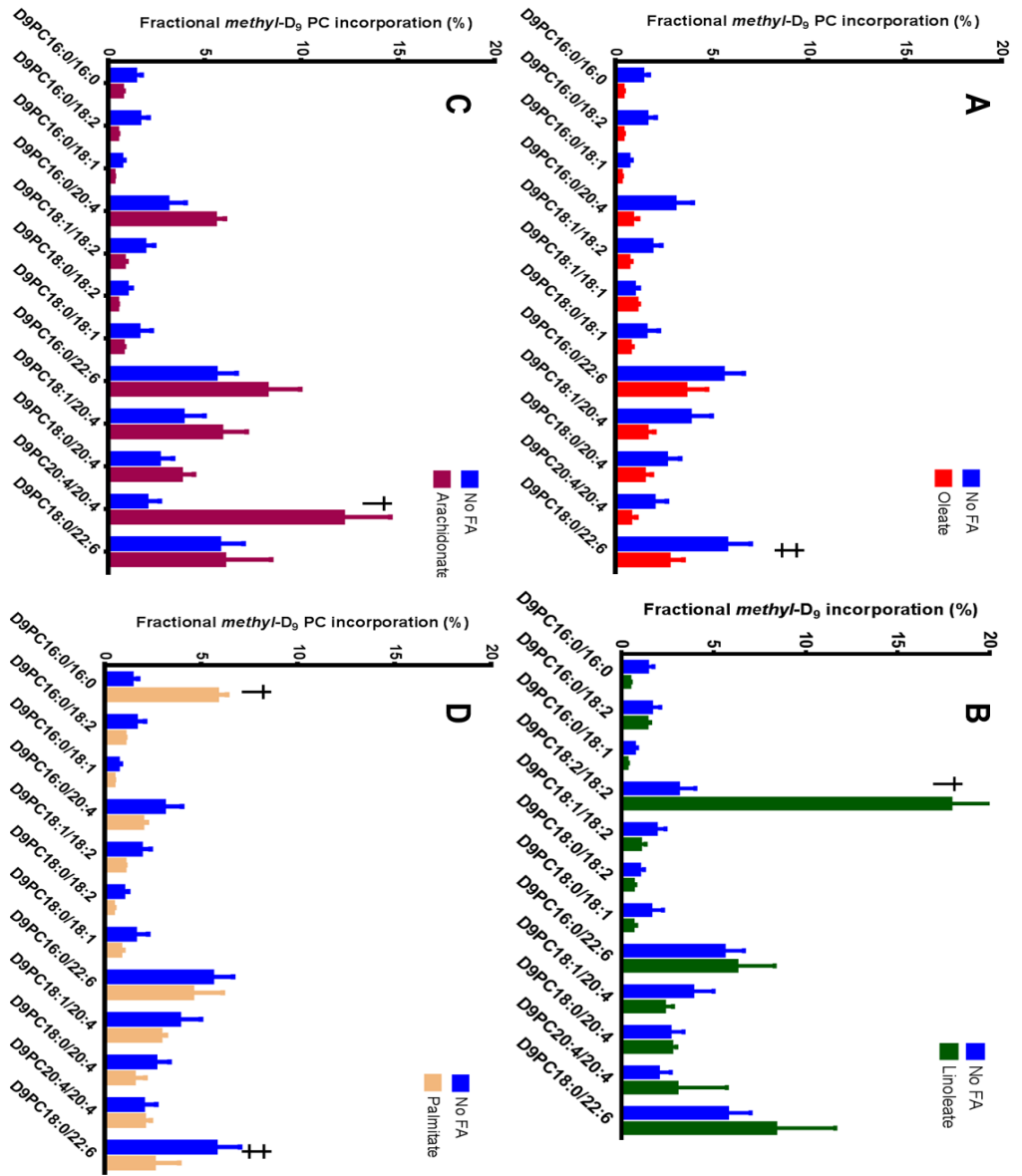


Figure 80: Fractional *methyl-D₉* incorporation in CD15+ neutrophils after fatty acids supplementation. **A:** Oleic acid (N=5), **B:** Linoleic acid (N=5), **C:** Arachidonic acid (n=5), **D:** Palmitic acid (N=5). Data presented as mean ± SEM, †; P<0.05 increase in fractional *methyl-D₉* incorporation, ‡; P<0.05 decrease in fractional *methyl-D₉* incorporation as assessed by two way ANOVA of variance with Bonferroni's corrections for multiple comparisons.

5.4.6 Functional variation of neutrophils following supplementation of fatty acids

Following the supplementation of free fatty acids, ex-vivo human neutrophils from whole blood were analysed for their cell surface expression of adhesion molecules CD11b, CD11a and CD62L (Figure 81). There were significant increases in neutrophil surface expression of CD11b and CD11a, following the supplementation of all fatty acids. However, arachidonate and palmitate supplementation resulted in much higher expression of CD11b compared to oleate or linoleate. Cell surface expression of CD62L is markedly reduced following the supplementation of all fatty acids (Figure 82).

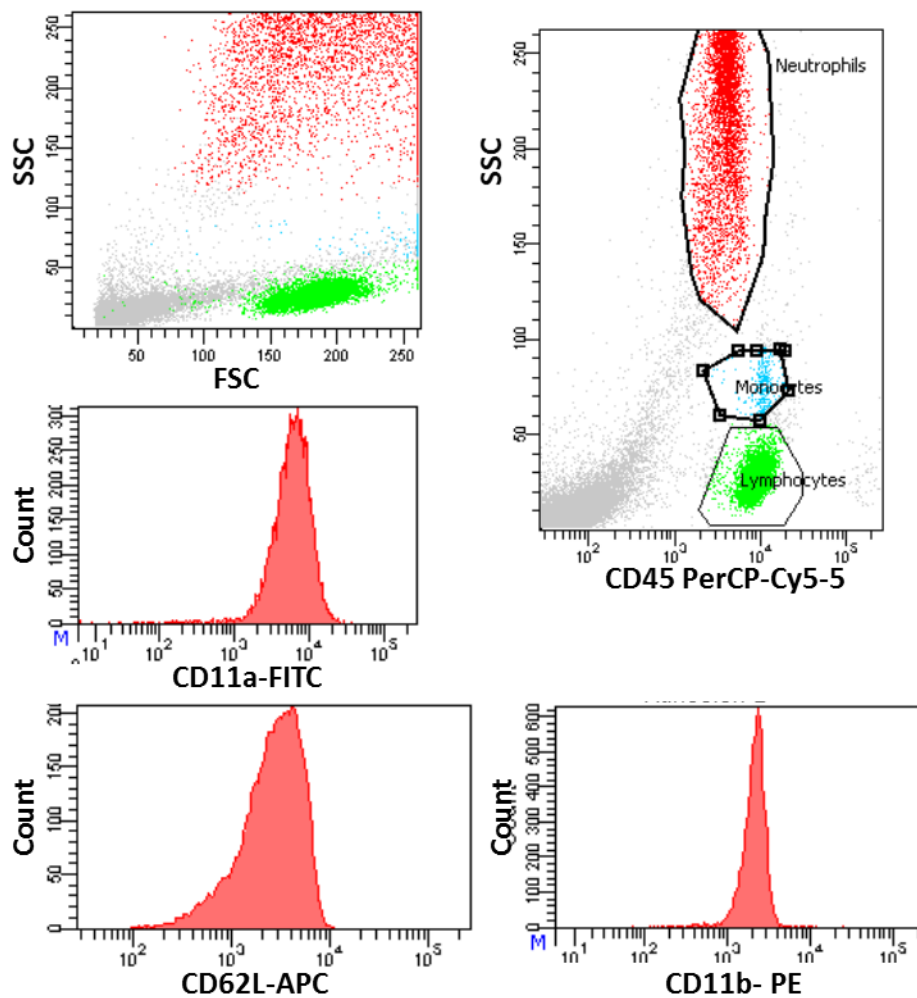
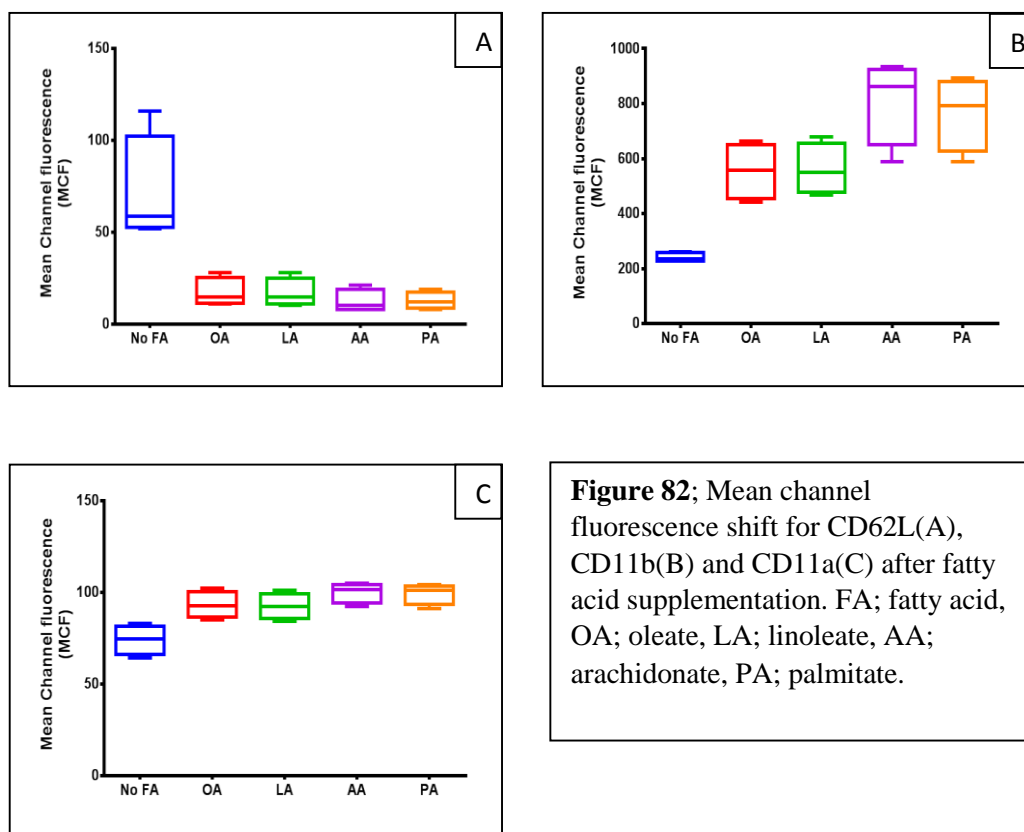


Figure 81; Human whole blood was incubated with fatty acids and neutrophils were assessed for their cell surface expression of activation markers (CD11a, CD11b, CD62L) on flow cytometry.



5.5 Discussion

ARDS is characterised by neutrophil mediated inflammatory response, leading to alveolar epithelial and endothelial injury (Ware LB and Matthay MA 2000). In addition to potent inflammatory cytokines, neutrophils also produce oxidised membrane mediators (eicosanoids/oxylin) such as prostaglandins and leukotrienes, which can potentiate local inflammation (Masclans JR et al 1999). These oxidised metabolites are generated from arachidonic acid, which is found in cell membranes as esterified to phosphatidylcholines. Importantly, as membrane phospholipid compositions are cell specific, inflammatory cells such as neutrophils and lymphocytes may have variable degree of substrate availability for oxylin synthesis. Furthermore, transcellular donations of substrates may also be possible from cell to cell on demand and has not been investigated before. Characterisation of cell membrane phospholipid composition and synthesis may improve the understanding of underlying mechanisms of oxylin synthesis and manipulations of substrate availability

and hence metabolic pathways. Moreover, it may also provide therapeutic targets for inflammatory conditions like ARDS. However, studies of such are lacking in *in-vivo* human models. Consequently, this study was aimed to assess the PC composition and dynamic turnover of individual molecular PC species in peripheral blood cells during the early stages of ARDS. Furthermore, direct supplementation of fatty acids provided novel insights into the molecular rearrangement of newly synthesised PC fraction in *ex-vivo* human neutrophils.

Red blood cells do not participate in *de-novo* phospholipid biosynthesis. However, passive exchange of phospholipids from plasma lipoproteins (Renooij W and Van Golde LM 1976) and acyl-remodelling mechanisms (Robinson M et al. 1986) are thought to maintain the flux and renewal of membrane phospholipids in red blood cells. There were significant alterations in plasma PC composition and metabolic pathways in patients with ARDS as outlined in chapter 4. These alterations in the plasma may influence remodelling and hence the final composition of phospholipids in red blood cells. Consequently, in this chapter red blood cell phospholipids composition and dynamic PC turnover were assessed. Most of the compositional changes were evident in the PC fraction, where there were significant increases in PC16:0/18:1 in both unlabelled and *methyl-D₉* labelled fraction and decreases in PC16:0/18:2 (Figure 61). Assessment of unlabelled endogenous concentrations of PC showed, significant decreases for PC species (in particular polyunsaturated PC species), with the exception of PC16:0/16:0, PC16:0/18:1 and PC18:0/18:1. Concentrations of *methyl-D₉* labelled PC species corrected from controls at peak incorporation suggest, a specific molecular order of enrichment (16:0/16:0 > 18:0/18:1 > 16:0/18:1 > 18:0/18:2) (Figure 70). These changes may be due to alterations in the acyl-transferase activity in the red blood cells in patients with ARDS. In addition, there was an increase in total *methyl-D₉* incorporation suggesting increased activity likely to be due to increased demand. The fractional increase in concentrations of PC16:0/18:1 correlated positively to the fractional increase in plasma PC16:0/18:1 concentrations. From this it appears that RBC PC

remodelling mechanisms are closely related to the plasma PC composition. In the patient's group, there was a drop in the total *methyl-D₉* incorporation at 12 and 72 hours, possibly related to the turnover time of red blood cells, but this was not evident in healthy controls (Figure 68).

PC compositional changes in CD15+ neutrophils were different to that of red blood cells. There was a selective increase in unlabelled and *methyl-D₉* labelled pool of PC18:0/18:2 in patients (Figure 72). The dedicated m/z for this PC is 786, and it is entirely plausible, that the changes noted were due to PC18:1/18:1 rather than PC18:0/18:2. Fractional *methyl-D₉* incorporation was higher for sn-2 arachidonyl PC species in both patients and controls. However, the increment in the incorporation among patients was much more evident for only 2 species PC16:0/18:1 and PC18:0/18:2 (or PC18:1/18:1). This highlights the specific alterations in the neutrophil PC synthetic and remodelling mechanism in patients with ARDS. This is the first study to demonstrate these phospholipid changes in neutrophils from ARDS patients. However, the exact clinical significance of these changes are not known.

Lymphocytes are involved in adaptive immune response and have been implicated in the recruitment of neutrophils during acute lung injury (Venet F 2009). The PC fractional composition of lymphocytes is enriched with arachidonyl species (Postle AD et al. 2004) and it is possible that they are donors of arachidonic acid for eicosanoid synthesis by other cells (Goldyne ME 1988), (Wu KK et al. 1987). PC labelling patterns of lymphocytes were not assessed due to the smaller quantity. Lymphocytes isolated from patients had significantly lower composition of sn-2 arachidonyl PC species (Figure 77). In addition, there were fractional changes in other PC species such as PC16:0/18:1 and PC18:0/18:2 (or PC18:1/18:1) (Figure 76). The latter finding was similar to that of neutrophils.

In-vitro fatty acid supplementation can influence cell membrane composition and demonstrated in various cell lines such as C₆-Glioma cells (Kim HY and Hamilton J 2000),

CaCo₂-enterocytes (Dias VC and Parsons HG 1995), human monocytes (Galella G et al. 1993), HL-60 cultured cells (Heung YM and Postle AD 1995), IMR- 32 cells (Hunt AN 2002), RAW264.7 cells and macrophages (Rouzer CA et al. 2007). Although several *in-vitro* (Tou JS 1984), (Chilton FH et al. 1987) and *in-vivo* studies (Chilton FH et al. 1993), (Healy DA et al. 2000), (Stanke-Labesque F et al. 2008) demonstrated the capability of modulating neutrophil membrane composition by external fatty acid supplementation, the molecular specificity of the final PC composition is not fully defined. Isotope labelling of deuteriated choline has been utilised to demonstrate dynamic incorporation of labelled PC to assess synthetic patterns in lymphocytes and neutrophils (Postle AD et al. 2004). Using the same methodology, we have assessed the final unlabelled and *methyl-D₉* labelled PC species composition in neutrophils after various fatty acids incubated for 3 hours. It appears that specific incorporation pattern of PC species with both sn-1 and sn-2 were prioritised for PC synthesis by all fatty acids. There was increased fractional synthesis of PC18:1/18:1 following oleic acid, PC18:2/18:2 following linoleic acid, PC20:4/20:4 following arachidonic acid and PC16:0/16:0 after palmitic acid supplementation (Figure 79). However, this pattern of incorporation was not uniform for all PC species. For instance, supplementation of arachidonic acid resulted in increased fractional synthesis of all arachidonyl PC species, but in the order of 20:4/20:4 > 16:0/20:4 > 18:1/20:4 > 18:0/20:4. Whereas incubation with oleic acid, linoleic acid and palmitic acid only resulted in the increased synthesis of one PC species, with both sn-1 and sn-2 of that particular fatty acid composition (Figure 79). In addition to these changes, the rest of the PC species showed reductions in their fractional synthesis. These modifications seem to alter the cell surface expression of activation markers in neutrophils. From these findings, it is possible to postulate that changes in plasma PC composition, may influence final PC composition and function of inflammatory cells.

5.6 *Conclusions*

This study demonstrates significant changes in the phospholipid composition and dynamic turnover in peripheral blood cells in patients with ARDS. Some changes particularly in the case of red blood cells, are likely to be related to plasma PC composition. The increased composition of PC18:0/18:2 (or PC18:1/18:1) in labelled and unlabelled fraction in neutrophils may have pathological consequence and further functional studies are needed to establish its exact role of this PC in neutrophil mediated inflammation. The depletion of arachidonyl PC species in lymphocytes suggests the possibility of substrate donation for other cells to participate in eicosanoids synthesis. This study also demonstrates the possibility of manipulation of neutrophil final PC composition by external fatty acid supplementation and further studies are warranted to assess the clinical importance of this in neutrophil function and in ARDS.

CHAPTER 6

Examination of phospholipid composition and kinetics from various endobronchial compartments in human healthy adults

6.1 Introduction

Pulmonary surfactant plays a crucial role in maintaining alveolar surface tension and preventing premature airway collapse. Surfactant abnormalities are evident in various acute and chronic lung conditions and ARDS is a typical example of an acute inflammatory process, characterised by significant alterations in surfactant composition and function (Hallman M et al. 1982). Altered surfactant composition is also a recognised feature of chronic inflammatory airway conditions such as asthma (Winkler C and Hohlfeld JM 2013) and cystic fibrosis (Mander A et al. 2002). Surfactant is generally recovered from alveolar epithelial lining by bronchoalveolar lavage (BAL). However, induced sputum as well as tracheal aspirate has been used to recover surfactant phospholipids by several studies (Bernard W et al. 2004) (Simonato M et al. 2011).

Surfactant PC is consistently identified in airway secretions and their function is to maintain airway patency (Enhorning G 2008). Cellular fractions of induced sputum are a valuable tool in the assessments of several lung diseases and can be comparable to cell fractions extracted by BALF (Silkoff PE et al. 2003). However, in the case of surfactant, the phospholipid extracts may represent two different respiratory anatomical sites; while the BALF may be more representative of alveolar origin, the induced sputum is from secretions of lower airways. Nevertheless, evidence from animal radiolabelled studies indicate that all surfactant PC is of alveolar in origin. Furthermore, the surfactant phospholipid composition from induced sputum is similar to that of alveolar composition

and primarily consisted of disaturated-PC species (Bernhard W et al. 2004) (Wright SM et al. 2000). However, the quality of the sputum samples may vary according to the extraction techniques, origin of sputum, and degree of contamination by salivary secretions. Consequently, subsequent fractions may vary in surfactant phospholipid composition during multiple inductions (Bernhard W et al. 2004).

Bronchoalveolar lavage is an invasive procedure, which requires sedation and may cause cardio-respiratory complications. Although, BALF is generally a safe procedure in mechanically ventilated patients, some may develop significant de-saturations during the procedure. In the case of ARDS, this is particularly important, as these patients suffer with severe hypoxic respiratory failure. Consequently, these patients will need increased sedation and frequently paralysis during the procedure.

Tracheal aspirate compared to induced sputum reflects secretions from more proximal large airways. The phospholipid composition of tracheal aspirates in neonates, closely resembles that of alveolar surfactant composition and has been widely used to study surfactant phospholipid kinetics in this population (Poets CF et al 1997), (Bunt JE et al. 1998). However, the tracheal aspirate phospholipid kinetics may vary from that of alveolar surfactant and possibly influenced by several factors, including mucociliary transit time of surfactant up along the airways. So far no studies have compared surfactant phospholipid kinetics from these different endobronchial compartments.

In Chapter 3, all ARDS patients had serial small volume BALF as the surfactant isolation method. This is not practically feasible to perform in a large cohort of patients. The primary aim of these studies is to translate the applicability of this methodology in a large scale, to identify potential patients with underlying phenotypes of surfactant synthesis and metabolism prior to therapeutic replacement strategies. In this chapter, the molecular composition and turnover of endobronchial phospholipid fractions was investigated from induced sputum, tracheal wash (TW) and small volume BALF. Such information is

valuable in the understanding of mechanisms of alveolar surfactant synthesis and metabolism, which may be applicable in diseases characterised by surfactant dysfunction. Furthermore, refining surfactant isolation methods with less invasive techniques will minimise potential complications, associated with BALF during surfactant studies.

6.2 Objectives

1. To assess the phospholipid composition and kinetics from different endobronchial fractions in healthy adult volunteers.

6.3 Summary of methods

Ten healthy volunteers without any pre-existing lung diseases were recruited. After informed consent, they had an intravenous infusion of *methyl-D₉* choline chloride (3.6mg/kg body weight) for a period of 3 hours. Sputum was induced by nebulised 4.5% hypertonic saline at 0, 8, 24, 48, 72 and 96 hours after choline infusion. Tracheal wash and BALF samples were obtained by a fiberoptic bronchoscope at 24 and 48 hours after choline infusion. All samples were filtered through a 100µm cell strainer and centrifuged at 400g for 10 minutes at 4°C to remove cellular debris. The supernatant was aspirated and the phospholipid fraction was extracted by modified Bligh and Dyer approach, after the addition of 1nmol of dimyristoyl-PC (PC14:0/14:0), 0.1nmol of LPC17:0 and 0.2nmol of dimyristoyl-PG (PG14:0/14:0) as internal standards. Phospholipid molecular composition was analysed by ESI-MS/MS. SP-D concentrations were determined by ELISA. Data are presented in mean ± SD, unless stated otherwise. Methodology is more detailed in chapter 2.

6.4 Results

6.4.1 Demographics

Ten healthy volunteers were recruited of whom 6 males and 4 females. All participants had sputum induction, but one subject was unable to tolerate bronchoscopy leaving BALF/TW analysis for the rest of the nine participants. The clinical data and summary of

demographics are listed in table 14. BALF recovery (42%) was higher than that of TW (31%). There was no significant drop in FEV₁ or oxygen saturation during sputum induction. The lowest oxygen saturation during bronchoscopy was 87% for one subject; however the mean drop in saturation during the procedure was from 99% to 94%.

Characteristics	
Age (Range)	26 (18-36)
M:F	6:4
FEV₁ (L)	4.22 ± 0.91*
Weight (kg)	78 ± 12*
Choline dose infused (mgs)	275 ± 54*
BALF Volume recovery (%)	42 ± 20*
TW Volume recovery (%)	31 ± 12*

Table 14; Characteristics of healthy subjects recruited (M;male, F;female, FEV₁; forced expiratory volume in 1 second, BALF; bronchoalveolar lavage fluid, TW; tracheal wash. *(Expressed as mean ±SD)

6.4.2 Total Phospholipid, PC and SP-D concentrations

Phospholipids are the principal component accounting for 80% of human pulmonary surfactant composition. BALF offers a practical approach to isolate surfactant material from alveolar epithelial lining fluid. However, quantification of the alveolar surfactant pool is dependent on several factors, and measurement of absolute concentrations of surfactant phospholipids and proteins can be inconsistent due to variable recovery of BALF. Consequently, in our study there was a considerable variation in total phospholipid, PC and SP-D concentrations among subjects and sampling methods.

The mean total phospholipid concentration (expressed as the sum of each phospholipid classes) in BALF was 64.4 (range 29.1-145.1) nmol/ml, TW 51.8 (range 13.5- 158.7) nmol/ml and IS 8.0 (Range 3.2-14.1) nmol/ml. The total PC concentration in BALF was relatively high (49.9 range 18.6-121.8nmol/ml) followed by TW (37.2 range 8.5-134.7

nmol/ml) compared to IS (5.8 range 2.4-10.5 nmol/ml). The mean SP-D concentration was 30.3 (range 9.9-67.6) ug/ml for BALF, 24.4 (range 11.8-48.1) ug/ml for TW and 17.5 (range 1.5-85.0) ug/ml for IS. The ratio of total SP-D/PC was much higher for IS, suggesting the possibility of additional secretion of SP-D from airway Clara cells (Table 15).

	BALF	TW	IS
Total PL	64.4 ± 37.1	51.8 ± 44.6	†8.0 ± 3.8
(nmol/ml)	(29.1-145.1)	(13.5-158.7)	(3.2-14.1)
Total PC	49.9 ± 32.8	37.2 ± 39.1	†5.8 ± 2.9
(nmol/ml)	(18.6-121.8)	(8.5-134.7)	(2.4-10.5)
SP-D	30.3 ± 16.6	24.4 ± 13.9	*17.5 ± 25.3
(µg/ml)	(9.9-67.6)	(11.8-48.1)	(1.5-85.0)
SP-D:PC	0.61	0.66	3.0

Table 15; Total phospholipid, phosphatidylcholine and surfactant protein D concentrations for all sampling methods. BALF, bronchoalveolar lavage fluid; TW, tracheal wash; IS, induced sputum; PL, phospholipid; PC, phosphatidylcholine; SP-D, surfactant protein D. *P<0.05, † P<0.01 when compared with BALF by student's T- test, data expressed as mean ± SD.

The total phospholipid concentrations were measured from all compartments. To assess the consistency of BALF and tracheal wash between both time points, correlation graphs were used. There was no positive correlation between BALF performed at 24 and 48 hours ($r^2=0.4118$, $P=0.06$) (Figure 83A). There was also a lack of correlation in total phospholipid concentrations between tracheal wash at 24 and 48 hours ($r^2=0.4201$, $P=0.06$) (Figure 83B).

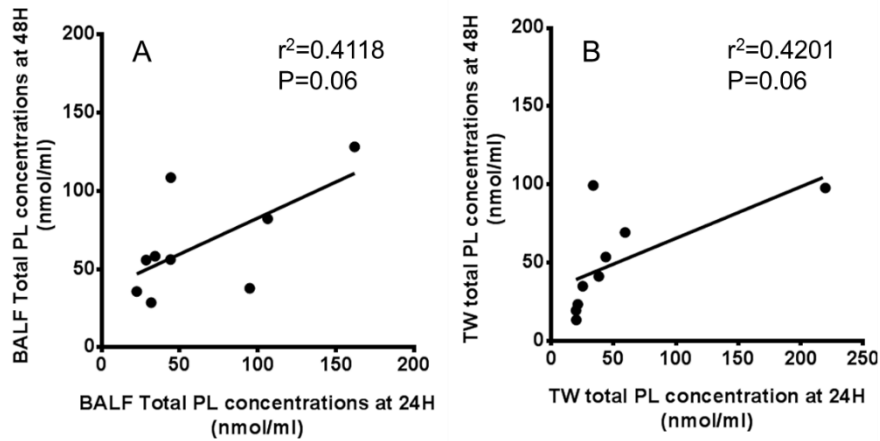


Figure 83; Correlations of bronchoalveolar lavage and tracheal wash phospholipid concentrations (nmol/l) for both time points studied (24 and 48 hours). There was no correlation between bronchoalveolar lavage (A) or tracheal wash (B) phospholipid concentrations for both time points, as analysed by Pearson's correlation coefficient. BALF, bronchoalveolar lavage fluid; TW, tracheal wash; PL, phospholipid.

For the comparison between BALF and TW total phospholipid concentrations extracted, there was a statistical significance ($r^2 = 0.6209$, $P=0.01$), but the analysis was dependent on one data point (Figure 84A). There was no positive correlation in total PL concentrations between BALF and induced sputum ($r^2=0.0453$, $P=0.61$) (Figure 84B). Furthermore, there were significant variations in the phospholipid concentrations between patients at each time points, highlighting the lack of consistency in the reproducibility between BALF, TW and induced sputum and among patients.

The total PC concentration varied between isolation methods and individuals. There was relatively higher concentration of PC in BALF (49.9 ± 32.8 nmol/ml), followed by TW (37.2 ± 39.1 nmol/ml) compared to the induced sputum (5.8 ± 2.3 nmol/ml). The total PC concentrations correlated positively between BALF and TW ($r^2=0.6402$, $P=0.01$) (Figure 84C), but not for BALF and induced sputum ($r^2=0.0255$, $P=0.70$) (Figure 84D). The both BALF and TW total PC concentration varied between individuals and one participant had consistently higher concentrations of PC in all three compartments (Figure 85).

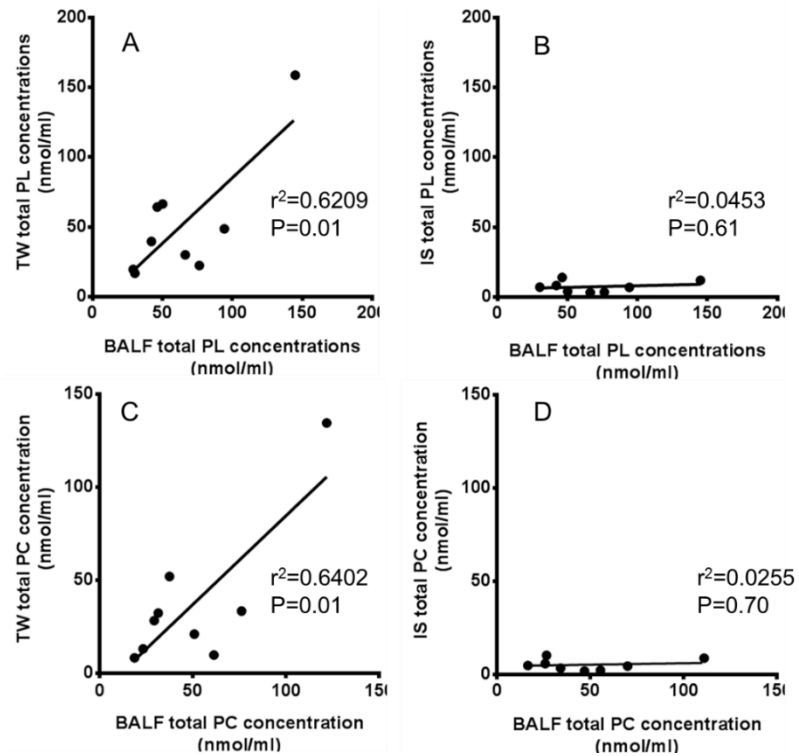


Figure 84; Correlation between bronchoalveolar lavage fluid (BALF), tracheal wash (TW), and induced sputum (IS) phospholipid (PL) and phosphatidylcholine (PC) concentrations. A, comparison between BALF and TW for total phospholipid concentration; B, BALF and IS for total phospholipid concentration. C, BALF and TW for total phosphatidylcholine concentration; D, BALF and IS for total phosphatidylcholine concentration. Assessed by Pearson’s correlation coefficient.

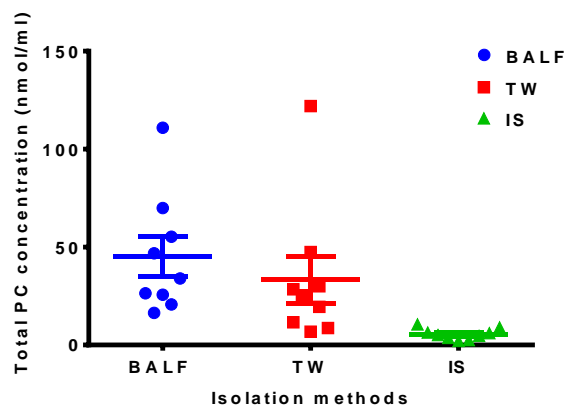


Figure 85; Variation in the total phosphatidylcholine concentrations (nmol/ml) from all sampling methods. BALF, bronchoalveolar lavage fluid; TW, tracheal wash; IS, induced sputum; PC, phosphatidylcholine. There was no significant difference between BALF and TW PC concentrations (mean difference of 11.8nmol/l, $P=0.42$). There was a significant difference between BALF and IS (mean difference 39.6nmol/l, $P=0.02$). Analysis by ANOVA of variance with Bonferroni’s corrections for multiple comparisons.

6.4.3 Surfactant phospholipid composition

6.4.3.1 Phospholipid classes

The fractional phospholipid composition was investigated by measuring the relative proportions of total PC, PG, PI, SPH and LPC, each determined as the sum of these individual molecular species. PE and PS were present at low concentrations and would have required additional analytical scans to assess molecular composition and consequently, these components are not presented here. PC (75%) followed by PG (13%) were the most abundant phospholipids. Although IS had a fractional increase in LPC and SPH, the phospholipid molecular composition was comparable among all sample types without any statistical difference (Figure 86).

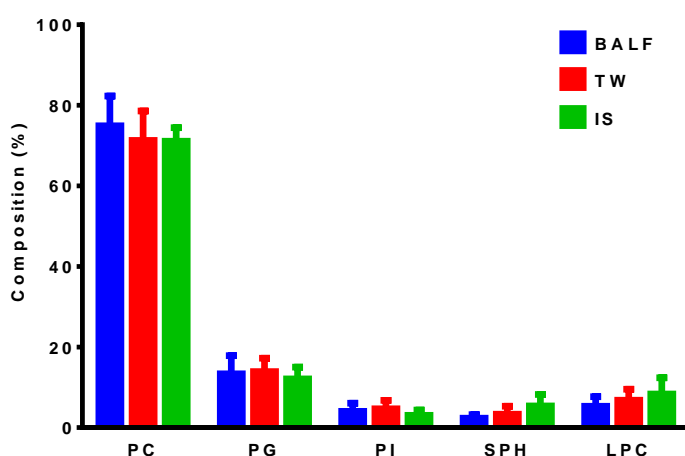


Figure 86; Fractional phospholipid composition from all sampling methods. BALF, bronchoalveolar lavage fluid; TW, tracheal wash; IS, induced sputum; PC, phosphatidylcholine; PG, phosphatidylglycerol; PI, phosphatidylinositol; SPH, sphingomyelin; LPC, lyso-phosphatidylcholine. (Expressed as mean \pm SD). There was no significant difference in overall phospholipids composition between isolation methods.

6.4.3.2 Phosphatidylcholine composition

In BALF, di-saturated PC16:0/16:0 was the dominant PC accounting for more than 50% of total PC. This was followed by PC16:0/18:1 (13%), PC16:0/16:1 (9%), PC16:0/14:0 (9%) and PC16:0/18:2 (6%). 1-alkyl 2-acyl-PC species and polyunsaturated containing PC species were in lesser proportion. These findings are consistent with previously published

data (Postle AD et al. 2001). When BALF PC composition was compared with other isolation methods (TW / induced sputum), significantly lower proportion of PC16:0/16:0 was noted in TW (mean difference (MD) of 4.5% lower, $P < 0.05$) and induced sputum (MD of 7.4% lower, $P < 0.05$). Additionally, induced sputum also had significantly lower proportions of PC16:0/14:0 and PC16:0/16:1 and higher composition of PC16:0/18:1 and PC18:0/18:2 compared to BALF (Table 16). These differences suggest the possibility of dilution of surfactant PC by phospholipids derived from non-alveolar origin in induced sputum.

PC Composition (%)			
PC Species	BALF	TW	IS
PC 16:0/14:0	8.81 (± 0.90)	7.93 (± 1.26)	*6.97 (± 1.58)
PC 16:0a/16:0	2.58 (± 0.39)	2.46 (± 0.42)	3.02 (± 0.63)
PC 16:0/16:1	9.00 (± 1.53)	8.10 (± 1.87)	*7.02 (± 1.31)
PC 16:0/16:0	53.27 (± 3.56)	*48.75 (± 6.39)	*45.83 (± 7.55)
PC 16:0/18:2	5.73 (± 1.07)	6.92 (± 1.78)	*7.56 (± 1.77)
PC 16:0/18:1	12.62 (± 1.65)	13.90 (± 1.93)	*15.27 (± 2.44)
PC 16:0/20:4	1.37 (± 0.42)	1.84 (± 0.80)	1.88 (± 0.68)
PC 18:1/18:2	1.63 (± 0.47)	2.26 (± 0.99)	2.86 (± 0.94)
PC 18:0/18:2	2.67 (± 0.97)	4.02 (± 2.04)	*5.36 (± 1.97)
PC 18:0/18:1	1.33 (± 0.59)	2.07 (± 1.17)	2.89 (± 1.26)
PC 18:1/20:4	0.37 (± 0.16)	0.60 (± 0.38)	0.50 (± 0.17)
PC 18:0/20:4	0.62 (± 0.40)	1.16 (± 0.89)	0.86 (± 0.43)

Table 16; Phosphatidylcholine molecular composition of phospholipid fraction from all sampling methods. (PC, Phosphatidylcholine; BALF, bronchoalveolar lavage fluid; TW, tracheal wash; IS, induced sputum. * $P < 0.05$. Data are expressed as % (mean \pm SD). Analysed by two-way ANOVA of variance with Bonferroni's corrections for multiple comparisons.

6.4.3.3 Phosphatidylglycerol and phosphatidylinositol composition

The relative composition of PG and PI are thought to contribute to surfactant stability and more recently, the importance of PG in immunological functions has been increasingly appreciated (Numata M et al. 2012). Compositional alterations of these anionic phospholipids may lead to dysfunctional surfactant film formation and an increased ratio of PI/PG is characteristic of ALI and ARDS (Schmidt R et al. 2001). Thus, the distribution of molecular variation among these acidic phospholipids may influence the functional characteristics of surfactant in health and disease. Consequently, PG and PI molecular composition was assessed and variation between isolation methods were compared.

In contrast to PC, BALF surfactant PG and PI molecular compositions were dominated by unsaturated species. BALF surfactant PG molecular composition consisted of PG16:0/18:1 (35%), PG18:0/18:1 (20%), and PG18:1/18:1(19%). This was followed by PG16:0/16:0 (9%), PG16:0/18:2 (6%) and PG18:1/8:2 (4%). There was no significant difference in PG composition between BALF and TW. However, there were small but significant differences in PG16:0/18:1 (MD of 3.3% lower, $P=0.01$) and PG18:1/18:1 (3.1% lower, $P=0.02$) in induced sputum compared to BALF (Figure 87A).

PI species from BALF also dominated by monounsaturated species such as PI18:0/18:1 (22%), PI18:1/18:1(21%) and PI16:0/18:1 (20%). There was no significant compositional variation in individual PI species between BALF and TW. There was a significantly higher proportion of polyunsaturated PI species in IS compared to BALF (MD 4.8% higher, $P=0.02$) (Figure 87B). This finding of unsaturated molecular species enrichment among PG and PI species is consistent with previously published data (Postle AD et al. 2001) (Wright SM et al. 2000).

6.4.3.4 Sphingomyelin composition

Sphingomyelin is a minor component of pulmonary surfactant and is an essential constituent of plasma and cellular membranes. Although the importance of sphingolipids in cellular integrity is increasingly recognised, the exact role of these in surfactant function is not known. However, the lecithin/SPH (L/S) ratio has been utilised in the past to assess the degree of cellular contamination in pulmonary surfactant in ARDS patients (Hallman M et al 1982) and in amniotic fluid L/S ratio is used as a marker of fetal lung maturity (Spillman T and Cotton DB 1989).

SPH species contain the same phosphocholine head group as PC and consequently can be readily detected by precursor scans of $m/z184^+$ in ESI-MS/MS. Major SPH species of BALF surfactant were SPH16:0 (65%), SPH24:1 (20%) and SPH24:0 (10%). Other minor species (SPH16:1, SPH18:0, SPH18:1, SPH18:2 and SPH20:4) were detected at much lower abundance (<3%). There were no significant differences in SPH molecular composition between BALF and TW. However, significant compositional differences with relative decrease in SPH16:0 (MD 2.9% lower, $P=0.0003$) and increase in SPH24:1 (MD 1.8% higher, $P=0.04$) was noted in IS compared to BALF (Figure 87C).

6.4.3.5 LPC composition

Lyso-PC species can be readily identified in the region of m/z 400-600 during precursor scans of $m/z184^+$ and this enabled the assessment of LPC molecular composition from all compartments. The BALF surfactant LPC was primarily composed of LPC16:0 (71%), followed by LPC18:1 (13%), LPC18:0 (6%), LPC18:2 (6%) and LPC20:4 (3%). TW had a lower proportion of LPC16:0, whereas IS had lower proportions of LPC16:0 and higher proportions of LPC 18:1 and LPC 18:2 (Figure 87D).

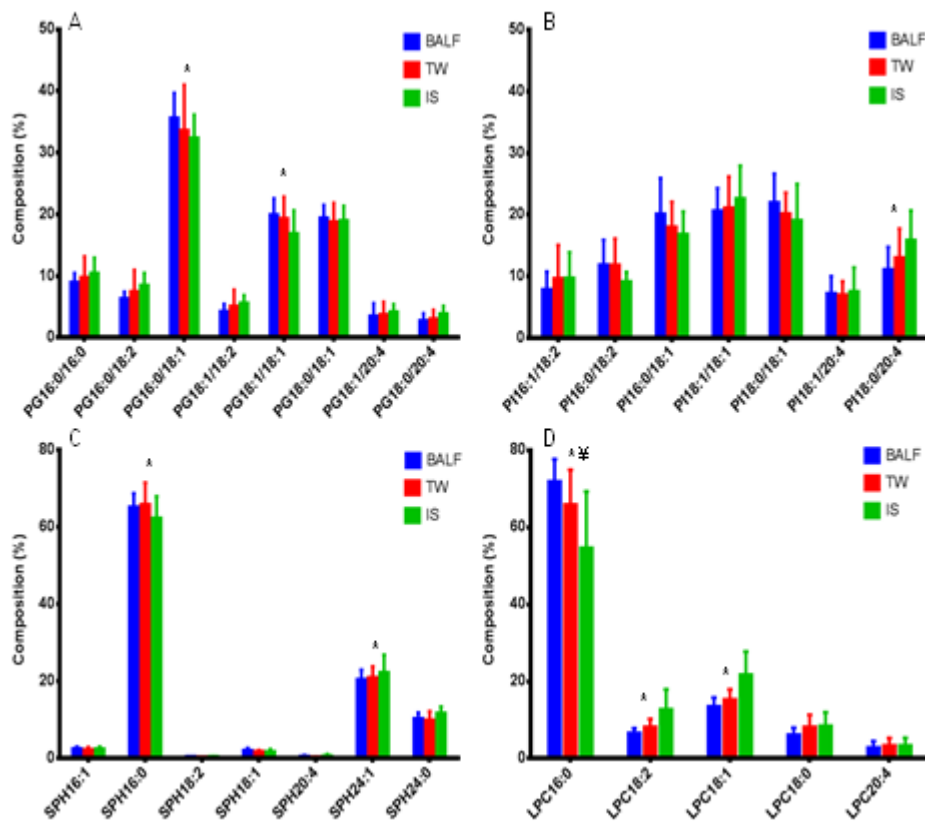


Figure 87; Comparison of surfactant phospholipid subclass molecular composition from all three sampling methods. PI; phosphatidylinositol, PG; phosphatidylglycerol, SPH; sphingomyelin, LPC; lysophosphatidylcholine, BALF, bronchoalveolar lavage fluid; TW, tracheal wash; IS, induced sputum. * $P < 0.05$ comparison between BALF and IS, † $P < 0.05$ comparison between BALF and TW. Data are expressed as % (mean \pm SD) composition of total selected species and analysed by two- way ANOVA of variance with Bonferroni's corrections for multiple comparisons.

6.4.4 Total and fractional PC *methyl-D₉* Incorporation

Methyl-D₉-choline incorporation was measured at two time points (24 and 48 hours) for BALF and TW and five time points (8, 24, 48, 72 and 96 hours) for induced sputum. In BALF, the total *methyl-D₉*-choline incorporation into surfactant PC was $0.35 \pm 0.17\%$ at 24 hours and $0.52 \pm 0.15\%$ at 48 hours with a rate of incorporation of $0.011 \pm 0.002\%$ per hour until 48 hours (Figure 88A). There was no difference in total PC *methyl-D₉*-choline incorporation between BALF and TW (Figure 88A). In addition, there was a positive correlation between BALF and TW for both time points ($r^2 = 0.8344$, $P < 0.0001$) for each individuals (Figure 89A).

The induced sputum surfactant PC *methyl-D₉*-choline incorporation was $0.13 \pm 0.03\%$ at 8 hours and showed a linear incorporation until 48 hours ($r^2=0.9984$, $P=0.02$) at a rate of $0.012 \pm 0.0005\%$ per hour and achieved a steady state between 48-96 hours. The sputum PC *methyl-D₉* incorporation was delayed initially but reached equilibrium with other sample types at 48 hours (Figure 88A). Although there was a positive correlation between BALF and induced sputum for both time points ($r^2=0.3572$, $P=0.03$), this association was much weaker than that of TW and BALF (Figure 89B).

Methyl-D₉ PC16:0/16:0 incorporation was again similar for both BALF and TW at 24 hours ($0.31 \pm 0.06\%$ and $0.29 \pm 0.05\%$) and 48 hours ($0.51 \pm 0.05\%$ and $0.49 \pm 0.04\%$) respectively. However, for induced sputum the PC16:0/16:0 incorporation was much lower at 24 hours ($0.17 \pm 0.13\%$) compared to BALF or TW, but at 48 hours the incorporation reached to similar values of other sampling methods at $0.48 \pm 0.06\%$ (Figure 88B). The *methyl-D₉* PC16:0/16:0 incorporation had linear correlation for BALF and TW. Despite statistical correlation, this association was much weaker for induced sputum (Figure 89C and 89D).

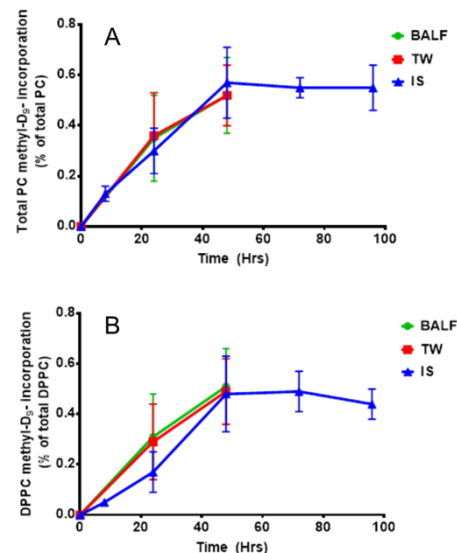


Figure 88; Total phosphatidylcholine (A) and fractional PC16:0/16:0 *methyl-D₉*-incorporation (B) for all sampling methods. Data expressed as mean \pm SD. PC, phosphatidylcholine; DPPC, dipalmitoylphosphatidylcholine; BALF, bronchoalveolar lavage fluid; TW, tracheal wash; IS, induced sputum.

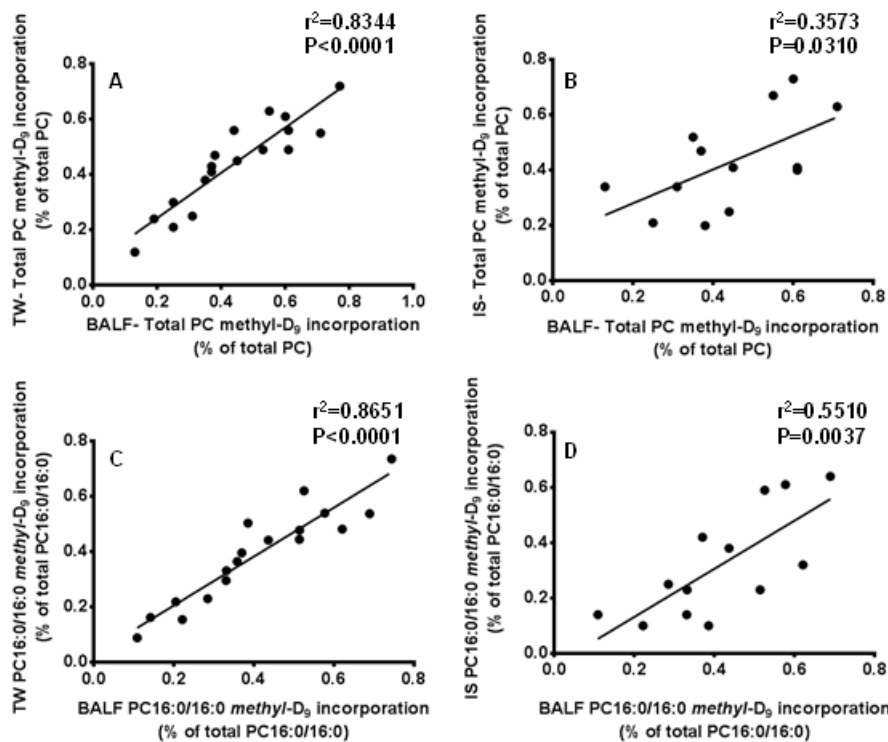


Figure 89; Correlation graphs for the total phosphatidylcholine and fractional PC16:0/16:0 *methyl-D₉*-incorporations for all sampling methods. BALF, bronchoalveolar lavage fluid; TW, tracheal wash; IS, induced sputum; PC, phosphatidylcholine. **A;** Total phosphatidylcholine *methyl-D₉* incorporation for BALF versus TW, **B;** total *methyl-D₉* incorporation for BALF versus IS, **C;** PC16:0/16:0 *methyl-D₉* incorporation for BALF versus TW and **D;** PC16:0/16:0 *methyl-D₉* incorporation for BALF versus IS. Analysed by Pearson’s correlations coefficient.

Relative fractional *methyl-D₉* incorporation of other PC species was assessed for all sampling methods. For BALF surfactant PC species, at 24 hours the *methyl-D₉*-incorporation ranged between 0.31-0.50%, lowest for PC 16:0/16:0 (0.31%) and highest for PC18:1/20:4 (0.50%). At 48 hours the incorporation showed less variation between molecular species ranging between 0.48- 0.57% of total PC. This is likely due to the molecular variation in *methyl-D₉*- incorporation patterns and acyl remodeling mechanisms among PC species (Figure 90). There is also variation in total PC and fractional PC16:0/16:0 *methyl-D₉* incorporation between individuals (Figure 91).

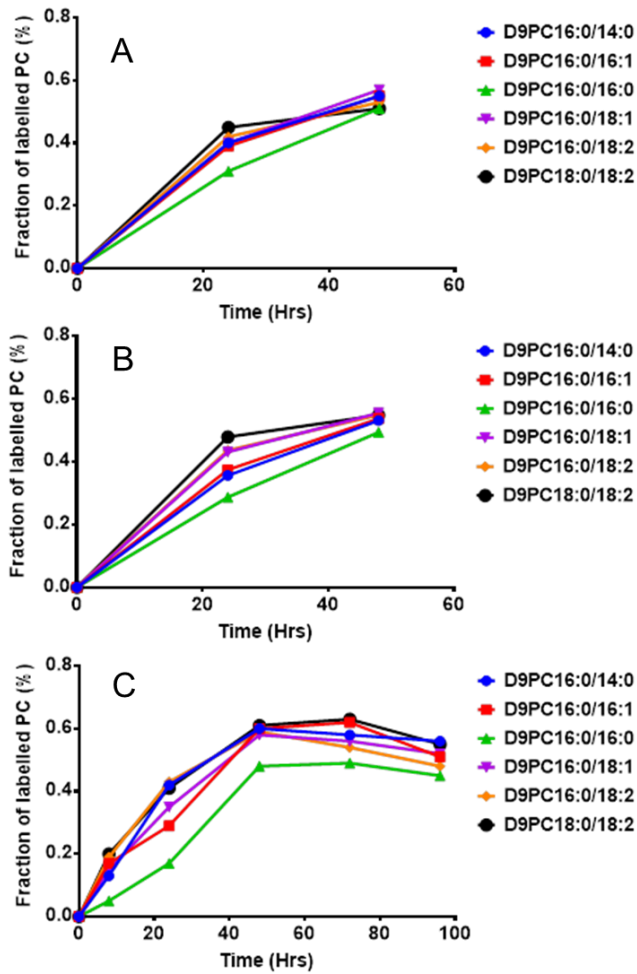


Figure 90; Fractional *methyl-D₉*-incorporation of major surfactant phosphatidylcholine species (PC16:0/14:0, PC16:1/16:0, PC16:0/16:0 and PC16:0/18:1) for all sampling methods. (**A**- Bronchoalveolar lavage fluid, **B**- tracheal wash and **C**- induced sputum).

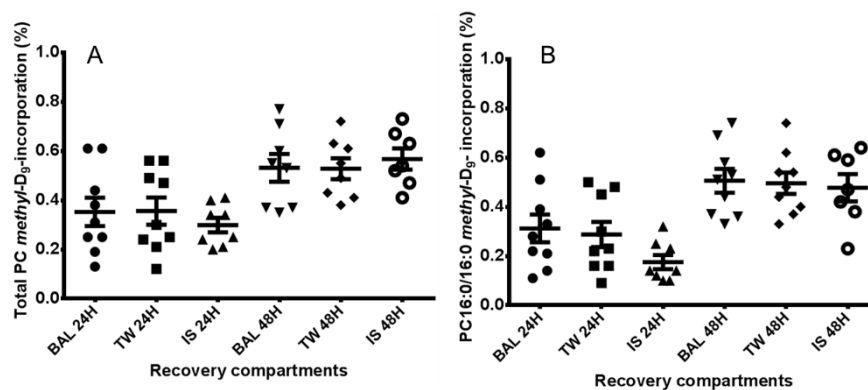


Figure 91; Individual variation in total phosphatidylcholine (**A**) and fractional *methyl-D₉*-PC16:0/16:0 incorporation (**B**). PC, phosphatidylcholine; BAL, bronchoalveolar lavage; TW, tracheal wash; IS, induced sputum.

6.4.5 Molecular specificity of *methyl-D₉*-labelled PC species

Molecular specificity of *methyl-D₉* labelled surfactant showed a much lesser proportion of *methyl-D₉*-labelled PC16:0/16:0 at 24 hours, which equilibrated with the unlabelled fraction at 48 hours. All sampling methods followed the same pattern. *Methyl-D₉*-labelled PC16:0/16:0 from IS showed the most difference, where at 24 hours the *methyl-D₉*-labelled PC16:0/16:0 accounted for only 24% of the labelled PC fraction. At 48 hours, induced sputum and TW showed significant differences in *methyl-D₉*-labelled PC16:0/16:0 compared to BALF (Table 17).

<i>Methyl-D₉</i> -labelled molecular PC composition at 24 and 48 hours						
	24 Hours			48 Hours		
PC species (%)	BALF	TW	IS	BALF	TW	IS
PC16:0/14:0	10.0(±2.5)	7.8 (±2.8)	7.9 (±3.2)	8.8 (±1.0)	7.5 (±1.0)	7.3 (±1.9)
PC16:0a/16:0	2.6(±0.6)	2.4 (±0.6)	4.0 (±2.9)	2.3 (±0.5)	2.3 (±0.5)	3.5 (±0.9)
PC16:0/16:1	10.0(±2.5)	8.9 (±2.4)	7.03 (±2.0)	9.3 (±1.7)	8.1 (±2.1)	7.6 (±2.0)
PC16:0/16:0	46.9(±3.0)	*39.4(±8.5)	*22.5(±7.9)	50.6(±3.8)	*45.4(±7.3)	*40.4(±5.8)
PC16:0/18:2	6.9 (±1.8)	8.32 (±2.7)	*12.6(±2.3)	6.1 (±1.4)	8.0 (±2.4)	8.3 (±0.9)
PC16:0/18:1	14.5 (±1.7)	17.5 (±2.8)	18.2 (±4.5)	13.9 (±1.9)	14.9 (±1.8)	15.9 (±2.2)
PC16:0/20:4	1.5 (±0.6)	2.2 (±0.9)	4.5 (±1.7)	1.5 (±0.5)	2.0 (±0.7)	2.1 (±1.0)
PC18:1/18:2	1.9 (±0.7)	3.1 (±1.5)	5.8 (±1.9)	2.0 (±0.6)	2.7 (±0.9)	3.5 (±1.4)
PC18:0/18:2	3.2 (±0.9)	5.4 (±2.8)	*9.1 (±3.0)	2.8 (±1.1)	4.6 (±2.3)	6.0 (±1.9)
PC18:0/18:1	1.3 (±0.6)	2.5 (±1.2)	4.7 (±2.3)	1.5 (±0.8)	2.3 (±1.8)	3.3 (±1.1)
PC18:1/20:4	0.5 (±0.2)	0.9 (±0.5)	1.5 (±1.1)	0.4 (±0.2)	0.7 (±0.4)	0.9 (±0.4)
PC18:0/20:4	0.7 (±0.4)	1.7 (±0.9)	2.1 (±0.9)	0.7 (±0.5)	1.3 (±1.1)	1.1 (±0.4)

Table 17; Fractional *methyl-D₉* labelled phosphatidylcholine composition from all sampling methods at 24 and 48 hours. BALF, bronchoalveolar lavage fluid; TW, tracheal wash; IS, induced sputum; PC, phosphatidylcholine. (* P<0.05 significant difference when compared with BALF by two-way ANOVA of variance with Bonferroni's corrections for multiple comparisons).

When compared to unlabelled PC composition, the fractional enrichment of PC16:0/16:0 is lower at 24 hours for all compartments BALF (47% vs. 51% $P < 0.05$) TW (39% vs. 45% $P < 0.05$) and IS (24% vs. 40% $P < 0.05$) (Figure 92). *Methyl-D₉*-labelled PC16:0/16:0 fraction was at equilibrium with unlabelled fraction for all compartments BALF (50.6% vs. 52.4% $P = ns$), TW (45.4% vs. 48% $P = ns$) and induced sputum (40.4% vs. 46% $P = ns$) at 48 hours (Figure 92). The fractional enrichments for all other PC species were in equilibrium with unlabelled PC composition at 24 hours.

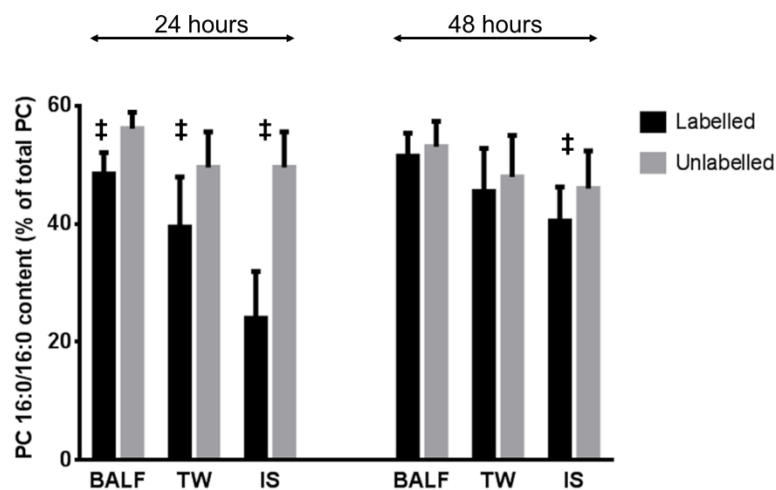


Figure 92; Molecular specificity of *methyl-D₉*-choline incorporation into PC16:0/16:0 synthesis (black bars), expressed as a percentage of *methyl-D₉* labelled PC, was compared with that of unlabelled PC16:0/16:0 (grey bars) at both 24 and 48 hours for bronchoalveolar lavage fluid (BALF), tracheal wash (TW) and induced sputum (IS) (mean \pm SD; ‡ $P < 0.001$ calculated by two way ANOVA of variance with Bonferroni's corrections for multiple comparisons).

6.4.6 BALF LPC assessment and fractional labelling

LPC was assessed for all compartments. The assessment of LPC *methyl-D₉* incorporation for induced sputum was limited by overall lower concentration of phospholipids present in the sputum. The data presented here is only for the BALF. The LPC composition mainly consisted of LPC16:0 (72%), LPC18:1 (13%) and LPC18:2 (6%). At 24 hours *methyl-D₉* labelled LPC16:0 is much lower (57%) than the unlabelled LPC16:0 composition (74%). *Methyl-D₉* labelled LPC composition for all other species were at near equilibrium and

mirrored the unlabelled LPC composition at 24 and 48 hours (Figure 93). Overall, total LPC incorporation was higher (~1%) than total PC incorporation (~0.50%). LPC16:0 *methyl-D₉* incorporation had a positive correlation with PC16:0/16:0 *methyl-D₉* incorporation for both 24 and 48 hours, but with doubled the rate. (Figure 94).

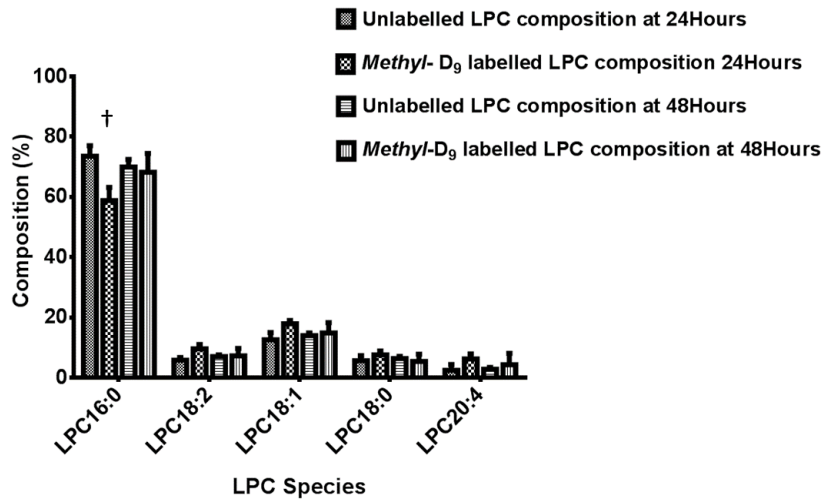


Figure 93; Comparison of bronchoalveolar lavage unlabelled and *methyl-D₉* labelled lysophosphatidylcholine composition at 24 and 48 hours. †P<0.05 when compared between unlabelled LPC composition and *methyl-D₉* labelled LPC composition at 24 hours, analysed by student’s T- test.

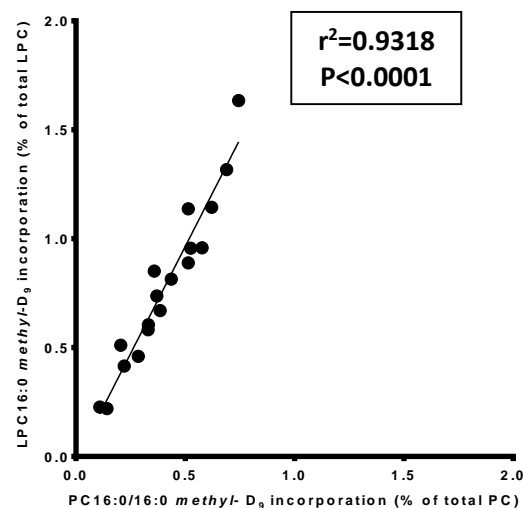


Figure 94; Correlation between LPC16:0 and PC16:0/16:0 *methyl-D₉* incorporation of bronchoalveolar lavage surfactant from healthy volunteers. Analysed by Pearson’s correlation coefficient.

6.5 Discussion

This study demonstrates for the first time the molecular compositions of various bronchialveolar compartments in a human model and the surfactant molecular PC kinetics from all these compartments. The results showed that surfactant extracted by TW closely resembled that of BALF. As AT-II cells are the only source of pulmonary surfactant phospholipids, the significant positive correlation of *methyl-D₉*-choline incorporation between BALF and TW suggests that the surface pressure, as well as mucociliary transit time of surfactant up along the airways had no significant impact on surfactant PC kinetics. It seems that despite the presence of already secreted surfactant along the small and large airways epithelial lining, the entire pulmonary surfactant is at equilibrium within the lung.

Induced sputum had variable phospholipid composition and kinetics compared to BALF, possibly due to several reasons (Table 16 and 17, Figure 87). Firstly, induced sputum phospholipids may represent pools of surfactant with different temporal origins, with some material newly secreted from the alveolus, and combined with previously secreted surfactant embedded within the mucus layer. Secondly, sputum induction is a complex process and the exact origin of the induced sputum is not always known. Furthermore, the contamination from saliva and other non-surfactant phospholipids may have interfered with surfactant assessment. Although induced sputum had qualitatively similar composition to that of alveolar surfactant, it may not be an ideal model to study alveolar surfactant metabolism. Thirdly, the relatively high content of sphingomyelin in induced sputum suggests a proportion of induced sputum phospholipid may be of cellular not surfactant origin (Figure 87C). Such a cellular origin of IS phospholipid may become more significant in disease states characterized by increased airway inflammatory cell infiltration.

Surfactant PC is synthesised *de-novo* by the CDP-choline pathway. However, about 50% of PC16:0/16:0 is produced by acyl-remodelling mechanisms catalysed by the sequential

actions of phospholipase-A₂ and lysophosphatidylcholine acyltransferase activities (Batenburg JJ 1992). It is widely assumed that surfactant PC synthesis and acyl-remodeling processes precede subsequent secretion (Batenburg JJ 1992). However, this study challenges this established concept. If the surfactant PC is secreted after acyl-remodeling and maturation process, the secreted surfactant PC16:0/16:0 compositions should reflect the unlabelled composition at all-time points. This study shows that the proportion of *methyl-D₉*-labelled PC16:0/16:0 is equilibrated with unlabelled PC16:0/16:0 composition only at 48 hours, which implies that a certain proportion of PC is secreted even before the acyl-remodeling mechanisms are complete (Figure 92).

This is the first to study to demonstrate the feasibility of assessing surfactant lyso-PC metabolism *in-vivo* in human subjects. This study shows that LPC16:0 is the principle lyso-PC in pulmonary surfactant, but that total LPC *methyl-D₉* incorporation was twice as that of total PC. The *methyl-D₉*-incorporation of LPC16:0 is much higher than that of PC16:0/16:0 at both 24 and 48 hours (Figure 94). This finding challenges the paradigm that the LPC is formed by hydrolysis of secreted surfactant PC. The much higher fractional incorporation of LPC compared to PC precludes LPC coming from hydrolysis of newly synthesised PC and emphasizes the complexity of the underlying mechanisms of surfactant synthesis and secretion. These observations strongly support the possibility, at least in healthy individuals, that LPC is secreted together with the other surfactant phospholipid rather than simply being a consequence of hydrolysed PC. While phospholipase-mediated hydrolysis of secreted surfactant phospholipid remains a possibility in inflammatory lung disease, a further implication of these results, supported by the strong correlation of stable isotope label incorporations into LPC16:0 and PC16:0/16:0 is that secreted LPC may be ultimately a consequence of acyl remodelling mechanisms within AT-II cells.

Surfactant PC kinetics was analysed from induced sputum in a previous study using *methyl-D₉*-choline, that has demonstrated the feasibility of performing such studies in humans (Bernard W et al. 2004). However, this study was limited by the use of induced

sputum to study surfactant kinetics, which may have not reflected the alveolar surfactant kinetics. Further, there was variability in each fractions of sputum obtained suggesting the lack of consistency and difficulty using this technique to study surfactant kinetics. However, the results were comparable with this study and showed that fractional enrichment of PC16:0/16:0 equilibrates with the unlabelled fraction only at 48 hours. This was demonstrable for all sampling methods.

In this thesis, small volume bronchoalveolar lavages were used instead of quantitative lavage, which has been generally used to study surfactant composition. Small volume lavage may reflect lower airway surfactant rather than alveolar composition. Nevertheless, the PC compositional analysis was comparable to other studies of ARDS patients (Hallman M et al. 1982) (Schmidt R et al. 2007). In-addition, small volume lavages were performed for practical reasons, where it may not be ethical to perform consecutive quantitative lavages on human subjects and this study was conducted on the assumption that this methodology may be utilised in patients with severe ARDS. In the latter context it is not ideal to perform consecutive quantitative lavages which may potentially dilute the endogenous surfactant pool and lead to worsening of airway collapse. Further, this study was not intended to quantify the absolute alveolar surfactant pool, rather the measurements of the dynamic incorporations against the background of unlabelled endogenous composition. The bronchoscope was wedge far enough distally to ensure entrapment of alveolar samples.

Acute lung injury and ARDS are characterised by significant quantitative and qualitative alterations in surfactant phospholipids composition. Despite this understanding, therapeutic attempts with exogenous surfactant remain unhelpful in this population (Meng H et al. 2012). The complexity of ARDS pathogenesis suggests several possible reasons (such as impaired synthesis, increased breakdown and functional inhibition) for surfactant dysfunction. However, *in-vivo* human models investigating such complex underlying mechanisms are lacking. Deficiency in our understanding into patterns of surfactant

synthesis and metabolism in this disease cohort may in part explain the lack of anticipated clinical benefits from exogenous surfactant replacement strategies. Application of stable isotope studies in this population, may possibly identify underlying phenotypes to characterise patients according to pathological mechanisms of surfactant dysfunction. Tracheal washings substituted for quantitative bronchoalveolar lavage may be an alternative for surfactant isolation in patients otherwise unable to tolerate invasive procedures without clinical compromise. However, this technique may need to be validated in disease population.

There is evidence for increased secretory phospholipase-A₂ activity and increased concentrations of lyso-PC in patients with ARDS (Kim DK et al. 1995). This alludes the possibility of increased phospholipase- A₂ mediated hydrolysis of surfactant phospholipids during acute lung injury. As a result this may lead to alterations in the spatial balance of surfactant PC and LPC. Consequently, assessment of LPC kinetics in relation to PC may improve our understanding of surfactant synthesis and recycling via acyl remodelling mechanisms during disease states. However, so far no studies have addressed this in *in-vivo* human models of ARDS.

Surfactant abnormalities are evident in several chronic lung and airway diseases. Although studies have addressed compositional alterations in disease states, so far no studies have assessed dynamic surfactant kinetics. Access to surfactant material involves invasive procedures like bronchoscopy which may preclude performing such studies in large population. Induced sputum may be of value as a non-invasive method to study surfactant metabolism within its inherent limitations.

6.6 Conclusions

This study comprehensibly demonstrates the feasibility of performing stable isotope labelling to study surfactant phospholipid kinetics from bronchoalveolar compartments in healthy adults. Tracheal secretions were more closely resembled alveolar surfactant

composition compared to induced sputum. Although several differences were noted in induced sputum phospholipid composition and turnover compared to BALF, the overall relative changes were small. This study illustrates the utility of various sampling methods to study *in-vivo* surfactant metabolism in humans which can be applied in disease states to possibly identify variation in surfactant metabolism among patients.

Chapter 7

General discussion and future directions

ARDS imposes significant health burden with substantial morbidity and mortality. There are no specific pharmacological therapies available and supportive management with protective lung ventilation remains the main stay of treatment. The heterogeneous nature of the disease coupled with failure of diagnostic definitions to identify specific phenotypes has contributed to the lack of positive clinical outcomes in the many randomised controlled trials in this area (Table 5). Lack of understanding of the complex nature of surfactant metabolism in ARDS remains a major obstacle for any future surfactant related clinical trials. *In-vivo* human models investigating the underlying mechanisms of surfactant metabolism in lung diseases are lacking due to several methodological limitations.

This is the first study to characterise dynamic surfactant molecular PC metabolism in patients with ARDS. This study not only demonstrated the feasibility of using stable isotope labelling to investigate surfactant metabolism, it has also provided novel insights into the patterns of fractional PC synthesis and dynamic *methyl-D₉* incorporation in patients with ARDS. This has never been examined before. In healthy controls and patients, the labelled fraction of PC16:0/16:0 was much lower than expected at earlier time points and only achieved equilibrium with unlabelled fraction at 48 hours after choline infusion (Figure 92). This contradicts the established paradigm that the surfactant is synthesised, acyl-remodelled and subsequently secreted (Batenburg JJ 1992). If this were true, the labelled surfactant PC16:0/16:0 extracted from alveolus would have the same composition as the unlabelled fraction at all time points. This was not the case and the equilibrium was only achieved after 48 hours suggesting the acyl remodelling was only

complete by this time point. Moreover, in some patients, this equilibrium was delayed indicating disruptions in acyl remodelling mechanisms of PC16:0/16:0.

In addition, the total PC and fractional PC16:0/16:0 *methyl-D₉* incorporation was much higher in patients than healthy controls (Figure 21). This may be due to the compensatory response of increased surfactant synthesis by AT-II cells during acute lung injury. Calculations of *methyl-D₉* incorporation was corrected for the background unlabelled fractional PC concentrations as measured by precursor scans of $m/z184^+$. If there were reductions in unlabelled endogenous compositions, the fractional incorporations may have been falsely elevated. This may be other possible explanation for the increased *methyl-D₉* incorporation measured in patients with ARDS. However, this increase was not appreciable in some patients, suggesting that these patients may lack the capacity to increase surfactant PC synthesis during disease processes. These patients may also correspond to a specific cohort with significant AT-II cell injury and paucity of surfactant synthesis. Surfactant phospholipid composition and dynamic synthesis had no correlations with clinical parameters such as compliance, PaO_2/FiO_2 ratio and mortality (Figure 9). This may be due to the small number of patients studied so far and consequent lack of statistical power. Furthermore, mortality of these patients in general is due to multi-organ failure, rather than intractable respiratory failure. Ongoing enrolment of patients into this study is essential to identify clinical correlations with underlying pathophysiological mechanisms of surfactant metabolism.

Surfactant phospholipids are synthesised from choline, glucose, glycerol and free fatty acids. In the past, several studies have utilised labelling of these precursor substances to study surfactant metabolism. Animal studies with radio isotope labelled precursors has helped to assess synthetic and turnover rates of total PC and specific PC species such as PC16:0/16:0 (Jobe A 1980) (Jobe A 1988) (Jacobs H et al. 1982). Stable isotopes with ^{13}C glucose (Bunt JE et al. 1998), ^{13}C palmitic acid and ^{13}C linoleic acid (Cacicchioli P et al.

2001) has been successfully used in pre-term infants to assess fractional synthetic rate (FSR) (% of labelled surfactant synthesised per day) and ^{13}C enrichment into fatty acid. These studies have used total saturated PC (after oxidation with OsO_4) as a surrogate for PC16:0/16:0 or specific fatty acids such as palmitic acid or linoleic acid to quantify enrichment. Various analytical methods such as isotope ratio mass spectrometry, gas chromatography mass spectrometry (GC/MS) and tandem mass spectrometry have been utilised by these studies (Carnielli VP et al. 2009). Although these studies are highly informative they have significant inherent limitations. First, these methodologies initially used osmium tetroxide oxidation of unsaturated phospholipid to generate a SatPC fraction. Consequently, minimal information can be obtained about the molecular specificity of surfactant PC metabolism and, additionally, SatPC composition itself is heterogeneous containing a variable amount of other disaturated species such as PC16:0/14:0 as well as PC16:0/16:0 (Goss V et al. 2013). Second, the laborious sample preparation required for these studies has precluded the early diagnostic application of these methodologies to individuals with lung diseases. In contrast, stable isotope labelling with *methyl-D₉*-choline chloride and analytical methods combining with ESI-MS/MS to monitor incorporation requires minimal sample preparation and has the potential to generate diagnostic surfactant kinetic results in a time scale ideal for clinical treatment decisions for individual patients with acute respiratory compromise.

The essential first stage during surfactant kinetic studies is the isolation of appropriate surfactant material from the alveolar epithelial lining. Although traditional methods involved large volume BALF to quantify fractional compositions, more recently induced sputum and tracheal aspirates have been utilized to study surfactant metabolism in healthy adults and ARDS population respectively (Bernhard W et al. 2004) (Simonato M et al. 2011). However, despite the compositional similarities in the phospholipid fraction recovered from various sampling methods, so far no studies have assessed how this might influence the kinetic data. Furthermore, if the phospholipid kinetics of the alveolar lining

is in equilibrium with the rest of the endobronchial compartments, tracheal aspirates via the endotracheal tube may be a lesser invasive method to extract surfactant than BALF in ARDS patients. To investigate this further, in Chapter 6, healthy volunteers were recruited and phospholipid fractions with kinetic assessments were made from induced sputum, tracheal washings and small volume BALF. Phospholipid fractions extracted from tracheal wash has close resemblance to that of alveolar surfactant in both composition and kinetics (Table 16 and Figure 88). This preliminary study suggests the possibility of using tracheal aspirate as an alternative to BALF to isolate surfactant material from patients in the future. There are several advantages of tracheal aspirate compared to BALF. Tracheal aspirate is less invasive, can be performed by a nursing staff and would not require any additional sedation. This will undoubtedly facilitate patient recruitment for future surfactant related studies.

Endogenous PC synthesis is dependent on two essential synthetic pathways. CDP-choline pathway is utilised by all nucleated cells (Li Z and Vance DE 2008). Whereas, hepatocytes utilise PEMT pathway for about third of their PC synthesis and output (Waite KA et al. 2002). Liver is the primary source for lipid synthesis and export. ARDS is characterised by multi-organ failure and hepatic impairment is also a recognised feature (Schwartz DB et al. 1989). The alterations in the surfactant phospholipid metabolism evident in ARDS patients may not be limited to the endobronchial compartments. Furthermore, despite their capability to produce specific fatty acids, AT-II cells are dependent on the availability of phospholipids from external sources for effective surfactant synthesis. Patterns of phospholipid synthesis and metabolism have not been investigated before in patients with ARDS, particularly outside the lung. With this in mind, it was essential to investigate both PC synthetic pathways and their molecular specificity to explore systemic and hepatic patterns of PC synthesis.

Surfactant synthesis is dependent on intact AT-II cells to produce PC via CDP-choline pathway. In addition to the alterations in surfactant metabolism, there were global changes in phospholipid composition in circulating plasma lipids and peripheral cells. Significant reductions in LDL, HDL, cholesterol and total PC concentrations coupled with specific increases in selective PC species were noted in patients with ARDS (Table 13, Figure 28). There were gradual improvements in these circulating plasma lipids over time except for PC. The reductions in plasma circulating lipids are likely to be due to increased usage, or possibly reduced synthesis by the liver and peripheral cells. A unique finding was that patient's plasma was highly enriched in PC16:0/18:1 with increased fractional synthesis of the same PC molecule (Figures 32 and 43). The clinical significance of this is not entirely clear. But it's possible that PC16:0/18:1 acts as a hierarchy of PC species which is later acyl remodelled into other PC species depending on the need.

In ARDS patients, despite the substantial increase in the flux through CDP-choline pathway, this was not enough to increase the total PC concentrations in the plasma (Figure 29). Additionally, the flux through PEMT pathway was significantly reduced even in patients with normal markers of hepatic synthetic function. This switching of PC synthetic pathways may be part of natural selection to selectively increase CDP-choline pathway products, such as mono and di-unsaturated PC species during a state of insult. This switching of selective changes in PC synthetic pathways has not demonstrated before in any disease states either in animal or human models. This is the first study to demonstrate this phenomenon in a specified adult human disease. One patient had overt liver failure and had virtually no PEMT mediated PC synthesis, but had relatively normal total PC concentration, with significant increase in PC flux through CDP-choline pathway. PEMT mediated PC synthesis is selective for PUFA-based PC species and paucity of PEMT activity may influence plasma concentrations and modify subsequent generation of inflammatory mediators through arachidonic acid pathways.

This is the first study to utilise two ESI-MS/MS analytical modes to quantify the molecular specificity of PC flux through PEMT pathway in a defined patient cohort. Parent scans of $m/z184^+$, $m/z187^+$ and $m/z190^+$ enabled assessment of unlabelled and one and two deuterium labelled methyl group enriched PC species with subsequent estimation of *methyl-D₃-SAM* enrichment. However, ARDS patients had significantly lower PC flux through PEMT pathway with very low concentrations of *methyl-D₆* PC enrichment. For this instance, specific neutral loss scans were additionally used to assess *methyl-D₆* enrichment with subsequent estimation of *methyl-D₃-SAM* enrichment. These two methods correlated well with each other for the estimation of *methyl-D₃-SAM* enrichment in both patients and healthy controls (Figure 51). These novel approaches may enable the assessment of PEMT activity non-invasively in human patients with real clinical conditions in the future. So far such studies have been mainly conducted in animal models and normally would require hepatic tissue for the assessment of PEMT activity.

Cellular phospholipids are essential not only for the physical properties of membranes, but have diverse functions including intra-cellular cell signalling and provide substrates for the generation of pro and anti-inflammatory lipid mediators. The phospholipids of cellular membranes are highly controlled and dependent on several cellular processes such as biosynthesis, remodelling, degradation, recycling and intracellular and trans-cellular lipid transfer. The fatty acid composition and phospholipid synthetic pathways have been extensively studied in several cultured cell lines (MacDonald JIS and Sprecher H 1991). However, little is known about the variations in molecular phospholipid composition and synthesis in disease states. Moreover, traditional analytical methods of fatty acid analysis using gas chromatographic in cell membranes, lacks specific information regarding molecular composition and synthesis (Postle AD et al. 2007). In contrast, ESI-MS/MS combined with stable isotope labelling is a novel technique to assess molecular PC synthesis in human cell lines (Postle AD et al. 2003).

Studies of cultured cell lines indicate, membrane phospholipid molecular composition can be manipulated by the presence of external fatty acids. Chapter four demonstrated that there were significant alterations in plasma PC molecular composition in ARDS patients. From this one can postulate, that the phospholipid compositional changes evident in plasma may influence the final membrane composition in circulating peripheral blood cells and hence their function. To investigate this, the molecular PC composition and dynamic incorporation of *methyl-D₉* choline into cellular PC of red blood cells, CD15+ neutrophils and CD3+ lymphocytes were assessed. However, due to the smaller quantity of the lymphocytes, kinetic data for these cells was not obtained. In ARDS patients, there were significant PC compositional changes evident in all cell lines investigated. Red blood cells showed increases in the fractional composition and incorporation of PC16:0/18:1 (Figures 61 and 67). Whereas, CD15+ neutrophils had specific increase in fractional composition and synthesis of PC18:0/18:2 (or possibly PC18:1/18:1) (Figure 73). Furthermore, CD3+ lymphocytes showed strikingly diminished concentrations of arachidonyl PC species (Figure 77). This is the first time these findings are demonstrated in a specific human disease. Further studies are needed to establish a functional or clinical correlation with these global phospholipid changes evident in peripheral blood cells including inflammatory cells.

This pilot study confirms the feasibility of performing stable isotope labelling to investigate phospholipid metabolism in various biological samples. The variability in the surfactant phospholipid synthetic patterns in ARDS patients, indicate the presence of underlying phenotypes of surfactant metabolism. Ongoing enrolment of adequate numbers patients will help to explore this further and future studies should attempt to elicit clinical correlations. Moreover, studies should also consider assessing the fate of exogenously supplemented surfactant by using this investigative model, which may be of significance for future randomised clinical trials of surfactant replacement. This thesis also confirms that phospholipid fractions and kinetics of tracheal aspirates closely resemble that of BALF

in healthy adults. Another study is underway to establish correlation between endobronchial phospholipid fractions in intensive care intubated patients. The use of tracheal aspirates instead of BALF to assess phenotypic variation of surfactant metabolism is potentially useful in minimising side effects and may facilitate translational studies in the future.

This thesis further expanded our insight into hepatic and cellular PC synthetic patterns in ARDS. The specific changes in PC molecular composition may be of value as biomarkers of disease severity or progression. Utilising these methodologies, a study is currently underway, to establish cohorts of large-scale systematic phenotyping of critically-ill patients, according to phospholipid metabolism. This will enable a comprehensive analysis of alveolar and systemic lipid mediators and their contribution in critical illness and multi-organ dysfunction. Furthermore, future studies should target therapeutic dietary modifications, to manipulate hepatic and cellular synthetic patterns of phospholipids and consequently minimising the down-stream release of systemic inflammatory lipid mediators to moderate inflammation.

Appendix- 1. Publications

Phospholipid composition and kinetics in different endobronchial fractions from healthy volunteers. **Dushianthan A**, Goss V, Cusack R, Grocott MPW, Postle AD (2014). *BMC Pulmonary Medicine*; 14 (1): 10.

Surfactant phospholipid kinetics in patients with acute respiratory distress syndrome (ARDS). **Dushianthan A**, Cusack R, Pappachan J, Goss V, Postle AD, Grocott MPW (2013). *Journal of Intensive Care Society*; 14(1); S08-S09.

Altered phosphatidylcholine synthetic pathways in acute respiratory distress syndrome (ARDS). **Dushianthan A**, Cusack R, Goss V, Postle AD, Grocott MPW (2013). *British Journal of Anaesthesia*; 110 (5); 860-885.

Neutrophil phospholipid profiling in patients with Acute Respiratory Distress syndrome (ARDS). **Dushianthan A**, Cusack R, Goss V, Grocott M, Postle AD (2012). *Intensive Care Med*; 38(Suppl 1):S258.

Phenotypic characterisation of patients with Acute Respiratory Distress syndrome (ARDS) according to surfactant synthetic function. **Dushianthan A**, Cusack R, Goss V, Pappachan J, Postle A, Grocott MPW (2012). *Intensive Care Med*; 38 (Suppl 1): S258

Surfactant phospholipid kinetics in patients with Acute Respiratory Distress syndrome (ARDS). **Dushianthan A**, Cusack R, Goss V, Postle AD, Grocott MPW (2012). *Thorax*;67(Suppl 2); A11.

Bronchoalveolar lavage, tracheal wash and induced sputum surfactant phospholipid kinetics from healthy volunteers. **Dushianthan A**, Cusack R, Goss V, Grocott MPW, Postle AD (2012). *Thorax*;67 (Suppl 2); A30.

Exogenous surfactant therapy for acute lung injury/acute respiratory distress syndrome – where do we go from here? **Dushianthan A**, Cusack R, Goss V, Postle AD, Grocott MPW (2012). *Critical Care*;16(6):238.

Exogenous surfactant therapy in acute lung injury/acute respiratory distress syndrome: the need for a revised paradigm approach. **Dushianthan A**, Cusack R, Grocott M, Postle AD (2012). *J Cardiothorac Vasc Anesth*;26(5):e50.

Acute Respiratory distress Syndrome and Acute Lung Injury. **Dushianthan A**, Grocott MP, Postle AD, Cusack R (2011). *Postgrad Med J*;87(1031):612-22

References

Abel SJ, Finney SJ, Brett SJ, Keogh BF, Morgan CJ, Evans TW. Reduced mortality in association with the acute respiratory distress syndrome (ARDS). *Thorax* 1998 Apr;53(4):292-4.

Abraham E, Carmody A, Shenkar R, Arcaroli J. Neutrophils as early immunologic effectors in hemorrhage- or endotoxemia-induced acute lung injury. *Am J Physiol Lung Cell Mol Physiol* 2000 Dec;279(6):L1137-L1145.

Adhikari N, Burns KE, Meade MO. Pharmacologic treatments for acute respiratory distress syndrome and acute lung injury: systematic review and meta-analysis. *Treat Respir Med* 2004;3(5):307-28.

Andreeva AV, Kutuzov MA, Voyno-Yasenetskaya TA. Regulation of surfactant secretion in alveolar type II cells. *Am J Physiol Lung Cell Mol Physiol* 2007 Aug;293(2):L259-L271.

Arbibe L, Koumanov K, Vial D, Rougeot C, Faure G, Havet N, et al. Generation of lyso-phospholipids from surfactant in acute lung injury is mediated by type-II phospholipase A2 and inhibited by a direct surfactant protein A-phospholipase A2 protein interaction. *J Clin Invest* 1998 Sep 15;102(6):1152-60.

ARDS Network 2000a. Ventilation with lower tidal volumes as compared with traditional tidal volumes for acute lung injury and the acute respiratory distress syndrome. The Acute Respiratory Distress Syndrome Network. *N Engl J Med* 2000 May 4;342(18):1301-8.

ARDS Network 2000b. Ketoconazole for early treatment of acute lung injury and acute respiratory distress syndrome: a randomized controlled trial. The ARDS Network. *JAMA* 2000 Apr 19;283(15):1995-2002.

ARDS Network 2002. Randomized, placebo-controlled trial of lisofylline for early treatment of acute lung injury and acute respiratory distress syndrome. *Crit Care Med* 2002 Jan;30(1):1-6.

Artigas A, Bernard GR, Carlet J, Dreyfuss D, Gattinoni L, Hudson L, et al. The American-European Consensus Conference on ARDS, part 2: Ventilatory, pharmacologic, supportive therapy, study design strategies, and issues related to recovery and remodeling. Acute respiratory distress syndrome. *Am J Respir Crit Care Med* 1998 Apr;157(4 Pt 1):1332-47.

Ashbaugh DG, Bigelow DB, Petty TL, Levine BE. Acute respiratory distress in adults. *Lancet* 1967 Aug 12;2(7511):319-23.

Avery ME, Mead J. Surface properties in relation to atelectasis and hyaline membrane disease. *AMA J Dis Child* 1959 May;97(5, Part 1):517-23.

Bachofen M, Weibel ER. Alterations of the gas exchange apparatus in adult respiratory insufficiency associated with septicemia. *Am Rev Respir Dis* 1977 Oct;116(4):589-615.

Batenburg JJ. Surfactant phospholipids: synthesis and storage. *Am J Physiol* 1992 Apr;262(4 Pt 1):L367-L385.

Bernard GR, Artigas A, Brigham KL, Carlet J, Falke K, Hudson L, et al. The American-European Consensus Conference on ARDS. Definitions, mechanisms, relevant outcomes, and clinical trial coordination. *Am J Respir Crit Care Med* 1994 Mar;149(3 Pt 1):818-24.

Bernhard W, Pynn CJ, Jaworski A, Rau GA, Hohlfeld JM, Freihorst J, et al. Mass spectrometric analysis of surfactant metabolism in human volunteers using deuteriated choline. *Am J Respir Crit Care Med* 2004 Jul 1;170(1):54-8.

Bersten AD, Edibam C, Hunt T, Moran J. Incidence and mortality of acute lung injury and the acute respiratory distress syndrome in three Australian States. *Am J Respir Crit Care Med* 2002 Feb 15;165(4):443-8.

Bligh EG, Dyer WJ. A rapid method of total lipid extraction and purification. *Can J Biochem Physiol* 1959 Aug;37(8):911-7.

Bonnans C, Levy BD. Lipid mediators as agonists for the resolution of acute lung inflammation and injury. *Am J Respir Cell Mol Biol* 2007 Feb;36(2):201-5.

Boyum A. Isolation of leucocytes from human blood. Further observations. Methylcellulose, dextran, and ficoll as erythrocyteaggregating agents. *Scand J Clin Lab Invest Suppl* 1968;97:31-50.

Boyum A, Lovhaug D, Tresland L, Nordlie EM. Separation of leucocytes: improved cell purity by fine adjustments of gradient medium density and osmolality. *Scand J Immunol* 1991 Dec;34(6):697-712.

Brewer LA, Burbank B, . The wet lung in war casualties. *Ann Surg* 1946 Mar;123:343-62.

Brower RG, Lanken PN, MacIntyre N, Matthay MA, Morris A, Ancukiewicz M, et al. Higher versus lower positive end-expiratory pressures in patients with the acute respiratory distress syndrome. *N Engl J Med* 2004 Jul 22;351(4):327-36.

Bridges JP, Davis HW, Damodarasamy M, Kuroki Y, Howles G, Hui DY, et al. Pulmonary surfactant proteins A and D are potent endogenous inhibitors of lipid peroxidation and oxidative cellular injury. *J Biol Chem* 2000 Dec 8;275(49):38848-55.

Brun-Buisson C, Minelli C, Bertolini G, Brazzi L, Pimentel J, Lewandowski K, et al. Epidemiology and outcome of acute lung injury in European intensive care units. Results from the ALIVE study. *Intensive Care Med* 2004 Jan;30(1):51-61.

Bunt JE, Zimmermann LJ, Wattimena JL, van Beek RH, Sauer PJ, Carnielli VP. Endogenous surfactant turnover in preterm infants measured with stable isotopes. *Am J Respir Crit Care Med* 1998 Mar;157(3 Pt 1):810-4.

Burford TH, Burbank B. Traumatic wet lung; observations on certain physiologic fundamentals of thoracic trauma. *J Thorac Surg* 1945 Dec;14:415-24.

Burgoyne RD, Barclay JW. Splitting the quantum: regulation of quantal release during vesicle fusion. *Trends Neurosci* 2002 Apr;25(4):176-8.

Caesar PA, Wilson SJ, Normand CS, Postle AD. A comparison of the specificity of phosphatidylcholine synthesis by human fetal lung maintained in either organ or organotypic culture. *Biochem J* 1988 Jul 15;253(2):451-7.

Caironi P, Ichinose F, Liu R, Jones RC, Bloch KD, Zapol WM. 5-Lipoxygenase deficiency prevents respiratory failure during ventilator-induced lung injury. *Am J Respir Crit Care Med* 2005 Aug 1;172(3):334-43.

Calder PC. Long-chain fatty acids and inflammation. *Proc Nutr Soc* 2012 May;71(2):284-9.

Carnielli VP, Zimmermann LJ, Hamvas A, Cogo PE. Pulmonary surfactant kinetics of the newborn infant: novel insights from studies with stable isotopes. *J Perinatol* 2009 May;29 Suppl 2:S29-S37.

Cavicchioli P, Zimmermann LJ, Cogo PE, Badon T, Giordano G, Torresin M, et al. Endogenous surfactant turnover in preterm infants with respiratory distress syndrome studied with stable isotope lipids. *Am J Respir Crit Care Med* 2001 Jan;163(1):55-60.

Chabot S, Koumanov K, Lambeau G, Gelb MH, Balloy V, Chignard M, et al. Inhibitory effects of surfactant protein A on surfactant phospholipid hydrolysis by secreted phospholipases A2. *J Immunol* 2003 Jul 15;171(2):995-1000.

Chander A, Chen XL, Naidu DG. A role for diacylglycerol in annexin A7-mediated fusion of lung lamellar bodies. *Biochim Biophys Acta* 2007 Oct;1771(10):1308-18.

Chevalier G, Collet AJ. In vivo incorporation of choline- 3 H, leucine- 3 H and galactose- 3 H in alveolar type II pneumocytes in relation to surfactant synthesis. A quantitative radioautographic study in mouse by electron microscopy. *Anat Rec* 1972 Nov;174(3):289-310.

Chilton FH, Hadley JS, Murphy RC. Incorporation of arachidonic acid into 1-acyl-2-lyso-sn-glycero-3-phosphocholine of the human neutrophil. *Biochim Biophys Acta* 1987 Jan 13;917(1):48-56.

Chilton FH, Patel M, Fonteh AN, Hubbard WC, Triggiani M. Dietary n-3 fatty acid effects on neutrophil lipid composition and mediator production. Influence of duration and dosage. *J Clin Invest* 1993 Jan;91(1):115-22.

Clements JA. Surface tension of lung extracts. *Proc Soc Exp Biol Med* 1957 May;95(1):170-2.

Cockshutt AM, Possmayer F. Lysophosphatidylcholine sensitizes lipid extracts of pulmonary surfactant to inhibition by serum proteins. *Biochim Biophys Acta* 1991 Oct 15;1086(1):63-71.

Cole LK, Vance JE, Vance DE. Phosphatidylcholine biosynthesis and lipoprotein metabolism. *Biochim Biophys Acta* 2012 May;1821(5):754-61.

Connors AF, Jr., Speroff T, Dawson NV, Thomas C, Harrell FE, Jr., Wagner D, et al. The effectiveness of right heart catheterization in the initial care of critically ill patients. SUPPORT Investigators. *JAMA* 1996 Sep 18;276(11):889-97.

da Costa KA, Sanders LM, Fischer LM, Zeisel SH. Docosahexaenoic acid in plasma phosphatidylcholine may be a potential marker for in vivo phosphatidylethanolamine N-methyltransferase activity in humans. *Am J Clin Nutr* 2011 May;93(5):968-74.

DeLong CJ, Shen YJ, Thomas MJ, Cui Z. Molecular distinction of phosphatidylcholine synthesis between the CDP-choline pathway and phosphatidylethanolamine methylation pathway. *J Biol Chem* 1999 Oct 15;274(42):29683-8.

den Breejen JN, Batenburg JJ, Van Golde LM. The species of acyl-CoA in subcellular fractions of type II cells isolated from adult rat lung and their incorporation into phosphatidic acid. *Biochim Biophys Acta* 1989 Apr 26;1002(3):277-82.

Dias VC, Parsons HG. Modulation in delta 9, delta 6, and delta 5 fatty acid desaturase activity in the human intestinal CaCo-2 cell line. *J Lipid Res* 1995 Mar;36(3):552-63.

Dushianthan A, Cusack R, Goss V, Postle AD, Grocott MP. Clinical review: Exogenous surfactant therapy for acute lung injury/acute respiratory distress syndrome - where do we go from here? *Crit Care* 2012 Nov 22;16(6):238.

Edelson JD, Vadas P, Villar J, Mullen JB, Pruzanski W. Acute lung injury induced by phospholipase A2. Structural and functional changes. *Am Rev Respir Dis* 1991 May;143(5 Pt 1):1102-9.

Enhörning G. Surfactant in airway disease. *Chest* 2008 Apr;133(4):975-80.

Fuchimukai T, Fujiwara T, Takahashi A, Enhörning G. Artificial pulmonary surfactant inhibited by proteins. *J Appl Physiol* (1985) 1987 Feb;62(2):429-37.

Fujiwara T, Maeta H, Chida S, Morita T, Watabe Y, Abe T. Artificial surfactant therapy in hyaline-membrane disease. *Lancet* 1980 Jan 12;1(8159):55-9.

Furue S, Mikawa K, Nishina K, Shiga M, Ueno M, Tomita Y, et al. Therapeutic time-window of a group IIA phospholipase A2 inhibitor in rabbit acute lung injury: correlation with lung surfactant protection. *Crit Care Med* 2001 Apr;29(4):719-27.

Galella G, Marangoni F, Rise P, Colombo C, Galli G, Galli C. n-6 and n-3 fatty acid accumulation in thp-1 cell phospholipids. *Biochim Biophys Acta* 1993 Sep 8;1169(3):280-90.

Gao SF, Perkins GD, Gates S, Young D, McAuley DF, Tunnicliffe W, et al. Effect of intravenous beta-2 agonist treatment on clinical outcomes in acute respiratory distress syndrome (BALTI-2): a multicentre, randomised controlled trial. *Lancet* 2012 Jan 21;379(9812):229-35.

Garmany TH, Moxley MA, White FV, Dean M, Hull WM, Whitsett JA, et al. Surfactant composition and function in patients with ABCA3 mutations. *Pediatr Res* 2006 Jun;59(6):801-5.

Gattinoni L, Bombino M, Pelosi P, Lissoni A, Pesenti A, Fumagalli R, et al. Lung structure and function in different stages of severe adult respiratory distress syndrome. *JAMA* 1994 Jun 8;271(22):1772-9.

Glasser L, Fiederlein RL. The effect of various cell separation procedures on assays of neutrophil function. A critical appraisal. *Am J Clin Pathol* 1990 May;93(5):662-9.

Goldyne ME. Lymphocytes and arachidonic acid metabolism. *Prog Allergy* 1988;44:140-52.

Gordon BR, Parker TS, Levine DM, Saal SD, Wang JC, Sloan BJ, et al. Low lipid concentrations in critical illness: implications for preventing and treating endotoxemia. *Crit Care Med* 1996 Apr;24(4):584-9.

Goss V, Hunt AN, Postle AD. Regulation of lung surfactant phospholipid synthesis and metabolism. *Biochim Biophys Acta* 2013 Feb;1831(2):448-58.

Greene KE, Wright JR, Steinberg KP, Ruzinski JT, Caldwell E, Wong WB, et al. Serial changes in surfactant-associated proteins in lung and serum before and after onset of ARDS. *Am J Respir Crit Care Med* 1999 Dec;160(6):1843-50.

Gregory TJ, Longmore WJ, Moxley MA, Whitsett JA, Reed CR, Fowler AA, III, et al. Surfactant chemical composition and biophysical activity in acute respiratory distress syndrome. *J Clin Invest* 1991 Dec;88(6):1976-81.

Grommes J, Soehnlein O. Contribution of neutrophils to acute lung injury. *Mol Med* 2011 Mar;17(3-4):293-307.

Gunasekara L, Schoel WM, Schurch S, Amrein MW. A comparative study of mechanisms of surfactant inhibition. *Biochim Biophys Acta* 2008 Feb;1778(2):433-44.

Gunther A, Siebert C, Schmidt R, Ziegler S, Grimminger F, Yabut M, et al. Surfactant alterations in severe pneumonia, acute respiratory distress syndrome, and cardiogenic lung edema. *Am J Respir Crit Care Med* 1996 Jan;153(1):176-84.

Gust R, Kozlowski JK, Stephenson AH, Schuster DP. Role of cyclooxygenase-2 in oleic acid-induced acute lung injury. *Am J Respir Crit Care Med* 1999 Oct;160(4):1165-70.

Haagsman HP, Diemel RV. Surfactant-associated proteins: functions and structural variation. *Comp Biochem Physiol A Mol Integr Physiol* 2001 May;129(1):91-108.

Halliday HL. Surfactants: past, present and future. *J Perinatol* 2008 May;28 Suppl 1:S47-S56.

Hallman M, Spragg R, Harrell JH, Moser KM, Gluck L. Evidence of lung surfactant abnormality in respiratory failure. Study of bronchoalveolar lavage phospholipids, surface activity, phospholipase activity, and plasma myoinositol. *J Clin Invest* 1982 Sep;70(3):673-83.

Haslam PL, Baughman RP. Report of ERS Task Force: guidelines for measurement of acellular components and standardization of BAL. *Eur Respir J* 1999 Aug;14(2):245-8.

Haworth O, Levy BD. Endogenous lipid mediators in the resolution of airway inflammation. *Eur Respir J* 2007 Nov;30(5):980-92.

Healy DA, Wallace FA, Miles EA, Calder PC, Newsholm P. Effect of low-to-moderate amounts of dietary fish oil on neutrophil lipid composition and function. *Lipids* 2000 Jul;35(7):763-8.

Hermansson M, Hokynar K, Somerharju P. Mechanisms of glycerophospholipid homeostasis in mammalian cells. *Prog Lipid Res* 2011 Jul;50(3):240-57.

Herridge MS, Cheung AM, Tansey CM, Matte-Martyn A, Diaz-Granados N, Al-Saidi F, et al. One-year outcomes in survivors of the acute respiratory distress syndrome. *N Engl J Med* 2003 Feb 20;348(8):683-93.

Herridge MS, Tansey CM, Matte A, Tomlinson G, Diaz-Granados N, Cooper A, et al. Functional disability 5 years after acute respiratory distress syndrome. *N Engl J Med* 2011 Apr 7;364(14):1293-304.

Heung YM, Postle AD. Substrate selectivity of phospholipase D in HL60 granulocytes: effects of fatty acid supplementation. *Biochem Soc Trans* 1995 May;23(2):276S.

Hite RD, Seeds MC, Jacinto RB, Grier BL, Waite BM, Bass DA. Lysophospholipid and fatty acid inhibition of pulmonary surfactant: non-enzymatic models of phospholipase A2 surfactant hydrolysis. *Biochim Biophys Acta* 2005 Dec 30;1720(1-2):14-21.

Holm BA, Notter RH. Effects of hemoglobin and cell membrane lipids on pulmonary surfactant activity. *J Appl Physiol* (1985) 1987 Oct;63(4):1434-42.

Holm BA, Matalon S, Finkelstein JN, Notter RH. Type II pneumocyte changes during hyperoxic lung injury and recovery. *J Appl Physiol* (1985) 1988 Dec;65(6):2672-8.

Holm BA, Enhorning G, Notter RH. A biophysical mechanism by which plasma proteins inhibit lung surfactant activity. *Chem Phys Lipids* 1988 Nov;49(1-2):49-55.

Holm BA, Wang Z, Notter RH. Multiple mechanisms of lung surfactant inhibition. *Pediatr Res* 1999 Jul;46(1):85-93.

Hopkins RO, Herridge MS. Quality of life, emotional abnormalities, and cognitive dysfunction in survivors of acute lung injury/acute respiratory distress syndrome. *Clin Chest Med* 2006 Dec;27(4):679-89.

Hughes M, MacKirdy FN, Ross J, Norrie J, Grant IS. Acute respiratory distress syndrome: an audit of incidence and outcome in Scottish intensive care units. *Anaesthesia* 2003 Sep;58(9):838-45.

Hunt AN, Clark GT, Neale JR, Postle AD. A comparison of the molecular specificities of whole cell and endonuclear phosphatidylcholine synthesis. *FEBS Lett* 2002 Oct 23;530(1-3):89-93.

Jacobs H, Jobe A, Ikegami M, Jones S. Surfactant phosphatidylcholine source, fluxes, and turnover times in 3-day-old, 10-day-old, and adult rabbits. *J Biol Chem* 1982 Feb 25;257(4):1805-10.

Jacobs RL, Devlin C, Tabas I, Vance DE. Targeted deletion of hepatic CTP:phosphocholine cytidyltransferase alpha in mice decreases plasma high density and very low density lipoproteins. *J Biol Chem* 2004 Nov 5;279(45):47402-10.

Jacobs RL, Lingrell S, Zhao Y, Francis GA, Vance DE. Hepatic CTP:phosphocholine cytidyltransferase-alpha is a critical predictor of plasma high density lipoprotein and very low density lipoprotein. *J Biol Chem* 2008 Jan 25;283(4):2147-55.

Jain D, Dodia C, Fisher AB, Bates SR. Pathways for clearance of surfactant protein A from the lung. *Am J Physiol Lung Cell Mol Physiol* 2005 Dec;289(6):L1011-L1018.

Jobe A. Surfactant phospholipid metabolism in 3-day and 3-day postmature rabbits in vivo. *Pediatr Res* 1980 Apr;14(4 Pt 1):319-25.

Jobe A. Metabolism of endogenous surfactant and exogenous surfactants for replacement therapy. *Semin Perinatol* 1988 Jul;12(3):231-44.

Kerr MA, Stocks SC. The role of CD15-(Le(X))-related carbohydrates in neutrophil adhesion. *Histochem J* 1992 Nov;24(11):811-26.

Khovidhunkit W, Kim MS, Memon RA, Shigenaga JK, Moser AH, Feingold KR, et al. Effects of infection and inflammation on lipid and lipoprotein metabolism: mechanisms and consequences to the host. *J Lipid Res* 2004 Jul;45(7):1169-96.

Kim DK, Fukuda T, Thompson BT, Cockrill B, Hales C, Bonventre JV. Bronchoalveolar lavage fluid phospholipase A2 activities are increased in human adult respiratory distress syndrome. *Am J Physiol* 1995 Jul;269(1 Pt 1):L109-L118.

Kim HY, Hamilton J. Accumulation of docosahexaenoic acid in phosphatidylserine is selectively inhibited by chronic ethanol exposure in C-6 glioma cells. *Lipids* 2000 Feb;35(2):187-95.

Kumar KV, Rao SM, Gayani R, Mohan IK, Naidu MU. Oxidant stress and essential fatty acids in patients with risk and established ARDS. *Clin Chim Acta* 2000 Aug;298(1-2):111-20.

Lamb NJ, Gutteridge JM, Baker C, Evans TW, Quinlan GJ. Oxidative damage to proteins of bronchoalveolar lavage fluid in patients with acute respiratory distress syndrome: evidence for neutrophil-mediated hydroxylation, nitration, and chlorination. *Crit Care Med* 1999 Sep;27(9):1738-44.

Lee WL, Downey GP. Neutrophil activation and acute lung injury. *Curr Opin Crit Care* 2001 Feb;7(1):1-7.

Lewis JF, Ikegami M, Jobe AH. Altered surfactant function and metabolism in rabbits with acute lung injury. *J Appl Physiol* (1985) 1990 Dec;69(6):2303-10.

Li Z, Vance DE. Phosphatidylcholine and choline homeostasis. *J Lipid Res* 2008 Jun;49(6):1187-94.

Luhr OR, Antonsen K, Karlsson M, Aardal S, Thorsteinsson A, Frostell CG, et al. Incidence and mortality after acute respiratory failure and acute respiratory distress syndrome in Sweden, Denmark, and Iceland. The ARF Study Group. *Am J Respir Crit Care Med* 1999 Jun;159(6):1849-61.

MacDonald JI, Sprecher H. Phospholipid fatty acid remodeling in mammalian cells. *Biochim Biophys Acta* 1991 Jul 9;1084(2):105-21.

Mallampalli RK, Salome RG, Bowen SL, Chappell DA. Very low density lipoproteins stimulate surfactant lipid synthesis in vitro. *J Clin Invest* 1997 Apr 15;99(8):2020-9.

Mander A, Langton-Hewer S, Bernhard W, Warner JO, Postle AD. Altered phospholipid composition and aggregate structure of lung surfactant is associated with impaired lung function in young children with respiratory infections. *Am J Respir Cell Mol Biol* 2002 Dec;27(6):714-21.

Markart P, Ruppert C, Wygrecka M, Colaris T, Dahal B, Walmrath D, et al. Patients with ARDS show improvement but not normalisation of alveolar surface activity with surfactant treatment: putative role of neutral lipids. *Thorax* 2007 Jul;62(7):588-94.

Masclans JR, Bermejo B, Pico M, de Latorre FJ, Rodriguez-Roisin R, Planas M. [The prognostic value of eicosanoids in the acute respiratory distress syndrome]. *Med Clin (Barc)* 1999 Jan 30;112(3):81-4.

Mason RJ, Nellenbogen J, CLEMENTS JA. Isolation of disaturated phosphatidylcholine with osmium tetroxide. *J Lipid Res* 1976 May;17(3):281-4.

Matthay MA, Brower RG, Carson S, Douglas IS, Eisner M, Hite D, et al. Randomized, placebo-controlled clinical trial of an aerosolized beta(2)-agonist for treatment of acute lung injury. *Am J Respir Crit Care Med* 2011 Sep 1;184(5):561-8.

McGuire WW, Spragg RG, Cohen AB, Cochrane CG. Studies on the pathogenesis of the adult respiratory distress syndrome. *J Clin Invest* 1982 Mar;69(3):543-53.

McPhail LC, Qualliotine-Mann D, Agwu DE, McCall CE. Phospholipases and activation of the NADPH oxidase. *Eur J Haematol* 1993 Nov;51(5):294-300.

Meng H, Sun Y, Lu J, Fu S, Meng Z, Scott M, et al. Exogenous surfactant may improve oxygenation but not mortality in adult patients with acute lung injury/acute respiratory distress syndrome: a meta-analysis of 9 clinical trials. *J Cardiothorac Vasc Anesth* 2012 Oct;26(5):849-56.

Mermis JD, Simpson SQ. HMG-CoA Reductase Inhibitors for Prevention and Treatment of Severe Sepsis. *Curr Infect Dis Rep* 2012 Oct;14(5):484-92.

Miles PR, Ma JY, Bowman L. Degradation of pulmonary surfactant disaturated phosphatidylcholines by alveolar macrophages. *J Appl Physiol* (1985) 1988 Jun;64(6):2474-81.

Moss M, Guidot DM, Steinberg KP, Duhon GF, Treece P, Wolken R, et al. Diabetic patients have a decreased incidence of acute respiratory distress syndrome. *Crit Care Med* 2000 Jul;28(7):2187-92.

Moss M, Parsons PE, Steinberg KP, Hudson LD, Guidot DM, Burnham EL, et al. Chronic alcohol abuse is associated with an increased incidence of acute respiratory distress syndrome and severity of multiple organ dysfunction in patients with septic shock. *Crit Care Med* 2003 Mar;31(3):869-77.

Murray JF, Matthay MA, Luce JM, Flick MR. An expanded definition of the adult respiratory distress syndrome. *Am Rev Respir Dis* 1988 Sep;138(3):720-3.

Nakos G, Kitsioulis EI, Tsangaris I, Lekka ME. Bronchoalveolar lavage fluid characteristics of early intermediate and late phases of ARDS. Alterations in leukocytes, proteins, PAF and surfactant components. *Intensive Care Med* 1998 Apr;24(4):296-303.

Noga AA, Vance DE. A gender-specific role for phosphatidylethanolamine N-methyltransferase-derived phosphatidylcholine in the regulation of plasma high density and very low density lipoproteins in mice. *J Biol Chem* 2003 Jun 13;278(24):21851-9.

Numata M, Kandasamy P, Voelker DR. Anionic pulmonary surfactant lipid regulation of innate immunity. *Expert Rev Respir Med* 2012 Jun;6(3):243-6.

Okuyama H, Yamada K, Miyagawa T, Suzuki M, Prasad R, Lands WE. Enzymatic basis for the formation of pulmonary surfactant lipids by acyltransferase systems. *Arch Biochem Biophys* 1983 Feb 15;221(1):99-107.

Osanai K, Mason RJ, Voelker DR. Pulmonary surfactant phosphatidylcholine transport bypasses the brefeldin A sensitive compartment of alveolar type II cells. *Biochim Biophys Acta* 2001 Apr 30;1531(3):222-9.

Osanai K, Tsuchihara C, Hatta R, Oikawa T, Tsuchihara K, Iguchi M, et al. Pulmonary surfactant transport in alveolar type II cells. *Respirology* 2006 Jan;11 Suppl:S70-S73.

Paggiaro PL, Chanez P, Holz O, Ind PW, Djukanovic R, Maestrelli P, et al. Sputum induction. *Eur Respir J Suppl* 2002 Sep;37:3s-8s.

Parks EJ, Hellerstein MK. Thematic review series: patient-oriented research. Recent advances in liver triacylglycerol and fatty acid metabolism using stable isotope labeling techniques. *J Lipid Res* 2006 Aug;47(8):1651-60.

Pattle RE. Properties, function and origin of the alveolar lining layer. *Nature* 1955 Jun 25;175(4469):1125-6.

Petty TL, Silvers GW, Paul GW, Stanford RE. Abnormalities in lung elastic properties and surfactant function in adult respiratory distress syndrome. *Chest* 1979 May;75(5):571-4.

Phua J, Badia JR, Adhikari NK, Friedrich JO, Fowler RA, Singh JM, et al. Has mortality from acute respiratory distress syndrome decreased over time?: A systematic review. *Am J Respir Crit Care Med* 2009 Feb 1;179(3):220-7.

Poets CF, Arning A, Bernhard W, Acevedo C, von der HH. Active surfactant in pharyngeal aspirates of term neonates: lipid biochemistry and surface tension function. *Eur J Clin Invest* 1997 Apr;27(4):293-8.

Postle AD, Heeley EL, Wilton DC. A comparison of the molecular species compositions of mammalian lung surfactant phospholipids. *Comp Biochem Physiol A Mol Integr Physiol* 2001 May;129(1):65-73.

Postle AD, Madden J, Clark GT, Wright SM. Electrospray ionisation mass spectrometry analysis of differential turnover of phosphatidylcholine by human blood leukocytes. *Phys. Chem. Chem. Phys* 2004;6: 1018-1021.

Postle AD, Wilton DC, Hunt AN, Attard GS. Probing phospholipid dynamics by electrospray ionisation mass spectrometry. *Prog Lipid Res* 2007 May;46(3-4):200-24.

Postle AD, Hunt AN. Dynamic lipidomics with stable isotope labelling. *J Chromatogr B Analyt Technol Biomed Life Sci* 2009 Sep 15;877(26):2716-21.

Postle AD, Henderson NG, Koster G, Clark HW, Hunt AN. Analysis of lung surfactant phosphatidylcholine metabolism in transgenic mice using stable isotopes. *Chem Phys Lipids* 2011 Sep;164(6):549-55.

Pynn CJ, Picardi MV, Nicholson T, Wistuba D, Poets CF, Schleicher E, et al. Myristate is selectively incorporated into surfactant and decreases dipalmitoylphosphatidylcholine without functional impairment. *Am J Physiol Regul Integr Comp Physiol* 2010 Nov;299(5):R1306-R1316.

Pynn CJ, Henderson NG, Clark H, Koster G, Bernhard W, Postle AD. Specificity and rate of human and mouse liver and plasma phosphatidylcholine synthesis analyzed in vivo. *J Lipid Res* 2011 Feb;52(2):399-407.

Ranieri VM, Rubenfeld GD, Thompson BT, Ferguson ND, Caldwell E, Fan E, et al. Acute respiratory distress syndrome: the Berlin Definition. *JAMA* 2012 Jun 20;307(23):2526-33.

Reddy AJ, Kleeberger SR. Genetic polymorphisms associated with acute lung injury. *Pharmacogenomics* 2009 Sep;10(9):1527-39.

Renooij W, Van Golde LM. The exchange of phospholipids between rat erythrocytes and plasma, and the translocation of phosphatidylcholine across the red cell membrane, are temperature dependent processes. *FEBS Lett* 1976 Dec 1;71(2):321-4.

Rice KL, Duane PG, Archer SL, Gilboe DP, Niewoehner DE. H₂O₂ injury causes Ca²⁺-dependent and -independent hydrolysis of phosphatidylcholine in alveolar epithelial cells. *Am J Physiol* 1992 Oct;263(4 Pt 1):L430-L438.

Rice TW, Wheeler AP, Thompson BT, deBoisblanc BP, Steingrub J, Rock P. Enteral omega-3 fatty acid, gamma-linolenic acid, and antioxidant supplementation in acute lung injury. *JAMA* 2011 Oct 12;306(14):1574-81.

Rice TW, Mogan S, Hays MA, Bernard GR, Jensen GL, Wheeler AP. Randomized trial of initial trophic versus full-energy enteral nutrition in mechanically ventilated patients with acute respiratory failure. *Crit Care Med* 2011 May;39(5):967-74.

Robinson M, Blank ML, Snyder F. Highly unsaturated phospholipid molecular species of rat erythrocyte membranes: selective incorporation of arachidonic acid into phosphoglycerides containing polyunsaturation in both acyl chains. *Arch Biochem Biophys* 1986 Nov 1;250(2):271-9.

Rodriguez-Capote K, Manzanares D, Haines T, Possmayer F. Reactive oxygen species inactivation of surfactant involves structural and functional alterations to surfactant proteins SP-B and SP-C. *Biophys J* 2006 Apr 15;90(8):2808-21.

Rouzer CA, Ivanova PT, Byrne MO, Brown HA, Marnett LJ. Lipid profiling reveals glycerophospholipid remodeling in zymosan-stimulated macrophages. *Biochemistry* 2007 May 22;46(20):6026-42.

Rubenfeld GD, Caldwell E, Granton J, Hudson LD, Matthay MA. Interobserver variability in applying a radiographic definition for ARDS. *Chest* 1999 Nov;116(5):1347-53.

Rubinfeld GD, Caldwell E, Peabody E, Weaver J, Martin DP, Neff M, et al. Incidence and outcomes of acute lung injury. *N Engl J Med* 2005 Oct 20;353(16):1685-93.

Ryan AJ, Medh JD, McCoy DM, Salome RG, Mallampalli RK. Maternal loading with very low-density lipoproteins stimulates fetal surfactant synthesis. *Am J Physiol Lung Cell Mol Physiol* 2002 Aug;283(2):L310-L318.

Schmidt R, Meier U, Yabut-Perez M, Walmrath D, Grimminger F, Seeger W, et al. Alteration of fatty acid profiles in different pulmonary surfactant phospholipids in acute respiratory distress syndrome and severe pneumonia. *Am J Respir Crit Care Med* 2001 Jan;163(1):95-100.

Schmidt R, Markart P, Ruppert C, Wygrecka M, Kuchenbuch T, Walmrath D, et al. Time-dependent changes in pulmonary surfactant function and composition in acute respiratory distress syndrome due to pneumonia or aspiration. *Respir Res* 2007;8:55.

Schwartz DB, Bone RC, Balk RA, Szidon JP. Hepatic dysfunction in the adult respiratory distress syndrome. *Chest* 1989 Apr;95(4):871-5.

Seeger W, Elssner A, Gunther A, Kramer HJ, Kalinowski HO. Lung surfactant phospholipids associate with polymerizing fibrin: loss of surface activity. *Am J Respir Cell Mol Biol* 1993 Aug;9(2):213-20.

Seeger W, Grube C, Gunther A, Schmidt R. Surfactant inhibition by plasma proteins: differential sensitivity of various surfactant preparations. *Eur Respir J* 1993 Jul;6(7):971-7.

Serhan CN. Novel lipid mediators and resolution mechanisms in acute inflammation: to resolve or not? *Am J Pathol* 2010 Oct;177(4):1576-91.

Silkoff PE, Trudeau JB, Gibbs R, Wenzel S. The relationship of induced-sputum inflammatory cells to BAL and biopsy. *Chest* 2003 Mar;123(3 Suppl):371S-2S.

Simonato M, Baritussio A, Ori C, Vedovelli L, Rossi S, Dalla ML, et al. Disaturated-phosphatidylcholine and surfactant protein-B turnover in human acute lung injury and in control patients. *Respir Res* 2011;12:36.

Singh TK, Abonyo B, Narasaraju TA, Liu L. Reorganization of cytoskeleton during surfactant secretion in lung type II cells: a role of annexin II. *Cell Signal* 2004 Jan;16(1):63-70.

Spector AA, Yorek MA. Membrane lipid composition and cellular function. *J Lipid Res* 1985 Sep;26(9):1015-35.

Spillman T, Cotton DB. Current perspectives in assessment of fetal pulmonary surfactant status with amniotic fluid. *Crit Rev Clin Lab Sci* 1989;27(4):341-89.

Stanke-Labesque F, Moliere P, Bessard J, Laville M, Vericel E, Lagarde M. Effect of dietary supplementation with increasing doses of docosahexaenoic acid on

neutrophil lipid composition and leukotriene production in human healthy volunteers. *Br J Nutr* 2008 Oct;100(4):829-33.

Steinberg KP, Hudson LD, Goodman RB, Hough CL, Lanken PN, Hyzy R, et al. Efficacy and safety of corticosteroids for persistent acute respiratory distress syndrome. *N Engl J Med* 2006 Apr 20;354(16):1671-84.

Strong P, Kishore U, Morgan C, Lopez BA, Singh M, Reid KB. A novel method of purifying lung surfactant proteins A and D from the lung lavage of alveolar proteinosis patients and from pooled amniotic fluid. *J Immunol Methods* 1998 Nov 1;220(1-2):139-49.

Suwabe A, Mason RJ, Voelker DR. Calcium dependent association of surfactant protein A with pulmonary surfactant: application to simple surfactant protein A purification. *Arch Biochem Biophys* 1996 Mar 15;327(2):285-91.

Thiel A, Scheffold A, Radbruch A. Immunomagnetic cell sorting--pushing the limits. *Immunotechnology* 1998 Oct;4(2):89-96.

Tou JS. Incorporation of arachidonic acid and eicosapentaenoic acid into phospholipids by polymorphonuclear leukocytes in vitro. *Lipids* 1984 Aug;19(8):573-7.

Trapnell BC, Whitsett JA. Gm-CSF regulates pulmonary surfactant homeostasis and alveolar macrophage-mediated innate host defense. *Annu Rev Physiol* 2002;64:775-802.

Uddin M, Levy BD. Resolvins: natural agonists for resolution of pulmonary inflammation. *Prog Lipid Res* 2011 Jan;50(1):75-88.

Ueland PM. Choline and betaine in health and disease. *J Inherit Metab Dis* 2011 Feb;34(1):3-15.

Van Helvoort A, de BA, Ottenhoff R, Brouwers JF, Wijnholds J, Beijnen JH, et al. Mice without phosphatidylcholine transfer protein have no defects in the secretion of phosphatidylcholine into bile or into lung airspaces. *Proc Natl Acad Sci U S A* 1999 Sep 28;96(20):11501-6.

Vance DE. Physiological roles of phosphatidylethanolamine N-methyltransferase. *Biochim Biophys Acta* 2013 Mar;1831(3):626-32.

Veldhuizen RA, Inchley K, Hearn SA, Lewis JF, Possmayer F. Degradation of surfactant-associated protein B (SP-B) during in vitro conversion of large to small surfactant aggregates. *Biochem J* 1993 Oct 1;295 (Pt 1):141-7.

Venet F, Chung CS, Huang X, Lomas-Neira J, Chen Y, Ayala A. Lymphocytes in the development of lung inflammation: a role for regulatory CD4+ T cells in indirect pulmonary lung injury. *J Immunol* 2009 Sep 1;183(5):3472-80.

Villar J, Blanco J, Anon JM, Santos-Bouza A, Blanch L, Ambros A, et al. The ALIEN study: incidence and outcome of acute respiratory distress syndrome in the era of lung protective ventilation. *Intensive Care Med* 2011 Dec;37(12):1932-41.

Vockeroth D, Gunasekara L, Amrein M, Possmayer F, Lewis JF, Veldhuizen RA. Role of cholesterol in the biophysical dysfunction of surfactant in ventilator-induced lung injury. *Am J Physiol Lung Cell Mol Physiol* 2010 Jan;298(1):L117-L125.

von Neergaard K. Neue Auffassungen über einen Grundbegriff der Atemmechanik. Die Retraktionskraft der Lunge, abhängig von der Oberflächenspannung in den Alveolen. *Z Gesamte Exp Med* 1929;66: 373–394.

Waite KA, Cabilio NR, Vance DE. Choline deficiency-induced liver damage is reversible in *Pemt*(-/-) mice. *J Nutr* 2002 Jan;132(1):68-71.

Walkey CJ, Donohue LR, Bronson R, Agellon LB, Vance DE. Disruption of the murine gene encoding phosphatidylethanolamine N-methyltransferase. *Proc Natl Acad Sci U S A* 1997 Nov 25;94(24):12880-5.

Ware LB, Matthay MA. The acute respiratory distress syndrome. *N Engl J Med* 2000 May 4;342(18):1334-49.

Ware LB, Koyama T, Billheimer DD, Wu W, Bernard GR, Thompson BT, et al. Prognostic and pathogenetic value of combining clinical and biochemical indices in patients with acute lung injury. *Chest* 2010 Feb;137(2):288-96.

Watkins SM, Zhu X, Zeisel SH. Phosphatidylethanolamine-N-methyltransferase activity and dietary choline regulate liver-plasma lipid flux and essential fatty acid metabolism in mice. *J Nutr* 2003 Nov;133(11):3386-91.

Webster NR, Cohen AT, Nunn JF. Adult respiratory distress syndrome--how many cases in the UK? *Anaesthesia* 1988 Nov;43(11):923-6.

Wendel M, Paul R, Heller AR. Lipoproteins in inflammation and sepsis. II. Clinical aspects. *Intensive Care Med* 2007 Jan;33(1):25-35.

Wheeler AP, Bernard GR, Thompson BT, Schoenfeld D, Wiedemann HP, deBoisblanc B, et al. Pulmonary-artery versus central venous catheter to guide treatment of acute lung injury. *N Engl J Med* 2006 May 25;354(21):2213-24.

Wiedemann HP, Wheeler AP, Bernard GR, Thompson BT, Hayden D, deBoisblanc B, et al. Comparison of two fluid-management strategies in acute lung injury. *N Engl J Med* 2006 Jun 15;354(24):2564-75.

Winkler C, Hohlfeld JM. Surfactant and allergic airway inflammation. *Swiss Med Wkly* 2013;143:w13818.

Wirtz HR, Dobbs LG. Calcium mobilization and exocytosis after one mechanical stretch of lung epithelial cells. *Science* 1990 Nov 30;250(4985):1266-9.

Wright SM, Hockey PM, Enhorning G, Strong P, Reid KB, Holgate ST, et al. Altered airway surfactant phospholipid composition and reduced lung function in asthma. *J Appl Physiol* (1985) 2000 Oct;89(4):1283-92.

Wu KK, Papp AC, Manner CE, Hall ER. Interaction between lymphocytes and platelets in the synthesis of prostacyclin. *J Clin Invest* 1987 Jun;79(6):1601-6.

Yao ZM, Vance DE. The active synthesis of phosphatidylcholine is required for very low density lipoprotein secretion from rat hepatocytes. *J Biol Chem* 1988 Feb 25;263(6):2998-3004.

Young D, Lamb SE, Shah S, MacKenzie I, Tunnicliffe W, Lall R, et al. High-frequency oscillation for acute respiratory distress syndrome. *N Engl J Med* 2013 Feb 28;368(9):806-13.

Zeisel SH. Choline: an essential nutrient for humans. *Nutrition* 2000 Jul;16(7-8):669-71.

Zeisel SH, Mar MH, Howe JC, Holden JM. Concentrations of choline-containing compounds and betaine in common foods. *J Nutr* 2003 May;133(5):1302-7.

